REGULATION OF CELL-MEDIATED IMMUNE (CMI) RESPONSES ASSOCIATED WITH EXPERIMENTAL IMMUNOSUPPRESSION

By

TATHAGATA MUKHERJEE

LIFE11201604008

National Institute of Science Education and Research, an OCC of HBNI, Bhubaneswar

A thesis submitted to the Board of Studies in Life Sciences in partial fulfillment of requirements for the Degree of

DOCTOR OF PHILOSOPHY

of

HOMI BHABHA NATIONAL INSTITUTE

August 2024

Homi Bhabha National Institute

Recommendations of the Viva Voce Committee

As members of the Viva Voce Committee, we certify that we have read the dissertation prepared by Tathagata Mukherjee entitled "Regulation of Cell-mediated Immune (CMI) Responses Associated with Experimental Immunosuppression" and recommend that it may be accepted as fulfilling the thesis requirement for the award of Degree of Doctor of Philosophy.
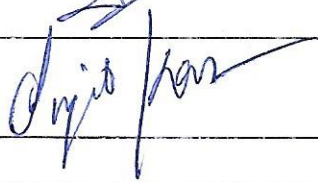
Chairman – Prof. Chandan Goswami _Chandan Goswami_ Date: 07/08/2024

Guide / Convener – Dr. Subhasis Chattopadhyay _Subhasis Chattopadhyay_ Date: 07/08/2024

Co-guide - Date:

Examiner - Prof. Dr. Sankar Maiti _Sankar Maiti_ Date: 07-08-2024

Member 1 – Dr. Asima Bhattacharyya Date: 7.8.2024

Member 2 – Dr. Harapriya Mahapatra Date: 07/08/2024

Member 3 – Dr. Sanjib Kar _Sanjib Kar_ Date: 07/08/2024

Final approval and acceptance of this thesis is contingent upon the candidate's submission of the final copies of the thesis to HBNI.

I/We hereby certify that I/we have read this thesis prepared under my/our direction and recommend that it may be accepted as fulfilling the thesis requirement.

Date : 07/08/2024

Place : NISER, Bhubaneswar

Signature
Co-guide (if any)

Signature
Guide

ii

STATEMENT BY AUTHOR

This dissertation has been submitted in partial fulfillment of requirements for an advanced degree at Homi Bhabha National Institute (HBNI) and is deposited in the Library to be made available to borrowers under the rules of the HBNI.

Brief quotations from this dissertation are allowable without special permission, provided that accurate acknowledgment of the source is made. Requests for permission for extended quotation from or reproduction of this manuscript in whole or in part may be granted by the Competent Authority of HBNI when in his or her judgment the proposed use of the material is in the interests of scholarship. In all other instances, however, permission mustbe obtained from the author.

Tathagata Mukherjee

DECLARATION

I hereby declare that I am the sole author of this thesis in partial fulfillment of the requirements for a postgraduate degree from the National Institute of Science Education and Research (NISER). I authorize NISER to lend this thesis to other institutions or individuals for the purpose of scholarly research.

Tathagata Mukherjee

List of Publications

Publications

1. Telmisartan Restricts Chikungunya Virus Infection In Vitro and In Vivo through the AT1/PPAR-γ/MAPKs Pathways. Saikat De, Prabhudutta Mamidi, Soumyajit Ghosh, Supriya Suman Keshry, Chandan Mahish, Sweta Smita Pani, Eshna Laha, Amrita Ray, Ankita Datey, Sanchari Chatterjee, Sharad Singh, **Tathagata Mukherjee**, Somlata Khamaru, Subhasis Chattopadhyay, Bharat Bhusan Subudhi, Soma Chattopadhyay. Antimicrobial Agents Chemotherapy, 2022, DOI: 10.1128/AAC.01489-21.

2. # Elevation of TRPV1 expression on T-cells during experimental immunosuppression. P Sanjai Kumar*, **Tathagata Mukherjee***, Somlata Khamaru, Anukrishna Radhakrishnan, Dalai Jupiter Nanda Kishore, Saurabh Chawla, Subhransu Sekhar Sahoo, Subhasis Chattopadhyay. Journal of Biosciences, 2022, DOI: https://doi.org/10.1007/s12038-022-00279-2. (Joint first authors)

3. Understanding the Role of Ca^{2+} via Transient Receptor Potential (TRP) Channel in Viral Infection: Implications in Developing Future Antiviral Strategies. P. Sanjai Kumar, Anukrishna Radhakrishnan, **Tathagata Mukherjee**, Somlata Khamaru, Soma Chattopadhyay, and Subhasis Chattopadhyay. Virus Research, 2022, DOI: https://doi.org/10.1016/j.virusres.2022.198992. (Review Article).

4. # TRPA1 activation and Hsp90 inhibition synergistically downregulate macrophage activation and inflammatory responses in vitro. Anukrishna Radhakrishnan*, **Tathagata Mukherjee***, Chandan Mahish, P Sanjai Kumar, Chandan Goswami, Subhasis Chattopadhyay. BMC Immunology, 2023, DOI: https://doi.org/10.1186/s12865-023-00549-0. (Joint first authors)

5. TLR4 is one of the receptors for Chikungunya virus envelope protein E2 and regulates virus induced pro-inflammatory responses in host macrophages. Chandan Mahish, Saikat De, Sanchari Chatterjee, Soumyajit Ghosh, Supriya Suman Keshry, **Tathagata Mukherjee**, Somlata Khamaru, Kshyama Subhadarsini Tung, Bharat

Bhusan Subudhi, Soma Chattopadhyay and Subhasis Chattopadhyay. Frontiers in Immunology, 2023, DOI: https://doi.org/10.3389/fimmu.2023.1139808.

6. Salicylic acid conjugate of telmisartan inhibits CHIKV infection and inflammation. Rudra N Dash, Amrita Ray, Prabhudutta Mamidi, Saikat De, Tapas K Mohapatra, Alok K Moharana, **Tathagata Mukherjee**, Soumyajit Ghosh, Subhasis Chattopadhyay, Bharat B Subudhi and Soma Chattopadhyay. ACS Omega, 2023, DOI: 10.1021/acsomega.3c00763.

7. # Upregulation, functional association, and correlated expressions of TRPV1 and TRPA1 during Telmisartan-driven immunosuppression of T cells. **Tathagata Mukherjee**, Kshyama Subhadarsini Tung, Parthasarathi Jena, Chandan Goswami, Subhasis Chattopadhyay. Immunological Investigations, 2024 (accepted, in press). (First author)

8. Chikungunya virus regulates T cell and macrophage directed immune responses towards B16-F10 mediated immune-suppression: An insight of the viral infection in tumor cells, macrophages and associated regulation of cell mediated immunosuppression. Somlata Khamaru*, **Tathagata Mukherjee***, Kshyama Subhadarsini Tung, P. Sanjai Kumar, Saumya Bandyopadhyay, Chandan Mahish, Soma Chattopadhyay, Subhasis Chattopadhyay (under review). (Joint first authors)

9. Differential expression of toll-like receptor 4 (TLR4) during B16F10-culture supernatant (B16F10-CS)- and FK506-mediated suppression of T cells. **Tathagata Mukherjee**, Parthasarathi Jena, Situl Mahanta, Subhasis Chattopadhyay. (manuscript under preparation)

# Pertaining to thesis; * Equal contribution

 Conferences

1. Oral Presentation entitled "Regulation of Anti-Cancer T Cell Responses Associated to Cell-Mediated Immunity: Implication in Cellular and Molecular Contexts of Tumor Microenvironment Driven Immune Suppression." **Tathagata Mukherjee** (**Presenting Author**), Saumya Bandyopadhyay, Somlata Khamaru, P Sanjai Kumar, Subhransu

Sekhar Sahoo, Subhasis Chattopadhyay. Indo Oncology Summit-18, 2nd - 4th, February 2018 at Bhubaneswar, India. ISBN: 97881-935941-1-7. (**Awarded First Prize for the Best Oral Presentation**)

2. Presented Poster entitled "Elevation of TRPV1 expression on T cells during experimental immunosuppression." P Sanjai Kumar, **Tathagata Mukherjee** (**Presenting Author**), Somlata Khamaru, Anukrishna Radhakrishnan, Dalai Jupiter Nanda Kishore, Saurabh Chawla, Subhransu Sekhar Sahoo, and Subhasis Chattopadhyay. Immunocon 2022, 8th - 9th, July 2022, Banaras Hindu University, Varanasi. Poster no. PP111.

 Workshops

1. "Workshop on Microtomy/Ultra-microtomy, Staining and Imaging Techniques" organized by Institute of Life Sciences, Bhubaneswar. 12th – 13th, April 2018.

2. "Light Microscope and Live Cell Imaging", Pre-Conference Workshop EMSI 2018 organized by Electron Microscope Society of India (EMSI) and National Institute of Science Education and Research. 16th – 17th, July 2018.

3. "4th Orientation Workshop on Laboratory Animal Sciences" jointly organized by National Institute of Science Education and Research & Institute of Life Sciences, Bhubaneswar. 11th – 15th, March 2019.

TATHAGATA MUKHERJEE
Name & Signature of the Student

Dedicated to

My parents . . .

ACKNOWLEDGEMENTS

hands, and significant suggestions. I would like to thank Saikat, Soumyajit, Sanchari, Koustavda, Amritadi, Supriya, Ankita, Anjali, Ipshitadi, Eshna, Sharad, and Raj of ILS Bhubaneswar, for their constant and unwavering support. I thank all my SBS seniors and juniors for their friendly and responsive cooperation.

I would love to express my profound and heartful gratitude to my family members, especially to my father, Mr. Prabir Mukherjee, and to my mother, Mrs. Krishna Mukherjee, for their unconditional and absolute support at every single step of my life. I'm really gratified to the wonderful lady Ms. Manideepa Saha for having faith and believing me in my tough time and my heartiest appreciation for her constant and unconditional heart-warming support.

I am grateful to my wonderful friends, especially Aranyadip, Ram, Abhrojyoti, Abhishek, Susobhan, Subham, and Sanjay for their endless support and encouragement during my difficult days, providing me with the best time at NISER. A Special thanks to my buddies Shoumik, Ritutama, Sroddha, and Madhumanti for being an important part of my life.

Last but not least, I am blissful to the Almighty God for all the blessings.

ABSTRACT

Macrophages and T cells play an important role in executing cell-mediated immune (CMI) responses by regulating different immune functions. Various altered physiological conditions, including cancer, different drugs, and many immunosuppressive modulators are attributed to induce systemic immunosuppression alleviating effector immune responses. Transient receptor potential vanilloid 1 (TRPV1) and transient receptor potential ankyrin 1 (TRPA1) channels regulate various physiological processes by mediating different cellular pathways. Modulation of TRPV1 and TRPA1 is known to regulate T cell- and macrophage-associated immune responses. However, the possible association of these channels towards immunosuppression requires further investigation. Here, we have found that elevation of TRPV1 expression occurs during FK506 (Tacrolimus, an immunosuppressive drug) or B16F10 (a metastatic immunosuppressive mouse melanoma cell line) culture supernatant (B16F10-CS) mediated immunosuppression of T cells, and it was found to play an important role in regulating the immunosuppression-driven accumulation of intracellular Ca^{2+} levels in T cells. Moreover, expression of TRPA1 was found to be elevated during 17-AAG (Tanespimycin; 17-N-allylamino-17-demethoxygeldanamycin)-driven suppression of proinflammatory responses of macrophages through Hsp90 inhibition, and it was found to regulates LPS/PMA/17-AAG-mediated pro-inflammatory cytokine productions, phospho-mitogen-activated protein kinase (p-MAPK) expressions, and Ca^{2+} influx, *in vitro*. In addition, both TRPV1 and TRPA1 expressions were found to be elevated in Telmisartan (TM)-driven immunosuppression of T cells, *in vitro*. TRPV1 activation during TM-mediated immunosuppression overrides TRPA1 activation-mediated suppression of T cells by upregulating T cell activation and effector cytokine productions, *in vitro*. Collectively, this study could be important in understanding the functional regulation of CMI responses

associated with immunosuppression in altered physiological conditions and may have implications for devising better strategies for future therapeutics.

Contents

SUMMARY

Immunosuppression is characterized by the abated effector responses associated with immune cells, accompanied by the modulation of the cellular events important to mount an effective immune response, followed by the reduced ability to recognize and/or counter foreign antigens. Several diseases, including cancer, are observed to progress through alleviating immune responses, causing systemic immunosuppression. The tumor microenvironment plays an important role in cancer progression and metastasis by employing an immunosuppressive network suppressing anti-tumor immune responses. B16F10, a murine transplantable melanoma cell line, has been reported to hinder T cell function, *in vivo* and *in vitro*. Similarly, various medications, including drugs used in transplantation, and several modulators function through the inhibition of effector immune responses associated with antigen-presenting cells (APC), lymphocytes, and other accessory immune cells. Transient receptor potential vanilloid 1 (TRPV1) and transient receptor potential ankyrin 1 (TRPA1) are polymodal, non-selective cation channels present in different cell types and are reported to regulate effector responses associated with various immune cells, including macrophages, dendritic cells, and T cells. However, the information towards the possible involvement of these channels in immunosuppression associated with T cells and macrophages remains scanty. In this study, first, we have explored the possible role of TRPV1 in FK506- and B16F10-CS-mediated immunosuppression of T cells. It was observed that induction of TRPV1 expression occurs during experimental immunosuppression and TRPV1 plays an important role in regulating immunosuppression-mediated Ca^{2+} influx. Next, we have investigated the possible role of TRPA1 in 17-AAG-induced Hsp90 inhibition-mediated suppression of pro-inflammatory responses associated with macrophages. It has been found that TRPA1

induction ensues during Hsp90 inhibition-mediated suppression of macrophages, and it plays an anti-inflammatory role in regulating pro-inflammatory responses. Next, we have studied the possible association of TRPV1 and TRPA1 channels in Telmisartan (TM) (an anti-hypertension drug)-mediated immunosuppression of T cells. It was found that both TRPV1 and TRPA1 expressions were elevated in TM-driven immunosuppression of T cells, *in vitro*. TRPV1 activation during TM-mediated immunoregulation overrides TRPA1 activation-mediated suppression of T cells by upregulating T cell activation and effector cytokine productions, *in vitro*. This study may have implications for understanding the functional regulation of cell-mediated immune (CMI) responses associated with immunosuppression in altered physiological conditions toward devising better strategies for future therapeutics.

ABBREVIATIONS

Ab: Antibody

AD: Atopic Dermatitis

ADCC: Antibody-Dependent Cellular Cytotoxicity

AF: Alexa Fluor

Ag: Antigen

AIDS: Acquired Immunodeficiency Syndrome

AITC: Allyl isothiocyanate

AM: Acetoxymethyl ester

AMP: Antimicrobial Peptide

ANOVA: Analysis of Variance

APC: Allophycocyanin

APC: Antigen Presenting Cells

APS: Ammonium Persulfate

ATG: Antithymocyte Globulins

AP-1: activator protein 1

ATP: Adenosine Triphosphate

BALT: Bronchus-Associated Lymphoid Tissues

BCR: B Cell Antigen Receptor

BSA: Bovine Serum Albumin

B16F10-CS: B16F10 cell culture supernatant

CCR: CC Chemokine Receptor

CD: Cluster of Differentiation

CLIP: Class II-associated Invariant Chain Peptide

CMI: Cell-Mediated Immunity

CS: Cell Surface Staining

CsA: Cyclosporine A

CSF: Colony-Stimulating Factors

CTL: Cytotoxic T Lymphocytes

CTLA4: Cytotoxic T-Lymphocyte Associated Protein 4

CVA21: Coxsackievirus A21

CX3CR: CX3C Chemokine Receptor

DAG: Diacylglycerol

DAMP: Danger-Associated Molecular Patterns

DC: Dendritic Cell

DDT: Dithiothreitol

DMEM: Dulbecco's Modified Eagle Medium

DMSO: Dimethyl Sulfoxide

DN: Double Negative

DP: Double Positive

DTH: Delayed-Type Hypersensitivity

EAE: Experimental Autoimmune Encephalomyelitis

EDTA: Ethylenediaminetetraacetic Acid

ELISA: Enzyme-Linked Immunosorbent Assay

ER: Endoplasmic Reticulum

ERAP: Endoplasmic Reticulum Amino-peptidase

ERK: Extracellular Signal-Regulated Kinase

Fab: Fragment Antigen Binding

FACS: Fluorescence-Activated Cell Sorting

FBS: Fetal Bovine Serum

FC: Flow Cytometry

Fc: Fragment Crystallizable

FcR: Fragment Crystallizable Receptor

FK506: Tacrolimus

FKBP: FK506-binding protein

FoxP3: Forkhead box P3

FSC: Forward Scattering

GALT: Gut-Associated Lymphoid Tissue

GATA3: GATA Binding Protein 3

GITR: Glucocorticoid-Induced TNFR-Related protein

GM-CSF: Granulocyte-Macrophage Colony-Stimulating Factor

HC-030031: 1,2,3,6-Tetrahydro-1,3-dimethyl-N-[4-(1-methylethyl) phenyl]-2,6-dioxo-7H-purine-7- acetamide,2-(1,3-Dimethyl-2,6-dioxo-1,2,3,6-tetrahydro-7H-purin-7-yl)-N-(4-isopropylphenyl) acetamide

HIV: Human Immunodeficiency Virus

HLA: Human Leukocyte Antigen

HPLC: High-Performence Liquid Chromatography

HRP: Horseradish Peroxidase

HSCs: Hematopoietic Stem Cells

Hsp: Heat Shock Protein

HSV: Herpes Simplex Virus

IAEC: Institutional Animal Ethics Committee

ICS: Intracellular Staining

IFN: Interferon

Ig: Immunoglobulin

IL: Interleukin

iMC: Immature Myeloid Cell

IRF: Interferon Regulatory Factor

ITAM: Immunoreceptor Tyrosine-Based Activation Motif

iTregs: Induced Regulatory T Cells

JNK: c-Jun N-Terminal Kinase

KO: Knockout

LAT: Linker for the Activation of T Cells

Lck: Lymphocyte-Specific Protein Tyrosine Kinase

LPS: Lipopolysaccharide

mAb: Monoclonal Antibodies

MAIT cells: Mucosal-Associated Invariant T Cells

MALT: Mucus Associated Lymphoid Tissues

MAPK: Mitogen-Activated Protein Kinase

MCP: Monocyte Chemotactic Proteins

MFI: Mean Fluorescence Intensity

MHC: Major Histocompatibility Complex

Min: Minutes (Time unit)

MIP: Macrophage Inflammatory Protein

mM: Millimolar

MS: Multiple Sclerosis

NaCl: Sodium Chloride

NALT: Nasal Associated Lymphoid Tissues

NaN3: Sodium Azide

NFAT: Nuclear Factor of Activated T Cells

NFκB: Nuclear Factor Kappa B

NK Cell: Natural Killer Cell

NKT cells: Natural Killer T cells

nM: Nanomolar

nm: Nanometer

NO: nitric oxide

nTregs: Natural Regulatory T cells

PAMP: Pathogen-Associated Molecular Patterns

pAPCs: Professional Antigen Presenting Cells

PBS: Phosphate-Buffered Saline

PE: Phycoerythrin

PFA: Paraformaldehyde

PHSC: Pluripotent Hematopoietic Stem Cell

PLC: Phospholipase C

PLO: Primary Lymphoid Organ

PMA: Phorbol 12-Myristate 13-Acetate

PRR: Pattern Recognition Receptor

PVDF: Polyvinylidene Fluoride or Polyvinylidene Difluoride

RA: Rheumatoid Arthritis

RAG: Recombination Activating Gene

RANTES: Regulated Upon Activation Normally T Expressed and Secreted

RBC: Red Blood Cell

RER: Rough Endoplasmic Reticulum

RIPA: Radio Immunoprecipitation Assay

RORγt: RAR-related Orphan Receptor gamma t

ROS: Reactive Oxygen Species

RPMI-1640: Roswell Park Memorial Institute-1640

RT: Room Temperature

SAPK: Stress-Activated Protein Kinase

SCID: Severe Combined Immunodeficiency

SDS: Sodium Dodecyl Sulphate

SDS-PAGE: Sodium Dodecyl Sulfate Polyacrylamide Gel Electrophoresis

SEM: Standard Error of the Mean

SLE: Systemic Lupus Erythematosus

SLOs: Secondary Lymphoid Organs

SOCE: Store-Operated Calcium Entry

SP: Single Positive

SSC: Side Scattering

SR: Sarcoplasmic Reticulum

TAM: Tumor-Associated Macrophages

TAP: Transporters Associated with Antigen Processing

TBS: Tris-Buffered Saline

TBST: Tris-Buffered Saline Tween-20

Tc Cells: Cytotoxic T Cells

TCM: Central Memory T Cells

TCR: T Cell Receptor

Tef Cells: Effector T Cells

TEMED: Tetramethylethylenediamine

TGF-β: Transforming Growth Factor beta

TGS: Tris-Glycine-SDS

Th Cells: Helper T Cells

TiDC: Tumor-Induced Dendritic Cell

TLR: Toll-like Receptor

TM: Telmisartan

TMB: 3,3″,5,5″-Tetramethylbenzidine

TME: Tumor Microenvironment

TNF: Tumor Necrosis Factor

Tregs: Regulatory T cells

TRP: Transient Receptor Potential Channel

TRPA: Transient Receptor Potential Ankyrin Channel

TRPV: Transient Receptor Potential vanilloid Channel

T-VEC: Talimogene Laherparepvec

VEGF: Vascular Endothelial Growth Factor

v/v: Volume/Volume

w/v: Weight/Volume

WCL: Whole Cell Lysate

ZAP70: ζ-chain associated protein kinase of 70 kDa

2-ME: 2-Mercaptoethanol

5'-IRTX: 5'-iodoresiniferatoxin

7-AAD: 7-Aminoactinomycin D

17-AAG: 17-(allylamino)-17-demethoxygeldanamycin

LIST OF FIGURES

LIST OF TABLES

CHAPTER # 1

Introduction

1. Introduction

1.1. The immune system

The system, comprised of an intricate network of cells, tissues, and organs, that protect us from the external threats of foreign invaders like bacteria, viruses, etc., and aid in fighting those invasions, is the immune system. The study of the immune system is known as immunology. Constantly we are getting exposed through inhalation, ingestion, or injury to a plethora of foreign "non-self" entities like bacteria, viruses, pollens, or any other harmful substances. The immune system has the ability to distinguish between "self" and "non-self" components which helps an organism in the recognition and elimination of those foreign/"non-self" elements in a coordinated manner, which may otherwise have detrimental effects on the organism [1,2].

The complexity of the immune system increased with its evolution ranging from prokaryotes to eukaryotes, from bacteria to higher vertebrates, protecting organisms ever since [3–5]. However, a balanced and coordinated immune response is necessary and critical for the host's defense against a foreign invasion. Hyperactivation of the immune system results in aggravated responses causing severe inflammation and could be responsible for bystander lysis of the "self" cells. Moreover, malfunction in "self" and "non-self" recognition by the immune system may result in autoimmune diseases, namely rheumatoid arthritis (RA), systemic lupus erythematosus (SLE), multiple sclerosis (MS), etc. Immunodeficiency or decreased immune response, conversely, is also disadvantageous for any organism as a reduced immune response makes the host more susceptible towards less virulent strains of pathogens. To name a few, severe combined immunodeficiency (SCID), acquired immunodeficiency syndrome (AIDS), etc. [6,7].

The immune system is comprised of an array of defense strategies. Constantly the host is getting exposed to a variety of foreign invaders, trying to breach the protective

shield recruited by the immune system [8]. These invasions, depending on the load or type/nature of the pathogens, are recognized by different functional layers of the immune system and restrict the assaults through different modes of action [9]. Accordingly, different components (either cellular or secreted/soluble factors) of the immune system function in different layers, and based on the time of recruitment, mode of action, and function, the immune system is broadly classified into two distinct but overlapping arms known as the innate immune system and the adaptive immune system which are connected mutually.

1.2. Innate immune system

The innate immune system is the first line of defense against foreign invasion. It is an evolutionarily conserved defense strategy sharing features between plants, invertebrates, and vertebrates [10]. Almost all the tissues in a mammal are armed with innate defense mechanisms, especially the skin and mucosal surfaces of the respiratory and gastrointestinal tract. The innate immune defense can be engaged in either cell-dependent (cell-mediated) or independent (humoral) manner [11]. The cellular components of the innate immune system consist of cells such as basophils, dendritic cells, eosinophils, Langerhans cells, mast cells, monocytes, macrophages, neutrophils, NK cells, etc., which "sense" the incoming threats through germline-encoded "sensors" known as pattern recognition receptors (PRRs) that recognize the molecular patterns present on the pathogen known as pathogen-associated molecular patterns (PAMPs) and restrict the assaults mostly through phagocytosis or cytotoxicity. The cell-independent components of the innate defense consist of antimicrobial peptides (AMPs), complement proteins, cytokines/chemokines, chitinases/chitinase-like proteins, acute-phase proteins, etc. [12]. The innate immune response is rapid, less specific, and doesn't evoke any memory responses. However, recent studies shifted the paradigm towards "trained immunity" associated with the memory responses by natural killer cells and innate lymphoid cells [13,14].

1.3. Adaptive immune system

The adaptive or acquired immune system comes into the picture when an innate response is unsuccessful in clearing the invading pathogen out of the host's body. The adaptive response is slower than the innate response. However, it is highly specific towards pathogens and generates long-lived memory cells, which are capable of triggering rapid secondary effector responses after the encounter with the same pathogen. The adaptive immune system functions in either cell-depended (cell-mediated immunity) or an independent (humoral immunity) manner, similar to the innate system. The cellular components of the adaptive immune system are comprised of highly specialized lymphocytes such as T cells and B cells, whereas the cell-independent or humoral part consists of antibodies (secreted B cell antigen (Ag) receptor/immunoglobulin) secreted by plasma/activated B cells [15]. The specificity triggered by the adaptive immune cells is primarily based on the antigen-specific receptors, which are expressed by T or B cells through the process of somatic rearrangement of germ-line gene elements to form complete T cell receptors (TCRs) or B cell receptors (antibodies/immunoglobulin) [16,17]. Adaptive immune cells, after recognizing specific antigens presented through antigen-presenting cells, become activated and mount an effector response along with memory generation following proliferation and clonal expansion.

1.4. Components of the immune system

Bone marrow-derived leukocytes (granulocytes, monocytes, dendritic cells, lymphocytes, etc.) are the key mediators of immune responses. Lymphoid and myeloid cells are generated from pluripotent hematopoietic stem cells. Lymphoid cells (T cells and B cells) are the main players in the adaptive immune responses, whereas myeloid cells (granulocytes, monocytes, macrophages, dendritic cells, mast cells, etc.) are involved in both innate and adaptive immune responses [18]. Differentiated tissue macrophages and mast

cells are the front-line effector cells initiating the inflammation. Phagocytes, such as macrophages, dendritic cells, etc., initiate their function through phagocytosis and recruit granulocytes such as neutrophils, basophils, eosinophils, and other cells at the site of infection, mounting innate responses [19]. Ingested microbes are then processed into small antigenic peptides by these phagocytes. Macrophages and dendritic cells are specialized in their function, and after ingestion of the microbes, they migrate to the peripheral/secondary lymphoid organs to present the processed antigenic peptides (so are called antigen-presenting cells (APCs)) to lymphoid cells like T cells or B cells. Maturation of T and B

Table 1: Differences between Innate and Adaptive Immune Responses

Sl.No.	Characteristics	Innate Immunity	Adaptive immunity
1.	Presence	Gemline encoded.	Generates through somatic rearrangement of T cell receptor (TCR) or immunoglobulin/B cell receptor (BCR) gene elements.
2.	Specificity	Less-Specific, board spectrum recognition	Specific for a particular antigen
3.	Response	Against molecular patterns present on foreign invader	Against specific infection
4.	Response time	Rapid	Slow (7-14 days)
5.	Potency	Limited and Lower	Higher
6.	Inheritance	Inherited through parents	Acquired through infection.
7.	Memory	Doesn't generate a memory response.	Generates memory.
8.	Diversity	Low	High
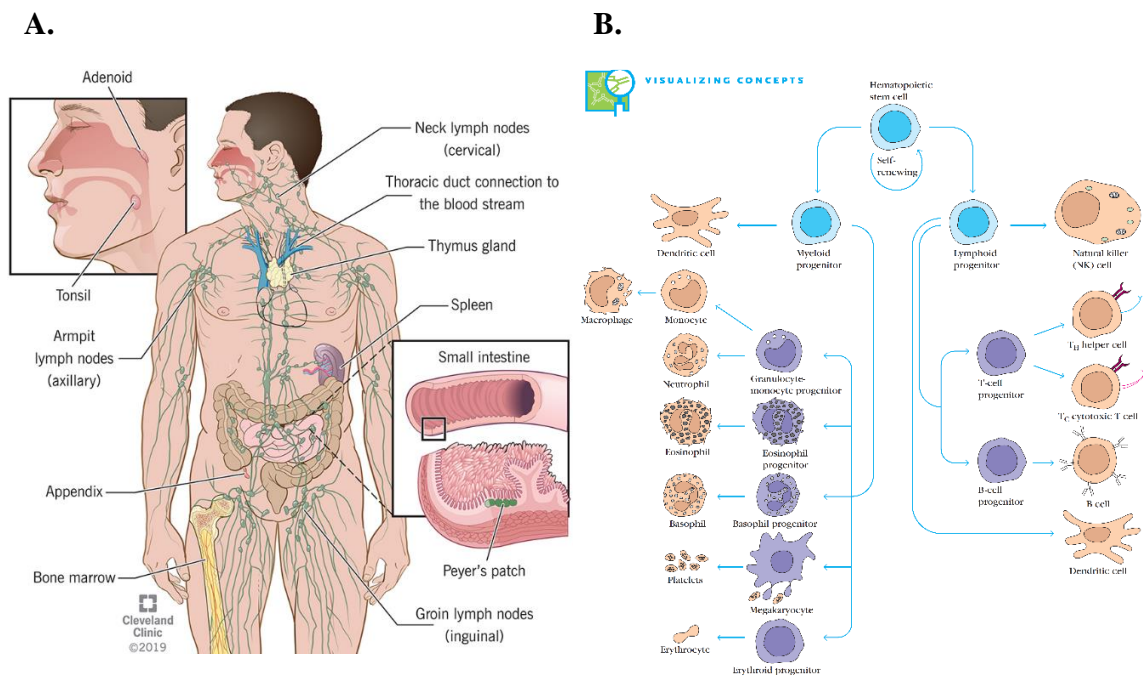
Figure 1: Human immune system and generation of blood cells through hematopoiesis. (A) The human immune system [20] and (B) generation of different blood cells through hematopoiesis (Kuby 7th edition).

lymphocytes occur in the primary lymphoid organs, such as the thymus and bone marrow, respectively. Major peripheral/secondary lymphoid organs include the spleen (accumulating antigens from the bloodstream), lymph nodes (accumulating antigens from the tissue), and mucosal-associated lymphoid tissues (MALT) (accumulating antigens from the epithelial surfaces). Recirculation of mature lymphocytes from blood to peripheral/secondary lymphoid organs and from peripheral/secondary lymphoid organs to blood occurs through lymphatic vessels. Recognition of specific antigens on the surface of macrophages/dendritic cells triggers an adaptive immunity following proliferation and differentiation, generating memory for the immune system [21,22].

1.5. Physical and chemical barriers to the immune system

Restrictions for the entry of pathogens inside the host's body are initiated by the physical and chemical barriers of innate immunity. The physical barriers include skin, gastrointestinal tract, respiratory tract, nasopharynx, cilia, eyelashes, and other body hairs, whereas the chemical barriers include body secretions, mucus, bile, gastric acid, saliva, sweat, antimicrobial peptides, etc. [23]. The thick epithelial lining, acidic pH (~ 5.5), and flora of beneficial bacteria inhibit the colonization and growth of pathogens on the skin surface. Specialized structures called cilia are present on the surface of the respiratory and gastrointestinal tract and help in sweeping out bacteria during respiration and ingestion. The mucus layer present in the respiratory tract, gastrointestinal tract, urogenital tract, ducts of exocrine secretory glands, etc., prevents the binding and entry of pathogens. Gastric pH (~ 1-3), pH of the vaginal fluid (~ 4.4), and lysozyme present in tears restrict microbial growth. However, breaching occurs owing to the damage or impairment to these barriers facilitating the entry of the pathogens inside the host, approaching contact with different immune cells [22,24].

1.6. Organs and cells of the immune system

Lymphoid organs are the principal players of the immune system facilitating the generation and supporting the development of the immune cells. The primary lymphoid organs include bone marrow and thymus, whereas the secondary or peripheral lymphoid organs are comprised of the spleen, lymph nodes, lymphatic vessels, tonsil, adenoid, skin, and liver. [25,26].

Bone marrow is the soft sponge-like tissue found inside the bone containing pluripotent hematopoietic stem cells, which give rise to most of the immune cells. These cells then migrate toward their particular organs or tissue through the bloodstream. Red bone marrow, at the time of birth, is found inside many bones; however, with time, the

marrow has been replaced by fatty tissue. The ribs, breastbone, and pelvis are the remaining bones that contain the marrow during adulthood.

The thymus is a gland-like structure found at the backside of the breastbone above the heart. The size of the thymus starts to shrink a few days after birth. Antigen education and maturation of T lymphocytes occur inside the thymus supported by other thymocytes.

Spleen resides in the left upper abdomen, below the diaphragm. It houses different immune cells which scavenge and filter microbes or debris present in the bloodstream. Spleen also helps in the breakdown of erythrocytes and thrombocytes.

The lymph nodes are bean-like small tissues residing across the lymphatic vessels. The main function of the lymph nodes is to filter out infections from the infected tissues. Pathogenic encounter with the circulating immune cells occurs inside the lymph nodes.

The tonsils reside in the throat and the palate, holding a significant amount of white blood cells which shield the entry of pathogens through the mouth and nose.

Other secondary lymphoid organs include MALT (mucus-associated lymphoid tissue), GALT (gut-associated lymphoid tissue), NALT (nasal-associated lymphoid tissue), BALT (bronchus-associated lymphoid tissue), Peyer's patches, etc.

Hematopoiesis is the process of the generation of blood and bone marrow cells. Hematopoietic stem cells (HSCs) are multipotent, capable of generating progenitor cells and have self-renewal ability. Hematopoiesis begins with the division of the multipotent progenitor cells into common myeloid progenitor and common lymphoid progenitor (**Figure 2**). These common progenitors lack the ability to self-renewal [27]. Common myeloid-progenitor cells give rise to dendritic cells, erythrocytes, monocytes, macrophages, neutrophils, basophils, mast cells, eosinophils, erythrocytes, and megakaryocytes, whereas common lymphoid progenitor cells generate T lymphocytes, B
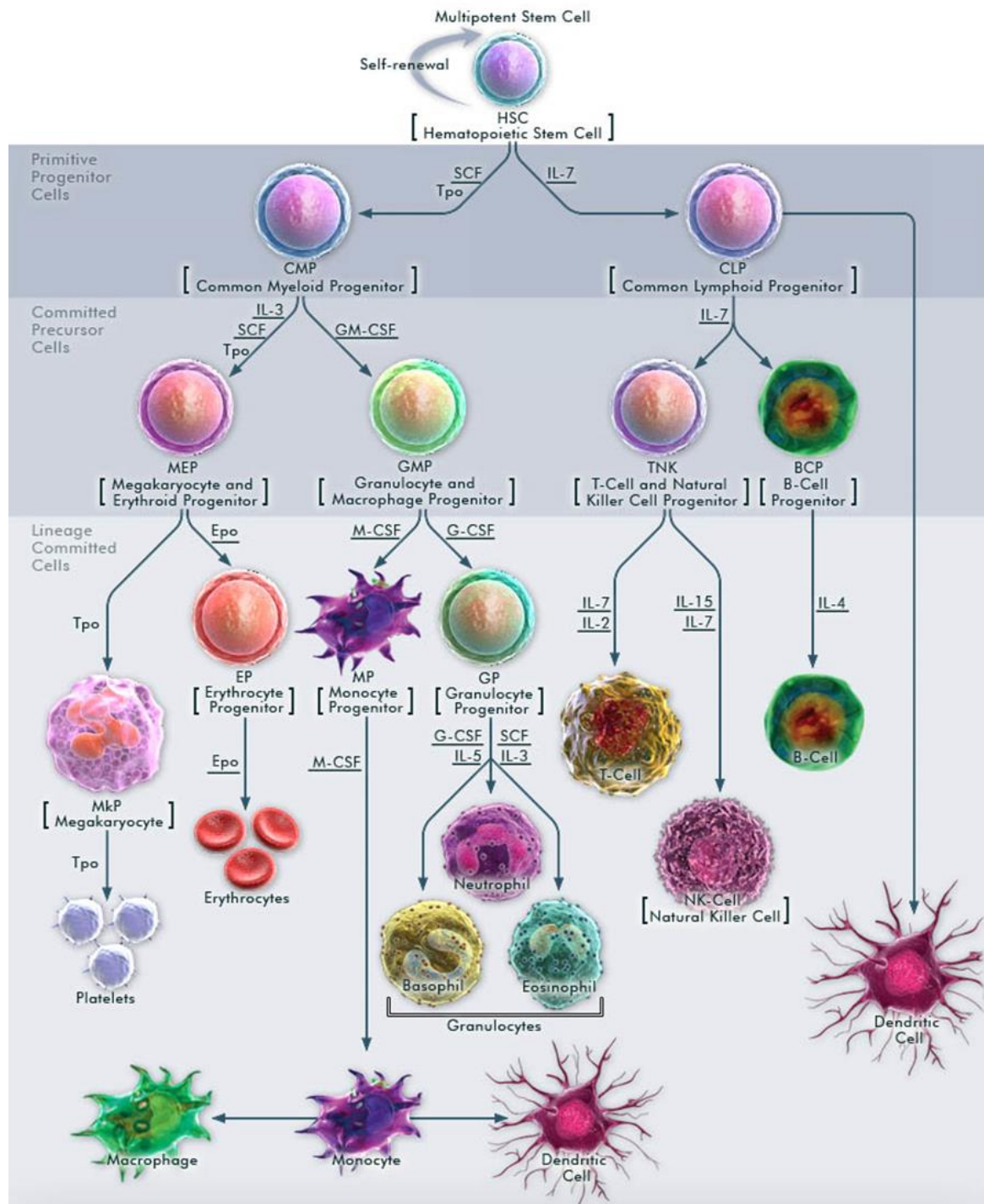
Figure 2: Differentiation of hematopoietic stem cells. Multipotent stem cells generate common myeloid and lymphoid progenitor cells. The common myeloid cells generate monocytes, macrophages, granulocytes, etc. The common lymphoid progenitors give rise to T cells, B cells, and natural killer cells [29].

lymphocytes, and natural killer cells (NK cells) [28]. The fate of the hematopoietic stem cells depends on different signaling molecules like interleukins (ILs), erythropoietin, and colony-stimulating factors (CSFs) generating specific niches of cells [30]. T cells and B cells are the main players in conducting the adaptive immune system, while monocyte macrophages, dendritic cells, etc., function both as innate and adaptive immune cells.

1.7. Antigen-presenting cells (APC)

The immune system is constantly exposed to foreign molecules and neo/unknown antigens. These "nonself" molecules must be recognized by the immune cells from the "self" elements. In order to mount an effective immune response, the immune cells must be trained against these "nonself" molecules. Accordingly, the training or priming of the immune cells against those foreign "nonself" molecules/antigens through phagocytic engulfment, processing, and presentation of the "nonself" molecules, in a recognizable form, is given by the so-called "trainers" known as antigen-presenting cells (APCs) [31]. Depending on the degree of presenting exogenous antigens and the expression of certain cell surface molecules present on these cells, the APCs can be classified as professional and non-professional APCs [31–33] (**Figure 3**).

Professional APCs include dendritic cells, macrophages, and B cells. These cells are specialized and much more efficient in presenting foreign/exogenous antigenic peptides through major histocompatibility complexes (MHCs). Dendritic cells and macrophages engulf microbes through phagocytosis, whereas B cells opt for receptor-mediated endocytosis. Constitutive expression of class II MHC (MHCII) molecules and costimulatory molecules such as CD80 (B7.1), and CD86 (B7.2) are the prominent features of professional antigen-presenting cells. Non-professional APCs include all nucleated cells, e.g., epithelial cells, fibroblasts, endothelial cells, glial cells, etc. These cells are mostly involved in presenting endogenous antigens through class I MHC

(MHCI). Non-professional APCs do not express MHCII or costimulatory molecules constitutively. However, the expression of
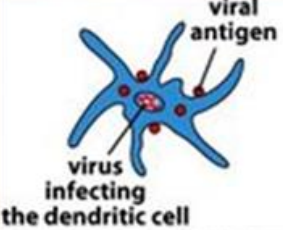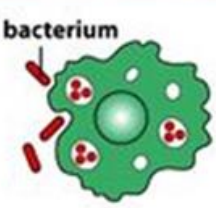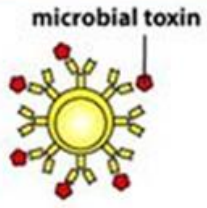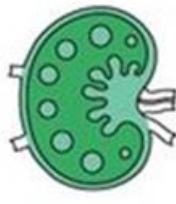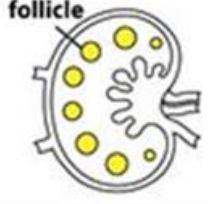
	Professional antigen-presenting cells		
	Dendritic cell	Macrophage	B cell
Cell type	viral antigen / virus infecting the dendritic cell	bacterium	microbial toxin
Location in lymph node	T-cell areas		follicle
Antigen uptake	+++ Macropinocytosis and phagocytosis by tissue dendritic cells Viral infection	Phagocytosis +++	Antigen-specific receptor (Ig) ++++
MHC expression	Low on tissue dendritic cells High on dendritic cells in lymphoid tissues	Inducible by bacteria and cytokines – to +++	Constitutive Increases on activation +++ to ++++
Co-stimulator delivery	Constitutive by mature, nonphagocytic lymphoid dendritic cells ++++	Inducible – to +++	Inducible – to +++
Antigen presented	Peptides Viral antigens Allergens	Particulate antigens Intracellular and extracellular pathogens	Soluble antigens Toxins Viruses
Location	Ubiquitous throughout the body	Lymphoid tissue Connective tissue Body cavities	Lymphoid tissue Peripheral blood

Figure 3: Differences between Professional APCs (The Immune System, Garland Science, 3rd Edition, 2009).

these molecules may appear in response to certain cytokines or other molecules involved in generating immune responses.

1.8. Antigen processing and presentation

Antigen processing and presentation are the primary steps for initiating an optimal adaptive immune response. Depending on the source of the antigens, APCs present the foreign peptides to different subsets of T lymphocytes via MHC molecules [34], generating protective T cell responses. Exogenous antigens are processed mostly by professional APCs and presented to CD4+ helper T cells (Th cells) via MHCII molecules, whereas endogenously expressed foreign antigens are presented by APCs to CD8+ cytotoxic T cells (Tc cells) via MHCI molecule. MHC molecules that are not loaded with antigenic peptides are unable to activate T lymphocytes. Exogenous antigens (e.g., bacteria) are processed and presented through the exogenous pathway, whereas endogenous antigens (viral proteins, transformed antigens, etc.) are processed and presented via the endogenous pathway of antigen processing and presentation [32,35].

The exogenous pathway of antigen processing and presentation begins with the internalization of the foreign pathogen/molecule either by phagocytosis (by dendritic cells and macrophages) or by endocytosis (by B cells). After getting internalized, the exogenous substances travel through a network of endosomes having different pHs, such as early endosome (pH 6 - 6.5), late endosome/endolysosome (pH 4.5 - 5), and lysosome (pH 4.5) and eventually end up in 13-18 amino acid (AA) long peptides with the action of different proteolytic enzymes. The invariant chain/CD74 (Li protein) protects the MHCII peptide binding groove in the rough endoplasmic reticulum (RER) from the binding of peptides designed for MHCI. After the transport of the MHCII molecules from RER to endolysosomal compartments via cis- and trans-Golgi network, the Li protein gets trimmed off, giving rise to CLIP (class II-associated invariant chain) protein in the endolysosome. A non-classical MHCII molecule, HLA-DM, facilitates the exchange of

CLIP with antigenic peptides. The peptide-MHCII complex is then transported to the cell membrane and presented to Th cells [36,37] (**Figure 4**).
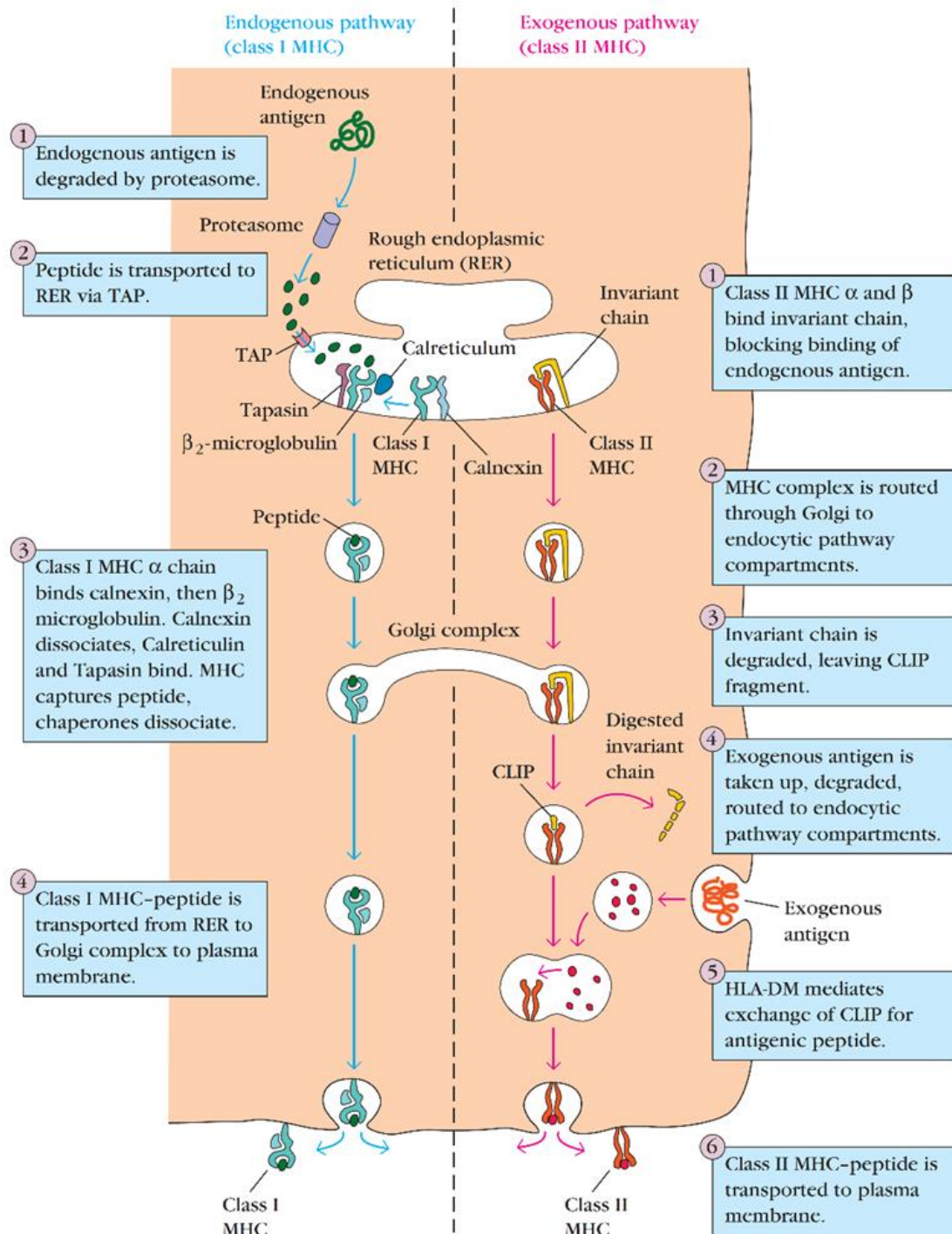
Figure 4: An overview of endogenous and exogenous pathways of antigen processing and presentation (Immunology, Kuby, 5th edition).

The endosomal pathway of antigen processing and presentation begins with the tagging of endogenously expressed "nonself" proteins with ubiquitination. Ubiquitinated proteins are then degraded with the help of proteasomal complexes creating small peptide fragments and transported from the cytoplasm to the RER lumen via TAP (Transportes associated with antigen processing) proteins. Endoplasmic reticulum aminopeptidases (ERAPs) then further chop the antigenic fragments into around 9 AA peptides. Calnexin, calreticulin, and tapasin proteins monitors and facilitate the proper binding of the antigenic peptide to the peptide binding cleft of MHCI. The MHCI-peptide complexes are then transported to the cell membrane through the cis- and trans-Golgi network and presented to Tc cells [32,38] (**Figure 4**).

However, having all the regulatory/monitoring mechanisms, cross-presentation occasionally occurs when the exogenous antigenic peptides are presented through MHCI molecules to Tc cells [39–42].

1.9. Antibodies

Antibodies (Ab) are the factors of the vertebrate adaptive immune system that protects the host from various pathogens, such as viruses, toxins, etc., and aid in neutralizing these foreign elements by recruiting various immune functions. Antibodies can be found in either soluble/secreted form or bound to the B cell membrane as B cell receptors. It possesses a "Y" shaped structure having two identical antigen binding sites on the tips known as the F_{ab} region, whereas the membrane binding site resides on the tail of the "Y", called the F_c region. Antibodies are made up of 4 polypeptide chains – two identical light chains and two identical heavy chains. The light chains are made up of one variable (V_L) and one constant region (C_L), whereas the heavy chain contains one variable (L_H) and 3 - 4 constant regions (C_H). Depending on the presence of distinctive heavy chains, the antibodies are classified as IgA, IgD, IgG, IgE, and IgM, having heavy chains

α, δ, γ, ε, and μ respectively. The light chains are either κ or λ. Either class of light chains can associate with any heavy chain to form the complete structure. The biological role of an antibody depends on the presence of a specific heavy chain. A particular clone of the B cell contains unique antibodies specific for a unique epitope of an antigen. During the development of B cells in the bone marrow, the antibody molecules remain in membrane-bound condition. In the periphery/secondary lymphoid organs, once the B cell receptors bind to its particular antigen along with other co-stimulatory signals, the B cells become activated following proliferation and differentiation. These activated B cells differentiate into either memory B cells or antibody-secreting plasma B cells that secret antibodies which have the same specificity. Antibodies mostly function in the neutralization of pathogens, phagocytosis, antibody-dependent cellular cytotoxicity (ADCC), complement-mediated lysis of the pathogen or the infected cells, etc. [22,24,43].

1.10. Cytokines and chemokines

Cytokines and chemokines (chemotactic cytokines) are important mediators regulating physiological responses having pleiotropic functions. These are small soluble/secretory protein molecules that control the growth and development of cells, generation of immune cells, lymphocyte recruitment, differentiation of cells, inflammation, etc., through an autocrine or paracrine, or endocrine manner by employing a vast signaling network between different cells. An immune response, triggered by the function of a group of cytokines, decides the phenotype of the forthcoming cellular outcomes [44,45]. Examples of cytokines include the interleukin (IL) superfamily of proteins such as IL-1, IL-2, IL-4, IL-6, IL-10, IL-11, IL-13, IL-15, IL-16, IL-17, IL-18. Cytokines, other than the IL superfamily, include interferons (IFNs), tumor necrosis factors (TNFs), transforming growth factors (TGFs), colony-stimulating factors (CSFs), fibroblast growth factor (FGF), vascular endothelial growth factor (VEGF), etc. Contingent on the cellular

outcome it facilitates, the cytokines can be broadly classified as pro-inflammatory and anti-inflammatory/regulatory.

Pro-inflammatory cytokine includes IL-1, IL-2 (also known as T cell growth factor), IL-6, IL-16, IL-17, IL-18, TNF, IFN, etc., whereas anti-inflammatory/regulatory cytokines include IL-10, TGF-β, IL-4 (mostly), IL-11, IL-13, etc. Examples of chemokine include macrophage inflammatory proteins (MIPs) (also known as IL-8), monocyte chemotactic proteins (MCPs), interferon-γ-inducing protein-10 (IP-10), Mig, regulated upon activation normally T expressed and secreted (RANTES), eotaxin, C10, KC/Gro-α, etc. [46,47].

1.11. Lymphocytes

Lymphocytes are critical players in mediating adaptive immune responses having the ability to recognize specific antigenic epitopes. It includes T and B cells. T cells mediate the cell-mediated immune responses by interacting with other cells, whereas the B cells mediate humoral immunity through antibody responses. Both types of lymphocytes possess similar morphology containing a large nucleus, compact heterochromatin structures, and less cytoplasmic volume with a few mitochondria, ribosomes, and lysosomes. The volume of the cytoplasm, along with the number of cytoplasmic organelles, increases with activation subsequent to specific antigenic encounters in the periphery. A particular antigenic epitope is recognized by a particular receptor present in T and B cells, known as the T cell receptor (TCR) and B cell receptor (BCR), respectively, having enormous phenotypic diversity generated through vigorous somatic recombination processes.

1.11.1. T lymphocytes

The development of T cells begins in the later stage of hematopoiesis in the bone marrow, where hematopoietic stem cells (HSCs) differentiate into multipotent progenitor

cells. A subset of these progenitor cells started expressing recombination activating genes 1 and 2 (RAG1 and RAG2), generating the common lymphoid progenitor cells. A small subset of common lymphoid progenitors migrates to the thymus and differentiates into TCR-beari-
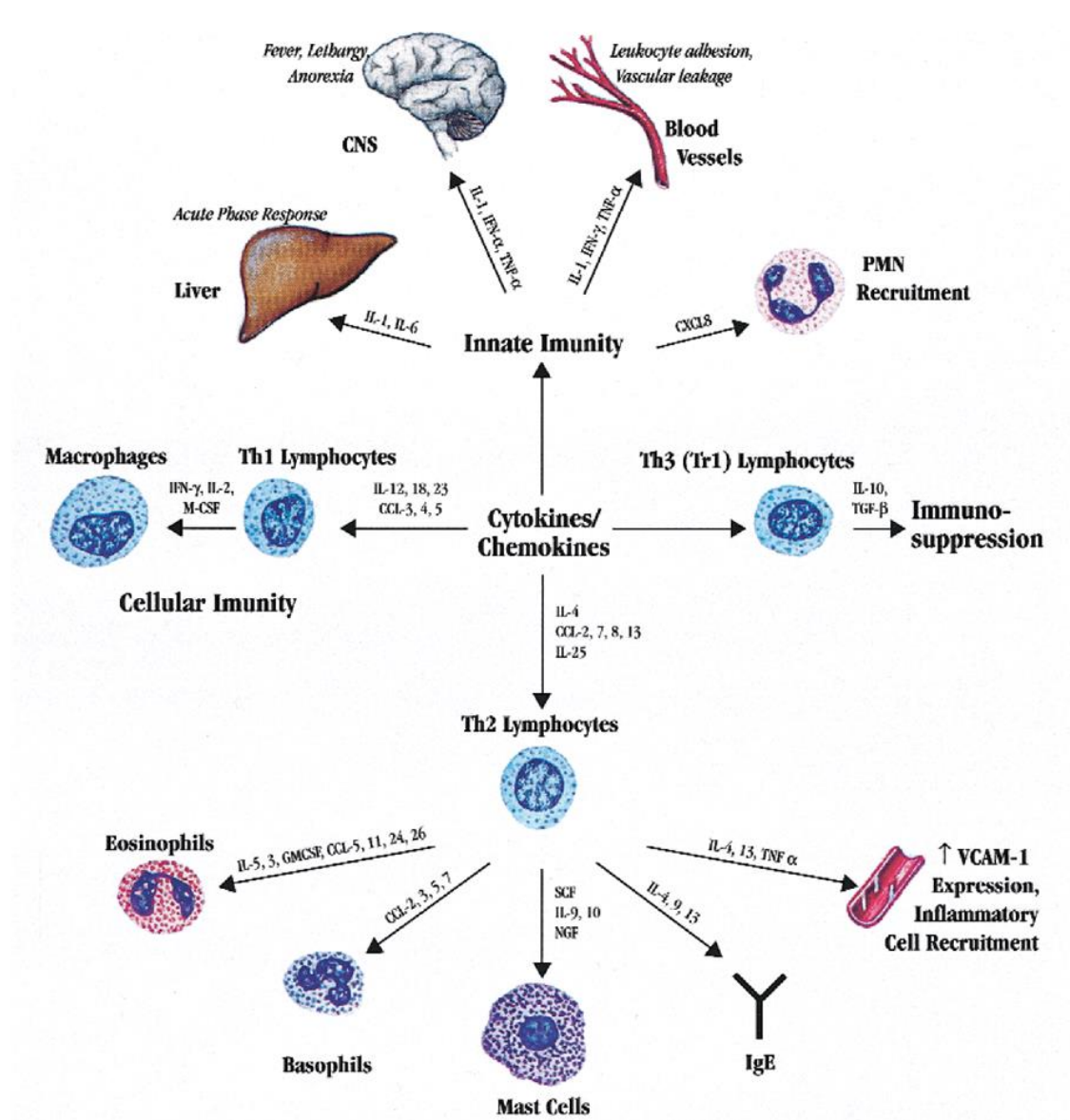
Figure 5: Overview of the role of different cytokines and chemokines in generating an immune response [45].

-ng T cells with the action of different signaling molecules, having either CD4 or CD8 as a co-receptor [48].

At the beginning of the maturation stage in the thymus, T cells bear both the co-receptors and are called CD4+CD8+ double positive (DP) cells. Positive selection of these cells in human channels through a "self" antigen presentation test where the epithelial cells of the thymic cortex present the "self" antigens via class I and class II human leukocyte antigens (HLA-I and HLA-II) molecules. Cells expressing TCRs that have an intermediate affinity towards those self-antigens get positively selected and differentiate into either CD4+CD8-/CD4-CD8+ single positive (SP) cells depending on the HLA recognition. Cells recognizing HLA-I differentiate into CD8+ cells, and cells recognizing HLA-II differentiate into CD4+ cells. Cells that are unable to bind the HLA molecules undergo apoptosis [49,50].

The negative selection of the SP cells takes place in the medulla of the thymus. Thymic epithelial cells of the medulla present a diverse range of self-antigens through HLA-I and HLA-II molecules. Cells expressing TCRs that bind to these self-peptides with high affinity undergo apoptosis, eliminating the autoreactive cells [50]. Surviving cells of the negative selection mature into naïve T cells and leave the thymus and migrate to secondary lymphoid organs for antigen priming.

The recognition of specific antigenic epitopes by T cells is mediated by the T cell receptors (TCRs). TCR is made up of the antigen binding chains and the accessory proteins forming the multiprotein TCR complex. The variable antigen binding chains include either αβ or γδ and the accessory proteins comprising the CD3γε, CD3δε, and CD3ζζ [51]. The CD3 ζ chains have an elongated cytoplasmic tail which facilitates the TCR-mediated T cell activation signals.

T cells constantly migrate through the lymph nodes, searching for their specific antigens. An optimal binding of TCRs with the MHC-peptide complex presented by the dendritic cells initiates T cell activation, differentiation, and proliferation, generating effector and memory T cells [52]. T cell signaling cascade originates from the phosphorylation of lymphocyte-specific protein tyrosine kinase (Lck) and Fyn associated with the CD4/CD8 co-receptors and CD3 ε chain, respectively, next to TCR engagement with the antigenic peptide. Through subsequent phosphorylation by kinase activities, the immunoreceptor tyrosine-based activation motif (ITAM) moiety of the CD3δε gets phosphorylated, which attracts the ζ-chain associated protein kinase of 70 kDa (ZAP70). ZAP70, in turn, activates the linker for the activation of T cells (LAT) and phospholipase C γ1 (PLCγ1). Activated LAT initiates actin reorganization, whereas PLCγ1 activates phosphatidylinositol 4, 5-bisphosphate (PIP2), diacylglycerol (DAG) and facilitates the expression of nuclear factor of activated T cells (NFAT), nuclear factor kappa B (NFκB), and activator protein 1 transcription factor (AP-1) transcription factors. NFAT, NFκB, and AP-1 facilitate the expression of IL-2, high-affinity IL-2 receptor alpha (IL-2Rα, also known as CD25), expression of cell adhesion molecules, costimulatory molecules, antiapoptotic proteins, etc. [53,54]. However, optimal T cell activation requires costimulatory signals referred to as the second signal of T cell activation (TCR-MHC-peptide being the first one) [55,56]. Examples of positive costimulatory molecules present on T cells include CD28, CD27, HVEM, etc. that interact with CD80/CD86 (B7.1/B7.2), CD70, and LIGHT molecules present on APCs, respectively. Negative costimulatory molecules on T cells include CTLA-4, PD-1 which interacts with CD80/CD86, and PDL-1/PDL-2 molecules present on the APCs. Positive costimulatory signals help in sustaining the activation state, whereas negative costimulatory signals reduce the degree of T cell activation inducing T cell anergy.

Antigen binding and co-stimulation initiate IL-2 and IL-2R expression in T cells. IL-2, after being secreted from the activated T cells, can function in either an autocrine or paracrine manner facilitating blastogenesis and clonal expansion of T cells giving rise to a large number of activated T cells having identical TCRs [57]. Subsequent to the clearance of the pathogen, effector T cells are eliminated from circulation through apoptosis initiated by the interaction with Fas-FasL, TNF-TNFRI/TNFRII, etc. [58].

Following activation, T cells are differentiated into different subpopulations depending on the nature of the antigenic peptide, APC type and its state of activation, cytokine microenvironment, and the type of co-stimulatory signals. The functions of the activated CD4+ helper T cells (Th cells) include helping other cells by further inducing the immune response through cytokine secretion, activating B cells to generate antibody-secreting plasma cells, etc. Based on the effector cytokines response, Th cells can be classified into several subclasses. Th1 cells secrete IFNγ and induce cell-mediated immune responses against pathogens, involved in autoimmunity and delayed-type hypersensitivity (DTH) [59]. Th2 cells secrete IL-4, IL-5, IL-9, IL-10, IL-13, etc., suppressing inflammatory responses, IgE class switching, airway hyperresponsiveness, mast cell recruitment, etc. [60]. Th9 cells secrete IL-9, IL-10, etc., and help in IgE class switching, mucus secretion, etc. [61]. Th17 cells secret IL-17, IL-6, IL-9, TNF-α, etc., and induces chemokine production, neutrophilia, etc. [62]. Th22 cells secrete IL-22, TNF-α, IL-13, etc., and help in antimicrobial peptide synthesis, keratinocyte proliferation, etc. [63]. Tfh (follicular helper T cells) secrets IL-21, IL-4, IL-10, etc., and helps in the formation of germinal centers, plasma cell production, development of B cells, etc. [64]. Regulatory T cells (Tregs) can be either CD4+ or CD8+. However, the prime functions of these cells are to regulate the immune function by suppressing inflammatory responses, promoting Th2 polarization, preventing autoimmunity, etc. Based on the origin, Tregs can be classified as

thymic Tregs (tTregs, originates in the thymus) and peripheral Tregs (pTregs, originates in the periphery) [65,66]. Activated CD8+ cytotoxic T cell functions by destroying the altered target cells (virus-infected cells, cancerous cells, etc.) directly through cytotoxicity. Exerted cytotoxicity by the CD8+ cytotoxic T cells that results in apoptosis of the target cell includes the release of different cytolytic granules (perforins, granzymes, etc.), expression of ligands for death receptors like FasL, etc. [67,68]. Perforin polymerization form pores in the target cell membrane destroying the osmotic equilibrium and allowing the entry of granzyme that degrades mitochondria or other intracellular entities through their proteolytic effects.

1.11.2. B lymphocytes

The generation and development of B cells initiate in the bone marrow. Multipotent hematopoietic stem cells (HSCs) give rise to common lymphoid progenitor (CLP) cells. CLPs then differentiate into CLP-2, generating the B cell lineage [69]. B cell development from CLP-2 is divided into several stages, namely early pro-B cells, late pro-B cells, pre-B cells, and immature B cells. Immature B cells, after generation, leave the bone marrow and migrates to the secondary lymphoid organs for an antigenic encounter.

B cell receptors (BCRs) are nothing but membrane-bound antibodies having a transmembrane and a cytoplasmic segment. Immature B cells contain either IgM or IgD on their surfaces; however, these immunoglobulin (Ig) molecules, having three amino acid-long cytoplasmic domains, are unable to transduce the signal through their cytoplasmic segments. Along with IgM/IgD, another accessory set of immunoglobulins (Ig) molecules, Igα and Igβ, constitutes the BCR complex. Igα and Igβ are required for the initiation of signal transduction through BCRs providing the ITAM motif to different kinases.

Different immunoglobulin gene segments codes for the heavy (H) and light (L) chains of the B cell receptor. H chains are made up of variable (V), diversity (D), and joining (J) gene segments, whereas L chains are consist of V and J segments of immunoglobulin genes. An enormous diversity of BCRs is generated through the recombination of different gene segments by the action of RAG1 and RAG2 enzymes [70]. Pre-BCRs are made up of a μ heavy chain and a surrogate lite chain (SLC). Optimal signaling through pre-BCR signifies successful heavy chain recombination and initiates the light chain gene recombination process followed by the proliferation of pre-B cells and differentiation into immature B cells. Immature B cells then migrate to the secondary lymphoid tissues and further mature in the germinal centers. Activation of immature B cells by subsets of helper T lymphocytes initiates the proliferation and somatic hypermutation in the variable region gene products, giving rise to a large number of B cells having numerous variations in the variable region of BCRs. During the antigenic encounter, high-affinity binding of the antigen with specific BCR-bearing B cells selects that particular clone of B cell and maturation of those particular clones occurs through the process of affinity maturation. Class switching of immunoglobulins takes place after affinity maturation through intrachromosomal deletion rearrangement in the constant region genes generating antibodies with different isotypes giving rise to IgG, IgA, and IgE [71,72].

BCR signaling initiates with specific antigenic binding. The signaling starts with the activation of SRC family kinases (SFKs) following the aggregation of BCRs. Activated SFKs such as Lyn, Fyn, Syk, etc. then phosphorylate the ITAM motifs of the accessory immunoglobulins Igα and Igβ and transduce the signaling through PLCγ2, PI3K, AKT, DAG, etc. pathways generating the transcription factors NFκB, ATF-2, Jun, FoxO, etc. leading to different gene expression, metabolic changes, cell proliferation,

cytoskeletal reorganization, migration, etc. [73]. B cell co-receptor complex includes CD19, CD21 (CR2), CD45, CD38, and CD81 molecules, helping in the amplification of the signals induced by BCR.

1.12. Antigen-presenting Cell (APC) – T cell interaction

Generation of antigen-specific immune responses towards foreign antigens is optimally devised by the mutual communication between APCs and the antigen-specific T cells [74–76]. The interface between APCs and T cells is known as an "immunological synapse". Naïve T cells require several activation signals for optimal activation. Signal 1 involves the recruitment of antigen-specific TCR present on the T cells and its interaction with the antigenic peptide presented through the MHC (MHCI/MHCII) molecules on the surface of APCs. Signal 2 includes several co-stimulatory signals, e.g., CD28-B7.1(CD80)/B7.2(CD86), CD40L(CD154)-CD40, etc., that help in enhancing as well as sustaining the TCR-mediated signal 1. CD4+ helper T cells constitutively express CD28 molecules. During antigen presentation, expression of co-stimulatory molecules such as B7.1, B7.2, etc. on APCs goes up, and interaction between TCR-antigenic peptide-MHC leads to T cell activation followed by increased IL-2, IFNγ production, CD25 expression, T cell proliferation, and survival [77]. TCR-MHC engagement enhances the expression of TNF receptor family proteins such as CD40L on T cells. CD40L interacts with CD40 on APCs, leading to subsequent up-regulation of certain adhesion molecules, MHCII expression, and cytokine production by APCs. Other up-regulated TNF receptor family protein includes OX40 (CD134), 4-1BB (CD137), and CD27 having co-stimulatory functions following T cell activation, providing the waves of signal 2, important for sustaining the activation cascade required for T cell differentiation, proliferation, and memory generation [78,79]. Following initial activation, T cells express CTLA4, an activation-induced negative costimulatory molecule that binds B7.1 and B7.2 with higher

affinity than CD28. Interaction of CTLA4 with B7 molecules induces T cell anergy following decreased T cell responses maintaining the homeostasis of the immune system. Other T cell inhibitory molecules include the PD-1 receptor that interacts with PDL-1 and PDL-2 on APCs, responsible for decreased immune responses, similar to CTLA4 [80,81].

1.13. CMI response following T cell activation

Engagement of antigen-specific TCR with MHC-peptide complex along with the co-stimulatory signals activates T cells resulting in T cell proliferation, differentiation, and memory generation. T cells are restricted towards the origin of the antigens and the type of MHC molecules that present the antigenic peptide to T cells. Exogenous antigens presented by APCs through MHCII molecules are recognized by CD4+ helper T cells (Th cells), whereas endogenous antigens presented by APCs through MHCI molecules are recognized by CD8+ cytotoxic T cells (Tc cells). Following recognition of specific antigens, depending on the cytokine milieu, Th and Tc cells recruit certain responses contingent on differentiation. Th cell activation leads to effector and memory cell generation. Effector Th cells secret various cytokines that help in the activation of Tc cells, B cells, macrophages, and other immune cells, further strengthening the protection against the foreign pathogen. Tc cell activation, under Th cell influence, results in the generation of cytotoxic T lymphocytes (CTLs) that exhibit cell killing/cytotoxic activity. CTL plays an important role in monitoring and eradicating altered self-cells, such as virus-infected cells, cancerous cells, etc., from the body [78,82–85].

1.14. Th1/Th2 polarization and function

Naïve T helper cells, after leaving the thymus, start migrating to the secondary lymphoid tissues as Th0 cells. Th0 cells, following activation through antigenic encounter, differentiate into effector T helper cells having the ability to polarize into Th1 or Th2 cells [86]. IL-2, IFNγ, lymphotoxin-α (LT-α), etc., are the cytokines released by matured Th1

cells, whereas mature Th2 cells produce IL-4, IL-5, IL-9, IL-10, and IL-13 [87,88]. However, a few human Th1 polarized cells have been reported to secrete IL-10 and IL-13, illustrating an overlap in cytokine profiles produced by Th1 and Th2 cells [89,90]. Other subtypes of helper T cells include Th3, T regulatory type 1 (Tr1), etc. Th3 cells secrete TGF-β regulating mucosal immunity, induce B cells to express IgA, etc., whereas, Tr1 cells produce IL-10 and a lesser amount of TGF-β suppressing overall immune responses [91–94]. IFNγ, a signature proinflammatory Th1 cytokine, plays an important role in inducing phagocytosis, the intracellular killing of microbes, oxidative burst and enhances the expression of MHCI/MHCII molecules, increasing antigen presentation to T cells [95–98]. Moreover, IFNγ and LT-α stimulate non-leukocytes such as endothelial cells, keratinocytes, fibroblasts, etc., inducing the expression of TNF and chemokines and facilitating blood vessel dilation, diapedesis of leukocytes, recruiting innate immune cells to the area of infection [99–102]. Th2 cytokines such as IL-4, IL-10, and IL-13, in contrast, induce B cell proliferation and antibody class switching [103,104]. IL-10, having a potent immunosuppressive activity, inhibits proinflammatory responses and reduces the degree of phagocytosis, oxidative burst, and antigen presentation [105–107]. IL-5 induces the production and chemotaxis of eosinophils from the bone marrow[108]. IL-4, IL-5, IL-9, and IL-13 play an important role in airway inflammation in asthma and reactive airway diseases [109–111]. Th1 and Th2 cells are also reported to cross-regulate each other. IFNγ, produced by Th1 cells, suppresses the production of IL-4 inhibiting Th2 polarization [112]. Conversely, IL-10 and IL-4 block the production of IL-12 and IFNγ, inhibiting Th1 polarization [113,114].

CHAPTER # 2

Review of Literature

2. Review of literature

2.1. Immunosuppression and immunosuppressive agents

Immunosuppression could be broadly described as the abated effector immune responses associated with macrophages, dendritic cells, lymphocytes, and other accessory immune cells. It is a state with a reduced ability to recognize or counter foreign antigens resulting from the modulation of signaling molecules involved in cellular pathways important to mount immune responses or by reducing the number of effector immune cells [115].

The causes of immunosuppression can be classified into two broad categories such as intrinsic/non-deliberate and extrinsic/deliberate. Intrinsic/non-deliberate immunosuppression includes persisting chronic diseases like HIV, cancer, aging, asplenia, etc. [116–122]. Extrinsic/deliberate immunosuppression includes therapeutic medications, radiation therapy, etc. [123,124]. Medications are generally used to suppress an aggravated immune response during autoimmunity, chronic inflammation, organ transplant, etc. Agents that induce immunosuppression include Antithymocyte Globulins (ATG) [125,126], Interleukin (IL) - 2 Receptor Antagonists (Basiliximab and Daclizumab) [127,128], Azathioprine (AZA) [129], Glucocorticosteroids [130], Calcineurin Inhibitors (Cyclosporine A (CsA) and Tacrolimus (Tace / FK506)) [131,132], etc. Table 2 contains a detailed list of immunosuppressive agents.

Table 2: List of immunosuppressive agents with brief mechanisms [123]

Name of the Agent/Drug	Mechanism of Action
rATG	Polyclonal antibodies against CD2, CD3, CD4, CD8, CD11a, CD18, CD25, CD44, HLA-DR, HLA I heavy chain
Basiliximab	Chimeric human/murine monoclonal IgG1κ against CD25/Tac subunit

Alemtuzumab	Humanized monoclonal IgG1κ against CD52
Muromonab-CD3	Murine monoclonal antibody against CD3 of T-cell receptor complex
Azathioprine	Converted to 6-mercaptopurine, inhibits purine biosynthesis and CD28 signaling
Glucocorticoids	Inhibits formation of free NF-κB and down-regulates expression of proinflammatory cytokines
Cyclosporine A	Binds cyclophilin and inhibits calcineurin, prevents activation of NFAT and expression of IL-2, stimulates TGF-β expression
Tacrolimus (FK506)	Binds FK-binding protein, inhibits calcineurin, prevents activation of NFAT and expression of IL-2, stimulates TGF-β expression
Mycophenolate mofetil	Inhibits inosine monophosphate dehydrogenase and de novo purine biosynthetic pathway
Mycophenolic acid	Enteric coated, inhibits inosine monophosphate dehydrogenase and de novo purine biosynthetic pathway
Sirolimus	Binds FK-binding protein and inhibits mammalian target of rapamycin (mTOR) pathway by binding mTOR complex 1 leading to blockade of activation of 70-kDa S6 protein kinases, expression of bcl-2 proto-oncogene, Ca^{2+}-independent CD28-induced costimulatory pathway
Belatacept	Fusion protein of modified CTLA-4-human Ig, blocks B7/CD28 costimulatory proteins
Leflunomide	Inhibits dihydroorotate dehydrogenase and pyrimidine biosynthesis
Eculizumab	Monoclonal antibody against complement C5
Rituximab	Monoclonal antibody against CD20 glycoprotein on B cells
IVIG	Suppress autoantibodies, cytokines, neutralize complements, up-regulate FcγRIIB, immunomodulation
17-AAG	Binds and inhibits Hsp90, suppresses inflammatory responses
Telmisartan (TM)	Angiotensin receptor blocker, used as a medicine to treat hypertension, inhibits inflammatory responses

Treatment of undesirable immune responses generated by allergic reactions, autoimmunity, and/or transplantation involves the use of anti-inflammatory, immunosuppressive, and cytotoxic drugs. Immunosuppressive drugs are currently used to

treat transplant patients to suppress the immune responses generated against the transplanted graft [133,134]. Experimental animal models have been studied extensively, targeting immunosuppression by inhibiting the responses against autoantigens, targeting cytokine microenvironment, modulating immune responses into a nonpathogenic pathway, etc. However, more number of human studies are prerequisite to further strengthening of the outcomes. Studies with only animals might pose a difficulty in understanding in a more appropriate clinical context.

2.2. Immunosuppressive agents modulating antigen-presenting cell (APC) – T cell interaction and T cell activation

Therapeutic agents directed against T cells mostly function by modulating either Signal 1 (the interaction of TCR on T cell with the MHC molecules present on APC containing the antigenic peptide; in case of transplant, the graft tissue itself acts as an antigen) or Signal 2 (costimulatory signals between T cell and APC) of T cell activation [124] (**Figure 6**). Molecules that inhibit further T cell proliferation and later signaling events are referred to as signal 3 inhibitors. Anti-TCR agent includes the murine anti-CD3 monoclonal antibody Muromonab-CD3 (OKT3), the first FDA-approved drug used to prevent graft rejection in kidney, heart, and liver transplants and functions through inhibiting CD3 subunit of TCR complex eliminating functional T cell populations [135]. Calcineurin-dependent signaling cascades are initiated downstream of TCR activation, followed by TCR-MHC interaction is required for T cell activation and effector function. Commonly used calcineurin inhibitors (Cyclosporin A and Tacrolimus (FK506) function by inhibiting calcineurin from dephosphorylating NFAT preventing downstream gene transcription [136,137]. Agents targeting costimulatory molecules include Abatacept and Belatacept. CD80/CD86 – CD28 interactions are required for optimal T cell activation. After getting fully activated, T cells started expressing CTLA4, a negative costimulatory molecule responsible for

downregulating T cell responses. Abatacept is a fusion of human Ig heavy chain and CTLA4 (CTLA4-Ig), mimicking the CTLA4 expression on T cells, and is used to treat autoimmune disorders [138]. Belatacept is a similar fusion protein to Abatacept, having a higher affinity towards CD80/CD86 molecules [139]. CD40-CD40L costimulation is important for T cell activation leading to the upregulation of CD80/CD86 molecules. Astellas, a fully humanized anti-CD40 antibody, targets CD40 preventing its interaction with CD40L and inhibiting optimal T cell activation [140].
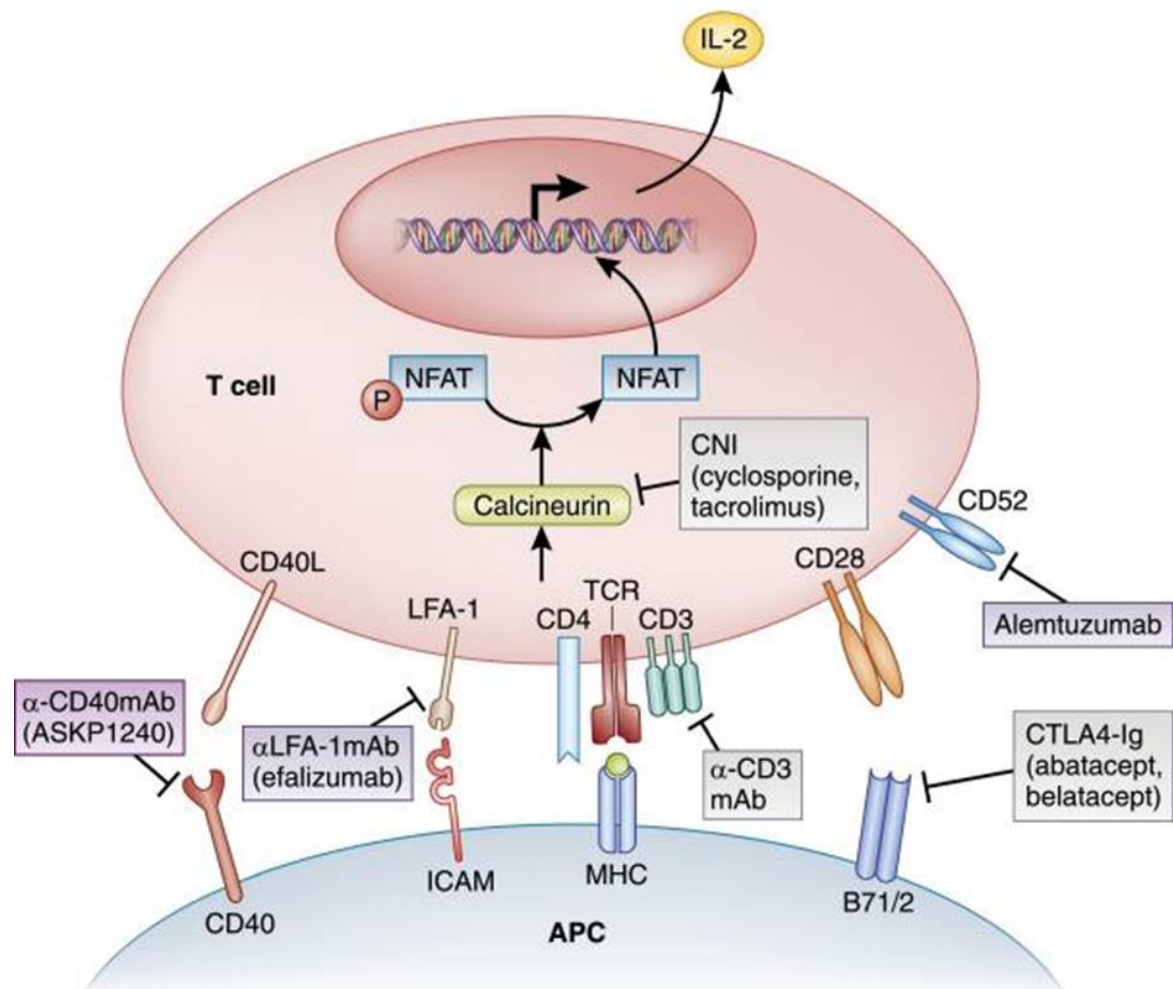
Figure 6: Immunosuppressive agents targeting T cell – APC interaction and T cell Activation [124]

2.3. Tacrolimus (FK506)

Tacrolimus, formerly known as FK506, is a macrolide antibiotic produced by *Streptomyces tsukubaensis* having an immunosuppressive activity [141]. FK506 is a primary immunosuppressive agent used in solid organ transplants [142,143]. It has been reported to function by downregulating IL-2 gene expression in CD4+ T cells, inhibiting proinflammatory responses [144,145]. FK506 binds and inhibits signaling molecules required for T cell activation. It binds to immunophilins such as FK506-binding proteins (FKBP) (FKBP12, FKBP13, FKBP25, and FKBP59) forming the FK506-FKBP complex [146,147]. Calcineurin, a calcium-dependent phosphatase, is a key player in downstream signal transduction and T cell activation. During T cell activation, calcineurin dephosphorylates NFAT and facilitates its nuclear translocation and IL-2 gene transcription. FK506-FKBP12 complex principally binds calcineurin preventing it from dephosphorylating NFAT, which results in reduced IL-2 expression and downregulation of T cell activation [148] (**Figure 7**). Further, the FK506-FKBP complex binds to intracellular ryanodine and IP3 receptor Ca^{2+} release channels present on the sarcoplasmic reticulum membrane regulating intracellular Ca^{2+} release [149,150] (**Figure 8**).
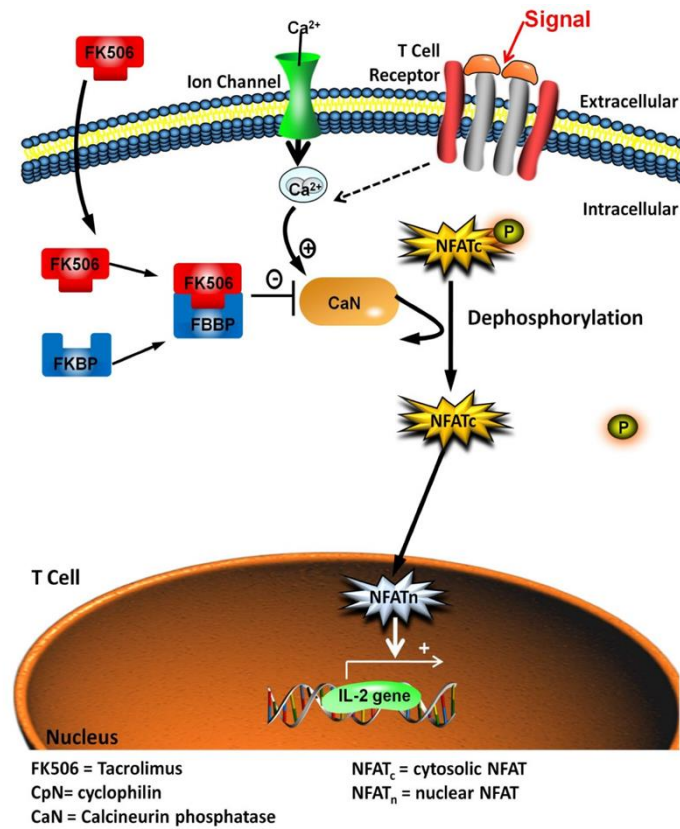
Figure 7: Mode of Action of Tacrolimus (FK506) facilitating T cell suppression [142].
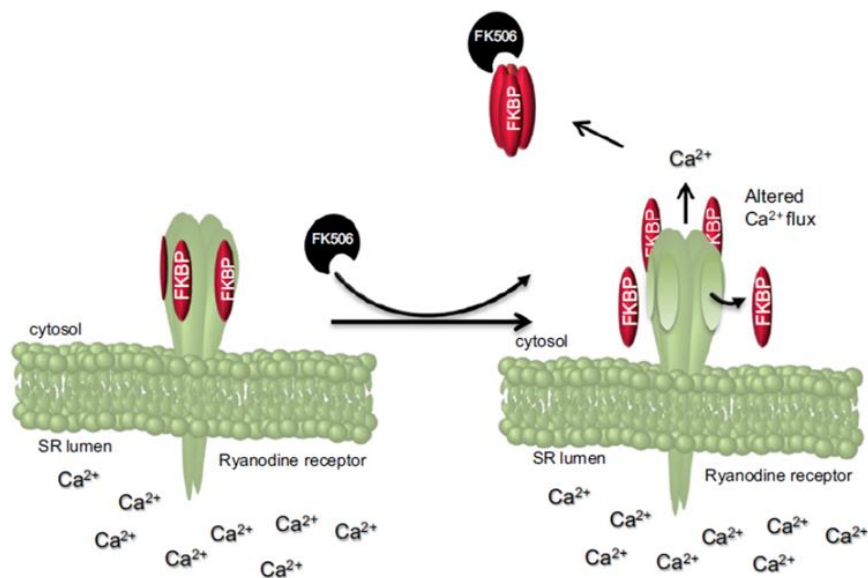
Figure 8: FK506-mediated Ca+2 release from the sarcoplasmic reticulum increasing intracellular calcium level [150].

2.4. Cancer and immunosuppression

Cancer could be defined as the uncontrolled growth and/or division of cells forming malignant tumors and the spreading of malignant cells to other parts of the body through metastasis. The prime cause of cancer is genetic mutations, mostly in the genes controlling cell growth and proliferation [151]. The tumor microenvironment (TME) plays an important role in tumor progression and inhibits anti-tumor immune responses [152]. The growth and metastasis of tumors evolve by employing an immunosuppressive network facilitated by soluble factors released by tumor cells encompassing the primary tumor site to secondary lymphoid organs and peripheral vessels [153,154] (**Figure 9**). Tumor-released VEGF attracts immature myeloid cells (iMCs) from the bone marrow to peripheral vessels and recruits immature myeloid cells (iMCs) to the tumor sites [155]. iMCs, such as immature dendritic cells (iDCs) and macrophages, are functionally and biochemically modulated in the TME, becoming tumor-induced DCs (TiDCs) and tumor-associated macrophages (TAMs) and gaining immunosuppressive activity. Recruitment of these immunosuppressive cells in the spleen, lymph nodes, and peripheral vessels employs further immunosuppression, recruits
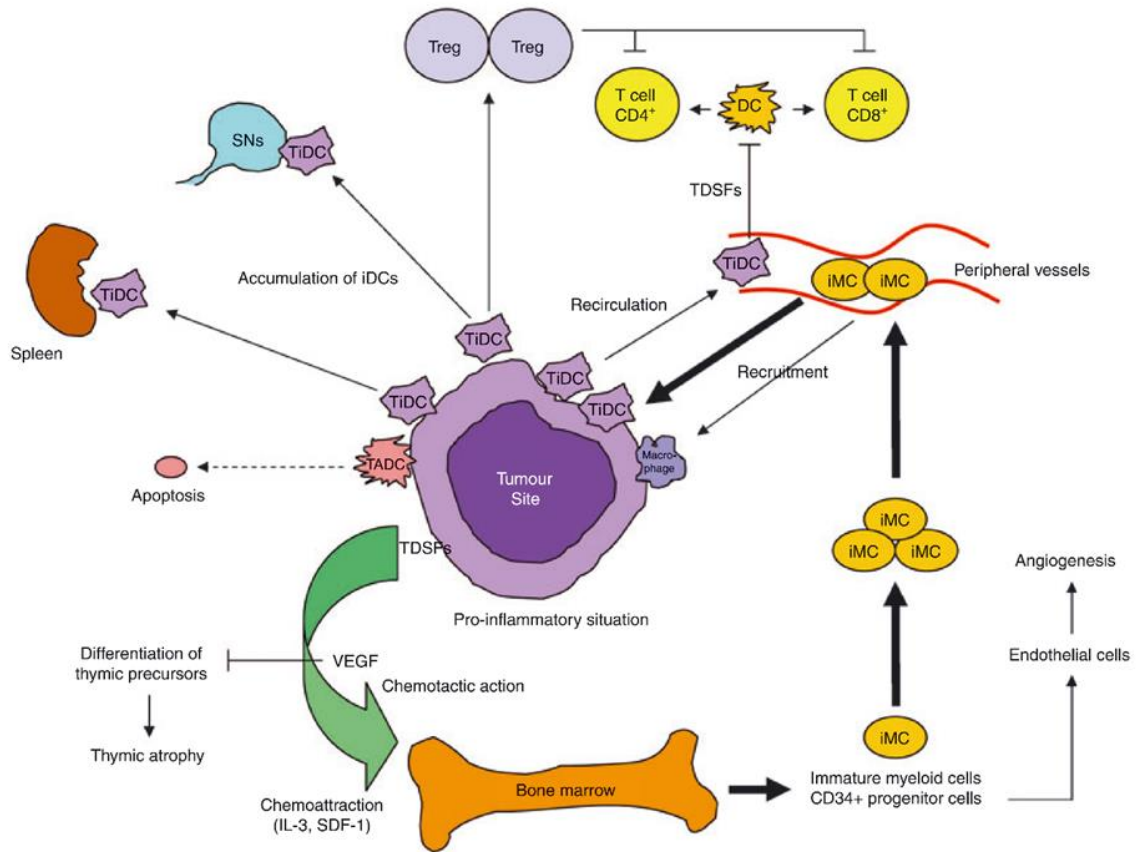
Figure 9: Cancer Immunosuppressive network extending from the tumor site to secondary lymphoid organs and peripheral vessels [156].

regulatory T cells (Tregs), and facilitates immune evasion of cancer cells [155–157].

2.5. B16F10 melanoma model

Malignancy of the melanocytes (melanin-producing skin cells) is known as melanoma. It is one type of skin cancer characterized by its highly metastatic nature and spreads abruptly to other parts of the body [158]. B16F10 is a murine (C57BL/6) transplantable melanoma cell line used as a model to study human melanoma, providing useful information towards solid tumor formation, tumor progression, and metastasis [159,160]. The culture supernatant derived from B16F10 melanoma cells (B16F10-CS) has been reported to have immunosuppressive activity suppressing effector immune responses [161–164]. Studies with murine mononuclear cells have revealed the immunomodulatory

effects of B16F10-CS associated with T cells, B cells, macrophages, and neutrophils [161–165]. However, the information towards the components of B16F10-CS is scanty and needs to be explored further.

2.6. 17-AAG

17-AAG, a derivative of geldanamycin, is one of the selective inhibitors of Hsp90 and is reported to be actively blocking various innate immune responses in rats and various *in vitro* models. 17-AAG administration has been shown to suppress TLR4 mediated pro-inflammatory cytokine production via blockade of the signaling cascade in rat LPS-induced auto-immune uveitis [166]. Dello Russo *et al.* reported that 17-AAG inhibits TLR4 stimulation *in vitro* and alleviates disease incidence and severity in myelin oligodendrocyte glycoprotein–peptide-induced experimental auto-immune encephalitis [167]. These reports suggest the immense therapeutic potential of Hsp90 inhibitors in auto-immune and pro-inflammatory diseases.

2.7. Hypertension, angiotensin receptor blockers (ARBs), and Telmisartan (TM)

Hypertension is a cardiovascular disease that has been attributed as a risk factor for stroke, peripheral artery disease, heart failure, myocardial infarction, atrial fibrillation, coronary heart disease, and chronic kidney disease [168–170]. Dysregulation of angiotensin (Ang) II, the key player of the renin-angiotensin system (RAS) that regulates and maintains blood pressure and fluid volume [171], is the prime cause of hypertension. Cellular receptors for Ang II are Ang II receptor type 1 (AT1R) and Ang II receptor type 2 (AT2R). Interaction of Ang II with AT1R causes vasoconstriction, sodium retention, aldosterone secretion, and cell proliferation, whereas Ang II and AT2R interaction causes vasodilation and growth inhibition, balancing AT1R-mediated responses [172].

Several AT1R blockers (ARBs) have been reported to be beneficial for treating hypertension and reducing hypertension-induced disease manifestations including

myocardial infarction, heart failure, and atrial fibrillation [173–175]. TM is one of the ARBs that is currently in use to treat patients having hypertension [176–178].

Recently, it has been shown that hypertensive responses involve the activation of various immune cells releasing several inflammatory mediators causing systemic inflammation [179,180]. The involvement of T cells in the development of hypertension has been attributed elsewhere [179,181,182]. Inhibition of T cells is reported to reduce renal Ang II levels and diminished disease manifestations in Dahl salt-sensitive rats [182]. Moreover, reduced T cell activity has been shown to prevent disease occurrence [183].

Telmisartan (TM) is an ARB that is currently used to treat patients having hypertension [176–178]. Reports indicate that TM reduces T cell responses by inhibiting the NFAT signaling and diminishing TNF-α-induced NF-κB activation [184,185]. Furthermore, the repurposing of TM has been documented to regulate various inflammatory immune diseases by its anti-inflammatory or immunosuppressive effects [186–188].

2.8. Transient receptor potential (TRP) channels

TRP channels are non-selective cation permeable polymodal ion channels having roles in sensory processes, cellular excitation, growth, migration, proliferation, transcription, differentiation, stress, and cell death [189–193]. TRP channels are functionally associated with different physiological processes. Mutations causing truncation in the structure or hindering the function of TRP channels are associated with various pathophysiological conditions [194–197].

TRP channels are divided into two groups depending on their sequence similarity and topological differences having seven subfamilies comprising the groups. The seven subfamilies include TRPC (canonical), TRPV (vanilloid), TRPA (ankyrin), TRPML (mucolipin), TRPM (melastatin), TRPP (polycystin), TRPN (NOMPC) [197,198]. The first group includes TRPC, TRPA, TRPV, TRPM, and TRPN whereas group 2 includes TRPP

and TRPML [198–200] (**Figure 10**). TRPC has seven members, TRPC1-TRPC7, which gets activated through the action of protein kinase C (PKC) facilitating PKC-mediated calcium (Ca^{2+}) influx [198,201,202]. TRPV has 6 members, TRPV1-TRPV6, and are reported to be activated in the presence of vanilloid compounds such as capsaicin, endocannabinoid, camphor, piperin, etc. [203–206]. TRPM consists of 8 members, TRPM1-TRPM8, which are cold-sensitive ion channels [207–210]. TRPA1 is the single member of the TRPA subfamily. It is a Ca^{2+} permeable channel activated in the presence of cold stimuli, mustard oil, cannabinoids, and PLC [209–211]. TRPN has only one member, TRPN1, having roles in mechanical gating [200,212]. TRPP has 5 members, TRPP1-TRPP5, which are reported to be modulated in the presence of PIP2 and EGF [213]. TRPML has three members, TRPML1-TRPML3, and is sensitive to pH [214–216]. Group 1 TRP channels share a similar topology of the TRP domain comprising the pore loop, ankyrin repeats, and TRP box 1 and 2, whereas group 2 channels are distantly related to group 1 members [217].
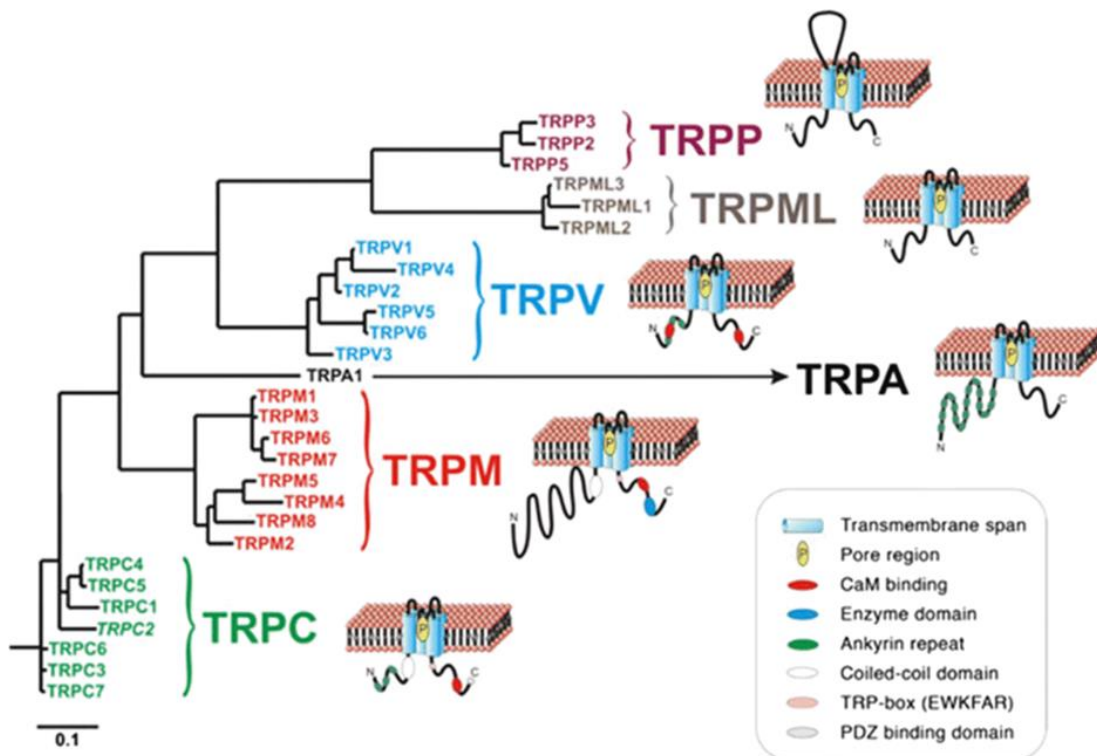
Figure 10: Phylogenetic distribution of mammalian TRP channels and their major structural features [218].

TRP channel consists of six transmembrane segments with intracellular N and C termini [219–221] having diverse activation mechanisms and cation selectivity [220] (**Figure 11**). The cytoplasmic N and C terminus comprise two structural and functional units, respectively. The pore that facilitates the passage of cations is present in between transmembrane segments five and six. Within the six transmembrane segments, segments one to four form the anchorage and senses voltage differences, while segments five and six form the ion pore [222]. Group 1 channels contain conserved N-terminal ankyrin repeats except for TRPM. Three TRPM members have N-terminal enzyme repeats known as chanzymes [220]. TRPP contains a large loop between the first two transmembrane segments. The N and C terminus domains of the TRP channels mediate the signaling and sensory functions and vary significantly between subfamilies depending on their specific roles [220,223].
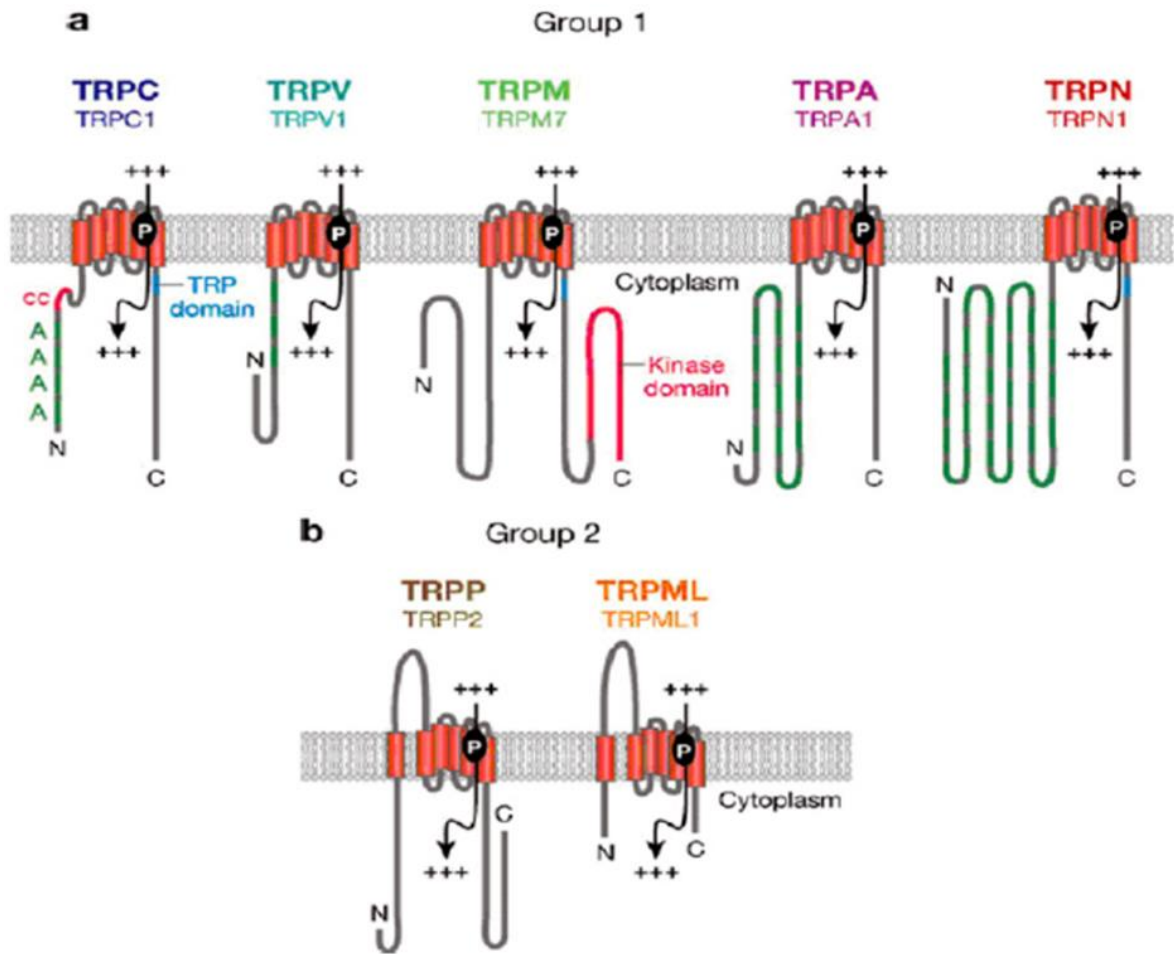
Figure 11: Schematic structure of different TRP subfamilies. (a) group 1 and (b) group 2 TRP subfamily [224].

2.9. TRP channels in macrophages and T cells

TRP channels play an important role in regulating immune function associated with monocytes, macrophages, dendritic cells, and T cells [225–228]. Macrophages have been reported to express several functional TRP channels, such as TRPV1, V2, A1, C1, C6, M2, M4, and M7, having roles in activation and effector function [229–232]. TRPC3 helps in macrophage development, polarization, and apoptosis [233,234]; TRPV1 has roles in macrophage activation and effector function [235,236]; TRPV2 has roles in cytokine

production, phagocytosis [237]; TRPM2 has roles in ROS production, migration, and Ca^{2+} entry [238,239]; TRPA1 has a role in the inhibition of ROS production [240], etc.

Ca^{2+} ions play an important role in T cells development, maturation, activation, and effector function [241,242]. Functional TRP channels in T lymphocytes are one of the important mediators facilitating Ca^{2+} flux regulating T cell function [241–243]. T lymphocytes express TRPC1, TRPC3, TRPC5, TRPC6, TRPV1, TRPV4, TRPV5, TRPV6, TRPM2, TRPM4, TRPM7, and TRPA1 [232,244]. TRPC1 has roles in T cell activation and Ca^{2+} entry [245]; TRPC3 has roles in TCR signaling and proliferation [246]; TRPM1 modulates Ca^{2+} entry [228]; TRPM2 has roles in proliferation, cytokine release, and development [246–248]; TRPV1 has roles in T cell activation, TCR signaling [249,250]; TRPML1 has a role in immunosuppression [251], etc.

Table 3 summarizes the TRP channels present in T cells and macrophages with brief functions.

Table 3: **TRP channels and their role in T cells and macrophages**

TRP Channel	Role in T Lymphocytes	Role in Macrophages
TRPC1	T cell activation, Ca^{2+} entry	Development, Polarization, Apoptosis
TRPC3	T cell signaling, proliferation	Regulation of apoptosis, cell survival
TRPC5	Autoimmunesuppression	M1 polarization, pain regulation
TRPV1	T cell activation, TCR signaling, effector function	Phagocytosis, activation, cytokine production
TRPV2	Ca^{2+} signal, activation, proliferation, effector function	Phagocytosis, migration, cytokine response
TRPV5	Ca^{2+} entry	Regulates osteoclastogenesis

TRPV6	T cell proliferation, Ca^{2+} entry	Osteoclast differentiation
TRPM1	Ca^{2+} entry	Cation entry
TRPM2	Development, effector function	Ca^{2+} entry, ROS production, cytokine release
TRPM4	Inhibits IL-2 production	Phagocytosis, cytokine release
TRPM7	Apoptosis	Proliferation, polarization
TRPM8	Immunosuppression	Cytokine production, differentiation
TRPA1	Activation, pro-inflammatory responses, cytokine release	Nitric oxide inhibition
TRPML1	Immunosuppression	Cytokine production, phagocytosis

2.10. Role of TRPV1 in macrophages and T cells

TRPV1 is an important regulator of macrophages having roles in survival and effector responses [236,252]. Activation of TRPV1 in the presence of capsaicin polarizes macrophages from M1 to M2 [253]. TRPV1 has been reported to regulate phagocytosis. TRPV1 knockout or inhibition through antagonism reduces the ability to clear pathogenic load compared to WT or control cells [252,254]. Moreover, orally administered capsaicin avert autoimmunity in Lewis rats [255]. Further, TRPV1 has been found to be involved in cross-cellular communications [256,257].

TRPV1 plays an important role in T cell survival, activation, proliferation, and effector function [232,244]. TRPV1 knockout impairs proteasome function, increases apoptosis of thymocytes, and reduction in CD4+ and CD8+ cell count compared to WT mice [258]. TRPV1 is an important mediator of Ca^{2+} influx required for T cell activation. Inhibition of TRPV1 leads to reduced T cell activation and effector function [250,259].

TRPV1 knockout reduces pain associated with Rheumatoid Arthritis [260]. CD4+ cells from mice and human PBMCs express functional TRPV1 constitutively and recently have been reported to mediate a separate passage for Ca^{2+} entry, which gets significantly reduced in TRPV1 knockout cells [249,258]. TRPV1 is further reported to be associated with the TCR cluster and regulating TCR signaling and p38/JNK activation [258].

2.11. Role of TRPA1 in macrophages and T cells

TRPA1 mediates numerous functions in macrophages, including activation, migration, effector function, and regulation of macrophage plasticity [261–263]. TRPA1 has been reported to be involved in macrophage infiltration in a mouse wound-healing model [264]. PMA-activated macrophages display reduced TRPA1 expression. TRPA1 knockout is associated with the overexpression of proinflammatory mediators and the infiltration of M1 macrophages in the kidneys [265,266]. Knockout and antagonistic study of TRPA1 has been shown to reduce atopic dermatitis (AD) symptoms in a mouse model [267].

TRPA1 is endogenously expressed in T lymphocytes and associated with T cell activation, proinflammatory responses, and effector function [232,235,244,268]. TRPA1 knockout increases Th1-biased and IFNγ-mediated proinflammatory responses in a colitis mouse model [259,269,270]. Further, reduced Ca^{2+} influx has been shown in TRPA1 knockout T cells compared to WT cells [259].

2.12. Role of TRP channels in immunosuppression

TRP channels have been well attributed to have a functional role associated with immune activation, inflammation, and effector responses [240,249,250,262,269,271–273]. However, the information towards the functional association of TRP channels associated with immunosuppression remains scanty. Immunosuppressive agents used to prevent transplant rejection, e.g., FK506, cyclosporin A, rapamycin, etc., has been reported to induce a rise in intracellular Ca^{2+} levels and modulate TRP channels [251,274–278]. Rapamycin has been shown

to directly activate lysosomal TRPML1 and modulates Ca^{2+} levels. Moreover, cells deficient in TRPML1 exhibit no effect of rapamycin *in vitro* [251]. Similarly, TRPM8 deficiency or antagonistic inhibition nullifies the effect of FK506 [278], suggesting TRP channels as molecular targets for immunosuppressive agents.

2.13. Heat Shock Protein 90 (Hsp90) and its immunomodulatory role

Hsp90 is a 90 kDa evolutionary conserved cytoplasmic molecular chaperon that facilitates the maturation and stabilization of "client" proteins involved in growth, differentiation, and apoptosis, thus maintaining cellular proteostasis [279–281]. Hsp90 is an important player in regulating various pathophysiological conditions, such as viral infection and autoimmune disorders [282–285]. Several "client" proteins are associated with tumor progression, metastasis, and immunosuppression, considering Hsp90 as a potential target for cancer therapy [286–289]. Hsp90-mediated regulation of immune responses through "client" protein modulation has been well documented [290–292]. Pharmacological inhibition of Hsp90 has been found to be effective in treating various inflammatory processes associated with innate and adaptive immune responses. [293–298]. Hsp90 antagonism with 17-AAG, a geldanamycin derivative, has been found to impede proinflammatory responses associated with autoimmune uveitis in rats [166]. Further, Hsp90 inhibition has been reported to attenuate disease severity in EAE (experimental autoimmune encephalomyelitis) model [299].

CHAPTER # 3

Hypothesis

&

Objectives

3. Hypothesis and Objectives

3.1. Hypothesis

There might be differential involvements of TRPV1 and TRPA1 during experimental immunosuppression of cell-mediated immunity (CMI) associated with the possible altered phenotypes and functions of T cells and macrophages.

3.2. Objectives

3.2.1. To investigate the functional expression of TRPV1 during experimental immunosuppression of T cells.

3.2.2. To study the role of TRPA1 in experimental immunoregulation of macrophages.

3.2.3. To compare the possible differential role of TRPV1 and TRPA1 during experimental immunosuppression of T cell responses.

CHAPTER # 4

Materials

&

Methods

4. Materials and Methods

4.1. Materials

4.1.1. Cell lines

B16F10 (ATCC® CRL-6475™), a mouse melanoma cell line was cultured in DMEM medium (Gibco™, Thermo Fisher Scientific, MA, USA) supplemented with 10% heat-inactivated fetal bovine serum (FBS) (PAN Biotech, Aiden Bach, Germany), 2 mM L-glutamine, 100 U/mL Penicillin and 0.1 mg/mL Streptomycin in a CO_2 incubator containing 5% CO_2 at 37°C. RAW 264.7 (ATCC® TIB-71™), a mouse macrophage cell line was cultured in HiGlutaXL™ RPMI-1640 medium (Himedia, Mumbai, India) supplemented with 10% heat-inactivated FBS (PAN Biotech, Aiden Bach, Germany), 2 mM L-glutamine and 100 U/mL Penicillin, and 0.1 mg/mL Streptomycin at 37°C inside a CO_2 incubator with 5% CO_2. THP-1 (ATCC® TIB-202™), an undifferentiated human leukemia monocytic cell line was cultured in RPMI-1640 (PAN Biotech, Aiden Bach, Germany) supplemented with 10% heat-inactivated FBS, 100 U/mL Penicillin, and 0.1 mg/mL Streptomycin at 37°C inside a CO_2 incubator with 5% CO_2.

4.1.2. Mice

6 to 8-week-old C57BL/6 mice were used for experimentation. All mice were supplied from the in-house animal facility of NISER. Protocols used for experiments were approved by the Institutional Animal Ethics Committee (IAEC), NISER following Committee for the Purpose of Control and Supervision of Experiments on Animals (CPCSEA) guidelines.

4.1.3. Antibodies

Table 4 contains the details of the antibody used with catalog numbers and the company name.

Table 4: Details of Antibodies used

Sl. No.	Antibody	Catalog No. (Clone)	Company
1	Anti-mouse CD90.2 APC	20-0903-U100 (30-H12)	Tonbo Biosciences, CA, USA
2	Anti-mouse CD90.2 PerCP-Cy5.5	65-0903-U100 (30-H12)	Tonbo Biosciences, CA, USA
3	Anti-mouse CD25 PE	50-0251-U500 (PC61.5)	eBioscience, CA, USA
4	Anti-mouse CD69 FITC	11-0691-85 (H1.2F3)	eBioscience, CA, USA
5	In vivo Ready™ anti-mouse CD3 (functional grade)	40-0032-U500 (17A2)	Tonbo Biosciences, CA, USA
6	In vivo Ready™ anti-mouse CD28 (functional grade)	40-0281-U500 (37.51)	Tonbo Biosciences, CA, USA
7	Anti-TRPV1 polyclonal antibody (1:200)	ACC-030 0.2 ml (NA)	Alomone Lab, Jerusalem, Israel
8	Anti-TRPA1 polyclonal antibody (1:200)	ACC-037 0.2 ml (NA)	Alomone Lab, Jerusalem, Israel
9	Chicken anti-mouse AF488	A21200 (NA)	Invitrogen, CA, USA
10	Goat anti-rabbit AF647	A21244 (NA)	Invitrogen, CA, USA
11	HRP-goat anti-mouse IgG (1:5000)	554002 (NA)	BD Biosciences, CA, USA
12	HRP-goat anti-rabbit IgG	554021	BD Biosciences,

		(1:5000)	(NA)	CA, USA
13	Isotype control FITC	35-4714-U100 (MOPC-21)	Tonbo Biosciences, CA, USA
14	Isotype control PE	559841 (A23-1)	BD Biosciences, CA, USA
15	Isotype control APC	553932 (R35-95)	BD Biosciences, CA, USA
16	CD80 (B7-1) mAb APC	17-0801-82 (16-10A1)	eBioscience, CA, USA
17	CD86 (B7-2) mAb APC	17-086282 (GL1)	eBioscience, CA, USA
18	PE Rat ant-mouse I-Ad/I-Ed	558593 (2G9)	BD Biosciences, CA, USA
19	Mouse IgG1 Isotype control	10-101 (MOPC31C)	Abgenex India Pvt. Ltd., BBS, India
20	Anti-mouse GAPDH	2118 (14C10)	Cell Signaling Technology, MA, USA
21	Purified anti-mouse Hsp90	610418 (68/Hsp90)	BD Biosciences, CA, USA
22	Cleaved caspase-3 (Asp175) Rabbit monoclonal antibody (mAb)	9664 (5A1E)	Cell Signaling Technology, MA, USA
23	p38 MAPK antibody	9212	Cell Signaling Technology, MA,

			USA
24	Phospho-p38 MAPK (Thr180/Tyr182) Rabbit mAb	4511 (D3F9)	Cell Signaling Technology, MA, USA
25	SAPK/JNK Rabbit mAb	9258 (56G8)	Cell Signaling Technology, MA, USA
26	Phospho-SAPK/JNK (Thr183/Tyr185) Rabbit mAb	4668 (81E11)	Cell Signaling Technology, MA, USA
27	p44/42 MAPK (Erk1/2)	4695 (137F5)	Cell Signaling Technology, MA, USA
28	Phospho-p44/42 MAPK (Erk1/2) (Thr202/Tyr204) Rabbit mAb	4370 (D13.14.4E)	Cell Signaling Technology, MA, USA

4.1.4. Reagents and Modulators

Table 5 contains the details of the reagents and modulators used with catalog numbers and the company name.

Table 5: Details of Reagents and Modulators used

Sl. No.	Reagent Name	Catalog No. (Clone)	Company
1	FK506	F4679-5MG	Sigma Aldrich,

			MO, USA
2	Fluo-4 AM	F14217	Invitrogen, CA, USA
3	7-AAD	559925	BD Biosciences, CA, USA
4	APC Annexin V	550474	BD Biosciences, CA, USA
5	10x Annexin V binding buffer	556454	BD Biosciences, CA, USA
6	17-Allylaminogeldanamycin (17-AAG)	100068	Merck Millipore, MA, USA
7	Saponin	47036-50GM	Sigma Aldrich, MO, USA
8	Bovine serum albumin fraction-V	GRM105-100G	Himedia Laboratories Pvt. Ltd., Mumbai, India
9	Triton X-100	MB031-500ML	Sigma Aldrich, MO, USA
10	Sodium deoxycholate	D6750-25G	Sigma Aldrich, MO, USA
11	Sodium dodecyl sulfate (SDS)	L6026	Sigma Aldrich, MO, USA
12	2-mercaptoehtanol (2-ME)	63689	Sigma Aldrich, MO, USA
13	PhosStop^{TM} (phosphatase	04906837001	Sigma Aldrich,

	inhibitors cocktail)		MO, USA
14	Complete EDTA-free Protease inhibitor	05892970001	Sigma Aldrich, MO, USA
15	Bromophenol blue	114391	Sigma Aldrich, MO, USA
16	Crystal violet	C6158	Sigma Aldrich, MO, USA
17	Bis-Acrylamide	MB005-250G	Himedia Laboratories Pvt. Ltd., Mumbai, India
18	Glycine	MB013-1KG	Himedia Laboratories Pvt. Ltd., Mumbai, India
19	Sodium chloride	GRM031-1KG	Himedia Laboratories Pvt. Ltd., Mumbai, India
20	Tris base	TC072-1KG	Himedia Laboratories Pvt. Ltd., Mumbai, India
21	Sodium azide	GRM123-100G	Himedia Laboratories Pvt. Ltd., Mumbai, India
22	EDTA	R066-500ML	Himedia Laboratories Pvt. Ltd., Mumbai, India

23	Glycerol	MB060-500ML	Himedia Laboratories Pvt. Ltd., Mumbai, India
24	Sulphuric acid (H_2SO_4)	AS016-500ML	Himedia Laboratories Pvt. Ltd., Mumbai, India
25	Tween-20	GRM156-500G	Himedia Laboratories Pvt. Ltd., Mumbai, India
26	Ammonium persulfate (APS)	161-0700	Bio-Rad, CA, USA
27	HPLC grade Methanol	AS061-2.5L	Himedia Laboratories Pvt. Ltd., Mumbai, India
28	Paraformaldehyde (PFA)	GRM-3660-500GM	Himedia Laboratories Pvt. Ltd., Mumbai, India
29	Acrylamide	MB068-1KG	Himedia Laboratories Pvt. Ltd., Mumbai, India
30	Antibiotic solution 100x liquid (10000 U Penicillin + 10 mg Streptomycin)	A001A-5x100ML	Himedia Laboratories Pvt. Ltd., Mumbai, India
31	10X Phosphate Buffered Saline	TL1032-500ML	Himedia Laboratories Pvt. Ltd., Mumbai, India

32	HiGlutaXL™ RPMI-1640	AL060G	Himedia Laboratories Pvt. Ltd., Mumbai, India
33	TEMED	MB026-100ML	Himedia Laboratories Pvt. Ltd., Mumbai, India
34	Fetal Bovine Serum (FBS), Australian origin	P30-1302	PAN Biotech, Aiden bach, Germany
35	10x RBC lysis buffer	R075-100ML	Himedia Laboratories Pvt. Ltd., Mumbai, India
36	20X TMB/H2O2	62160118010A	Bangalore Genei, Bangalore, India
37	Trypan blue	TC193	Himedia Laboratories Pvt. Ltd., Mumbai, India
38	Concanavalin A	C0412-5MG	Sigma Aldrich, MO, USA
39	5'-IRTX	I9281-1MG	Sigma Aldrich, MO, USA
40	DMEM	11995081	Gibco™, Thermo Fisher Scientific, MA, USA
41	HC-030031	H4415-10MG	Sigma Aldrich,

Sl. No.			MO, USA
42	AITC	36682-1G	Sigma Aldrich, MO, USA
43	DMSO	TC185-250ML	Himedia Laboratories Pvt. Ltd., Mumbai, India
44	Carboxyfluorescein diacetate succinimidyl ester (CFSE)	C34554	Invitrogen, CA, USA

4.1.5. Buffers

Table 6 contains the details of buffers and their compositions.

Table 6: Details of buffers and their compositions

Sl. No.	Buffer Name	Composition
1	Flow cytometry (FC) staining buffer	1% BSA, 0.01%NaN$_3$, 1x PBS
2	Permeabilization buffer for intracellular staining (ICS)	0.5% BSA (w/v), 0.1% saponin (w/v), 0.01% NaN3 (w/v), 1x PBS, (pH 7.2)
3	Blocking buffer for intracellular staining (ICS)	1% BSA (w/v), 0.1% saponin (w/v), 0.01% NaN3 (w/v), 1x PBS, (pH 7.2)
4	4% Paraformaldehyde (PFA)	1x PBS (pH 7.4-7.6), 4% paraformaldehyde (w/v)
5	Radio Immunoprecipitation Assay (RIPA) buffer	150 mM sodium chloride, 0.1% SDS (sodium dodecyl sulfate) (w/v), 1.0% NP-40 (v/v), 0.5% sodium deoxycholate (w/v), 50 mM Tris, adjust to pH 8.0

6	2x Laemmli buffer	4% SDS (w/v), 10% 2-mercaptoethanol (v/v), 20% glycerol (v/v), 0.125 M Tris HCl, 0.004% bromophenol blue (w/v), adjust to pH 6.8
7	1x SDS-PAGE running buffer	25 mM Tris base, 190 mM glycine, 0.1% SDS (w/v)
8	1x Transfer buffer	25 mM Tris base, 190 mM glycine, 20% HPLC grade methanol (v/v)
9	Blocking reagent Western blotting	3% BSA fraction-V in TBST
10	Tris-buffered saline (TBS)	0.0153 M Trizma HCl, 0.147 M NaCl in ultrapure water (MilliQ), pH adjusted to 7.6 by HCl
11	Tris-buffered saline Tween-20 (TBST)	0.05% (v/v) Tween-20 in 1x TBS

4.1.6. Experimental kits

Table 7 contains the details of the kits used.

Table 7: Details of the experimental kits

Sl. No.	Name of the Kit	Catalog No.	Company
1	Dynabeads™ Untouched™ Mouse T Cells Kit	11413D	Invitrogen, CA, USA
2	BD OptEIA™ Mouse IL-2 ELISA Set	555148	BD Biosciences, CA, USA

3	BD OptEIA™ Mouse IFN-γ ELISA Set	555138	BD Biosciences, CA, USA
4	BD OptEIA™ Mouse TNF ELISA Set II	558534	BD Biosciences, CA, USA
5	BD OptEIA™ Mouse IL-6 ELISA Set	555240	BD Biosciences, CA, USA
6	BD OptEIA™ Mouse IL-10 ELISA Set	555252	BD Biosciences, CA, USA

4.2. Methods

4.2.1. Mouse splenocytes isolation

Splenocytes were isolated as described in previous reports [250,269,300]. Briefly, spleens were aseptically harvested from C57BL/6 mice and kept in a 70 μM cell strainer containing complete RPMI-1640 medium. Then, using a syringe plunger, spleens were crushed and splenocytes were harvested in a 50 mL tube. Cells were then centrifuged at 350g for 5 min at 4°C. The supernatant was then discarded, and the pellet was broken by gently tapping. 1X RBC lysis buffer was added to the splenocytes and incubated for 1 min to lyse the RBCs. After incubation, RBC lysis buffer was diluted with an equal volume of 1X PBS and centrifuged at 350g for 5 min at 4°C. The supernatant was discarded, and the pellet was broken by gently tapping. Cells were then resuspended in complete RPMI-1640 medium and RBC debris was removed by slowly passing the cell suspension through a serological pipette. Splenocytes were then seeded in a 6-well plate and kept inside a CO_2 incubator for further processing.

4.2.2. T cell purification

T cell purification was carried out using dynabeads^{TM} untouched^{TM} mouse T cells kit (Invitrogen, CA, USA) as mentioned earlier [250,269,300]. Briefly, Splenocytes were harvested and centrifuged at 350g for 5 min at 4°C. The supernatant was discarded, and the pellet was broken by gently tapping. The cells were then counted and 50×10^6 splenocytes were resuspended in a 15 mL tube containing isolation buffer (2mM EDTA + 2% heat-inactivated FBS + 1X PBS). 100 μL of heat-inactivated FBS and 100 μL biotinylated antibody cocktail were added to the cell suspension and incubated for 20 min on ice. After incubation, excess isolation buffer was added to the cell suspension, and cells were centrifuged at 350g for 8 min at 4°C. The supernatant was then discarded, and the pellet was broken by gently tapping. Next, 1 mL washed streptavidin-conjugated magnetic beads were added to the cells and incubated for 15 min at room temperature (RT) with gentle mixing by keeping the 15 mL tube on a rocker or by slow vortexing. After incubation, 4 to 5 mL of isolation buffer was added to the cell-bead mixture and placed on a magnet for 2 to 3 min. The cell suspension will become clear after placing the 15 mL tube on the magnet containing T cells in the clear solution. The clear solution was then harvested and centrifuged at 350g for 5 min at 4°C, and the pellet containing T cells was resuspended in complete RPMI-1640 medium. The purity of the T cells was then assessed via Flow cytometry and found to be ≥ 95%.

4.2.3. B16F10 culture supernatant (B16F10-CS) preparation

B16F10 cells (ATCC® CRL-6475^{TM}) were cultured and maintained in complete DMEM medium (Gibco, Thermo Fisher Scientific, MA, USA) as mentioned in ATCC protocol. B16F10-CS was prepared as described in previous reports [164,301]. Briefly, when the B16F10 cells reach 60 to 70% confluency, the cell culture medium was removed, and fresh medium was added. Cells were then incubated for 24 h and the culture supernatant (B16F10-CS) was harvested, aliquoted, and stored at -80°C until further use.

4.2.4. Flow cytometry (FC)

FC and FC staining was performed as mentioned previously [250,269,300]. Briefly, for cell surface staining, cells were harvested and resuspended in FC staining buffer (1% BSA + 0.01% NaN$_3$ + 1X PBS). Next, an antibody cocktail containing fluorochrome-conjugated primary antibodies was added to the cells and incubated for 30 min on ice. Cells were then washed with FC staining buffer and centrifuged at 350g for 5 min at 4°C. Supernatants were then discarded, and pellets were broken by gentle tapping. Secondary fluorochrome-conjugated antibodies were then added in case primary antibodies were not fluorochrome-tagged and incubated for 30 min on ice. Cells were then washed with FC staining buffer and centrifuged at 350g for 5 min at 4°C. Supernatants were discarded and pellets were broken by gentle tapping followed by the addition of FC staining buffer with 1% paraformaldehyde (PFA) and stored at 4°C in dark until acquisition.

For intracellular staining, cells were first harvested and fixed with 4% PFA for 10 min at RT. Fixed cells were then washed, centrifuged, and permeabilized with permeabilization buffer (0.5% BSA + 0.1% saponin + 0.01% NaN3 + 1X PBS). Cells were then centrifuged, supernatants were discarded, and pellets were resuspended in blocking buffer (1% BSA in permeabilization buffer) and incubated for 30 min. Cells were then washed with permeabilization buffer, centrifuged, and resuspended in permeabilization buffer containing antibody cocktail followed by 30 min incubation at RT. Cells were then washed with permeabilization buffer, centrifuged, and supernatants were discarded. If the primary antibodies used were unconjugated, secondary antibodies having fluorochrome tags diluted in permeabilization buffer were added and incubated for 30 min followed by washing with permeabilization buffer. Cells were then centrifuged, supernatants were discarded, and pellets were resuspended in FC staining buffer. Cells were then stored at 4°C in dark until acquisition.

Cells were acquired using BD LSRFortessa™ or BD FACSCalibur™ (BD Biosciences, CA, USA) Flow cytometers. Appropriate unstained and isotype controls were used to determine background noises. Data were analyzed using FlowJo (BD Biosciences, CA, USA) software (v 10.8.1).

4.2.5. Sandwich enzyme-linked immunosorbent assay (Sandwich ELISA)

Sandwich ELISA for IL-2, IFNγ, TNF, IL-6, and IL-10 from cell-free supernatants was performed using BD OptEIA™ cytokine ELISA kits as mentioned in previous reports [250,269,300]. Briefly, 96-well strip immuno-plates (SPL Life Sciences, Korea) were coated with 100 μL of diluted capture antibody and incubated overnight at 4°C. After incubation, each well was washed 3 times with 300 μL of wash buffer (1X PBS with 0.05% Tween-20). Then 300 μL of assay diluent (1X PBS with 10% FBS) was added to each well and incubated for 1 h at RT. Wells were then washed 3 times with wash buffer followed by the addition of 100 μL standards and samples in respective wells and incubated for 2 h. Wells were then washed 5 times with wash buffer. 100 μL Diluted detection antibody + streptavidin HRP (working detector) was then added to each well and incubated for 1 h. The wells were then washed 7 times followed by the addition of 100 μL HRP substrate (TMB/H_2O_2 diluted in MilliQ H_2O) and incubated in dark for 30 min generating a blue color solution. The reaction was then stopped by the addition of 50 μL 2N H_2SO_4 to each well turning the blue color solution into yellow. The reading was then taken using a microplate reader (Epoch 2 microplate reader, BioTek, USA) at 450 nm. Concentrations (pg/mL) of the cytokines were determined from the standard curve.

4.2.6. Western blot

Western blot analysis was performed as described earlier [302,303]. Cells were harvested and centrifuged at 350g for 5 min. Supernatants were discarded and cell pellets were broken by tapping followed by the addition of RIPA buffer containing protease and

phosphatase inhibitor cocktail (Roche, Mannheim, Germany). Cells were then incubated for 1 h on ice, and vortexed every 15 min following the addition of RIPA buffer to ensure proper lysis of cells. Lysed cells were then centrifuged at 15000 rpm for 30 min at 4°C. Next, the supernatants containing cell lysates were harvested and concentrations were determined using Bradford reagent (Sigma Aldrich, MO, USA). 30 μg of proteins were then loaded on 10% SDS gel followed by running and transfer of proteins on a polyvinylidene fluoride (PVDF) membrane (Millipore, MA, USA). PVDF membranes were then blocked for 1 h in blocking buffer (3% BSA in 1X TBST) at RT followed by the addition of primary antibodies and incubated overnight at 4°C. Next, the membranes were washed 3 times with 1X TBST followed by the addition of HRP-conjugated secondary antibodies and incubated at RT for 2 h. Membranes were then washed 3 times with 1X TBST followed by the addition of chemiluminescent substrates (Merck Millipore, MA, USA) and detected by a ChemiDoc system (Bio-Rad, CA, USA). Blot images were further analyzed using ImageLab software (Bio-Rad, CA, USA).

4.2.7. Trypan blue exclusion assay

Trypan blue exclusion assays were performed to determine the cytotoxic effects of different modulators as reported earlier [300]. Cells were incubated with different drugs with various concentrations. Next, cells were harvested, and trypan blue was added to the cell suspensions. Under a brightfield microscope, the number of blue-colored cells was determined which signifies dead cells. The number of blue-colored cells was found to be higher in higher concentrations of modulators.

4.2.8. Annexin V/7-AAD staining

Annexin V/7-AAD staining was performed as reported earlier [302]. Cells were incubated with different modulators having various concentrations. Next, cells were harvested and washed with 1X PBS followed by centrifugation at 350g for 5 min at RT.

Then annexin V and 7-AAD were added to cell suspensions and incubated for 15 min at RT. Cells were then acquired using BD LSRFortessa™ or BD FACASCalibur™ (BD Biosciences, CA, USA). Data were further analyzed using FlowJo (BD Biosciences, CA, USA) software (v10.8.1).

4.2.9. Nitrite estimation

Supernatants were harvested from macrophage cultures with different experimental conditions. For NO estimation 100 µL of macrophage supernatants were used followed by the addition of 100 µL of 1% sulfanilamide and 100 µL of 0.1% N-1-naphthylenediamine dihydrochloride as described earlier [304]. Next, after 10 min of incubation, absorbance was measured at 540 nm. The concentration of NO was determined from a standard curve prepared in the presence of sodium nitrite of different concentrations.

4.2.10. Calcium influx study

Calcium influx studies were performed as reported earlier [250]. Cells were incubated with 2µM Ca^{2+} sensitive dye Fluo-4 AM (Invitrogen, CA, USA) for 30 min. Next, cells were washed twice with 1X PBS and kept inside an incubator for 15 min for de-esterification. Then Fluo-4 intensities were recorded using a Flow cytometer in presence of different treatments. The levels of intracellular Ca^{2+} were assessed with a minor modification of the above procedure. Fluo-4 AM and different treatments were added at the same time followed by an incubation of 60 min. Cells were then washed twice with 1X PBS and kept inside an incubator for 15 min for de-esterification followed by acquisition using a Flow cytometer. Data were further analyzed using FlowJo (BD Biosciences, CA, USA) software.

4.2.11. Statistical analysis

Statistical analysis was carried out using GraphPad 9 software (GraphPad Software Inc., San Diego, CA, USA). Comparison between groups was performed using either

student's t-test or one-way ANOVA or two-way ANOVA. Data were represented in mean ± SEM constituting 3 independent experiments. '*' represents statistical significance with $p \leq 0.05$. ns, non-significant; * $p \leq 0.05$; ** $p \leq 0.01$; *** $p \leq 0.001$; **** $p \leq 0.0001$.

CHAPTER # 5

Results

5. Results

5.1. Elevation of TRPV1 expression on T cells during experimental immunosuppression

TRPV1 has been reported to functionally regulate T cell activation and effector responses and is associated with the Ca^{2+} flux required for the generation of T cell-mediated effector immune responses [250,305,306]. Moreover, immunosuppressive drugs have been shown to induce a rise in intracellular calcium levels in T cells and other immune cells [149,275–277,307–309]. However, the role of TRPV1 towards the immunosuppression-mediated rise in intracellular Ca^{2+} levels has not been reported earlier. Accordingly, here we have investigated the association of TRPV1 towards FK505- and B16F10-mediated immunosuppression of T cells along with the effect of the above immunosuppressants towards T cell activation, proliferation, cytokine production, and Ca^{2+} influx.

5.1.1. Cell surface expression of TRPV1 on T cells

The expression of TRPV1 channels on purified murine T cells was determined using Flow cytometry (FC). It was observed that the frequency (percentage) of TRPV1-positive cells was $17.86 \pm 1.34\%$ as compared with isotype controls ($0.02 \pm 0.01\%$) (**Figure 12**). Further, the specificity of the TRPV1 antibody in T cells was tested by using control blocking peptide antigen. For that, T cells were stained with anti-TRPV1 antibody in the presence or absence of the blocking peptide. It was observed that the percentage of positive cells for TRPV1 was markedly reduced in a dose-dependent manner. These results indicate that TRPV1 is expressed on T cells, and the anti-TRPV1 antibody is specific towards TRPV1 expressed on T-cells (Figure 8).
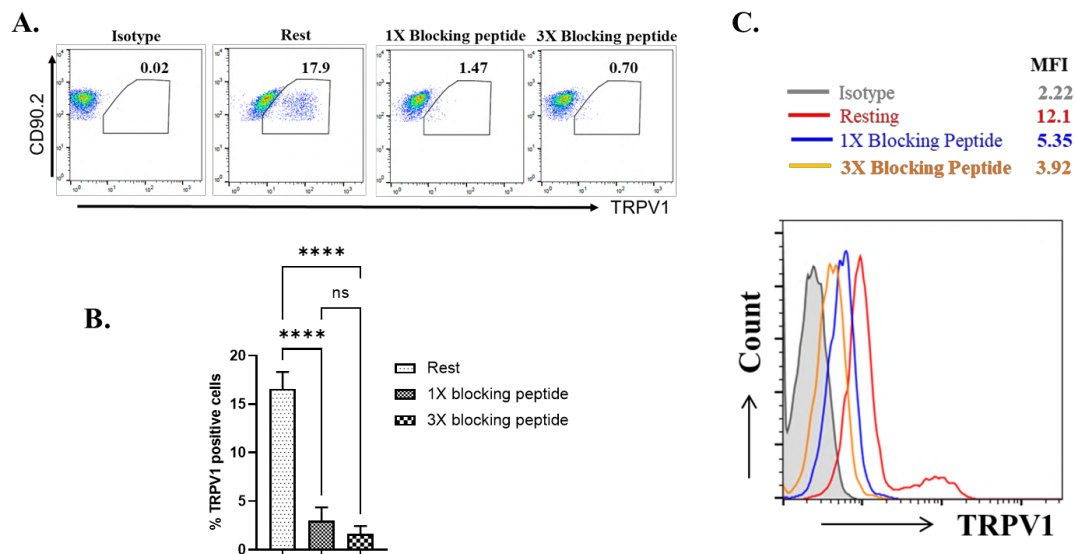
Figure 12: TRPV1 expression in purified mouse T cells. Resting T cells, after 48 h of culture, were stained with anti-TRPV1 antibody for 30 mins in Flow cytometry staining buffer followed by secondary antibody staining and acquired via Flow cytometry (FC). (A) Representative dot-plot showing TRPV1 expression on resting T cells in the presence or absence of control blocking peptide along with representative bar diagram shown in (B). (C) showing the Mean Fluorescence Intensity (MFI) of TRPV1 expression with corresponding MFI values. Representative data from three independent experiments are shown. One-way ANOVA was performed for significance calculation between the groups. **** $p < 0.0001$.

5.1.2. Cellular cytotoxicity assay of T cells in presence of B16F10-CS, FK506, and 5'-IRTX

The cellular cytotoxicity of 5'-IRTX, FK506, and B16F10-CS in purified mouse T cells was studied using the trypan blue exclusion method. It was observed that around 93% of the cells were viable for 5'-IRTX at 5 μM and FK506 at 5 μg/mL concentration, and around 95% of cells were viable at 20% B16F10-CS with respect to the total media volume (**Figure 13**). In all the experiments, either heat-killed or UV-treated T cells were

used as a positive control. Accordingly, we chose 5 μM 50-IRTX, 5 μg/mL FK506, and 20% of B16F10-CS for further experiments.
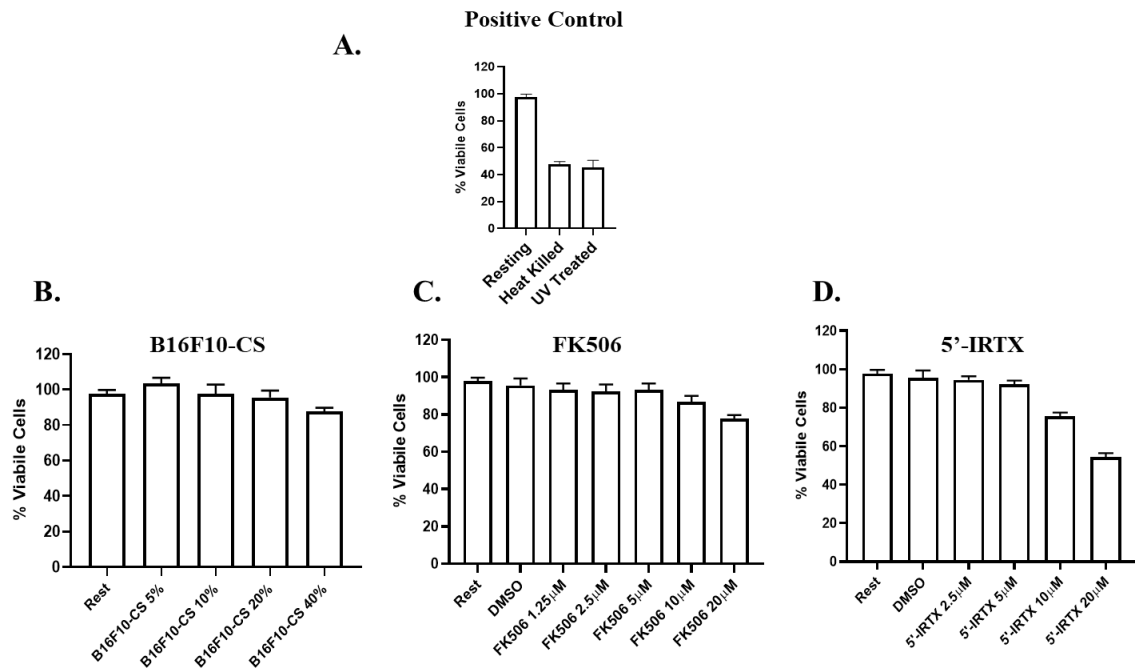
Figure 13: Cytotoxicity of B16F10-CS, FK506, and 5′-IRTX on T cells. Cytotoxicity of T cells in different doses of (B) B16F10-CS, (C) FK506, or (D) 5′-IRTX, as assessed by trypan blue exclusion assay. (A) depicts the percentage of viable cells in heat-killed or UV-treated T cells (positive controls).

5.1.3. FK506 and B16F10-CS mediated immunosuppression downregulates T cell activation

To determine the status of T cell activation during immunosuppressive treatment with either FK506 or B16F10-CS, T cell activation markers, including CD69 (an early T cell activation marker) and CD25 (a late T cell activation marker), were analyzed using FC [250] (**Figure 14**). It was observed that in T cells pre-treated with either FK506 (ConA + FK506: CD69: 5.08 ± 1.46%, CD25: 13.77 ± 3.55%; TCR + FK506: CD69: 3.50 ± 1.52%, CD25: 6.78 ± 2.44%) or B16F10-CS (ConA + B16F10-CS: CD69: 28.43 ± 1.07%, CD25: 63.8 ± 2.97%; TCR + B16F10-CS: CD69: 34.97 ± 2.57%, CD25:   62.90   ±   2.10%)

stimulated with ConA or TCR, both CD69 and CD25 decreased as compared with those in ConA- (CD69: 67.17 ± 6.73%; CD25: 74.63 ± 2.64%) or TCR-activated (CD69: 80.50 ± 3.10%; CD25: 84.53 ± 3.60%) T cells indicating a reduction of T cell activation.
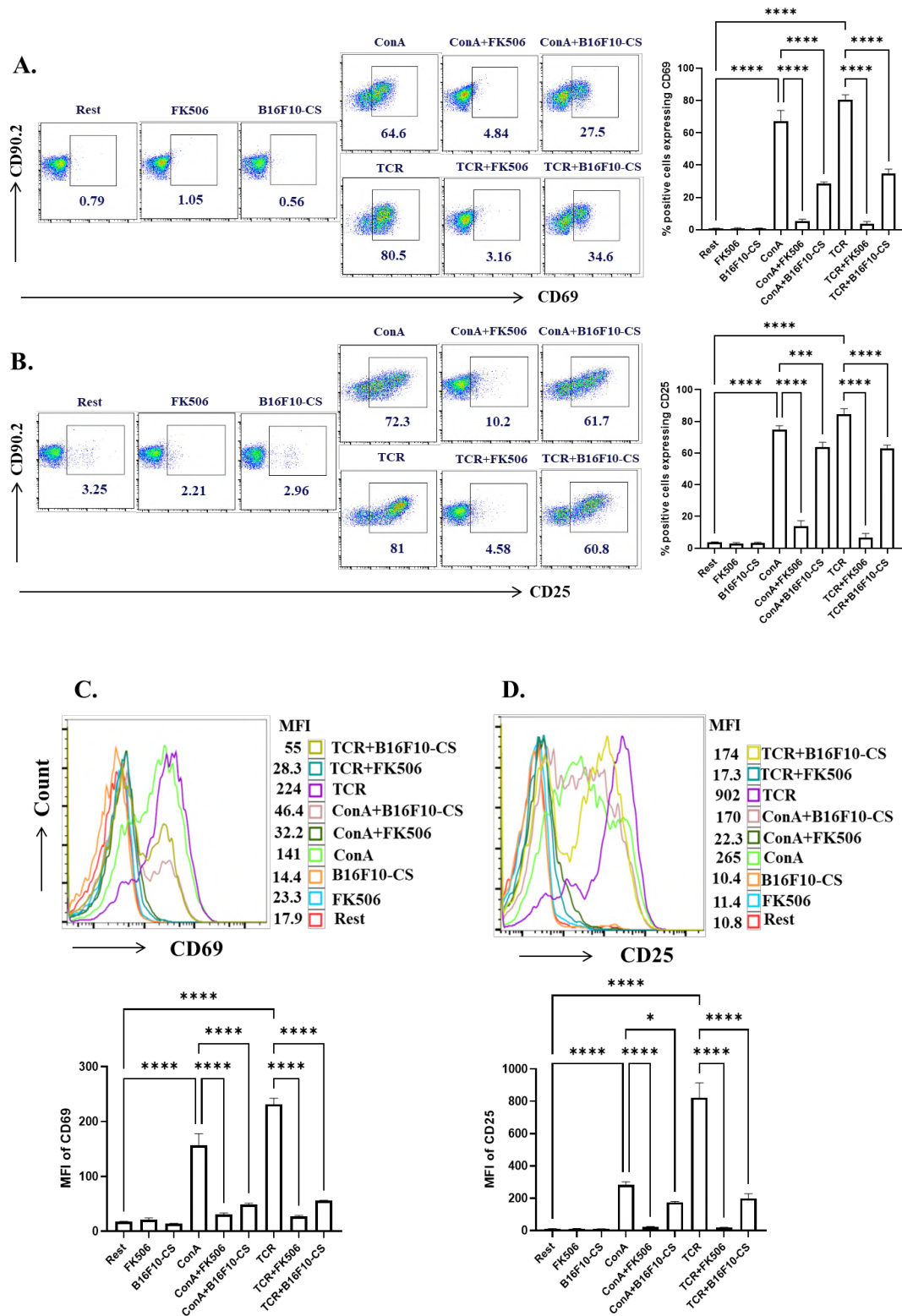
Figure 14: T cell activation in the presence of FK506 and B16F10-CS. Purified mouse T cells were treated with FK506 or B16F10-CS in the presence or absence of ConA or TCR. Cells were harvested after 48 h post-treatment, and T cell activation markers were assessed by FC. Flow cytometric dot-plots depicting T cell activation markers (A) CD69 and (B) CD25, along with the corresponding bar diagram. (C) and (D) depicts the MFI of CD69 and CD25 expression with corresponding MFI values. One-way ANOVA was performed for significance calculation between the groups. $P < 0.05$ was considered a statistically significant difference between the groups. * $p < 0.5$; *** $p < 0.001$; **** $p < 0.0001$.

5.1.4. FK506 and B16F10-CS mediated immunosuppression downregulates T cell proliferation

T cell activation is accompanied by T cell proliferation, as mentioned elsewhere [250,300]. To ascertain whether immunosuppressed T cell stimulation leads to reduced proliferation, we performed CFSE staining of T cells, and cells were analyzed via FC. It was observed that in T cells pre-treated with either FK506 (FK506 + ConA: $0.32 \pm 0.18\%$; FK506 + TCR: $0.62 \pm 0.22\%$) or B16F10-CS (B16F10-CS + ConA: $16.5 \pm 6.09\%$; B16F10-CS + TCR: $7.63 \pm 0.84\%$) stimulated with ConA or TCR, T cell proliferation was decreased as compared with the corresponding ConA ($84.53 \pm 1.33\%$) or TCR ($71.1 \pm 3.74\%$) controls (**Figure 15**). These results indicate that T cell proliferation is markedly reduced in immunosuppressed T cells.
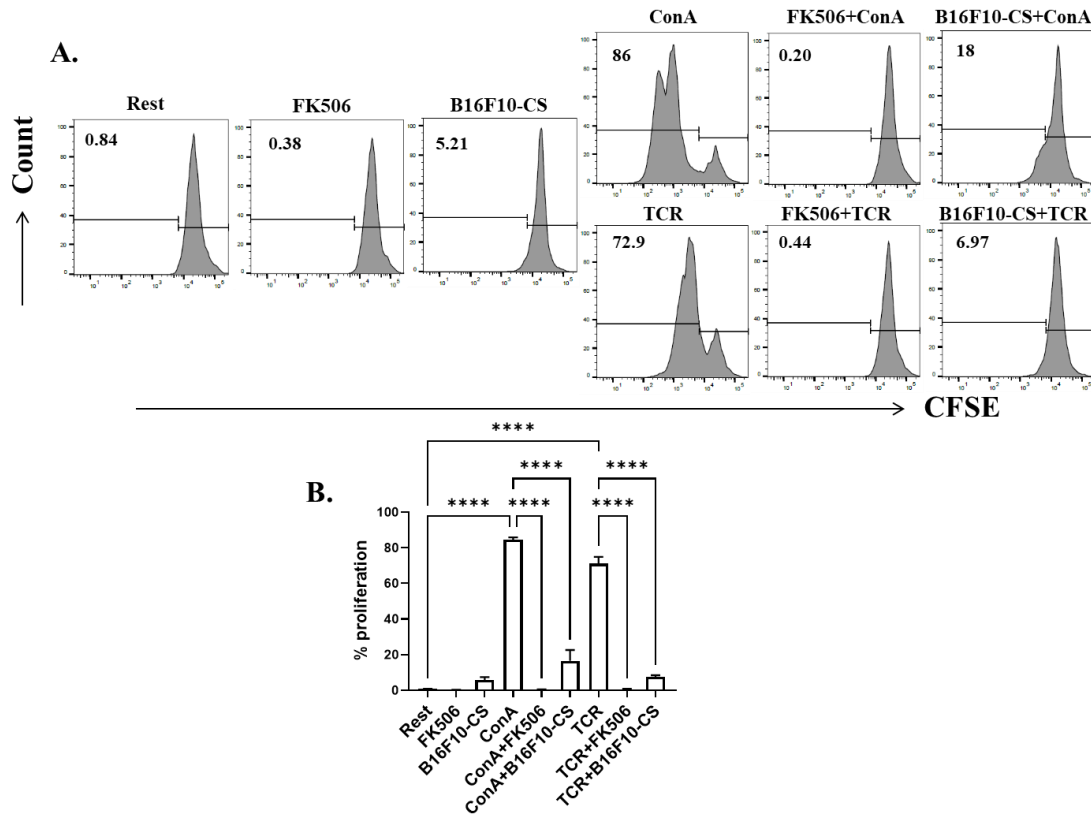
Figure 15: T cell proliferation in the presence of FK506 and B16F10-CS. Purified mouse T cells were stained with CFSE and then treated with FK506 or B16F10-CS in the presence or absence of ConA or TCR. Cells were harvested 96 h post-activation, and T cell proliferation was assessed by FC. (A) Flow cytometric histograms represent T cell proliferation as determined by CFSE staining along with its corresponding bar diagram shown in (B). One-way ANOVA was performed for significance calculation between the groups. $P < 0.05$ was considered a statistically significant difference between the groups (**** $p < 0.0001$).

5.1.5. Immunosuppression modulates proinflammatory cytokine release

T cell activation induces pro-inflammatory cytokine production [250,300]. Sandwich ELISAs were performed to quantitate the amount of IL-2, IFNγ and TNF released by T cells pre-treated with either FK506 or B16F10-CS stimulated with ConA or TCR as compared with the corresponding ConA or TCR controls (**Figure 16**). It was found that the production of pro-inflammatory cytokines increases with activation, which was

reduced in immunosuppressed T cells, suggesting a reduced effector cytokine responses by immunosuppressed T cells.
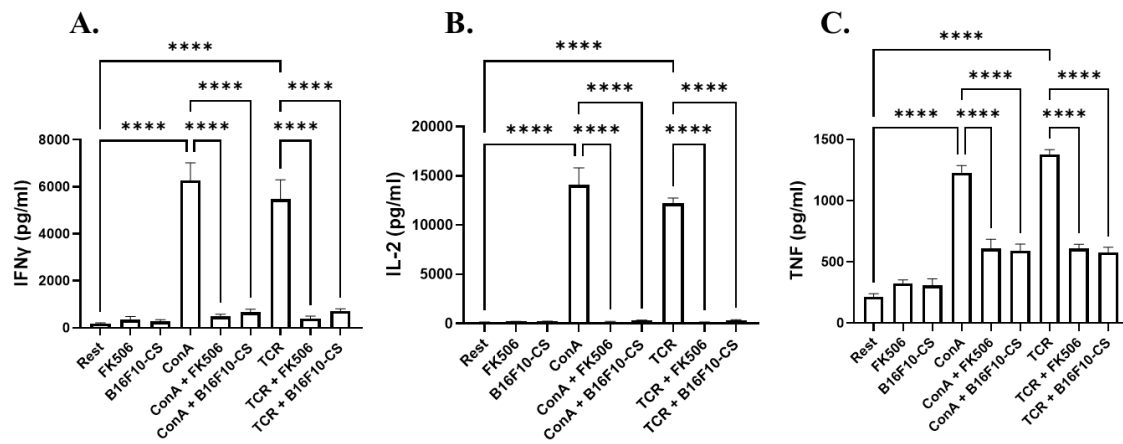
Figure 16: Cytokine response by immunosuppressed T cells. T cells were treated with FK506 or B16F10-CS in the presence or absence of ConA or TCR. The supernatant was collected at 48 h, and sandwich ELISA was performed to quantitate secreted cytokines, such as (A) IFN-γ, (B) IL-2, and (C) TNF. Representative data from three independent experiments are shown. One-way ANOVA was performed for significance calculation between the groups (**** $p < 0.0001$).

5.1.6. Expression of TRPV1 upregulated during immune activation and immunosuppression

The expression of TRPV1 was assessed in immunosuppressed T cells. Interestingly, TRPV1 expression levels significantly increased in T cells treated with FK506 or B16F10-CS (26.9 ± 1.11% or 23.97 ± 1.04%) as compared with resting T cells (16.5 ± 0.52%). Moreover, the TRPV1 expression further increased in FK506- or B16F10-CS-treated T cells with ConA or TCR stimulation. In FK506- or B16F10-CS-treated T cells stimulated with ConA or TCR, the TRPV1 expression was 34.53 ± 0.86% or 33.77 ± 0.85%, respectively, as compared with control ConA-activated T cells (28.83 ± 1.19%). Similarly, in TCR-activated FK506 or B16F10-CS treated T cells, the TRPV1 expression

was 33.97 ± 0.77 or 36.1 ± 1.31%, respectively, as compared with control TCR-activated

T cells (30.07 ± 0.20%) (**Figure 17**). Accordingly, the current findings indicate that the

TRPV1 expression also increases significantly in FK506 or B16F10-CS-treated

immunosuppressed T cells as compared with the resting T cells, which were further

elevated in FK506- or B16F10-CS-treated T cells stimulated with either ConA or TCR as

compared with ConA or TCR stimulation alone.
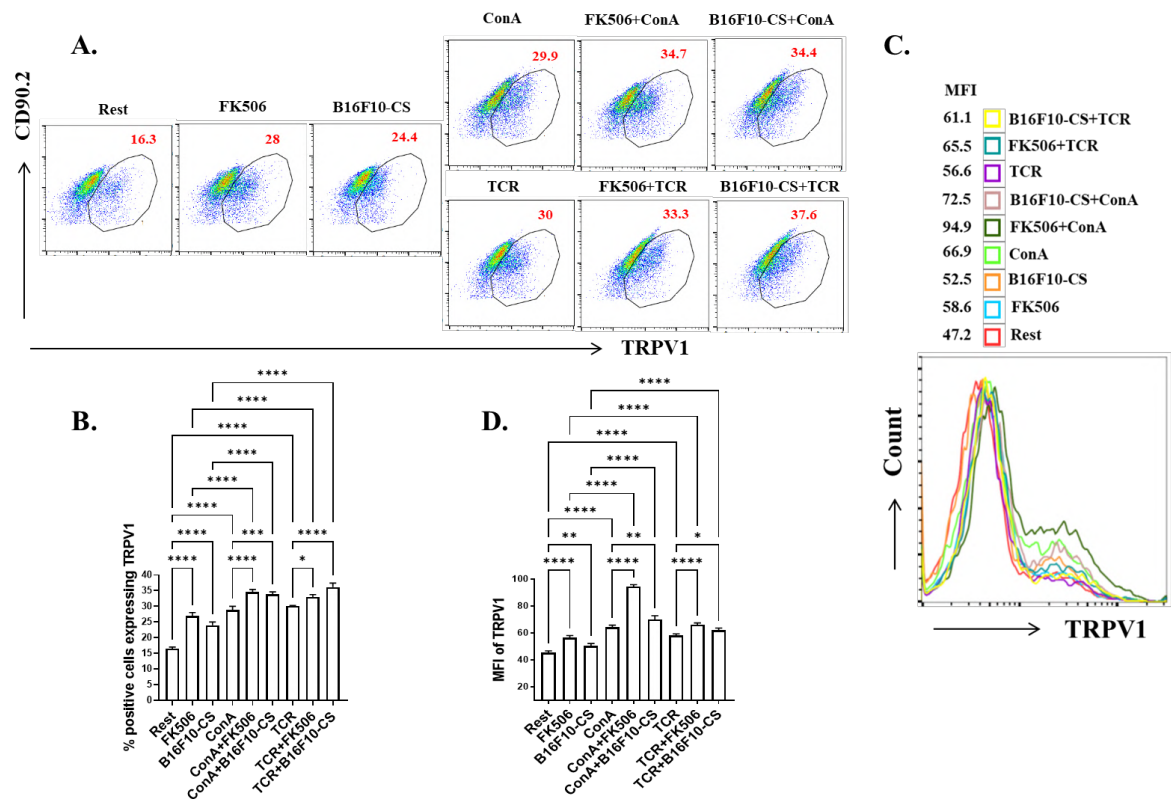
Figure 17: Expression of TRPV1 in activated and immunosuppressed T cells. Purified

mouse T cells were treated with FK506 or B16F10-CS in the presence or absence of ConA

or TCR. Cells harvested after 48 h post-treatment were assessed by FC. (A) FC dot-plots

show TRPV1 expression on T cells along with the corresponding bar diagram shown in

(B). (C) MFI of TRPV1 expression with the corresponding bar diagram depicted in (D).

Representative data from three independent experiments are shown. One-way ANOVA

was performed for significance calculation between the groups. P < 0.05 was considered

as a statistically significant difference between the groups (* p < 0.05; ** p < 0.01; *** p < 0.001; **** p < 0.0001).

5.1.7. Time kinetics study of TRPV1 expression on T cells and during reversal of immunosuppressive conditions

To determine the effect of FK506 and B16F10-CS on TRPV1, its expression with time, and during the reversal of immunosuppressive conditions, we performed a kinetic study via FC. It was observed that in FK506-treated T cells, the TRPV1 expression significantly increased at an early time point of 24 h, compared with resting T cells. Further, in B16F10-CS treated T cells, the TRPV1 expression significantly increased at 48 h as compared with resting T cells. The 48 h harvested T cells were washed to remove FK506 or B16F10-CS and were re-seeded with fresh media. These T cells were harvested at 60 h and 72 h. Intriguingly, it was observed that the TRPV1 expression levels also further heightened at 60 h and 72 h, as compared with T cells at 48 h (**Figure 18**). These results indicate that the FK506 or B16F10-CS-induced TRPV1 upregulation is irreversible even after the removal of these immunosuppressive conditions.
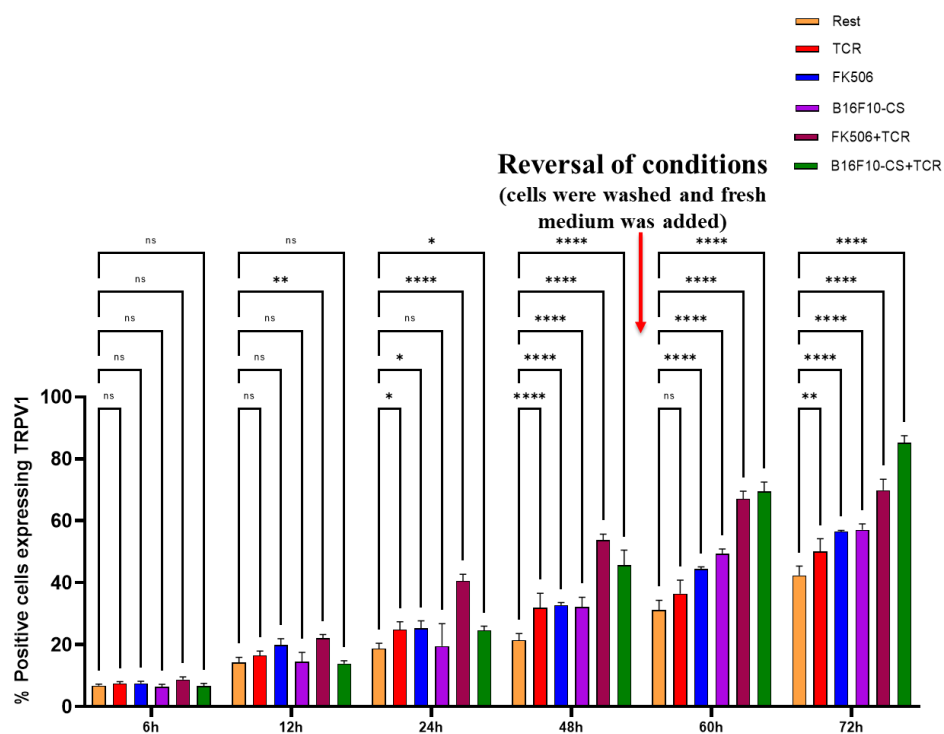
Figure 18: Time kinetics of TRPV1 expression on T cells and during reversal of conditions. The expression profile of TRPV1 on T cells at time points ranging from 6 h to 48 h. The 48 h T cells were washed and reseeded with fresh medium. Those reseeded T cells were later harvested at 60 h to 72 h and stained for TRPV1. Bar diagram showing the expression profile of TRPV1 at different time points. Representative data is from three independent experiments. Two-way ANOVA was performed for significance calculation between the groups (ns, non-significant; * $p < 0.05$; ** $p < 0.01$; *** $p < 0.001$, **** $p < 0.0001$).

5.1.8. TRPV1 regulates immunosuppression-mediated intracellular Ca^{2+} levels

5'-IRTX is a potent and specific functional inhibitor of the TRPV1 channel and can block TRPV1-directed Ca^{2+} influx [250,310]. Here, the intracellular Ca^{2+} levels were assessed by using the Ca^{2+}-sensitive dye Fluo-4 AM [250,269,310]. We have observed that in ConA- ($183.33 \pm 5.52\%$) or TCR-stimulated ($143.52 \pm 10.45\%$) T cells, the Ca^{2+} levels significantly increased compared with resting T cells (100%). Additionally, upon immunosuppressive treatment with FK506, the calcium levels further (FK506: $181.87 \pm 4.15\%$; FK506 + ConA: $235.04 \pm 38.69\%$; FK506 + TCR: $185.16 \pm 9.81\%$) increased significantly compared with ConA or TCR controls. However, in B16F10-CS immunosuppressive conditions, a modest albeit increase in Ca^{2+} levels was found (B16F10-CS: $115.42 \pm 6.11\%$, ConA + B16F10-CS: $189.71 \pm 14.34\%$, TCR + B16F10-CS: $146.90 \pm 11.00\%$) as compared with resting (100%), ConA, or TCR controls. Furthermore, in the presence of the TRPV1-specific inhibitor, 5'-IRTX, the calcium levels significantly decreased compared with their corresponding controls (**Figure 19**). These results indicate that other calcium channels fail to replenish the reduced Ca^{2+} levels due to TRPV1 blocking in T cells. This highlights the fact that TRPV1 is indispensable in

increasing intracellular Ca^{2+} levels in T-cells in both T-cell activation and immunosuppressive conditions.
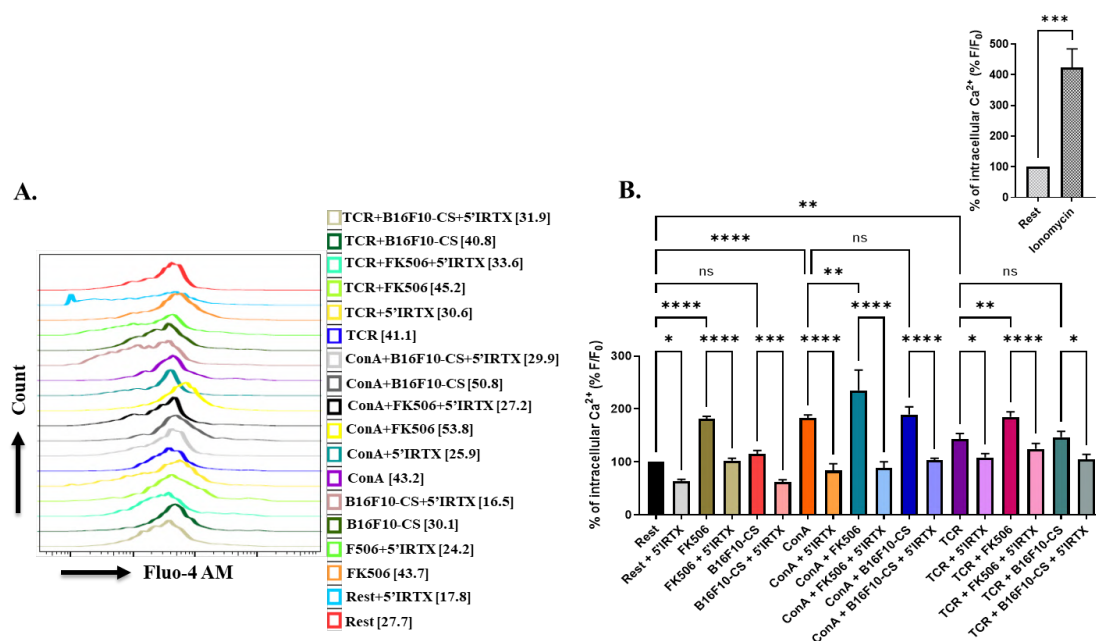
Figure 19: Regulation of immunosuppression-mediated intracellular Ca^{2+} in T cells via TRPV1 channel. T cells were incubated with Ca^{2+}-sensitive dye, Fluo-4 AM, along with different experimental conditions for 1 h as mentioned in material and methods and acquired via FC. The various experimental conditions were pre-treated with 5′-IRTX, followed by treatment as per the experimental setup. (A) Histogram analysis of Fluo-4 intensity representing intracellular Ca^{2+} in T cells. (B) Fluo-4 intensity representing intracellular Ca^{2+} has been expressed as a percentage normalized to resting control. The inset depicts the rise in intracellular Ca^{2+} levels in ionomycin-treated T cells. Representative data is from three independent experiments. One-way ANOVA was performed for significance calculation between the groups (ns, non-significant; * $p < 0.05$; ** $p < 0.01$; *** $p < 0.001$, **** $p < 0.0001$).

5.1.9. Time of action study of FK506 and B16F10-CS on T cell activation markers, CD69 and CD25

To investigate the time of action of FK506 and B16F10-CS on T cells, we have performed a kinetic study to elucidate the expression levels of CD69 and CD25 with respect to activation in the presence or absence of FK506 and B16F10-CS treatment. For that, purified mouse T cells were first pre-treated with FK506, or B16F10-CS, followed by activation. Next, cells were harvested at different time points (6, 12, 24, 48, 72 h) post-activation, followed by cell surface staining of CD69 and CD25 and analyzed by FC (**Figure 20**). The FC results show that the CD69 and CD25 expression decreases on FK506 treated T cells from 6 h onwards (FK506 + TCR: CD69: $1.53 \pm 0.44\%$, CD25: $2.92 \pm 0.71\%$), whereas in the case of B16F10-CS treatment, the CD69 and CD25 levels decrease from 48 h onwards (B16F10-CS + TCR: CD69: $19.43 \pm 2.63\%$, CD25: $35.83 \pm 2.76\%$) compared to the ConA and TCR controls (TCR 6 h: CD69: $31 \pm 2.91\%$, CD25: $10.76 \pm 1.60\%$; TCR 48 h: CD69: $56.20 \pm 2.62\%$, CD25: $61.90 \pm 2.82\%$), suggesting that FK506 is a fast-acting immunosuppressant, whereas B16F10-CS elucidates its effect lately.
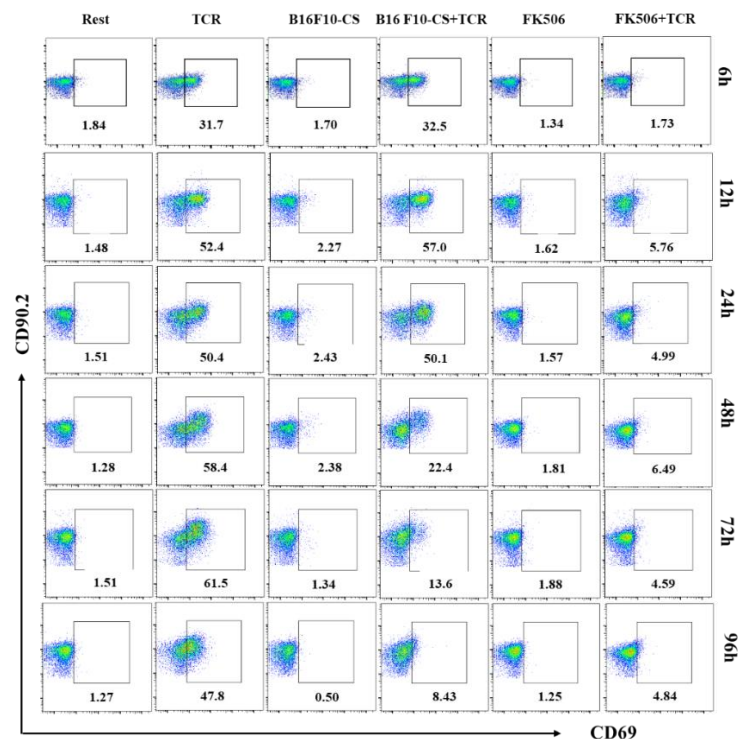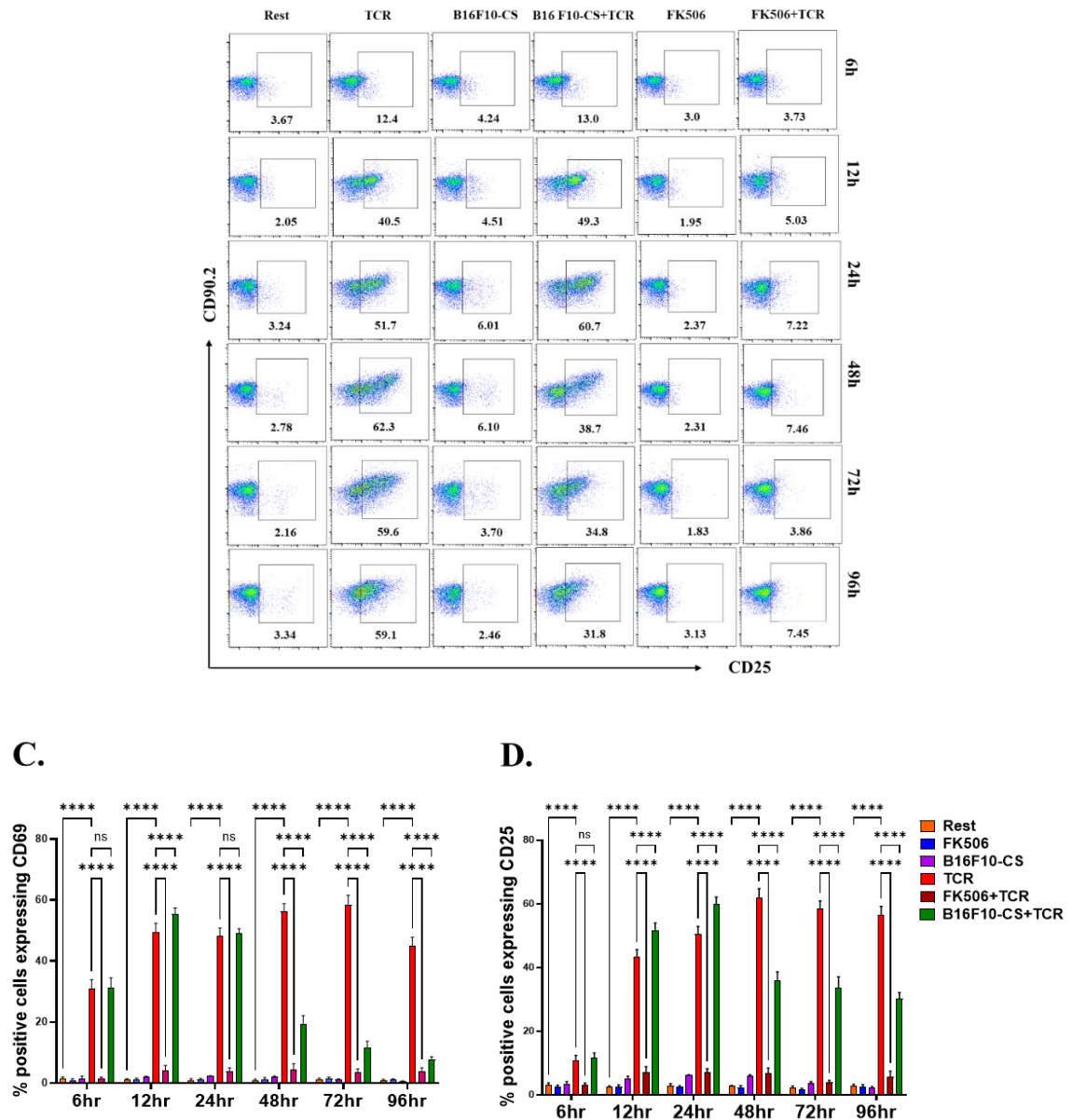
Figure 20: Time of action of FK506 and B16F10-CS on T cell activation with respect to CD69 and CD25 expression. T cells were activated with TCR. After treatment with different conditions, T cells were harvested at time points 6, 12, 24, 48, 72, and 96 h. (A) FC dot plots depicting the frequency of CD69 positive T cells along with the representative bar diagram (C) of three independent experiments. (B) FC dot plots depicting the frequency of CD25 positive T cells along with the representative bar diagram (D) of three independent experiments. Two-way ANOVA was performed for significance calculation between the groups (ns, non-significant; **** $p < 0.0001$).

5.1.10. Modulation CD69 and CD25 expression on T cell in the presence of TRPV1 inhibitor (5'-IRTX) along with FK506 and B16F10-CS

To study the cell surface expression of T cell activation markers CD69 and CD25 and whether these expressions are modulated in activated T cells in the presence of 5'-IRTX alone or 5'-IRTX + FK506/B16F10-CS with or without activation, purified mouse T cells were pre-treated with 5'-IRTX followed by the addition of FK506 or B16F10-CS in respective wells. Then cells were activated with either ConA or TCR. Next, cells were harvested 48 h post-activation, surface stained for CD69 and CD25, and analyzed via FC (**Figure 21**). From the FC data, it has been observed that CD69 and CD25 levels were significantly reduced in cells treated with ConA/TCR + 5'-IRTX compared to ConA/TCR controls. Similarly, as found earlier, CD69 and CD25 levels on T cells were alleviated in ConA/TCR + FK506/B16F10-CS treatment. Moreover, a further decrease in CD69 and CD25 levels were found in cells treated with ConA/TCR + FK506/B16F10-CS + 5'-IRTX compared to ConA/TCR + 5'-IRTX/FK506/B16F10-CS. These results suggest that TRPV1 inhibition induces T cell suppression, and the suppression was further elevated with FK506 and B16F10-CS treatment along with 5'-IRTX.

A.

Isotype 0.73 | Rest 1.20 | DMSO 1.02 | ConA 74.8 | ConA+DMSO 72.3 | TCR 83.6 | TCR+DMSO 82.4

5'-IRTX 2.08 | 5'-IRTX+ConA 3.49 | 5'-IRTX+TCR 2.90

B16 1.0 | B16+ConA 29.6 | B16+TCR 37.7 | B16+ConA+5'-IRTX 1.88 | B16+TCR+5'-IRTX 4.42

FK506 1.06 | FK506+ConA 6.04 | FK506+TCR 5.16 | FK506+ConA+5'-IRTX 4.0 | FK+TCR+5'-IRTX 3.19

CD90.2 (y-axis), CD69 (x-axis)

B.

Isotype 0.22 | Rest 3.68 | DMSO 3.24 | ConA 74.1 | ConA+DMS 75.1 | TCR 84.4 | TCR+DMSO 80.4

5'-IRTX 3.45 | 5'-IRTX+ConA 4.45 | 5'-IRTX+TCR 3.87

B16 3.04 | B16+ConA 62.5 | B16+TCR 65.0 | B16+ConA+5'-IRTX 4.01 | B16+TCR+5'-IRTX 4.74

FK506 2.68 | FK506+ConA 13.8 | FK506+TCR 6.36 | FK506+ConA+5'-IRTX 4.04 | FK506+TCR+5'-IRTX 3.67

CD90.2 (y-axis), CD25 (x-axis)

Figure 21: T cell activation in the presence of TRPV1 inhibitor (5'-IRTX) along with FK506 and B16F10-CS. Purified mouse T cells were pre-treated with 5'-IRTX, and then FK506 or B16F10-CS were added to respective wells, followed by ConA or TCR activation. Next, cells were harvested 48 h post-activation, and T cell activation markers (CD69 and CD25) were assessed by FC. Flow cytometric dot plots depicting T cell activation markers (A) CD69 and (B) CD25 along with the corresponding bar diagram in (C) and (D), respectively. One-way ANOVA was performed for significance calculation between the groups. P < 0.05 was considered a statistically significant difference between the groups. ns, non-significant; *** p < 0.001; **** p < 0.0001.

5.1.11. Modulation of pro-inflammatory cytokine production by T cells in the presence of TRPV1 inhibitor (5'-IRTX) along with FK506 and B16F10-CS

To find out the pro-inflammatory cytokine release by T cells in the presence of 5'-IRTX alone or 5'-IRTX + FK506/B16F10-CS with or without activation, purified mouse T cells were pre-treated with 5'-IRTX followed by the addition of FK506 or B16F10-CS in respective wells. Then cells were activated with either ConA or TCR. Next, cell-free T cell supernatants were harvested 48 h post-activation, and sandwich ELISAs were performed to quantitate the amount of IL-2, IFNγ, and TNF released by T cells (**Figure**

22). From the ELISA data, it has been observed that levels of IL-2, IFNγ, and TNF were significantly reduced in cells treated with ConA/TCR + 5'-IRTX compared to ConA/TCR controls. Similarly, as found earlier, pro-inflammatory cytokine levels secreted by T cells were significantly alleviated in ConA/TCR + FK506/B16F10-CS treatment. Moreover, a further decrease in cytokine levels was found in cells treated with ConA/TCR + FK506/B16F10-CS + 5'-IRTX compared to ConA/TCR + 5'-IRTX/FK506/B16F10-CS. These findings suggest that TRPV1 inhibition reduces pro-inflammatory cytokine production, which is further reduced with FK506 and B16F10-CS treatment along with 5'-IRTX.
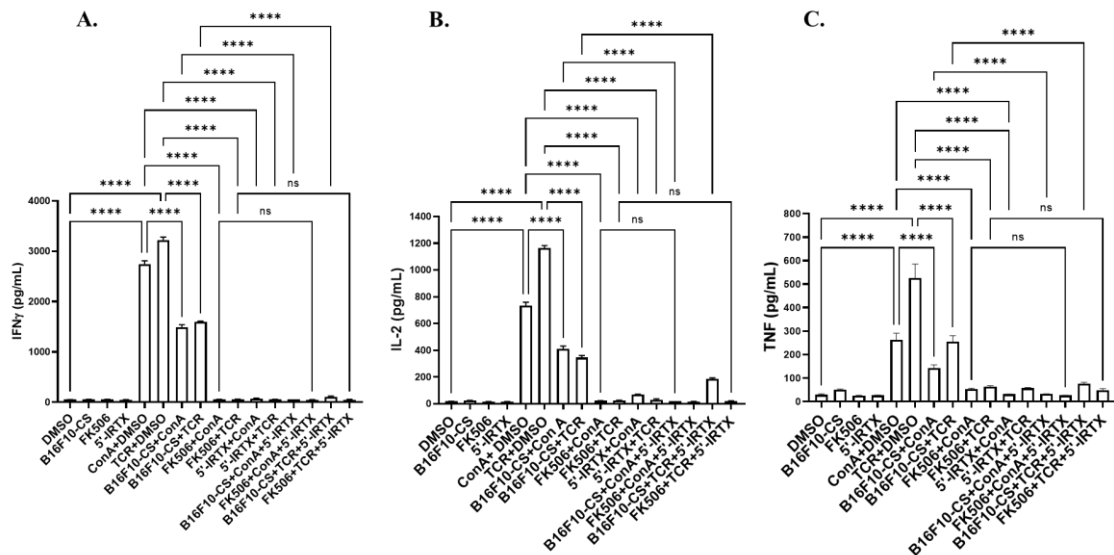
Figure 22: Cytokine response by T cells in the presence of TRPV1 inhibitor (5'-IRTX) along with FK506 and B16F10-CS. T cells were pre-treated with 5'-IRTX, and then FK506 and B16F10-CS were added, followed by ConA/TCR activation. The T cell supernatants were collected at 48 h post-activation, and sandwich ELISAs were performed to quantitate secreted cytokines, such as (A) IFN-γ, (B) IL-2, and (C) TNF. Representative data from three independent experiments are shown. One-way ANOVA was performed for significance calculation between the groups (ns, non-significant; **** $p < 0.0001$).

5.1.12. Modulation of TRPV1 expression and intracellular Ca^{2+} levels in B16F10 tumor-bearing mice

B16F10, a transplantable immunosuppressive mouse melanoma cell line, was injected subcutaneously (SC) in C57BL/6 mice, and tumor growths were monitored up to 21 days post-sc injection. In order to ascertain the modulation of TRPV1 expression and consequent changes in intracellular Ca^{2+} levels in murine splenic T cells, we performed FC and calcium influx studies comparing control and B16F10 tumor-bearing mice (SC) (**Figure 23**). It was observed that TRPV1 levels significantly increased in T cells isolated from B16F10 tumor-bearing mice (19.63 ± 1.10%) compared with control mice (15.83 ± 0.93%) (**Figure 23 B**). Next, we assessed whether the increase in TRPV1 expression was associated with a concurrent increase in intracellular Ca^{2+} levels. We found that the basal intracellular Ca^{2+} levels (Rest: 100%; ConA: 129.46 ± 14.08%; TCR: 113.66 ± 5.80%) also increased in T cells isolated from B16F10 tumor-bearing mice (Rest: 121.04 ± 9.55%; ConA: 143.08 ± 8.58%; TCR: 151.51 ± 6.17%) as compared with control mice (**Figure 23 C**). Altogether, these results indicate that TRPV1 expression increases in splenic T cells isolated from B16F10 tumor-bearing mice, and consequently, the intracellular Ca^{2+} levels were also increased as compared with control mice.
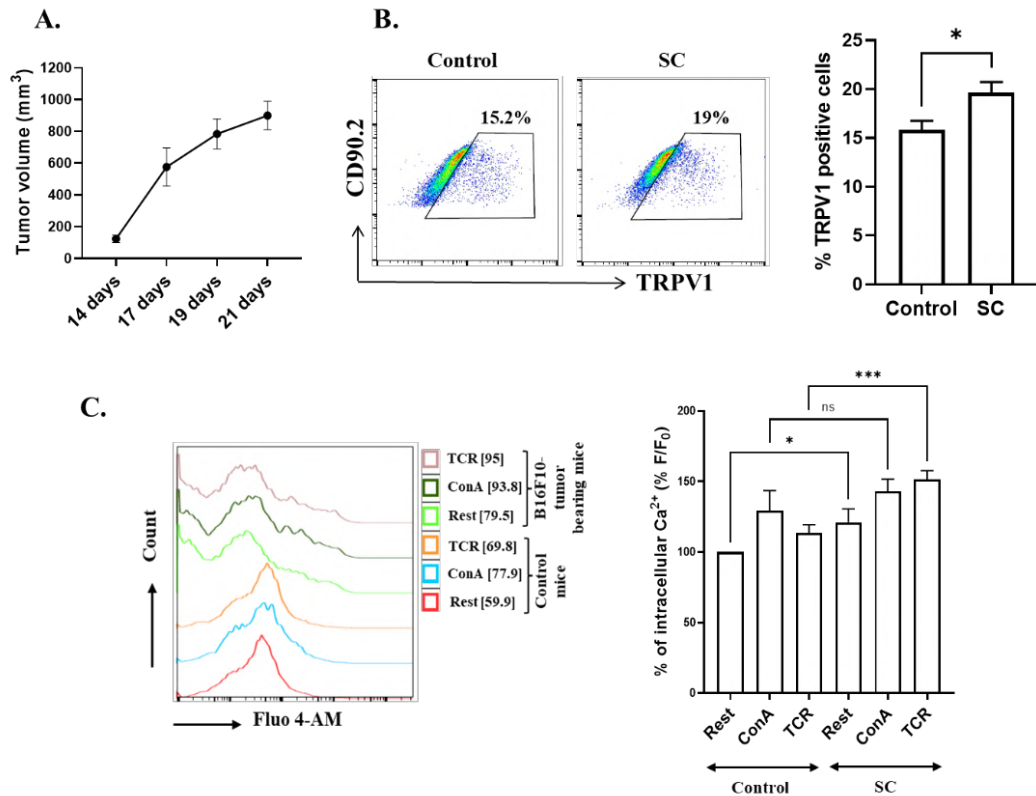
Figure 23: Modulation of TRPV1 expression and intracellular Ca^{2+} levels in splenic T cells from control and B16F10 tumor-bearing mice (SC). Splenic T cells were isolated from control and tumor-bearing mice (SC) and analyzed via FC. (A) B16F10-tumor growth progression in C57BL/6 mice. (B) FC dot-plots depict TRPV1 expression on T cells along with its corresponding bar diagram. (C) Histogram plot of intracellular Ca^{2+} levels in untreated, ConA, or TCR activated in B16F10 tumor-bearing mice as compared to control mice. Fluo-4 AM intensity representing intracellular Ca^{2+} has been expressed as a percentage normalized to resting T cells of control mice. Representative data from three independent experiments are shown. t-test (B) and One-way ANOVA (C) were performed for significance calculation between the groups (ns, non-significant; * $p < 0.05$; *** $p < 0.001$).

5.2. *Synergistic effect of TRPA1 activation and Hsp90 inhibition promotes the suppression of macrophage responses*

Functional TRPA1 channels have been attributed to regulate various immune functions associated with monocytes, macrophages, and T cells, modulating their activation and effector function [262,269,311,312]. Further, TRPA1 has been reported to be associated with lipopolysaccharide (LPS)-mediated inflammatory pathways [313–315], modulates nitric oxide (NO) production [240], and facilitates cell survival through the association of various proteins, including Hsp90 [268,316–318]. Hsp90, a cytoplasmic chaperon protein, has been observed to regulate various cellular processes by regulating different client proteins [319,320]. Moreover, Hsp90 has been shown to modulate different responses associated with immune cells [290,293–298]. However, the possible role of TRPA1 in the Hsp90-associated regulation of immune responses has not been investigated. Accordingly, here we have studied the association of TRPA1 towards Hsp90 inhibition-mediated modulation of immune responses in RAW 264.7 (mouse macrophage cell line), and THP-1 cells (human monocytic cell line) stimulated with LPS-, or phorbol 12-myristate 13-acetate (PMA).

5.2.1. Kinetics (dose and time) of TRPA1 expression in LPS/PMA-stimulated macrophages with or without Hsp90 inhibition

To investigate the dose kinetics of TRPA1 expression in the presence of LPS or PMA with or without 17-AAG, RAW 264.7 cells were incubated with different doses of these reagents, and the expression of TRPA1 was analyzed using FC. Similarly, a time kinetics study with a similar setup has been carried out with different time points. It has been found that the expression of TRPA1 is dose-dependent in the presence of either LPS or PMA, whereas it is dose-independent and reversible with a fixed concentration of LPS/PMA with varied 17-AAG concentrations (**Figure 24**). These results suggest that the

TRPA1 levels are modulated during LPS or PMA stimulation in a dose- and time-dependent manner.
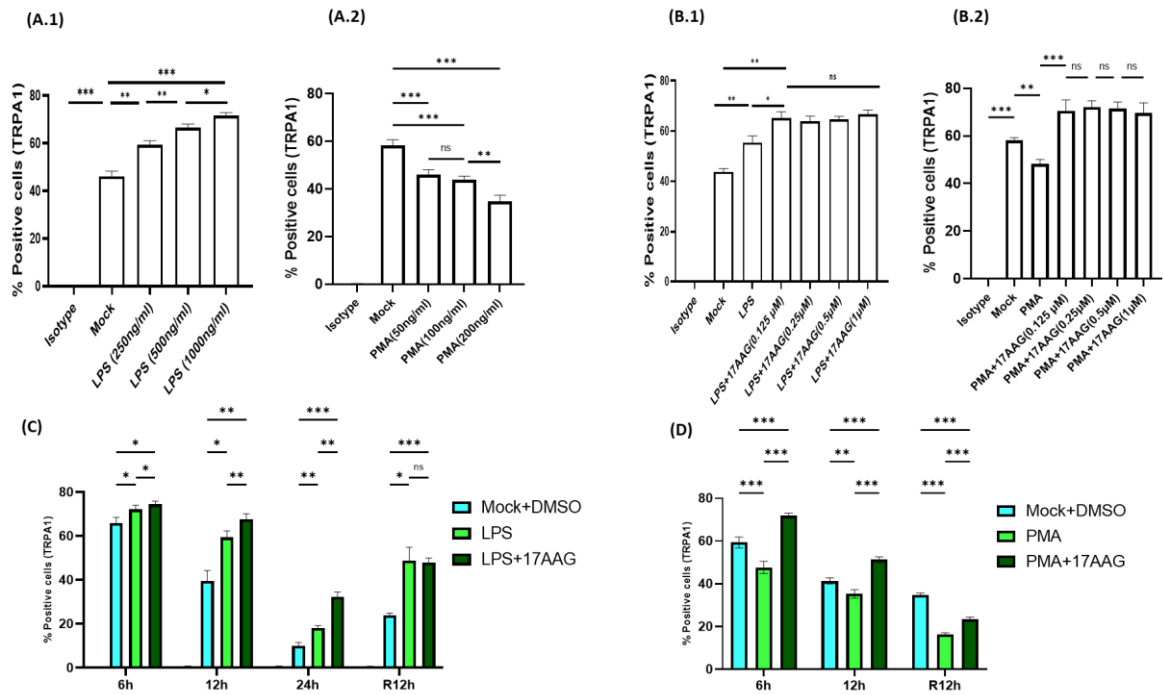
Figure 24: Dose and time kinetics of TRPA1 expression in LPS/PMA-stimulated and Hsp90-inhibited macrophages. (A) Bar graph representing the percentage of positive cells for TRPA1 with different doses of LPS (A.1)/PMA (A.2). (B) Bar graph representing the percentage of positive cells for TRPA1 for differential doses of LPS (B.1) / PMA (B.2) + 17-AAG (0.5 μM). (C) Bar graph comparing the percentage of positive cells for TRPA1 in the presence of LPS or LPS + 17AAG condition or (D) PMA, PMA + 17-AAG at different time points. R represents time points after the reversal of conditions. The data represent the mean ± SD of three independent experiments. One-way ANOVA was used for A and B, and two-way ANOVA was used for C. Differences between groups with a p-value less than 0.05 were considered statistically significant (ns, non-significant; *, $p < 0.05$; **, $p < 0.01$; ***, $p < 0.001$).

5.2.2. Cell viability assay for TRPA1 modulators (AITC and HC-030031) in Hsp90 inhibitor in macrophages

To study the cellular cytotoxicity of TRPA1 modulators (AITC and HC-030031) and Hsp90 inhibitor (17-AAG), RAW 264.7 cells were treated with different doses of these modulators, and cell viability was determined via FC using 7-AAD staining (**Figure 25**). First, it was found that more than 90% of the cells were viable at 0.5 μM concentration of 17-AAG, which was followed in further experiments. Next, the cytotoxicity levels of the TRPA1-specific modulators were assessed by 7-AAD staining via FC. The cells were treated with different concentrations of the serially diluted TRPA1 modulators HC-030031 (40, 20, 10, 5 μM) and AITC (40, 20, 10, 5 μM) in the presence of 17-AAG. DMSO was used as solvent control. It was observed that more than 95% of the cells were viable at 10 and 5 μM of HC-030031 + 17-AAG (0.5 μM), and similar results were observed at 20, 10, and 5 μM of AITC + 17-AAG (0.5 μM). Hence, 10 μM of AITC and 10 μM of HC-030031 were used for further experiments.

Figure 25: Cytotoxicity of TRPA1 modulators (AITC and HC-030031) in Hsp90-inhibited macrophages. RAW 264.7 cells were treated with different doses of 17-AAG or AITC and HC-030031 in the presence of 0.5 μM of 17-AAG. Cells were harvested at 24 h
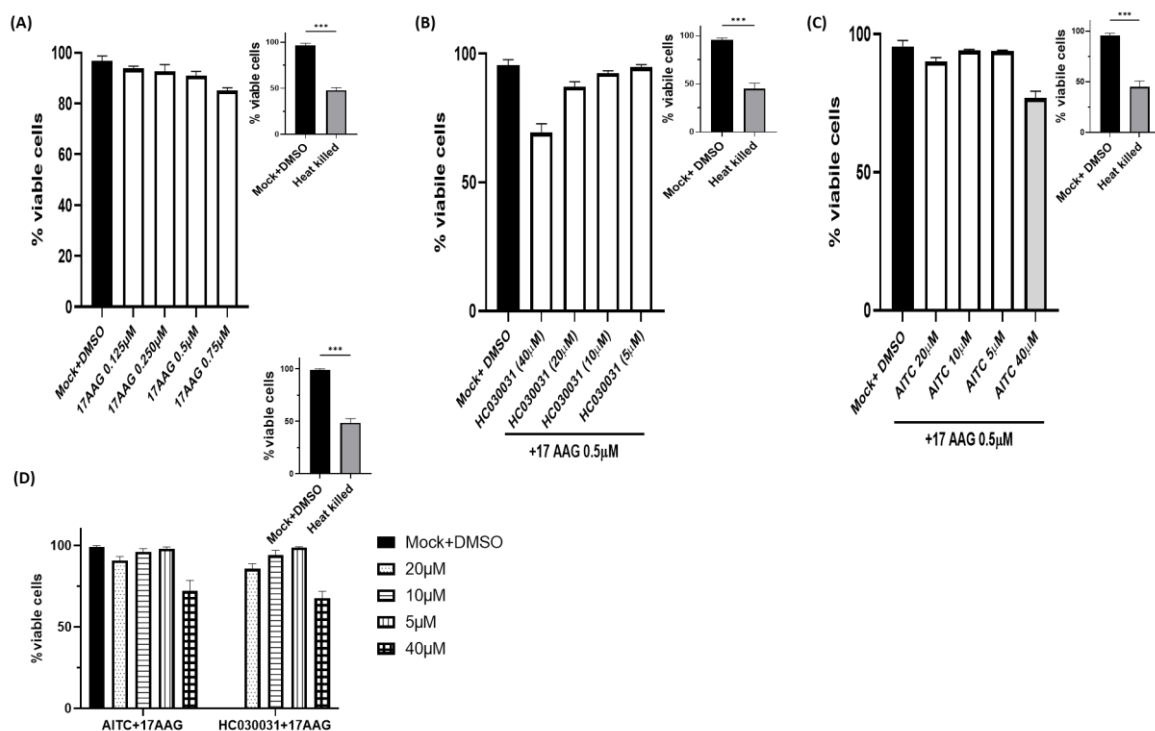
and immediately stained with 7-AAD and analyzed via FC. (A) Bar graph showing the percentage of viable RAW 264.7 cells at different doses of 17-AAG. (B) Bar graph showing the percentage of viable RAW 264.7 cells at different doses of AITC and (C) HC-030031 in Hsp90-inhibited macrophages. (D) bar graph showing the percentage of viable RAW 264.7 cells at different concentrations of AITC and HC-030031 with 17-AAG (0.5 µM). The data represent the mean ± SD of three independent experiments. One-way ANOVA has been performed for statistical significance analysis. Differences between groups with a p-value < 0.05 were considered statistically significant (***, $p < 0.001$).

5.2.3. TRPA1 is upregulated in Hsp90-inhibited and LPS-stimulated macrophages

TRPA1 is associated with a wide range of cellular and pathophysiological conditions [264,267,321]. It has a protective role in macrophage-mediated inflammation in several inflammatory diseases [232,244,259,266,272,322,323]. The Hsp90 inhibitor used in the study is 17-AAG, which is accredited as a potential anti-inflammatory agent during LPS stimulation in macrophages via blockade of TLR4 signaling pathways [166,299]. To investigate a possible association between TRPA1 and Hsp90-inhibition mediated impairment of inflammation in macrophages, RAW 264.7 cells or THP-1 macrophages were treated with either LPS/PMA or 17-AAG or together. The working concentration of LPS, PMA, and 17-AAG used were 500 ng/mL (as reported in the literature), 100 ng/ml (as reported in the literature), and 0.5 µM, respectively. These cells were then harvested, stained, and analyzed to check TRPA1 expression levels via FC (**Figure 26**). The TRPA1 antibodies used are specific for mouse TRPA1 proteins and the specificity was tested using blocking peptides (data not shown). The percentage of cells positive for TRPA1 was observed to be increased significantly in LPS-stimulated RAW 264.7 cells (83.4 ± 1.73%) as compared to resting RAW (mock) 264.7 cells (55.4 ± 3.73%) (**Figure 26 A**). Further, in macrophages treated with both 17-AAG and LPS, the TRPA1 levels were augmented

(94.6 ± 1.67%). Similarly, it was found that the percentage of cells positive for TRPA1 decreased significantly in PMA-stimulated RAW 264.7 cells (48.5 ± 1.74%) as compared to resting RAW 264.7 cells (59.5 ± 2.19%). Furthermore, in macrophages treated with both 17-AAG and PMA, the TRPA1 levels were higher (72.2 ± 1.90%) (**Figure 26 A**). The samples from each condition were assessed for TRPA1 protein quantification via Western blot. The highest band intensity for TRPA1 was obtained in LPS/PMA stimulated and 17-AAG treated conditions (**Figure 26 B.1 and B.2**). The THP-1 macrophages also followed a similar trend with reaching maximum TRPA1 levels in Hsp90-inhibited and LPS-stimulated macrophages (82.8 ± 2.53%), trailed by LPS-stimulated macrophages (69.7 ± 2.72%) and resting macrophages (56.6 ± 2.61%). The results indicate a possible modulation of TRPA1 expression in Hsp90-inhibited macrophages during LPS or PMA stimulation.
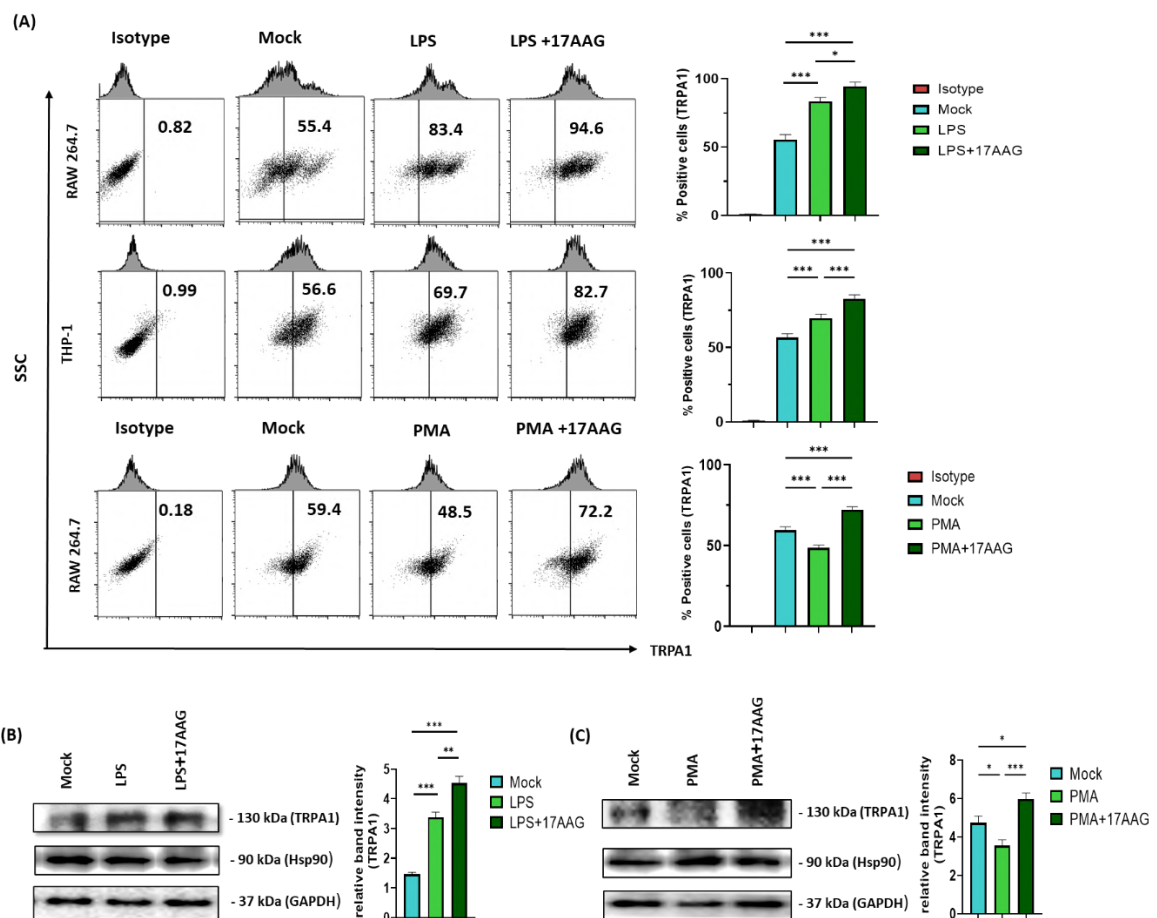
Figure 26: TRPA1 is upregulated in Hsp90-inhibited and LPS- or PMA-stimulated macrophages. Cells were treated with either LPS (500ng/ml, both RAW 264.7 and THP-1 macrophages) or PMA (100ng/ml, only in RAW 264.7) alone or together with 17-AAG for 6h. (A) FC dot-plot and bar graphs depicting the percentage of positive cells for TRPA1 in mock, LPS/PMA, and17-AAG + LPS/PMA (B) Western blot analysis and corresponding bar graphs of TRPA1 expression in RAW 264.7 cells stimulated with 500ng/ml LPS (B.1), 100ng/ml PMA (B.2), and 0.5µM 17-AAG + LPS/PMA for 6h. The data represent the mean ± SD of three independent experiments. Differences between groups with a p-value < 0.05 were considered statistically significant (*, $p < 0.05$; **, $p < 0.01$; ***, $p < 0.001$).

5.2.4. TRPA1 regulates the activation of Hsp90-inhibited macrophages

To determine whether TRPA1 has any role in regulating the activation of Hsp90-inhibited macrophages, cell surface expression of MHCII and CD80/86 were analyzed via FC; RAW 264.7 were stimulated with LPS or PMA in presence of TRPA1 modulators, and 17-AAG. The cells were harvested at 6 h post-stimulation, immunolabelled with MHCII, CD80, and CD86 antibodies, followed by their acquisition and analysis via FC. The expression levels of MHCII, CD80, and CD86 were represented in fold change compared to the isotype control (**Figure 27**). It was observed that inhibition of Hsp90 significantly decreases the expression of MHCII (6.99 ± 0.51), CD80 (17.4 ± 0.72), and CD86 (24.4 ± 0.94) as compared to the LPS stimulated cells (MHCII: 10.40 ± 1.23, CD80: 21.2 ± 1.14 and CD86: 28.1 ± 1.2). Furthermore, the pharmacological inhibition of TRPA1 with HC-030031 significantly downregulated the effect of Hsp90 inhibition (MHCII: 9.85 ± 0.87, CD80: 20.5 ± 0.68, and CD86: 30.3 ± 1.65) as compared to LPS + 17-AAG. Conversely, TRPA1 activation with AITC significantly enhanced the Hsp90-mediated downregulation of MHCII (4.63 ± 0.51), CD80 (15.2 ± 0.58), and CD86 (20.7 ±

1.09) as compared to LPS + 17-AAG (**Figure 27 A**). Similarly, It was observed that Hsp90 inhibition has significantly downregulated the expression of MHCII (7.90 ± 0.17), CD80 (11.1 ± 0.32), and CD86 (3.46 ± 0.16) as compared to the control PMA-stimulated cells (MHCII: 9.13 ± 0.195, CD80: 12.8 ± 0.59 and CD86: 3.95 ± 0.14). Further pharmacological inhibition of TRPA1 with HC-030031 significantly reduced the effect of Hsp90 inhibition (MHCII: 9.65 ± 0.73, CD80: 14.1 ± 0.55, and CD86: 3.98 ± 0.13) as compared to PMA + 17-AAG. Conversely, TRPA1 activation with AITC has significantly enhanced the Hsp90-mediated downregulation of MHCII (6.50 ± 0.424), CD80 (9.87 ± 0.06), and CD86 (3.01 ± 0.05) as compared to PMA + 17-AAG (**Figure 27 B**). These results indicate an important role of TRPA1 in the suppression of activation markers of macrophages, i.e., MHCII, CD80, and CD86, in Hsp90-inhibited conditions in the presence of LPS or PMA stimulation.
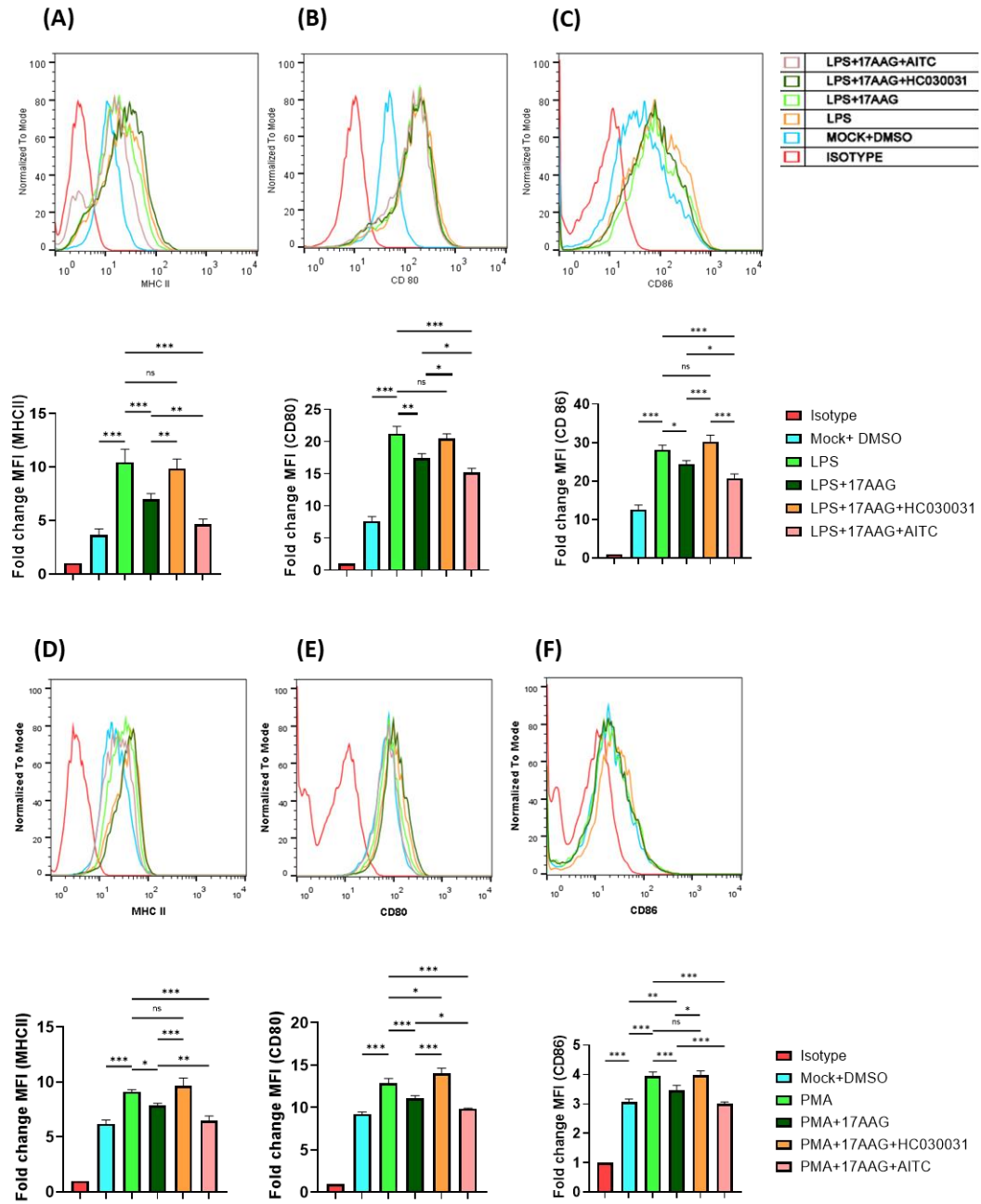
Figure 27: TRPA1 regulates the activation of macrophages in Hsp90-inhibited conditions. RAW 264.7 cells were treated with different conditions of 500ng/ml LPS/100ng/ml PMA, 0.5μM 17-AAG, 10μM HC030031, or 10μM AITC and harvested at 12 h. FC histogram depicting fold change in MFI of MHCII (A.1, B.1), CD80 (A.2, B.2), and CD86 (A.3, B.3) of macrophages treated with LPS (A-series) or PMA (B-series) along with their respective bar graphs. The data represent the mean ± SD of three independent experiments.

Differences between groups with a p-value < 0.05 were considered statistically significant (ns, nonsignificant; *, $p < 0.05$; **, $p < 0.01$; ***, $p < 0.001$).

5.2.5. TRPA1 impairs the nitric oxide (NO) production in Hsp90-inhibited macrophages

Hsp90 is an active modulator of reactive nitrogen species (RNS) and reactive oxygen species (ROS) [324,325]. To investigate the regulatory effect of TRPA1 in regulating the NO production by 17-AAG-mediated Hsp90 inhibited condition, RAW 264.7 and THP-1 macrophages were stimulated with LPS or PMA in the presence of TRPA1 modulators and 17-AAG. Griess assay was performed from the cell supernatants to assess the nitrite, a breakdown product of NO [326] (**Figure 28**). Upon LPS stimulation, it was observed that the nitrite production was upregulated at 24 h (78.7 ± 8.39 µM) as compared to the untreated cells (9.59 ± 0.831 µM). Further, upon Hsp90 inhibition with 17-AAG, the nitrite production was significantly downregulated (53.6 ± 2.42 µM). Surprisingly, in the presence of either HC-030031 (21.58 ± 1.42) or AITC (5.38 ± 0.667 µM), the NO levels decreased significantly (**Figure 28 A**). This trend was observed at 12 h, while no significant changes in NO production were observed at 6 h post-stimulation. A similar scenario was observed with THP-1 macrophages stimulated with LPS. Activation of TRPA1 along with 17-AAG (10.3 ± 0.6 µM) significantly impaired the NO production compared to the LPS 17.2 ± 0.891 µM) and LPS + 17-AAG (14.6 ± 0.97 µM) at 24 h conditions (**Figure 28 B**). Additionally, a significant uprise in nitrite production was observed in macrophages treated with PMA at 12 h and 24 h. Furthermore, TRPA1 activation diminished the nitrite production in 17-AAG treated and PMA stimulated macrophages successfully compared to the PMA and PMA + 17-AAG controls at 12 h and 24 h. Surprisingly no significant changes were observed with HC-030031 + 17-AAG conditions compared to 17-AAG control in PMA-stimulated macrophages (**Figure 28 C**).

These results indicate that TRPA1 activation augments the downregulation of NO production via Hsp90 inhibition in LPS/PMA-stimulated macrophages.
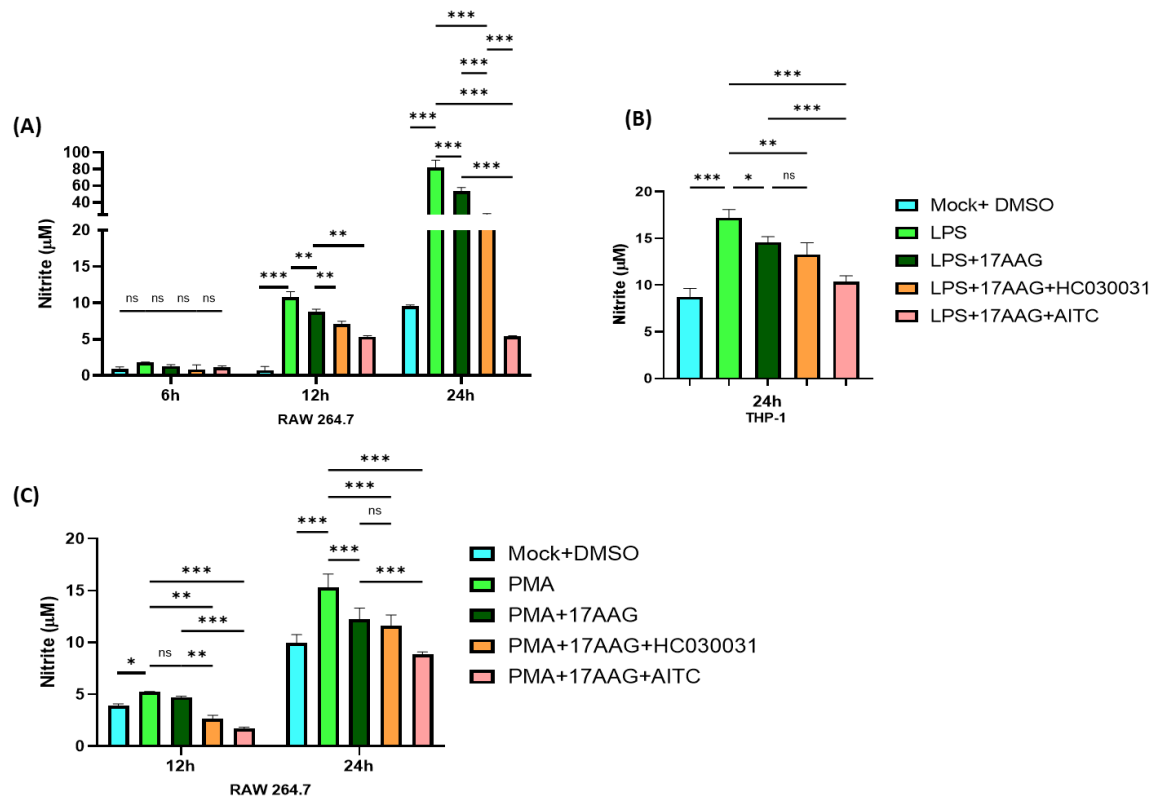
Figure 28: TRPA1 regulates the modulation of nitric oxide (NO) production in Hsp90-inhibited macrophages. RAW 264.7 and PMA-differentiated THP-1 cells were treated with different conditions of 500ng/mL LPS or 100ng/mL PMA, 0.5μM 17-AAG, 10μM HC030031, or 10μM AITC, and the supernatant was collected at 6 h, 12 h, and 24 h. Bar graph depicting nitrite production from RAW 264.7 cells treated with LPS (A) or PMA (C) or THP-1 macrophages treated with LPS at (B). The data represent the mean ± SD of three independent experiments. Differences between groups with a p-value < 0.05 were considered statistically significant (ns, nonsignificant; *, $p < 0.05$; **, $p < 0.01$; ***, $p < 0.001$).

5.2.6. TRPA1 enhances the Hsp90 inhibition-mediated downregulation of pro-inflammatory cytokine production in LPS or PMA-stimulated macrophages

Hsp90 has been reported to be essential for pro-inflammatory cytokine production by macrophages [327]. To investigate the regulatory effect of TRPA1 in regulating the pro-inflammatory cytokine production by 17-AAG-mediated Hsp90 inhibited condition, RAW 264.7 cells were subjected to LPS or PMA stimulation under differential conditions of TRPA1 modulation and 17-AAG treatment. The culture supernatant was assessed for TNF and IL-6 cytokine release profiles (**Figure 29**). In 17-AAG-mediated Hsp90 inhibited and LPS- or PMA-stimulated macrophages, the TNF and IL-6 levels reduced significantly at 6 h and 24 h post-LPS-stimulation compared to only LPS or only PMA controls. Further, the inhibition of TRPA1 by HC-030031 has increased and restored the pro-inflammatory cytokine production in Hsp90-inhibited and LPS-stimulated macrophages, nullifying the effect of 17-AAG as the TNF and IL-6 production of LPS + 17-AAG + HC-030031 or PMA + 17-AAG + HC-030031 samples were comparable to only LPS control. Conversely, activation of TRPA1 in the LPS + 17-AAG + AITC or PMA + 17-AAG + AITC conditions alleviated the pro-inflammatory cytokine production compared to Hsp90-inhibited and LPS- or PMA-stimulated macrophages (**Figure 29**). The TNF and IL-6 production were significantly downregulated compared to LPS or PMA, LPS + 17-AAG, and PMA + 17-AAG samples. Furthermore, AITC administration in LPS-stimulated macrophages could impair TNF and IL-6 production; however, HC-030031 could not significantly change LPS-stimulated macrophages (data not shown). Similar results were observed with LPS-stimulated THP-1 macrophages at 24 h (**Figure 29 B**). These results indicate an important role of TRPA1 in the development of anti-inflammatory responses in Hsp90-inhibited macrophages.
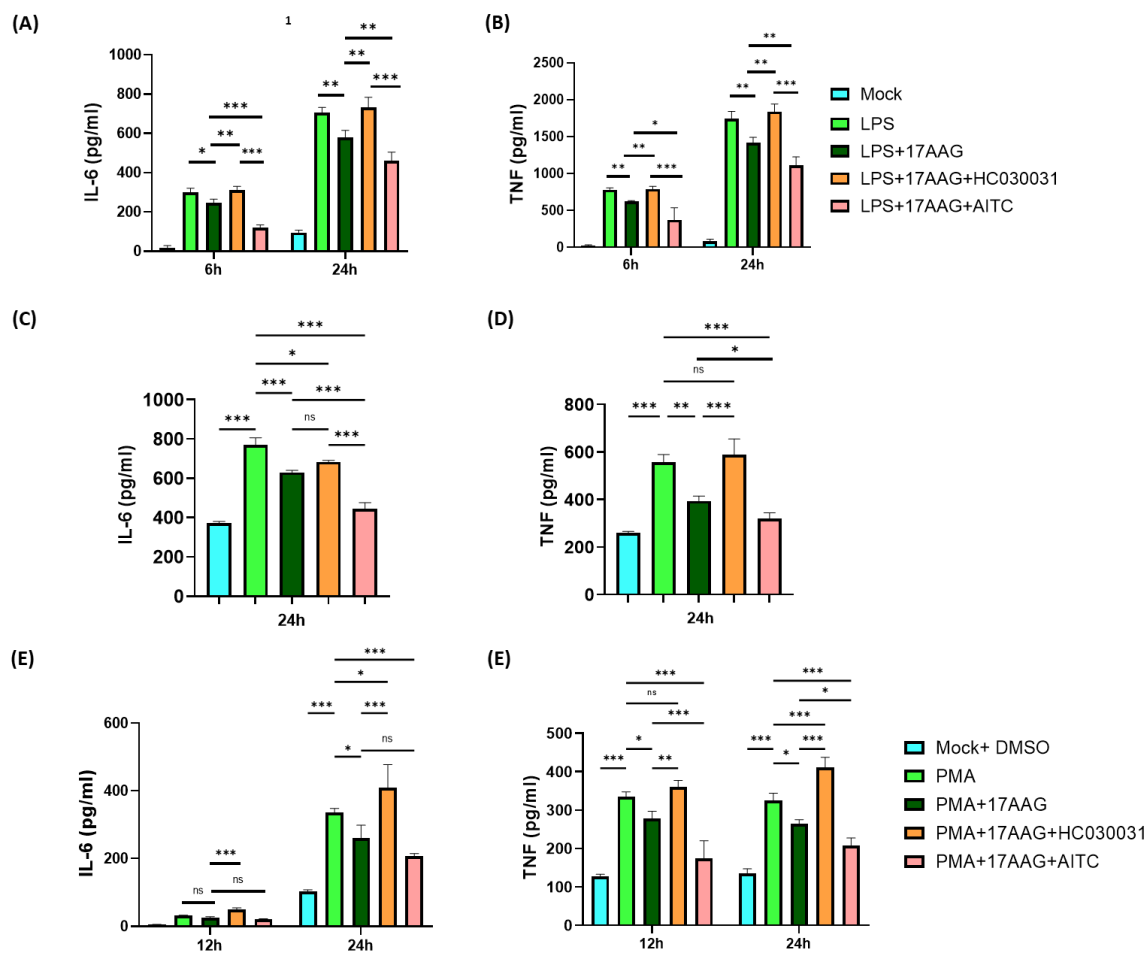
Figure 29: TRPA1 modulates inflammatory cytokine responses in activated macrophages. RAW 264.7 or PMA-differentiated THP-1 cells were subjected to different conditions of 500ng/ml LPS/100ng/ml PMA, 0.5μM 17-AAG, 10μM HC030031, or 10μM AITC, and the supernatant was collected at 6 h and 24 h and assessed for cytokine profile. Bar graph representing IL-6 (A.1, B.1, C.1) and TNF (A.2, B.2, C.2) levels in RAW 264.7 cells stimulated with either LPS (A)/PMA (C), and THP-1 cells stimulated with LPS (B). The data represent the mean ± SD of three independent experiments. Differences between groups with a p-value < 0.05 were considered statistically significant (ns, nonsignificant; *, p < 0.05; **, p < 0.01; ***, p < 0.001).

5.2.7. TRPA1 modulates the Hsp90 inhibition-mediated downregulation of MAPK activation during LPS stimulation in macrophages

Hsp90 has been well-attributed as a regulator of various signaling complexes of inflammation and associated responses [328]. Hsp90 and inhibitors of Hsp90 have been reported to be associated with the activation of ERK-MAPK signaling pathways and SAPK/JNK pathways in various immune models [329,330]. To investigate the role of TRPA1 in Hsp90-mediated regulation in MAPK pathways, RAW 264.7 cells were subjected to LPS (500 ng/mL) stimulation under differential conditions of TRPA1 modulators and 17-AAG for 15 min. Samples were collected and assessed to quantify signaling proteins, p38-MAPK, ERK 1/2, SAPK/JNK, and their respective phosphorylated proteins via Western blot (**Figure 30**). Interestingly, it was observed that Hsp90 inhibition via 17-AAG has significantly downregulated the LPS-induced p-p38-MAPK, p-ERK 1/2, and p-SAPK/JNK expression. Further, this development via 17-AAG was reversed with TRPA1 inhibition via HC-030031 treatment. The TRPA1 activation via AITC successfully diminished the expression of the proteins and signaling further compared to the respective 17-AAG + LPS and LPS conditions (**Figure 30**). These results indicate that the TRPA1 might be required for Hsp90 inhibition-mediated regulation of MAPK signaling cascades.
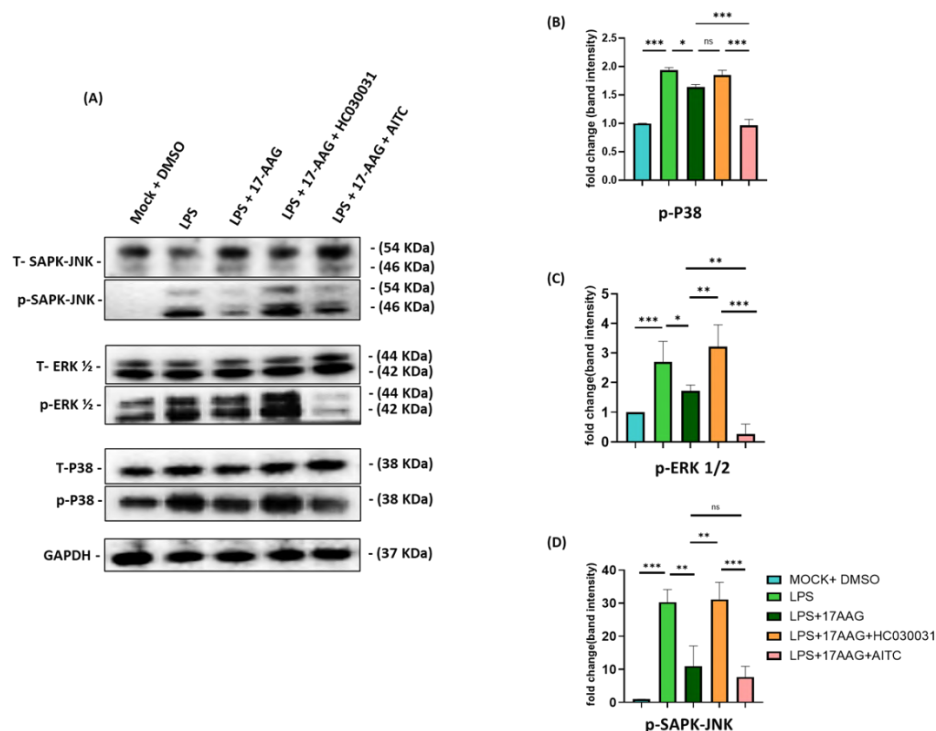
Figure 30: TRPA1 regulates the Hsp90 inhibition-mediated downregulation of MAPK signaling in LPS-stimulated macrophages. RAW 264.7 cells were subjected to different conditions of 500ng/ml LPS, 0.5μM 17-AAG, 10μM HC030031, or 10μM AITC, and harvested at 15 min and assessed for intracellular signaling proteins p38-MAPK, ERK 1/2, SAPK-JNK and their respective phosphorylated proteins via western blot. (A) Western blot images from the samples represent p38-MAPK, ERK 1/2, SAPK-JNK, and their respective phosphorylated proteins. Bar graph representing the fold change in band intensity of phospho-proteins p-p38-MAPK (B), p-ERK 1/2 (C), and p-SAPK-JNK (D) normalized to the corresponding GAPDH controls. The data represent the mean ± SD of three independent experiments. The data represent the mean ± SD of three independent experiments. Differences between groups with a p-value < 0.05 were considered statistically significant (ns, nonsignificant; *, p < 0.05; **, p < 0.01; ***, p < 0.001).

5.2.8. TRPA1 modulates Hsp90 inhibition-mediated apoptosis in activated macrophages

Hsp90 has been found to be involved in cell survival during various inflammatory and cancer models [331,332]. Additionally, our group has reported that Hsp90 inhibition by 17-AAG downregulates the CHIKV-induced apoptosis in host macrophages [302]. To investigate the regulatory role of TRPA1 in Hsp90 inhibition-mediated developments in LPS-induced apoptosis of macrophages, if any, RAW 264.7 cells were incubated with differential conditions of TRPA1 modulators, 17-AAG, and LPS or PMA and assessed for cell death. We have performed cell-death analysis (Annexin V and 7-AAD staining) via FC. The cells were harvested at 5 h and 24 h post-stimulation and assessed for apoptosis via Annexin V and 7-AAD staining, followed by FC analysis (**Figure 31**). We have found that cell death was increased significantly in LPS-stimulated macrophages at 5 h (12.2 ± 1.02%) and further augmented at 24 h (50.8 ± 2.30%) post-stimulation as compared to

untreated cells at 5 h (2.85 ± 0.71%) and 24 h (11.1 ± 2.87%). As expected, it was significantly diminished with 17-AAG administration at 5 h (9.65 ± 0.55%) and 24 h (40.1 ± 1.05%) compared to LPS-treated cells. Interestingly, the TRPA1 inhibition via HC-030031 and 17-AAG has significantly upregulated at both 5 h and 24 h (17.6 ± 1.40% and 51.1 ± 3.14%), the apoptosis compared to LPS + 17-AAG condition. Conversely, TRPA1 activation via AITC has dramatically diminished the apoptosis at 5 h and 24 h (7.17 ± 0.36%) and (25.1 ± 3.36%). Activation of TRPA1 via AITC exhibited an anti-apoptotic effect in LPS-stimulated macrophages as it diminished cell death compared to LPS-stimulated cells. However, HC-030031 has not modulated the cell death in LPS-stimulated macrophages (data not shown). Similar results were observed in the PMA-induced apoptosis of macrophages. RAW 264.7 cells treated with PMA (49.1 ± 1.46%) were susceptible to apoptosis at 24 h compared to untreated cells (19.4 ± 2.90%). The highest percentage of apoptotic cells at 24 h was observed in samples treated with PMA + 17-AAG + HC-030031 (60.9 ± 3.16%) and the lowest in cells treated with PMA + 17-AAG + AITC (29.2 ± 0.872%) compared to PMA + 17-AAG (41.7 ± 1.35%) and PMA controls (49.1 ± 1.46%) (**Figure 31 C**). These samples were also assessed for caspase 3 protein levels via western blot. Band intensity levels were the lowest for cleaved caspase 3 in LPS/PMA + 17-AAG + HC-030031 samples compared to LPS/PMA, LPS/PMA + 17-AAG, and LPS/PMA + 17-AAG + HC-030031. Inhibition of TRPA1 with HC-030031 augmented the cleaved caspase 3 levels to the respective LPS/PMA samples, nullifying the effect of 17-AAG, indicating the important role of TRPA1 towards regulating the Hsp90-associated apoptosis of macrophages.
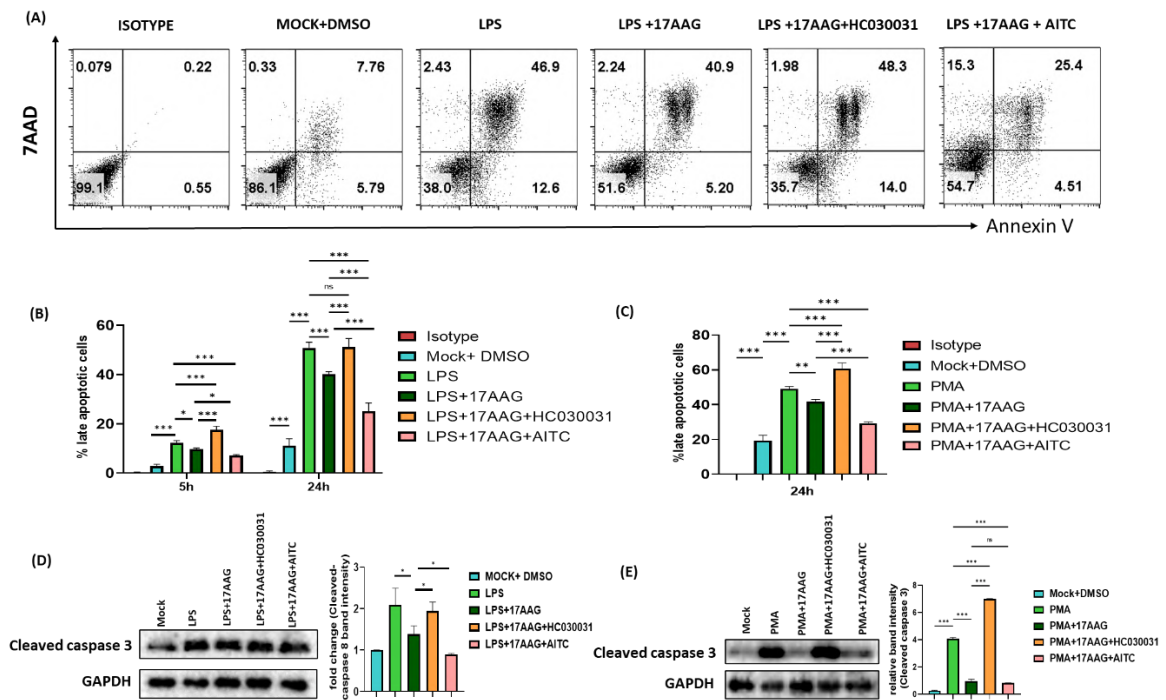
Figure 31: TRPA1 regulates apoptosis in Hsp90-inhibited and LPS/PMA-stimulated macrophages. RAW 264.7 cells were treated with different conditions of 500ng/ml LPS/100ng/ml PMA, 0.5μM 17-AAG, 10μM HC030031, or 10μM AITC. Cells were harvested at 5 h and 24 h. Heat-killed cells were used as a positive control. (A) FC dot plot representing the percentage of positive cells for Annexin V and 7-AAD at 24 h. Double-positive cells were considered either dead or late apoptotic. Representative bar graphs of the sample stimulated with LPS (B.1)/PMA (B.2). (C) Western blot image and bar graph representing fold change in band intensity for cleaved caspase 3 (C.1, C.2) for the respective samples. The data represent the mean ± SD of three independent experiments. Differences between groups with a p-value < 0.05 were considered statistically significant (ns, nonsignificant; *, $p < 0.05$; **, $p < 0.01$; ***, $p < 0.001$).

5.2.9. TRPA1 is an important contributor to intracellular Ca^{2+}-influx in Hsp90-inhibited and LPS-stimulated macrophages

Ca^{2+} currents via TRPA1 have been reported to modulate various immune responses and cell fate decisions [262,266,271,272,311,333,334]. Studies have reported that

intracellular Ca^{2+} increases after LPS stimulation [335]. To investigate the regulatory role of TRPA1 in intracellular Ca^{2+}-influx in Hsp90-inhibited and LPS-stimulated macrophages, Ca^{2+}-influx studies via FC were performed. RAW 264.7 cells were stained with Fluo-4 AM, and Ca^{2+}- influx was analyzed via FC continuously for 200s (**Figure 32**). The mean value for every 20s interval was obtained, and two-way ANOVA was carried out for statistical analysis (pairwise comparison and significance are not shown due to technical difficulties in representing comparisons of all the conditions in each interval). The intracellular Ca^{2+} levels were compared before and after the addition of TRPA1 modulators, 17-AAG, and LPS in different conditions. Colorless RPMI media was used as a vehicle. Interestingly, we observed that the Ca^{2+} levels were augmented upon LPS stimulation in macrophages compared to mock or vehicle-treated cells, whereas 17-AAG administration could not evoke any changes in Ca^{2+}-influx of its own (data not shown). Additionally, 17-AAG treatment along with LPS has significantly diminished the intracellular Ca^{2+} levels compared to the LPS-stimulation control. Similarly, HC-030031 administration reduced the elevated calcium levels during LPS stimulation, whereas the TRPA1 activation via AITC has upregulated it. HC-030031 treatment along with 17-AAG and LPS resulted in reduced Ca^{2+} levels compared to LPS only, LPS + 17-AAG, LPS + HC-030031. Additionally, the activation of TRPA1 via AITC along with 17-AAG and LPS resulted in elevated Ca^{2+} levels compared to LPS, or 17-AAG, LPS + 17-AAG, and LPS + AITC treated cells (**Figure 32**). These results indicate that TRPA1 might be an important contributor to Ca^{2+} influx in Hsp90-inhibited and LPS-stimulated macrophages.
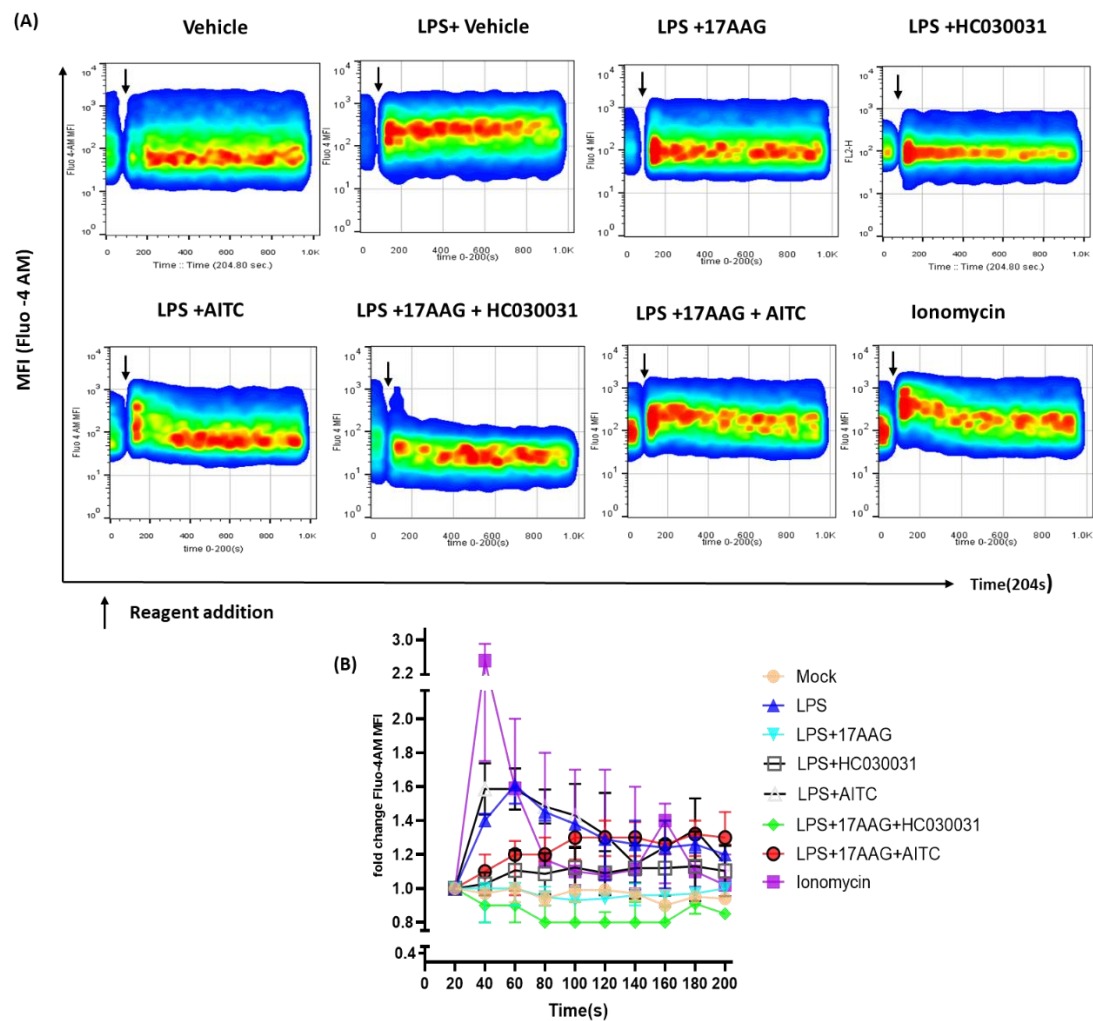
Figure 32: TRPA1 regulates intracellular calcium influx in LPS-stimulated and Hsp90-inhibited macrophages. RAW 264.7 cells were treated with Fluo-4 AM and assessed via FC for intracellular calcium levels upon combinatorial treatment with either Ionomycin, vehicle, LPS, LPS + 17-AAG, LPS + 17-AAG + HC-030031, and LPS + 17-AAG + AITC. (A) smoothened pseudo-color (red: high density; blue: Low density) dot plot representing time-lapse kinetics of intracellular calcium influx. (B) Representative line graph depicting fold changes in mean Fluo-4 intensity. The data represent the mean ± SD of three independent experiments.

5.3. *TRPV1 and TRPA1 differentially regulate Telmisartan-driven suppression of T cells*

TRPV1 and TRPA1 have been shown to functionally regulate T cell activation and effector functions and attribute towards Ca^{2+} flux [227,246,316,317]. Telmisartan (TM) (an angiotensin receptor blocker (ARB)), an anti-hypertension drug, has been reported to suppress T cell responses by inhibiting nuclear factor of activated T lymphocytes (NFAT) signaling and tumor necrosis factor-alpha (TNF-α)-induced nuclear factor-kappa B (NF-κB) activation [184,185]. Moreover, the repurposing of TM has been shown to modulate various inflammatory immune diseases through its anti-inflammatory or immunosuppressive effects [186–188]. However, the possible involvement of transient receptor potential (TRP) channels during TM-driven suppression of T cell responses has not been explored yet. In this study, we investigated the potential role of TRPV1 and TRPA1 during TM-driven experimental immunosuppression of T cells.

5.3.1. T cell viability in the presence of TM and different concentrations of TRPV1 and TRPA1 modulators

The cellular cytotoxicity assay in the presence of TM, RTX, BCTC, AITC, and HC in purified mouse T cells was carried out using the trypan blue exclusion method. It was observed that more than 90% of cells were found to be viable at 35 μM of TM, 100 nM RTX, 12.5 μM of AITC, 1.34 μM of BCTC, and 100 μM of HC (**Figure 33**). Accordingly, we chose these concentrations for further experiments. In all the experiments, either heat-killed or UV-treated T cells were used as a positive control.
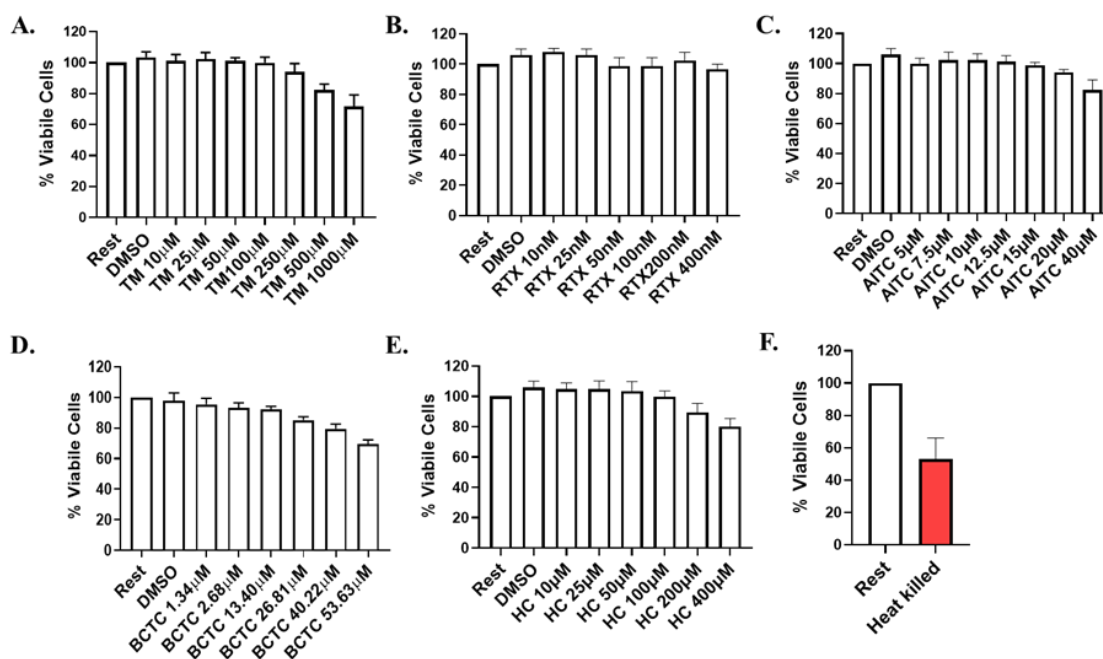
Figure 33: T cell viability in the presence of TM and different concentrations of TRPV1 and TRPA1 modulators. Purified murine T cells were incubated with different concentrations of Telmisartan (TM) (10 – 1000 μM), Resiniferatoxin (RTX) (TRPV1 activator, 25 – 400 nM), Allyl isothiocyanate (AITC) (TRPA1 activator, 5 – 40 μM), 4-(3-Chloro-2-pyridinyl)-N-[4-(1,1-dimethylethyl)phenyl]-1-piperazinecarboxamide (BCTC) (TRPV1 inhibitor, 1.34 – 53.63 μM), and 1,2,3,6-Tetrahydro-1,3-dimethyl-N-[4-(1-methylethyl)phenyl]-2,6-dioxo-7 H-purine-7-acetamide,2-(1,3-Dimethyl-2,6-dioxo-1,2,3,6-tetrahydro-7 H-purin-7-yl)-N-(4-isopropylphenyl)acetamide (HC-030031) (HC) (TRPA1 inhibitor, 10 – 400 μM) for 48 hours. Next, T cells were harvested, and trypan blue exclusion assays were performed to determine the viability of T cells. More than 90% of cells were found to be viable at (A) 35 μM of TM, (B) 100 nM RTX, (C) 12.5 μM of AITC, (D) 1.34 μM of BCTC, and (E) 100 μM of HC. Subsequently, these concentrations were used to carry out further experiments. (F) represents the positive control (heat-killed cells {red bar}; cells were heated at 55 °C for 10 min) for cell death. Bar diagrams represent the mean ± SD of three independent experiments.

5.3.2. Telmisartan (TM) suppresses TCR-induced T cell activation and proliferation

To determine the impact of TM on CD69 and CD25 levels, T cells were pre-incubated with either DMSO or 25 and 35 μM of TM, and experiments were conducted as described in the materials and methods (**Figure 34A – 34F**). No cytotoxicity was observed in the presence of 25 and 35 μM of TM; therefore, these concentrations were selected for further experiments (**Figure 33**). Flow cytometric dot-plots in **Figures 34A** and **34C** represent frequencies of CD69+ve and CD25+ve T cells along with the corresponding bar diagrams in **Figures 34B** and **34C**, respectively. **Figures 34E** and **34F** represent the MFI values of CD69 and CD25 expressions on T cells, respectively. Flow cytometric histograms in **Figure 34G** represent T cell proliferation along with the corresponding bar diagram in **Figure 34H**. Notably, 35 μM of TM significantly downregulated T cell activation (even in the presence of TCR, i.e., in TM+TCR condition) as the frequencies of both CD69+ve (53.7±3.90; $p \leq 0.0001$) and CD25+ve (40.3±3.94; $p \leq 0.0001$) T cells were reduced compared to only TCR (CD69: 72.26±2.36; CD25: 72.33±0.93) (**Figure 34A-34D**). This downregulation was consistent with the MFI values of CD69 (147.33±7.40; $p \leq 0.001$) and CD25 (50.6±3.88; $p \leq 0.0001$) in TM+TCR condition compared to TCR alone (CD69: 226.33±18.87; CD25: 383.33±11.02) (**Figure 34E and 34F**). Next, a T cell proliferation assay was carried out in the presence or absence of TM, revealing a significant downregulation of T cell proliferation in the TM+TCR condition (5.55±0.99; $p \leq 0.0001$) compared to only TCR (75.4±1.74) (**Figure 34G and 34H**).
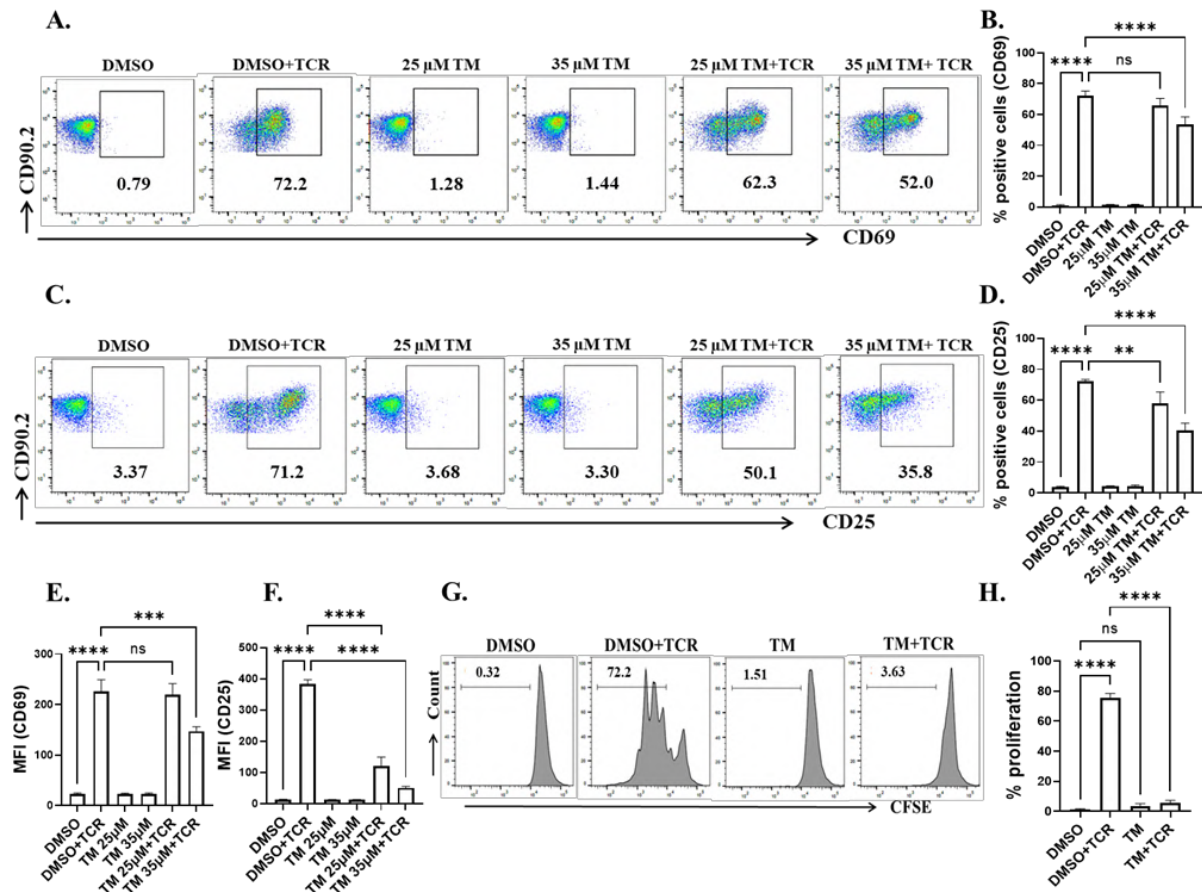
Figure 34: Telmisartan (TM) suppresses TCR-induced T cell activation and proliferation. A-F. Purified murine T cells were pre-incubated with either DMSO or TM (25 or 35 μM) for 1 hour. Cells were then activated with TCR (1 μg/mL of each anti-CD3 and anti-CD28 antibodies) in the presence or absence of TM. Next, cells were harvested and surface stained for CD69 (early activation marker) and CD25 (late activation marker), and analyzed via flow cytometry. Flow cytometric dot-plots of T cells showing frequencies of **(A)** CD69 and **(C)** CD25 positive T cells in different conditions. Bar diagrams (representing the mean ± SD of three independent experiments) showing **(B)** frequency of CD69 positive T cells, **(D)** frequency of CD25 positive T cells, **(E)** mean fluorescence intensity (MFI) of CD69 and **(F)** MFI of CD25. TM at 35 μM concentration downregulates both CD69 and CD25 levels significantly, and this concentration was used in further experiments. **G-H**. Flow cytometric histograms in **(G)** showing T cell

proliferation [proliferation assay of T cells stained with carboxyfluorescein succinimidyl ester (CFSE)] in the presence or absence of TM with or without activation along with the corresponding bar diagram in (H). Statistical analysis: One-way ANOVA; $p \leq 0.05$ was considered statistically significant. ns = non-significant; ** = $p \leq 0.01$; *** = $p \leq 0.001$; **** = $p \leq 0.0001$. The X and Y axes of the flow cytometric dot plots in (A) and (C) denote the log scale from 10^0 to 10^5. For the flow cytometric histograms in (G), the X-axis represents the log scale from 10^2 to 10^5 and the Y-axis denotes the count from 0 to 100.

5.3.3. Elevation of cell surface TRPV1 and TRPA1 on T cells during TM-mediated immunosuppression

To assess the cell surface expressions of TRPV1 and TRPA1 in TM-induced immunosuppressed T cells, purified murine T cells were pre-incubated with either DMSO or TM, and experiments were conducted as described in the materials and methods. Flow cytometric histograms in **Figures 35A** and **35C** represent MFIs of TRPV1 and TRPA1 expressions on T cells along with their corresponding bar diagrams in **Figures 35B** and **35C**, respectively. Flow cytometric density plots in **Figures 35E** and **35G** represent the frequencies of TRPV1+ve and TRPA1+ve T cells along with the corresponding bar diagrams in **Figures 35F** and **35H**, respectively. Interestingly, the frequencies of both TRPV1+ve and TRPA1+ve T cells were significantly elevated in TM+TCR (TRPV1: 39.2±1.34, $p \leq 0.0001$; TRPA1: 48.9±0.37, $p \leq 0.001$) and TM+ConA (TRPV1: 43.13±0.85, $p \leq 0.0001$; TRPA1: 53.73±0.89, $p \leq 0.001$) conditions compared to only TCR (TRPV1: 26.46±1.79; TRPA1: 43.1±1.08) or only ConA (TRPV1: 31.73±0.83; TRPA1: 47.86±0.40), respectively (**Figure 35E-35H**). Similar trends were observed for the MFIs of TRPV1 and TRPA1 in TM+TCR (TRPV1: 494.33±11.58, $p \leq 0.0001$; TRPA1: 145.33±4.92, $p \leq 0.001$) and TM+ConA (TRPV1: 538±8.52, $p \leq 0.0001$; TRPA1: 158.33±10.07, $p \leq 0.0001$) conditions as compared to only TCR (TRPV1: 316.33±6.84;

TRPA1: 120.5±6.5) or only ConA (TRPV1: 312.66±6.94; TRPA1: 120.33±6.18) controls, respectively (**Figure 35A-35D**).
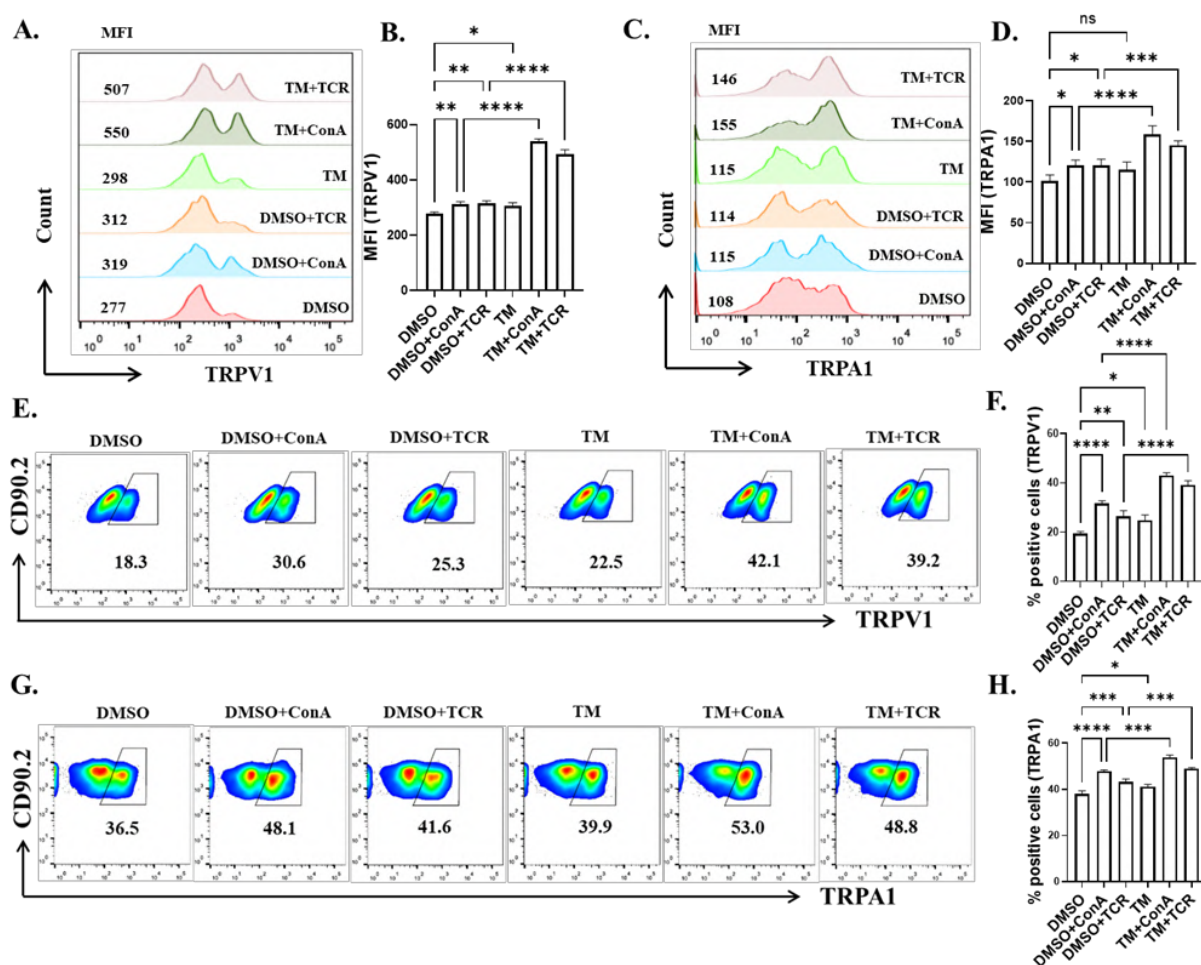
Figure 35: Elevation of cell surface TRPV1 and TRPA1 on T cells during TM-mediated immunosuppression. Purified murine T cells were pre-incubated with either DMSO or TM (35 μM) for 1 hour. Cells were then activated with either TCR (1 μg/mL of each anti-CD3 and anti-CD28 antibodies) or with ConA (5 μg/mL) stimulation in the presence or absence of TM and incubated for 48 hours. Next, cells were surface stained for TRPV1 and TRPA1 and analyzed by flow cytometry. Flow cytometric histograms of T cells show the mean fluorescence intensities (MFIs) of **(A)** TRPV1 and **(C)** TRPA1. Bar diagrams (representing the mean ± SD of 3 independent experiments) in **(B)** and **(D)** represent the MFIs of TRPV1 and TRPA1, respectively. Percentages of TRPV1 positive and TRPA1

positive T cells are shown in **(E)** and **(G)**, respectively, along with the corresponding bar diagrams in **(F)** and **(H)**. Statistical analysis: One-way ANOVA; $p \leq 0.05$ was considered statistically significant. ns = non-significant; * = $p \leq 0.05$; ** = $p \leq 0.01$; *** = $p \leq 0.001$; **** = $p \leq 0.0001$. The X and Y axes of the flow cytometric plots in **(E)** and **(G)** denote the log scale from 10^0 to 10^5.

5.3.4. TRPV1 activation during TM-mediated immunoregulation overrides TRPA1-driven suppression of T cell activation and effector cytokine responses

To determine the functional role of TRPV1 and TRPA1 in TM-induced immunosuppressed T cells, TRPV1 and TRPA1 were modulated with different functional modulators (no cytotoxicity was observed in each of the modulator's concentrations used for this study, **Figure 33B-33E**). Experiments were conducted as described in the materials and methods (**Figure 3** and **Figure 4**). Flow cytometric dot-plots in **Figures 3A** and **3F** represent the frequencies of CD69+ve and CD25+ve T cells, respectively. Bar diagrams in Figure 3B and 3G represent the frequencies of CD69+ve and CD25+ve T cells in TRP-activated conditions whereas Figure 3C and 3H represent the frequencies of CD69+ve and CD25+ve T cells in TRP-inhibited conditions, respectively. Bar diagrams in Figure 3D and 3I represent the MFIs of CD69 and CD25 expressions on T cells in TRP-activated conditions whereas **Figure 3E** and **3J** represent the MFIs of CD69 and CD25 expressions on T cells in TRP-inhibited conditions, respectively. It was observed that frequencies of both CD69+ve and CD25+ve T cells were significantly reduced in AITC+TCR (CD69: 47.6±2.49, $p \leq 0.001$; CD25: 41.8±2.29, $p \leq 0.0001$) and AITC+TM+TCR (CD69: 25.86±2.25, $p \leq 0.05$; CD25: 12.26±0.65, $p \leq 0.05$) conditions compared to TCR (CD69: 62±2.72; CD25: 57.4±1.92) and TM+TCR (CD69: 34.83±2.12; CD25: 18.16±0.85), respectively (**Figure 3A, 3B, 3F, and 3G**). RTX+TCR condition (CD69: 60.2±3.08; CD25: 55.26±1.26) showed no suppression of T cell activation, but maintained similar

trends (in TCR and RTX+TCR) of TCR-driven activation (TCR: CD69: 62±2.72; CD25: 57.4±1.92) compared to resting T cells (only DMSO) (CD69: 0.82±0.39; CD25: 1.99±0.43) or AITC+TCR treated T cells (CD69: 47.6±2.49; CD25: 41.8±2.29) (for AITC+TCR, the p-value: for CD69: $p \leq 0.01$; for CD25: $p \leq 0.0001$ respectively, as compared to RTX+TCR (CD69: 60.2±3.08; CD25: 55.26±1.26)). Moreover, the activation of both TRPV1 (by RTX) and TRPA1 (by AITC) in T cells treated with TM and TCR, i.e., in RTX+AITC+TM+TCR (CD69: 36.6±2.62, $p \leq 0.01$; CD25: 20.73±1.61, $p \leq 0.001$) condition partially yet significantly upregulated the frequencies of both CD69+ve and CD25+ve T cells as compared to AITC+TM+TCR (CD69: 25.86±2.25; CD25: 12.26±0.65) (**Figure 3A, 3B, 3F,** and **3G**). However, in the absence of TM, the AITC-driven T cell suppression in the presence of TCR (i.e., in AITC+TCR) as compared to TCR alone or RTX+TCR was not reversed by the RTX+AITC+TCR condition. The partial restoration of T cell activation was only observed in T cells treated with TM and TCR, where TRPV1 activation was found to override TRPA1 activation-driven T cell suppression (i.e., RTX+AITC+TM+TCR was found to restore T cell activation as compared to AITC+TM+TCR). However, no such reversal of T cell activation was observed in TCR-treated T cells (in the absence of TM), where TRPV1 activation was not found to override the TRPA1 activation-driven suppression (i.e., RTX+AITC+TCR did not restore T cell activation as compared to AITC+TCR) of T cells. Corresponding MFIs of CD69 and CD25 are depicted in **Figures 3D** and **3I**. Similar to the frequencies of CD69 and CD25, the MFI values of CD69 and CD25 in RTX+AITC+TM+TCR (CD69: 41.28±3.01, $p \leq 0.01$; CD25: 18.56±1.97, $p \leq 0.05$) condition moderately yet significantly upregulated the MFIs of both CD69 and CD25 expressions in T cells as compared to AITC+TM+TCR (CD69: 27.10±1.53; CD25: 10.90±0.41) (**Figure 3D** and **3I**). However, no reversal effects in the MFIs of CD69 and CD25 expressions were observed in the RTX+AITC+TCR (CD69:

59.73±4.92, non-significant; CD25: 48.10±3.082, non-significant) condition in the absence of TM as compared to AITC+TCR (CD69: 58.90±4.16; CD25: 46.76±3.99). The T cell activation in different conditions, as mentioned above, was further supported by cytokine levels (IFN-γ and TNF) (**Figure 4A** and **4B**). Bar diagrams in **Figure 4A** and **4B** represent the amount of IFN-γ and TNF released by T cells in TRP-activated conditions whereas **Figure 4C** and **4D** represent the amount of IFN-γ and TNF released by T cells in TRP-inhibited conditions, respectively. RTX+AITC+TM+TCR (IFN-γ: 1749±195.3, $p \leq 0.001$; TNF: 223.7±17.46, $p \leq 0.01$) condition partly yet significantly upregulated both IFN-γ and TNF productions by T cells as compared to AITC+TM+TCR (IFN-γ: 1119±153; TNF: 172.8±15.03) (**Figure 4A** and **4B**). However, no reversal effects in IFN-γ and TNF production were observed in the RTX+AITC+TCR (IFN-γ: 1124±129.8, p = ns; TNF: 186.2±22.27, non-significant) condition in the absence of TM as compared to AITC+TCR (IFN-γ: 1180±150.4; TNF: 195.4±17.28). In addition, no such reversal of T cell suppression was observed in the BCTC+HC+TM+TCR condition compared to BCTC+TM+TCR and HC+TM+TCR (**Figure 3A, 3C, 3E, 3F, 3H, 3J, 4C,** and **4D**).
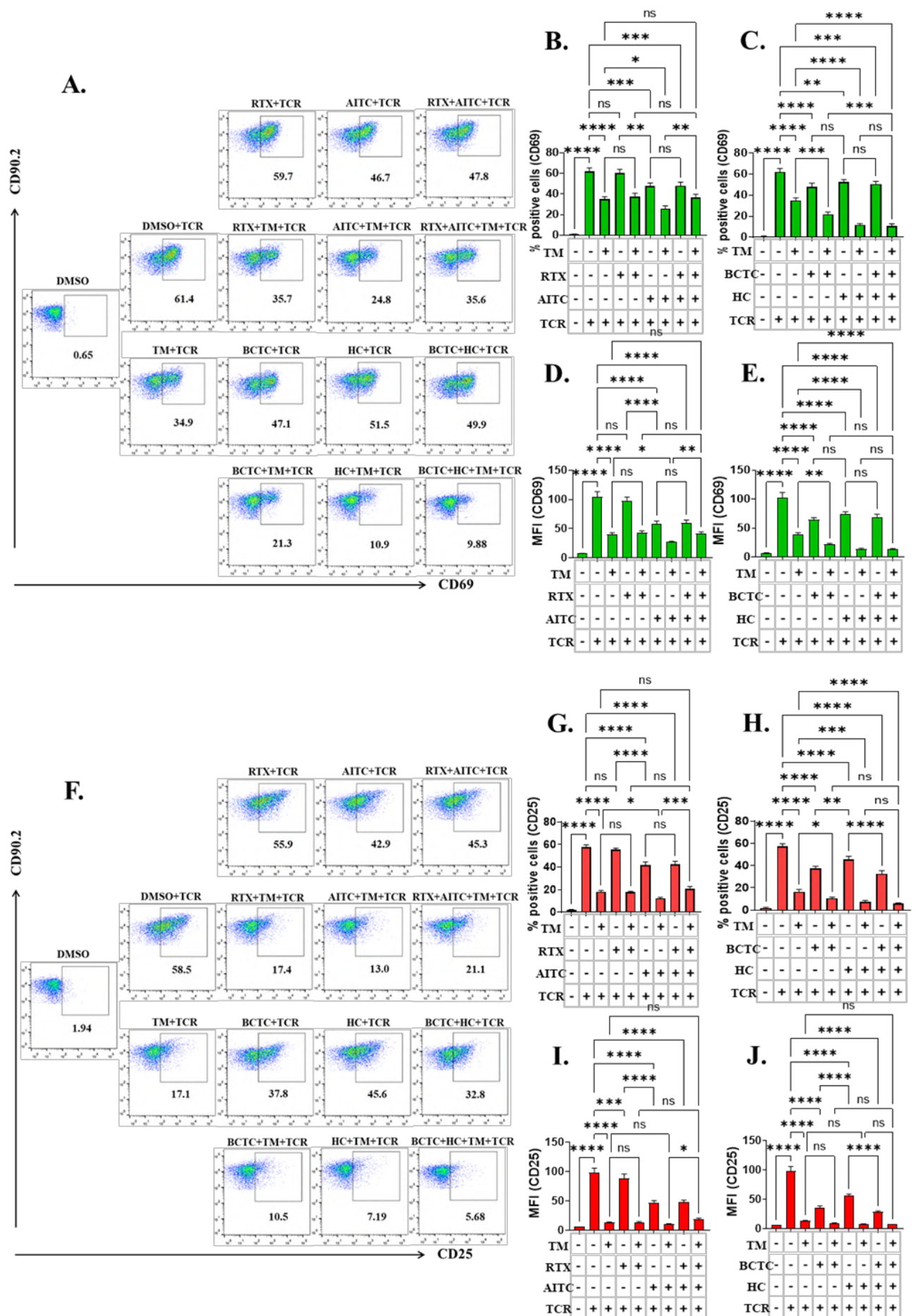
Figure 36: TRPV1 activation during TM-mediated immunoregulation overrides TRPA1-driven suppression of T cell activation. T cells were pre-incubated with RTX (TRPV1 activator, 100 nM), AITC (TRPA1 activator, 12.5 μM), BCTC (TRPV1 inhibitor, 1.34 μM), HC (TRPA1 inhibitor, 100 μM) to activate or inhibit TRPV1 and TRPA1 in the presence or absence of TM (35 μM) for 1 hour. After 48 hours of TCR stimulation (1 μg/mL of each anti-CD3 and anti-CD28 antibody), cells were harvested, surface stained for CD69 and CD25, and analyzed via flow cytometry. Flow cytometric dot-plots of T cells showing frequencies of **(A)** CD69 and **(F)** CD25 positive T cells in different experimental conditions. Bar diagrams (representing the mean ± SD of 3 independent experiments) showing frequency **(B)** and mean fluorescence intensity (MFI) **(D)** of CD69 positive T cells in TRPV1- and/or TRPA1-activated conditions. Bar diagrams showing frequency **(G)** and MFI **(I)** of CD25 positive T cells in TRPV1- and/or TRPA1-activated conditions. Bar diagrams showing frequency **(C)** and MFI **(E)** of CD69 positive T cells in TRPV1- and/or TRPA1-inhibited conditions. Bar diagrams showing frequency **(H)** and MFI **(J)** of CD25 positive T cells in TRPV1 and/or TRPA1-inhibited conditions. In each case, One-way ANOVA was performed. $p \leq 0.05$ was considered statistically significant. ns = non-significant; * = $p \leq 0.05$; ** = $p \leq 0.01$; *** = $p \leq 0.001$; **** = $p \leq 0.0001$. The X and Y axes of the flow cytometric dot plots in **(A)** and **(F)** denote the log scale from 10^0 to 10^5.

Figure 37: TRPV1 activation during TM-mediated immunoregulation overrides TRPA1-driven suppression of effector cytokine production by T cells. T cells were pre-incubated with RTX (TRPV1 activator, 100 nM), AITC (TRPA1 activator, 12.5 µM), BCTC (TRPV1 inhibitor, 1.34 µM), HC (TRPA1 inhibitor, 100 µM) to activate or inhibit TRPV1 and TRPA1 in the presence or absence of TM for 1 hour. After 48 hours of TCR stimulation (1 µg/mL of each anti-CD3 and anti-CD28 antibodies), culture supernatants were collected to quantify cytokine productions by T cells via sandwich ELISA. Bar diagrams (representing the mean ± SD of 3 independent experiments) showing productions of IFN-γ (A) and TNF (B) in TRPV1- and/or TRPA1-activated conditions. Bar diagrams showing productions of IFN-γ (C) and TNF (D) in TRPV1- and/or TRPA1-inhibited conditions. Statistical analysis: One-way ANOVA; $p \leq 0.05$ was considered statistically significant. ns = non-significant; * = $p \leq 0.05$; ** = $p \leq 0.01$; *** = $p \leq 0.001$; **** = $p \leq 0.0001$.

5.3.5. Expression of TRPV1 correlates well with TRPA1 in T cells in different immunological conditions

Correlation analyses were performed to assess the association between surface expressions of TRPV1 and TRPA1, as well as CD69 and CD25 in various experimental conditions (as shown in **Figure 5A**). Frequencies of TRPA1+ve and TRPV1+ve T cells in six different immunological conditions remain highly correlated (r = 0.9771; p ≤ 0.001) (**Figure 5A**). Comparable results were observed for MFIs of TRPA1 and TRPV1 (r = 0.9903; p ≤ 0.001) (**Figure 5B**). To explore the relationship between TRPV1 and TRPA1 in the context of T cell function, a standard pair of immune activation markers, i.e., a correlation between CD69 and CD25, was analyzed in sixteen different experimental conditions (as shown in **Figure 5C**). A high correlation between frequencies of CD69+ve and CD25+ve T cells (r = 0.9442; p ≤ 0.0001) and MFIs of CD69 and CD25 (r = 0.9303; p ≤ 0.0001) in various immunomodulated conditions was observed (**Figure 5C** and **5D**).

Figure 38: Expression of TRPV1 correlates well with TRPA1 in T cells in different immunological conditions. **(A)** Correlation between frequencies of TRPV1+ve with TRPA1+ve T cells in different conditions is shown. **(B)** Correlation between MFIs of

TRPV1 with TRPA1 in different conditions is shown. **(C)** Correlation between frequencies of CD69 with CD25 positive T cells in different conditions is shown. **(D)** Correlation between MFIs of CD69 and CD25 in different conditions is shown. Linear fit and correlation between points were used for the correlation analysis. In each case, the r and p values are indicated.

CHAPTER # 6

Discussion

6. Discussion

6.1. Elevation of TRPV1 expression on T cells during experimental immunosuppression

TRPV1, a vanilloid member of the TRP subfamily, has been well-cited to play an important role in a variety of cellular processes associated with macrophages, dendritic cells, and T cells regulating their effector responses [250,310]. Ca^{2+} plays an important role in T cell activation by integrating various cellular pathways modulating gene expression and function [336,337]. T cell mitogens (ConA), TCR induction, and various immunosuppressive drugs used during transplantation, e.g, cyclosporin A, rapamycin, and tacrolimus (FK506) are observed to increase intracellular Ca^{2+} levels [149,276,277]. TRPV1 also plays an important role, as published recently, in modulating ConA/TCR-mediated Ca^{2+} flux regulating T cell activation and effector function [250,338]. However, the role of TRPV1 towards immunosuppression and its functional association in regulating immunosuppression-mediated Ca^{2+} influx has not been investigated earlier. This study has provided the experimental indication that TRPV1 may also have a role in FK506 or B16F10-CS driven immunosuppression mediated Ca^{2+} influx in T cells. Further, the Fk506 and B16F10-CS mediated modulation of T cell activation, pro-inflammatory cytokine production, and proliferation has been highlighted.

Expression of TRPV1 increases during T cell activation [250,338]. In accordance, the TRPV1 level in T cells has been found to be higher in ConA/TCR treatment compared to resting cells. Interestingly, the TRPV1 expression was significantly increased in FK506 and B16F10-CS treatment compared to resting cells. Further, the expression of TRPV1 was elevated in FK506 and B16F10-CS treatment along with ConA/TCR activation compared to ConA/TCR controls. Additionally, the increased expression of TRPV1 was found to be irreversible as the removal of the treatment conditions also augmented TRPV1

expression. A similar trend with a significant increase in TRPV1 expression levels has been found in B16F10 tumor-bearing mice compared to the control group. These findings suggest that TRPV1 could be upregulated in an immunosuppressive environment.

Intracellular Ca^{2+} plays a significant role in regulating various cellular processes, including activation, cytokine production, migration, and differentiation [241,339]. 5'-IRTX, a specific TRPV1 inhibitor, was used to find out the involvement of TRPV1 towards FK506 and B16F10-CS-driven Ca^{2+} influx. Intracellular Ca^{2+} accumulation was increased significantly in FK506 treatment or treatment along with ConA/TCR, whereas pre-treatment with 5'-IRTX markedly decreased Ca^{2+} accumulation in T cells. However, a modest increase in intracellular Ca^{2+} accumulation was found with B16F10-CS treatment, yet a marked decrease was found with 5'-IRTX administration. Further, an increase in intracellular Ca^{2+} accumulation was observed in the splenic T cells isolated from B16F10 tumor-bearing mice compared to the control group. These findings may suggest that TRPV1 might be an important player in regulating activation- as well as immunosuppression-mediated intracellular Ca^{2+} levels in T cells.

FK506 is reported to increase intracellular Ca^{2+} levels [149]. Mechanistically, FK506-binding protein 12 (FKBP12) is found to be associated with ryanodine receptors present in the sarcoplasmic reticulum. The binding of FK506 with FKBP12 dissociates FKBP12 from ryanodine receptors facilitating Ca^{2+} release from the sarcoplasmic reticulum lumen, thus increasing intracellular Ca^{2+} levels. [150]. Additionally, FK506, after binding with FKBP12, targets calcineurin associated with inositol 1,4,5-trisphosphate receptor 1 (IP3R1). The binding of the FK506-FKBP12 complex with IP3R1-associated calcineurin modulates intracellular Ca^{2+} levels [275,340]. Conversely, B16F10-CS employs IL-10^{+} Bregs and PDL1^{hi} macrophages and suppresses T cell effector functions by engaging immunosuppressive activities [161,162,164,165,341]. Mechanistically, induction of the

immunosuppressive microenvironment through Ca^{2+}-induced activation of CaMKK2 has been reported. Further, deletion or inhibition of the CaMKK2 gene reduces tumor growth *in vivo* [342]. However, a detailed mechanistic study towards the possible association between increased calcium levels and immunosuppressive microenvironment is warranted.

Collectively, induction of TRPV1 expression occurs during both immune activation and immunosuppression in T cells. Immunosuppression induces a further rise in intracellular Ca^{2+} levels. TRPV1 regulates the elevated intracellular Ca^{2+} levels during experimental immunosuppression. A proposed working model is represented in **Figure 39**.
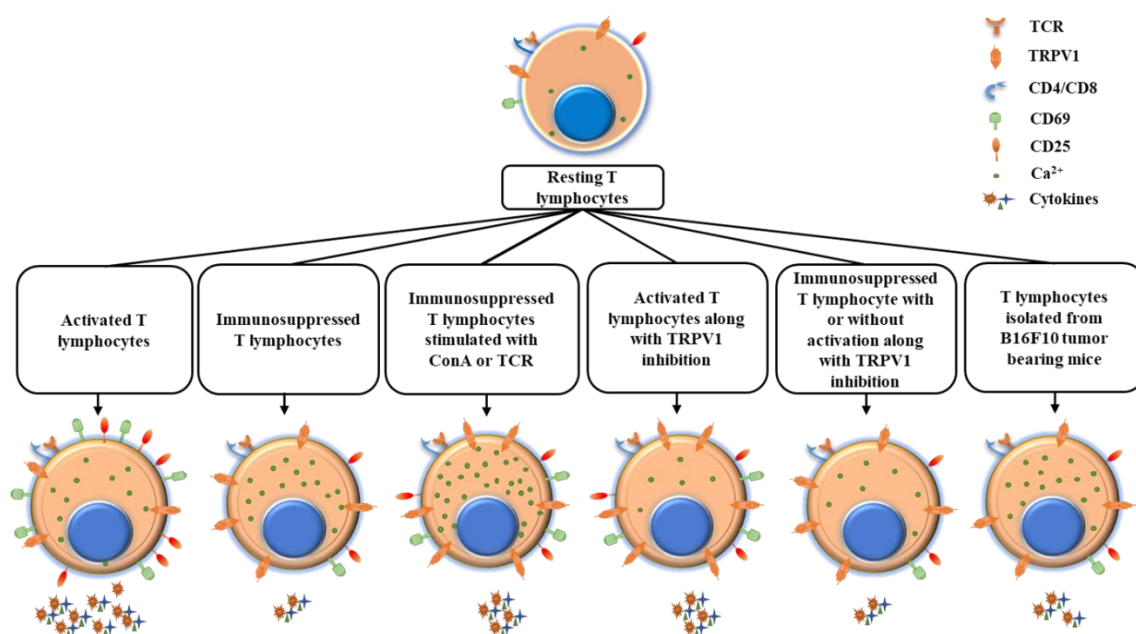
Figure 39: Proposed working model depicting functional expression of TRPV1 and intracellular calcium levels in activated and immunosuppressed T cells. Resting T cells maintain low levels of cytosolic Ca^{2+} and basal levels of TRPV1 expression. **(A)** During T cell activation with either ConA or TCR, both cytosolic Ca^{2+} level and TRPV1 expression were upregulated significantly, along with the induction of robust effector cytokine responses. **(B)** Upon treatment with immunosuppressive FK506 or B16F10-CS, TRPV1 expression increased significantly, and the cytosolic calcium increased either markedly (FK506) or modestly (B16F10-CS). **(C)** During experimental immunosuppression (treated

with either FK506 or B16F10-CS) of T cells in combination with ConA or TCR-driven stimulation, the cytokine responses markedly decreased. Further, in FK506 or B16F10-CS treated T cells stimulated with either ConA or TCR, the cytosolic Ca^{2+} either increased markedly or modestly, respectively. Moreover, TRPV1 expression increased significantly in FK506 or B16F10-CS treated T cells stimulated with either ConA or TCR, suggesting a possible induction of the TRPV1 channel on T cells during both immune activation and immunosuppression.

6.2. *Synergistic effect of TRPA1 activation and Hsp90 inhibition promotes the suppression of macrophage responses*

TRPA1, a member of the ankyrin subfamily of TRP channels, is an important player in regulating various cellular processes associated with different cell types, including monocytes, macrophages, and T cells [262,311,312,317,343]. Understanding TRPA1-mediated regulation of inflammatory pathways and its alliance with various intracellular proteins imparted insights into TRPA1-directed therapeutics in autoimmune disorders and various infectious diseases [262,266,273,313,314,344]. Hsp90, on the other hand, mediates several cellular pathways, including immune responses, by regulating various client proteins. Inhibition of Hsp90 has been found to be effective in regulating various inflammatory responses associated with monocytes and macrophages [282–286,331]. This study has provided the possible role of TRPA1 in regulating Hsp90 inhibition-mediated anti-inflammatory responses in macrophages. LPS/PMA stimulated RAW 264.7, and human THP-1 macrophages were used as an inflammatory model. 17-AAG-mediated inhibition of Hsp90 downregulated macrophage activation, inflammatory responses, and Ca^{2+} influx. Moreover, further modulation of TRPA1 channels in Hsp90-inhibited macrophages

modulates Hsp90 inhibition-mediated downregulation of macrophage inflammatory responses.

Induction of functional TRPA1 channels in various inflammatory conditions is well reported [232,240,323,345,244,259,266,271,272,311,312,322]. TRPA1 is upregulated in LPS-activated macrophages. However, the expression of TRPA1 goes down with PMA treatment. Yet, the expression further elevated significantly in both LPS or PMA treatment along with 17-AAG. Further, the augmentation of TRPA1 expression with 17-AAG-mediated Hsp90 inhibition is time-dependent and reversible. These results may suggest the possible association of TRPA1 and Hsp90-inhibition in macrophages.

17-AAG inhibits TLR4-mediated cellular inflammatory pathways [166,299]. LPS/PMA-stimulated macrophages treated with 17-AAG have been found to induce a reduced pro-inflammatory response with respect to macrophage activation markers, cytokine release, and NO production compared to activated macrophages. Moreover, inhibition of TRPA1 in Hsp90-inhibited macrophages augmented the pro-inflammatory responses, and activation led to a further reduction of macrophage activation. Similar results have been found with macrophage apoptosis. Hsp90 inhibition via 17-AAG reduced the frequency of apoptotic cells. Further, inhibition of TRPA1 in Hsp90-inhibited macrophages augmented the percentage of apoptotic cells, whereas activation leads to the reduction of apoptosis. Additionally, the expression of p-P38, p-ERK1/2, and p-SAPK-JNK was also found to follow a similar trend as above. These findings suggest that TRPA1 may have an anti-inflammatory role in Hsp90-inhibited macrophages.

Macrophage activation leads to augmented Ca^{2+} influx regulating various cellular functions [262,266,271,272,311,333,334]. Similarly, increased Ca^{2+} influx has been found with LPS stimulation, and a reduction has been observed in 17-AAG treatment. Further, TRPA1 activation in the Hsp90-inhibited condition upregulated Ca^{2+} influx, which gets reduced

with antagonism of TRPA1, suggesting TRPA1 regulates LPS/17-AAG-mediated Ca^{2+} influx.

Collectively, TRPA1 might have a possible association with 17-AAG-induced Hsp90 inhibition-mediated suppression of inflammatory responses in activated macrophages playing an important role as an anti-inflammatory mediator. A comprehensive working model is depicted in **Figure 40**.
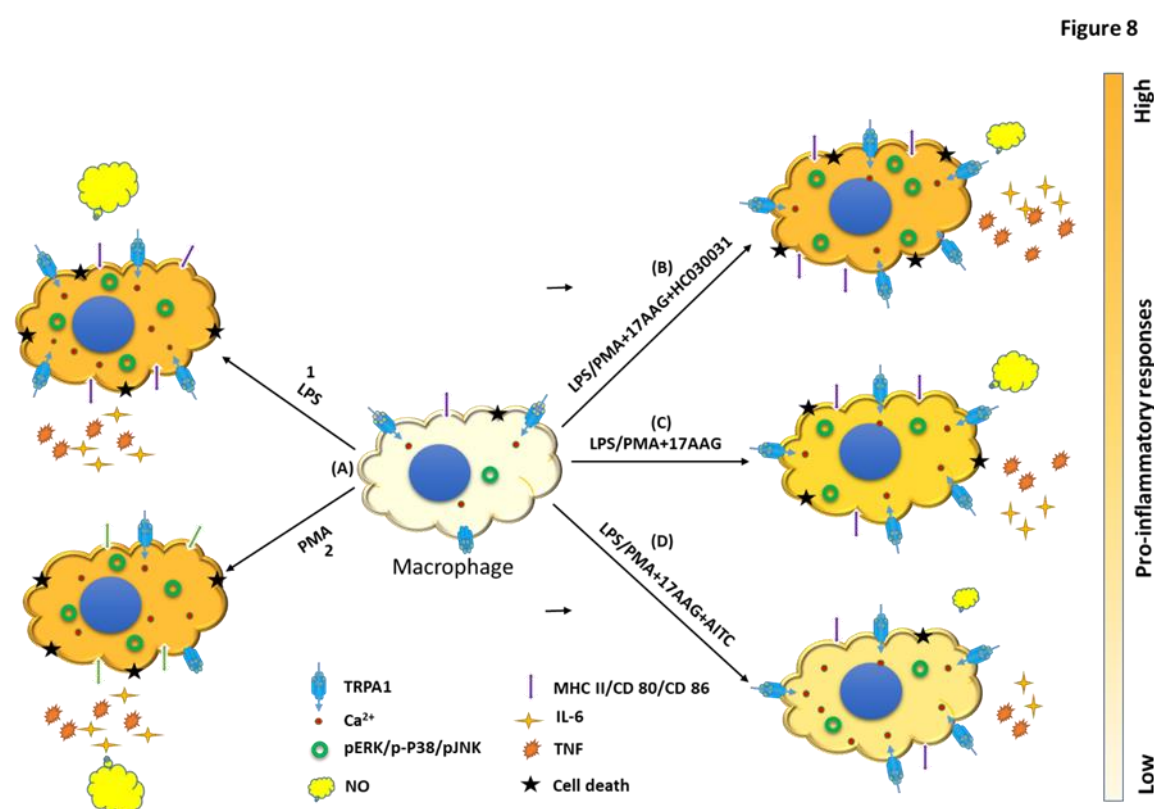
Figure 40: A proposed comprehensive working model. A proposed comprehensive working model depicting the role of TRPA1 in 17-AAG mediated inhibition of inflammation in LPS- or PMA-stimulated macrophages. TRPA1 is modulated upon LPS/PMA stimulation (**A**). Pro-inflammatory responses, including IL-6, TNF, MHCII, CD80/86, NO, intracellular calcium, and intracellular signaling proteins p38-MAPK, p-ERK 1/2, p-SAPK-JNK are significantly upregulated with LPS (**A.1**) or PMA stimulation (**A.2**). Upon administration of 17-AAG along with LPS or PMA, the pro-inflammatory responses are downregulated (**C**). Inhibition of TRPA1 via HC-030031 with 17-AAG and

LPS or PMA administration reverses the pro-inflammatory responses, intracellular signaling proteins p38-MAPK, p-ERK 1/2, p-SAPK-JNK back to the LPS or PMA stimulated levels with a further diminished intracellular calcium level **(B)**. Activation of TRPA1 via AITC and 17-AAG in LPS or PMA stimulated macrophages by impairing the pro-inflammatory responses, intracellular calcium, and intracellular signaling proteins p38-MAPK, p-ERK 1/2, p-SAPK-JNK to a greater extent exhibiting an anti-inflammatory property **(D)** the pro-inflammatory responses are represented according to the color code.

6.3. *TRPV1 and TRPA1 differentially regulate Telmisartan-driven suppression of T cells*

Many TRP channels, including TRPV1 and TRPA1 channels, are expressed in neurons and play a crucial role in transmitting a variety of sensory signals, such as inflammation, pain, and chemical and thermal nociception [346,347]. TRPV1 and TRPA1 are members of the TRP family and have been reported to be functionally associated with diverse immune cells, including macrophages, dendritic cells, T cells, and NK cells [250,269,348,349]. The functional role of TRPV1 and TRPA1 in TCR- or ConA-mediated T cell activation has been reported previously [250,269]. TM, an anti-hypertension drug, has been experimentally repurposed towards regulating various inflammatory disorders [179,187,188]. However, the possible involvement and association of TRPV1 and/or TRPA1 channels in TM-driven immunosuppression of T cells, if any, have not been reported until now. This study presents the initial evidence that both TRPV1 and TRPA1 participate in TM-driven suppression of T cell responses. Accordingly, our aim was to explore the possible functional involvement of TRPV1 and TRPA1 during TM-driven experimental immunosuppression of T cells. We observed that the surface expressions of TRPV1 and TRPA1 were elevated in TM-mediated immunosuppression of T cells. Moreover, TRPA1

activation-driven suppression of T cell responses during TM treatment was found to be partially yet significantly overridden by TRPV1 activation. Collectively, the data suggest that during immune activation from the basal level as well as in immunosuppressed conditions, expressions of TRPV1 and TRPA1 are upregulated, and these channels are functionally associated with T cell effector responses.

Immunosuppression promotes anti-inflammatory responses, demonstrating a critical impact in both clinical and experimental cases of altered immunity [350,351]. In this study, we used TM, an anti-hypertension drug reported to induce immunosuppression by regulating inflammatory responses [185–188]. Pre-incubation of T cells with TM effectively reduces T cell responses (CD69 and CD25 expressions, proliferation, and cytokine profile), indicating that TM-induced immunosuppression predominates over TCR-mediated T cell activation. Additionally, under TM-induced immunosuppressed conditions, activation of TRPA1 by AITC further induced immunosuppression. However, such stringent levels of immunosuppression could be partially overcome through the activation of TRPV1. Furthermore, in TM-driven immunosuppressed conditions, activation of TRPV1 by RTX was found to enhance T cell activation and effector cytokine production by overriding TRPA1-driven suppression of T cell responses. In contrast, the inhibition of TRPV1 by BCTC and TRPA1 by HC was found to induce higher immunosuppression. Therefore, it appears that the activation of endogenous TRPV1 may enhance T cell activation, especially under stringent immunosuppressive conditions.

Elevation of TRPV1 and TRPA1 during T cell activation and their functional association with T cell effector responses have been previously reported [250,269]. In our recent work, we demonstrated an increase in cell surface expression of TRPV1 levels in immunosuppressed T cells [352]. Additionally, our previous findings indicated an

upregulation of different TRP channels during T cell activation [250,269,353], aligning well with the results presented in this study.

TRPV1 activation facilitates TCR-driven Ca^{2+}-influx, T cell signaling, and effector responses in $CD4^+$ T cells [305]. Additionally, pharmacological inhibition of TRPV1 or genetic knockout mice showed reduced disease scores, colitogenic T cell responses, and intestinal inflammation in the T cell-mediated colitis model [305]. Conversely, $IL-10^{-/-}$ $TRPA1^{-/-}$ mice in colitis and inflammatory bowel disease (IBD) models have been reported to develop more severe $CD4^+$ T cell-mediated chronic inflammation as compared to mice with only $IL-10^{-/-}$ [354]. Moreover, TRPA1 knockout mutation has also been associated with sustained TCR-driven Ca^{2+} influx, leading to Th1 (IFN-γ, IL-2 producing type 1 $CD4^+$ helper T cells) polarization and the production of IFN-γ and IL-2 [354]. Furthermore, TRPA1 has been shown to play a suppressive role in regulating macrophage activation and proinflammatory responses [355]. In addition, immunosuppression has been reported elsewhere to upregulate intracellular Ca^{2+} concentrations [149,342,352,356], and both TRPV1 and TRPA1 have been found to play an important functional role in regulating intracellular Ca^{2+} levels associated with immunosuppression [352,355]. However, the underlying mechanisms involving immunosuppression-driven elevation of TRPV1 and TRPA1 and their possible association in regulating T cell functions require further exploration in future studies. It could be speculated that TRPV1 and TRPA1 might differentially contribute to the regulation of immune function, in addition to their upregulated expressions during cell-mediated immunosuppression.

In addition to pharmacological modulations, various endogenous molecules have been shown to have agonistic effects on TRPV1 and TRPA1 [357–361]. These include lysophosphatidic acid, N-acyl-ethanolamines, N-acyl-dopamines, oxytocin ATP, hydrogen sulfide, nitric oxide, arachidonic acid and lipoxygenase products, ammonia, intracellular

pH, divalent cations (Ca^{2+}, Mg^{2+}), which have been reported to activate TRPV1 channels [360,361]. In contrast, alkenyl aldehydes (4-hydroxynonenal, 4-oxo-nonenal, and 4-hydroxyhexenal), hydrogen peroxide, 15-deoxy-Δ12,14-prostaglandin J2, reactive oxygen species, and reactive nitrogen species have been shown to activate TRPA1 channels [357–359]. However, further investigations are warranted to decipher the direct involvement of various endogenous molecules in activating TRPV1 and TRPA1 in T cells.

Our data further indicate the existence of a strong correlation between surface expressions of TRPV1 and TRPA1 in T cells in different immunological conditions, such as resting, activated, and immunosuppressed states. Notably, the correlation between TRPV1 and TRPA1 surface expressions is at least the equal range, if not stronger than the CD69 and CD25, suggesting that TRPV1 and TRPA1 could be considered as contextual immunoregulatory markers. Nevertheless, the high correlation between the surface expressions of TRPV1 and TRPA1 in T cells is striking. This is also relevant as in the diverse cellular systems, both TRPV1 and TRPA1 engage in reciprocal signaling functions.

Based on these findings, we suggest that functional modulation of TRPV1 and TRPA1 could be helpful in regulating the immunosuppression of T cells. A proposed working model of the current study has been summarized in **Figure 41**. This study might have broad implications for the role of TRPV1 and TRPA1 in immunosuppressive diseases and might be important in designing strategies for possible future immunotherapy, especially the repurposing of TM in regulating TRP-directed cell-mediated immune responses associated with immune disorders. The current study may open future translational implications for other TRP channels in altered cell-mediated immune responses associated with various diseases.
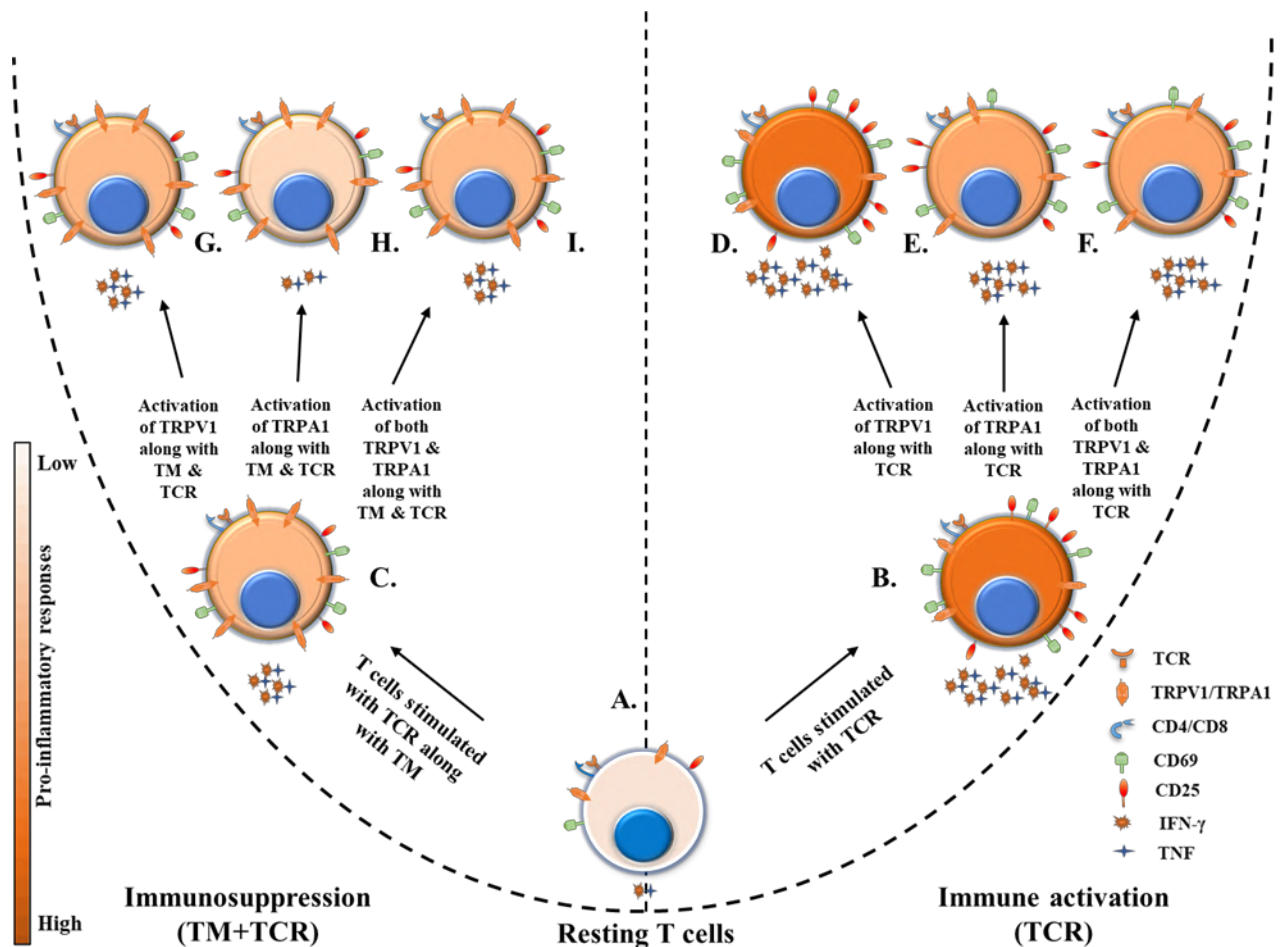
Figure 41: The proposed model depicting the possible involvement of TRPV1 and TRPA1 during TM-induced immunosuppression of T cells. Resting (condition **A**, i.e., T cells treated with only DMSO) murine T cells were activated by TCR (i.e., T cells pre-incubated with DMSO and then stimulated with TCR) in the presence **(C)** or absence **(B)** of TM. TCR activation upregulates T cell responses relating to T cell activation markers (CD69 and CD25 expressions) and effector cytokine (IFN-γ and TNF) production as compared to resting cells (i.e., T cells treated with only DMSO). TM treatment suppresses T cell responses by downregulating T cell activation markers (i.e., CD69 and CD25 expressions) and effector cytokine (IFN-γ and TNF) productions in TM+TCR condition (depicted by condition **C**) (i.e., pre-incubated with TM and then stimulated with TCR) as compared to only TCR activation (depicted by condition **B**). Cell surface expressions of TRPV1 and TRPA1 were upregulated in

TM-induced immunosuppressed T cells **(C)** as compared to T cells activated with only TCR stimulation **(B)**. TRPA1 activation by AITC reduces T cell responses by reducing T cell activation markers (CD69 and CD25 expressions) and effector cytokine (IFN-γ and TNF) productions in both AITC+TCR (depicted by condition **E**) (i.e., T cells pre-incubated with AITC and then activated with TCR stimulation) and AITC+TM+TCR **(H)** (i.e., T cells pre-incubated with TM and AITC and then stimulated with TCR) conditions. TRPV1 activation by RTX during TM-mediated immunoregulation overrides TRPA1-driven suppression of T cell responses by upregulating T cell activation markers (CD69 and CD25 expressions) and effector cytokine (IFN-γ and TNF) responses i.e., in RTX+AITC+TM+TCR condition (depicted in **I**, T cells pre-incubated with RTX, AITC, and TM and then stimulated with TCR) as compared to TRPA1-activated cells treated with TM and TCR, i.e., in AITC+TM+TCR condition (depicted in **H**, T cells pre-incubated with AITC and TM, and then stimulated with TCR). However, in the "absence of TM", activation of TRPV1 by RTX in TCR-activated cells fails to override TRPA1 activation (by AITC)-driven suppression of T cell responses, i.e., in RTX+AITC+TCR condition (depicted in **F**, i.e., T cells pre-incubated with RTX and AITC, and then stimulated with TCR) relating to T cell activation markers (CD69 and CD25 expressions) and effector cytokine (IFN-γ and TNF) productions as compared to TRPA1-activated cells treated with TCR, i.e., in AITC+TCR condition (depicted in **E**, T cells pre-incubated with AITC and then stimulated with TCR), suggesting a possible functional involvement of TRPV1 and TRPA1 in TM-mediated immunosuppression of T cells.

CHAPTER # 7

Future Direction

7. Future Direction

Immunosuppression is the prime cause of alleviated effector immune responses associated with macrophages, dendritic cells, T cells, and other accessory immune cells. Different diseases and several medications and modulators are reported to induce suppression of the immune cells by modulating cellular processes, including signaling cascades, gene expression, and/or cellular communications. In this study, immunosuppression-mediated regulation of T cell and macrophage functions, the association of TRPV1 and TRPA1 towards immunosuppression of T cells and macrophages, and the comparative possible differential role of TRPV1 and TRPA1 towards immunosuppression of T cells have been examined. However, the detailed mechanism underlying the association of immunosuppression with the induction of TRPV1 and TRPA1 in immune cells, along with their functions in regulating CMI responses, is yet to be elucidated. Moreover, the details of the cellular processes associated with cancer cell-mediated suppression of immune cells and signaling pathways altering the cancer cell-driven immunosuppression are still under investigation. It would be fascinating to further decode the information about the functional association of altered physiological conditions with immunosuppression towards regulating immune function along with the vertical exploration of the cellular events, which might have profound implications with better strategies for devising future therapeutics.

Bibliography

1.   Paul WE. Self/Nonself—Immune Recognition and Signaling: A new journal tackles a problem at the center of immunological science. *http://dx.doi.org/104161/self1110682*. 2010;1(1):2-3. doi:10.4161/SELF.1.1.10682

2.   Gonzalez S, González-Rodríguez AP, Suárez-Álvarez B, López-Soto A, Huergo-Zapico L, Lopez-Larrea C. Conceptual aspects of self and nonself discrimination. *http://dx.doi.org/104161/self2115094*. 2011;2(1):19-25. doi:10.4161/SELF.2.1.15094

3.   Buchmann K. Evolution of innate immunity: Clues from invertebrates via fish to mammals. *Front Immunol*. 2014;5(SEP):459. doi:10.3389/FIMMU.2014.00459/BIBTEX

4.   Cooper MD, Alder MN. The Evolution of Adaptive Immune Systems. *Cell*. 2006;124(4):815-822. doi:10.1016/J.CELL.2006.02.001

5.   Simon AK, Hollander GA, McMichael A. Evolution of the immune system in humans from infancy to old age. *Proc R Soc B Biol Sci*. 2015;282(1821). doi:10.1098/RSPB.2014.3085

6.   Janeway CA. The immune system evolved to discriminate infectious nonself from noninfectious self. *Immunol Today*. 1992;13(1):11-16. doi:10.1016/0167-5699(92)90198-G

7.   Janeway CA, Medzhitov R. Innate Immune Recognition. *https://doi.org/101146/annurev.immunol20083001084359*. 2003;20:197-216. doi:10.1146/ANNUREV.IMMUNOL.20.083001.084359

8.   Pratheek BM, Saha S, Maiti PK, Chattopadhyay SS, Chattopadhyay SS. Immune Regulation and Evasion of Mammalian Host Cell Immunity During Viral Infection. *Indian J Virol 2013 241*. 2013;24(1):1-15. doi:10.1007/S13337-013-0130-7

9. Dempsey PW, Vaidya SA, Cheng G. The Art of War: Innate and adaptive immune responses. *Cell Mol Life Sci C 2003 6012*. 2003;60(12):2604-2621. doi:10.1007/S00018-003-3180-Y

10. Bryant CE, Monie TP. Mice, men and the relatives: cross-species studies underpin innate immunity. *Open Biol*. 2012;2(APRIL). doi:10.1098/RSOB.120015

11. Galli SJ, Borregaard N, Wynn TA. Phenotypic and functional plasticity of cells of innate immunity: macrophages, mast cells and neutrophils. *Nat Immunol 2011 1211*. 2011;12(11):1035-1044. doi:10.1038/ni.2109

12. Gasteiger G, D'osualdo A, Schubert DA, Weber A, Bruscia EM, Hartl D. Cellular Innate Immunity: An Old Game with New Players. *J Innate Immun*. 2017;9(2):111-125. doi:10.1159/000453397

13. van der Meer JWM, Joosten LAB, Riksen N, Netea MG. Trained immunity: A smart way to enhance innate immune defence. *Mol Immunol*. 2015;68(1):40-44. doi:10.1016/J.MOLIMM.2015.06.019

14. Bedoui S, Gebhardt T, Gasteiger G, Kastenmüller W. Parallels and differences between innate and adaptive lymphocytes. *Nat Immunol 2016 175*. 2016;17(5):490-494. doi:10.1038/ni.3432

15. Bonilla FA, Oettgen HC. Adaptive immunity. *J Allergy Clin Immunol*. 2010;125(2 Suppl 2). doi:10.1016/J.JACI.2009.09.017

16. Flajnik MF, Kasahara M. Origin and evolution of the adaptive immune system: genetic events and selective pressures. *Nat Rev Genet 2010 111*. 2009;11(1):47-59. doi:10.1038/nrg2703

17. Chaplin DD. Overview of the immune response. *J Allergy Clin Immunol*. 2010;125(2

Suppl 2). doi:10.1016/J.JACI.2009.12.980

18. Nicholson LB. The immune system. *Essays Biochem*. 2016;60(3):275-301. doi:10.1042/EBC20160017

19. Quaresma JAS. Organization of the skin immune system and compartmentalized immune responses in infectious diseases. *Clin Microbiol Rev*. 2019;32(4). doi:10.1128/CMR.00034-18/ASSET/A9E536AD-5767-4FDA-BC46-249397E22759/ASSETS/GRAPHIC/CMR.00034-18-T003A.JPEG

20. Clinic C. Immune System: Parts & Common Problems. Published 2022. Accessed December 2, 2022. https://my.clevelandclinic.org/health/articles/21196-immune-system

21. Riera Romo M, Pérez-Martínez D, Castillo Ferrer C. Innate immunity in vertebrates: an overview. *Immunology*. 2016;148(2):125-139. doi:10.1111/IMM.12597

22. Charles A Janeway J, Travers P, Walport M, Shlomchik MJ. Immunobiology. *Immunobiology*. 2001;(14102):1-10. Accessed December 2, 2022. https://www.ncbi.nlm.nih.gov/books/NBK10757/

23. Gombart AF, Pierre A, Maggini S. A Review of Micronutrients and the Immune System–Working in Harmony to Reduce the Risk of Infection. *Nutr 2020, Vol 12, Page 236*. 2020;12(1):236. doi:10.3390/NU12010236

24. Bruce Alberts DBJLMRKRJW. Molecular Biology of the Cell - NCBI Bookshelf. Published 1994. Accessed December 2, 2022. http://www.ncbi.nlm.nih.gov/books/NBK20684/

25. Dutton RW. How does the immune system remember? *Curr Biol*. 1993;3(12):901-903. doi:10.1016/0960-9822(93)90232-D

26. Goronzy JJ, Weyand CM. The Innate and Adaptive Immune Systems. *Goldman's Cecil*

Med Twenty Fourth Ed. 2012;1:214-222. doi:10.1016/B978-1-4377-1604-7.00044-0

27.   Diamond JA, Phillips RA. StatPearls - NCBI Bookshelf. Hypertension Research. Published 2005. Accessed December 2, 2022. https://www.ncbi.nlm.nih.gov/books/NBK459329/%0Ahttps://www.ncbi.nlm.nih.gov/books/NBK448133/

28.   Zhang Y, Gao S, Xia J, Liu F. Hematopoietic Hierarchy - An Updated Roadmap. *Trends Cell Biol*. 2018;28(12):976-986. doi:10.1016/J.TCB.2018.06.001

29.   Hematopoiesis | Leaders in Pharmaceutical Business Intelligence (LPBI) Group. Accessed December 2, 2022. https://pharmaceuticalintelligence.com/2016/01/23/hematopoiesis/

30.   Haas S, Trumpp A, Milsom MD. Causes and Consequences of Hematopoietic Stem Cell Heterogeneity. *Cell Stem Cell*. 2018;22(5):627-638. doi:10.1016/J.STEM.2018.04.003

31.   Eiz-Vesper B, Schmetzer HM. Antigen-Presenting Cells: Potential of Proven und New Players in Immune Therapies. *Transfus Med Hemotherapy*. 2020;47(6):429-431. doi:10.1159/000512729

32.   Blum JS, Wearsch PA, Cresswell P. Pathways of antigen processing. *Annu Rev Immunol*. 2013;31:443-473. doi:10.1146/ANNUREV-IMMUNOL-032712-095910

33.   Nakayama M. Antigen presentation by MHC-dressed cells. *Front Immunol*. 2014;5(DEC):672. doi:10.3389/FIMMU.2014.00672/BIBTEX

34.   Pishesha N, Harmand TJ, Ploegh HL. A guide to antigen processing and presentation. *Nat Rev Immunol 2022 2212*. 2022;22(12):751-764. doi:10.1038/s41577-022-00707-2

35.   Vyas JM, Van Der Veen AG, Ploegh HL. The known unknowns of antigen processing and presentation. *Nat Rev Immunol 2008 88*. 2008;8(8):607-618. doi:10.1038/nri2368

36. Watts C. The exogenous pathway for antigen presentation on major histocompatibility complex class II and CD1 molecules. *Nat Immunol 2004 57*. 2004;5(7):685-692. doi:10.1038/ni1088

37. Harryvan TJ, de Lange S, Hawinkels LJAC, Verdegaal EME. The ABCs of Antigen Presentation by Stromal Non-Professional Antigen-Presenting Cells. *Int J Mol Sci 2022, Vol 23, Page 137*. 2021;23(1):137. doi:10.3390/IJMS23010137

38. Lee MY, Jeon JW, Sievers C, Allen CT. Antigen processing and presentation in cancer immunotherapy. *J Immunother Cancer*. 2020;8(2):e001111. doi:10.1136/JITC-2020-001111

39. Embgenbroich M, Burgdorf S. Current concepts of antigen cross-presentation. *Front Immunol*. 2018;9(JUL):1643. doi:10.3389/FIMMU.2018.01643/BIBTEX

40. Muntjewerff EM, Meesters LD, van den Bogaart G. Antigen Cross-Presentation by Macrophages. *Front Immunol*. 2020;11:1276. doi:10.3389/FIMMU.2020.01276/BIBTEX

41. Joffre OP, Segura E, Savina A, Amigorena S. Cross-presentation by dendritic cells. *Nat Rev Immunol 2012 128*. 2012;12(8):557-569. doi:10.1038/nri3254

42. Sánchez-Paulete AR, Teijeira A, Cueto FJ, et al. Antigen cross-presentation and T-cell cross-priming in cancer immunology and immunotherapy. *Ann Oncol*. 2017;28:xii44-xii55. doi:10.1093/ANNONC/MDX237

43. Forthal DN. Functions of antibodies. *Antibodies Infect Dis*. 2015;2(4):25-48. doi:10.1128/9781555817411.ch2

44. Dinarello CA. Historical insights into cytokines. *Eur J Immunol*. 2007;37(S1):S34-S45. doi:10.1002/EJI.200737772

45. Borish LC, Steinke JW. 2. Cytokines and chemokines. *J Allergy Clin Immunol*.

2003;111:S460-S475. Accessed December 2, 2022. https://pubmed.ncbi.nlm.nih.gov/12592293/

46. Turner MD, Nedjai B, Hurst T, Pennington DJ. Cytokines and chemokines: At the crossroads of cell signalling and inflammatory disease. *Biochim Biophys Acta - Mol Cell Res*. 2014;1843(11):2563-2582. doi:10.1016/j.bbamcr.2014.05.014

47. Chaperone-Mediated Autophagy -- Madame Curie Bioscience Database -- NCBI Bookshelf. Accessed December 2, 2022. http://www.ncbi.nlm.nih.gov/bookshelf/br.fcgi?book=eurekah&part=A34781

48. Yang Q, Jeremiah Bell J, Bhandoola A. T-cell lineage determination. *Immunol Rev*. 2010;238(1):12-22. doi:10.1111/J.1600-065X.2010.00956.X

49. Klein L, Hinterberger M, Wirnsberger G, Kyewski B. Antigen presentation in the thymus for positive selection and central tolerance induction. *Nat Rev Immunol 2009 912*. 2009;9(12):833-844. doi:10.1038/nri2669

50. Anderson G, Takahama Y. Thymic epithelial cells: working class heroes for T cell development and repertoire selection. *Trends Immunol*. 2012;33(6):256-263. doi:10.1016/J.IT.2012.03.005

51. Wucherpfennig KW, Gagnon E, Call MJ, Huseby ES, Call ME. Structural Biology of the T-cell Receptor: Insights into Receptor Assembly, Ligand Recognition, and Initiation of Signaling. *Cold Spring Harb Perspect Biol*. 2010;2(4):a005140. doi:10.1101/CSHPERSPECT.A005140

52. Bousso P. T-cell activation by dendritic cells in the lymph node: lessons from the movies. *Nat Rev Immunol 2008 89*. 2008;8(9):675-684. doi:10.1038/nri2379

53. Siebenlist U, Brown K, Claudio E. Control of lymphocyte development by nuclear factor-

κB. *Nat Rev Immunol 2005 56*. 2005;5(6):435-445. doi:10.1038/nri1629

54.   Müller MR, Rao A. NFAT, immunity and cancer: a transcription factor comes of age. *Nat Rev Immunol 2010 109*. 2010;10(9):645-656. doi:10.1038/nri2818

55.   Chen L, Flies DB. Molecular mechanisms of T cell co-stimulation and co-inhibition. *Nat Rev Immunol 2013 134*. 2013;13(4):227-242. doi:10.1038/nri3405

56.   Kroczek RA, Mages HW, Hutloff A. Emerging paradigms of T-cell co-stimulation. *Curr Opin Immunol*. 2004;16(3):321-327. doi:10.1016/j.coi.2004.03.002

57.   Boyman O, Sprent J. The role of interleukin-2 during homeostasis and activation of the immune system. *Nat Rev Immunol 2012 123*. 2012;12(3):180-190. doi:10.1038/nri3156

58.   Malek TR, Bayer AL. Tolerance, not immunity, crucially depends on IL-2. *Nat Rev Immunol 2004 49*. 2004;4(9):665-674. doi:10.1038/nri1435

59.   Kaiko GE, Horvat JC, Beagley KW, Hansbro PM. Immunological decision-making: how does the immune system decide to mount a helper T-cell response? *Immunology*. 2008;123(3):326-338. doi:10.1111/J.1365-2567.2007.02719.X

60.   Ho IC, Tai TS, Pai SY. GATA3 and the T-cell lineage: essential functions before and after T-helper-2-cell differentiation. *Nat Rev Immunol 2009 92*. 2009;9(2):125-135. doi:10.1038/nri2476

61.   Ma CS, Tangye SG, Deenick EK. Human Th9 cells: inflammatory cytokines modulate IL-9 production through the induction of IL-21. *Immunol Cell Biol*. 2010;88(6):621-623. doi:10.1038/ICB.2010.73

62.   Miossec P, Korn T, Kuchroo VK. Interleukin-17 and type 17 helper T cells. *N Engl J Med*. 2009;361(9):888-898. doi:10.1056/NEJMRA0707449

63. Wolk K, Witte E, Witte K, Warszawska K, Sabat R. Biology of interleukin-22. *Semin Immunopathol*. 2010;32(1):17-31. doi:10.1007/S00281-009-0188-X/FIGURES/3

64. King C. New insights into the differentiation and function of T follicular helper cells. *Nat Rev Immunol 2009 911*. 2009;9(11):757-766. doi:10.1038/nri2644

65. Schmetterer KG, Neunkirchner A, Pickl WF. Naturally occurring regulatory T cells: markers, mechanisms, and manipulation. *FASEB J*. 2012;26(6):2253-2276. doi:10.1096/FJ.11-193672

66. Sakaguchi S, Miyara M, Costantino CM, Hafler DA. FOXP3+ regulatory T cells in the human immune system. *Nat Rev Immunol 2010 107*. 2010;10(7):490-500. doi:10.1038/nri2785

67. Cox MA, Kahan SM, Zajac AJ. Anti-viral CD8 T cells and the cytokines that they love. *Virology*. 2013;435(1):157-169. doi:10.1016/J.VIROL.2012.09.012

68. Lieberman J. The ABCs of granule-mediated cytotoxicity: new weapons in the arsenal. *Nat Rev Immunol 2003 35*. 2003;3(5):361-370. doi:10.1038/nri1083

69. Pieper K, Grimbacher B, Eibel H. B-cell biology and development. *J Allergy Clin Immunol*. 2013;131(4):959-971. doi:10.1016/J.JACI.2013.01.046

70. Herzog S, Reth M, Jumaa H. Regulation of B-cell proliferation and differentiation by pre-B-cell receptor signalling. *Nat Rev Immunol*. 2009;9(3):195-205. doi:10.1038/NRI2491

71. Shlomchik MJ, Weisel F. Germinal center selection and the development of memory B and plasma cells. *Immunol Rev*. 2012;247(1):52-63. doi:10.1111/J.1600-065X.2012.01124.X

72. Cerutti A, Cols M, Puga I. Marginal zone B cells: virtues of innate-like antibody-producing lymphocytes. *Nat Rev Immunol 2013 132*. 2013;13(2):118-132.

doi:10.1038/nri3383

73. Choi MY, Kipps TJ. Inhibitors of B-cell receptor signaling for patients with B-cell malignancies. *Cancer J*. 2012;18(5):404-410. doi:10.1097/PPO.0B013E31826C5810

74. Daniels MA, Teixeiro E. TCR signaling in T cell memory. *Front Immunol*. 2015;6(DEC):617. doi:10.3389/FIMMU.2015.00617/BIBTEX

75. Hwang JR, Byeon Y, Kim D, Park SG. Recent insights of T cell receptor-mediated signaling pathways for T cell activation and development. *Exp Mol Med 2020 525*. 2020;52(5):750-761. doi:10.1038/s12276-020-0435-8

76. Gaudino SJ, Kumar P. Cross-talk between antigen presenting cells and T cells impacts intestinal homeostasis, bacterial infections, and tumorigenesis. *Front Immunol*. 2019;10(MAR):360. doi:10.3389/FIMMU.2019.00360/BIBTEX

77. Acuto O, Michel F. CD28-mediated co-stimulation: a quantitative support for TCR signalling. *Nat Rev Immunol 2003 312*. 2003;3(12):939-951. doi:10.1038/nri1248

78. Pennock ND, White JT, Cross EW, Cheney EE, Tamburini BA, Kedl RM. T cell responses: Naïve to memory and everything in between. *Am J Physiol - Adv Physiol Educ*. 2013;37(4):273-283.
doi:10.1152/ADVAN.00066.2013/ASSET/IMAGES/LARGE/ZU10041328140004.JPEG

79. Watts TH. TNF/TNFR family members in costimulation of T cell responses. *Annu Rev Immunol*. 2005;23:23-68. doi:10.1146/ANNUREV.IMMUNOL.23.021704.115839

80. Fife BT, Bluestone JA. Control of peripheral T-cell tolerance and autoimmunity via the CTLA-4 and PD-1 pathways. *Immunol Rev*. 2008;224(1):166-182. doi:10.1111/J.1600-065X.2008.00662.X

81. Buchbinder EI, Desai A. CTLA-4 and PD-1 Pathways: Similarities, Differences, and

Implications of Their Inhibition. *Am J Clin Oncol*. 2016;39(1):98-106. doi:10.1097/COC.0000000000000239

82.   Moskophidis D, Kioussis D. Contribution of Virus-specific CD8+ Cytotoxic T Cells to Virus Clearance or Pathologic Manifestations of Influenza Virus Infection in a T Cell Receptor Transgenic Mouse Model. *J Exp Med*. 1998;188(2):223-232. doi:10.1084/JEM.188.2.223

83.   Guo T, Qiu Z, Guo T, Qiu Z. The effects of CTL immune response on HIV infection model with potent therapy, latently infected cells and cell-to-cell viral transmission. *Math Biosci Eng 2019 66822*. 2019;16(6):6822-6841. doi:10.3934/MBE.2019341

84.   Manaster Y, Shipony Z, Hutzler A, et al. Reduced CTL motility and activity in avascular tumor areas. *Cancer Immunol Immunother*. 2019;68(8):1287-1301. doi:10.1007/S00262-019-02361-5/FIGURES/5

85.   Braun MW, Iwakuma T. Regulation of cytotoxic T-cell responses by p53 in cancer. *Transl Cancer Res*. 2016;5(6):692-697. doi:10.21037/TCR.2016.11.76

86.   Röcken M, Müller KM, Saurat JH, Hauser C. Lectin-mediated induction of IL-4-producing CD4+ T cells. Journal of immunology (Baltimore, Md. : 1950). Published 1991. Accessed December 3, 2022. http://www.ncbi.nlm.nih.gov/pubmed/1670948

87.   Seder RA, Paul WE. Acquisition of Lymphokine-Producing Phenotype by CD4+ T Cells. *https://doi.org/101146/annurev.iy12040194003223*. 2003;12:635-673. doi:10.1146/ANNUREV.IY.12.040194.003223

88.   Del Prete G, Maggi E, Romagnani S. Human Th1 and Th2 cells: functional properties, mechanisms of regulation, and role in disease. *Lab Invest*. 1994;70(3):299-306.

89.   Yssel H, De Waal Malefyt R, Roncarolo MG, et al. IL-10 is produced by subsets of human

CD4+ T cell clones and peripheral blood T cells. *J Immunol*. 1992;149(7):2378-2384.

90. Malefyt RDW, Abrams JS, Zurawski SM, et al. Differential regulation of IL-13 and IL-4 production by human CD8+ and CD4+ Th0, Th1 and Th2 T cell clones and EBV-transformed B cells. *Int Immunol*. 1995;7(9):1405-1416. doi:10.1093/INTIMM/7.9.1405

91. Chen Y, Kuchroo VK, Inobe JI, Hafler DA, Weiner HL. Regulatory T Cell Clones Induced by Oral Tolerance: Suppression of Autoimmune Encephalomyelitis. *Science (80-)*. 1994;265(5176):1237-1240. doi:10.1126/SCIENCE.7520605

92. Fukaura H, Kent SC, Pietrusewicz MJ, Khoury SJ, Weiner HL, Hafler DA. Induction of circulating myelin basic protein and proteolipid protein-specific transforming growth factor-beta1-secreting Th3 T cells by oral administration of myelin in multiple sclerosis patients. *J Clin Invest*. 1996;98(1):70-77. doi:10.1172/JCI118779

93. Powrie F, Carlino J, Leach MW, Mauze S, Coffman RL. A critical role for transforming growth factor-beta but not interleukin 4 in the suppression of T helper type 1-mediated colitis by CD45RB(low) CD4+ T cells. *J Exp Med*. 1996;183(6):2669-2674. doi:10.1084/JEM.183.6.2669

94. Hafler DA, Kent SC, Pietrusewicz MJ, Khoury SJ, Weiner HL, Fukaura H. Oral Administration of Myelin Induces Antigen-specific TGF-β1 Secreting T Cells in Patients with Multiple Sclerosisa. *Ann N Y Acad Sci*. 1997;835(1):120-131. doi:10.1111/J.1749-6632.1997.TB48623.X

95. Szulc B, Piasecki E. Effects of interferons, interferon inducers and growth factors on phagocytosis measured by quantitative determination of synthetic compound ingested by mouse bone marrow-derived macrophages. *Arch Immunol Ther Exp (Warsz)*. 1988;36(5):537-545.

96. Johnston RBJ, Kitagawa S. Molecular basis for the enhanced respiratory burst of activated macrophages. *Fed Proc*. 1985;44(14):2927-2932.

97. Diamond RD, Lyman CA, Wysong DR. Disparate effects of interferon-gamma and tumor necrosis factor-alpha on early neutrophil respiratory burst and fungicidal responses to Candida albicans hyphae in vitro. *J Clin Invest*. 1991;87(2):711-720. doi:10.1172/JCI115050

98. Lapierre LA, Fiers W, Pober JS. Three distinct classes of regulatory cytokines control endothelial cell MHC antigen expression. Interactions with immune gamma interferon differentiate the effects of tumor necrosis factor and lymphotoxin from those of leukocyte alpha and fibroblast beta interferons. *J Exp Med*. 1988;167(3):794-804. doi:10.1084/JEM.167.3.794

99. Goebeler M, Yoshimura T, Toksoy A, Ritter U, Bröcker EB, Gillitzer R. The chemokine repertoire of human dermal microvascular endothelial cells and its regulation by inflammatory cytokines. *J Invest Dermatol*. 1997;108(4):445-451. doi:10.1111/1523-1747.EP12289711

100. Teunissen MBM, Koomen CW, De Waal Malefyt R, Wierenga EA, Bos JD. Interleukin-17 and interferon-gamma synergize in the enhancement of proinflammatory cytokine production by human keratinocytes. *J Invest Dermatol*. 1998;111(4):645-649. doi:10.1046/J.1523-1747.1998.00347.X

101. Rathanaswami P, Hachicha M, Sadick M, Schall TJ, McColl SR. Expression of the cytokine RANTES in human rheumatoid synovial fibroblasts. Differential regulation of RANTES and interleukin-8 genes by inflammatory cytokines. *J Biol Chem*. 1993;268(8):5834-5839. doi:10.1016/S0021-9258(18)53395-0

102. Nickoloff BJ, Naidu Y. Perturbation of epidermal barrier function correlates with initiation

of cytokine cascade in human skin. *J Am Acad Dermatol*. 1994;30(4):535-546. doi:10.1016/S0190-9622(94)70059-1

103. Punnonen J, de Vries JE. IL-13 induces proliferation, Ig isotype switching, and Ig synthesis by immature human fetal B cells. *J Immunol*. 1994;152(3):1094-1102.

104. Lundgren M, Persson U, Larsson P, et al. Interleukin 4 induces synthesis of IgE and IgG4 in human B cells. *Eur J Immunol*. 1989;19(7):1311-1315. doi:10.1002/EJI.1830190724

105. Fiorentino DF, Zlotnik A, Vieira P, et al. IL-10 acts on the antigen-presenting cell to inhibit cytokine production by Th1 cells. *J Immunol*. 1991;146(10):3444-3451.

106. Romani L, Puccetti P, Mencacci A, et al. Neutralization of IL-10 up-regulates nitric oxide production and protects susceptible mice from challenge with Candida albicans. *J Immunol*. 1994;152(7):3514-3521.

107. Waal Malefyt R De, Haanen J, Spits H, et al. Interleukin 10 (IL-10) and viral IL-10 strongly reduce antigen-specific human T cell proliferation by diminishing the antigen-presenting capacity of monocytes via downregulation of class II major histocompatibility complex expression. *J Exp Med*. 1991;174(4):915-924. doi:10.1084/JEM.174.4.915

108. PARSONS JC, COFFMAN RL, GRIEVE RB. Antibody to interleukin 5 prevents blood and tissue eosinophilia but not liver trapping in murine larval toxocariasis. *Parasite Immunol*. 1993;15(9):501-508. doi:10.1111/J.1365-3024.1993.TB00637.X

109. Lukacs NW, Strieter RM, Chensue SW, Kunkel SL. Interleukin-4-dependent pulmonary eosinophil infiltration in a murine model of asthma. *https://doi.org/101165/ajrcmb1058179915*. 2012;10(5):526-532. doi:10.1165/AJRCMB.10.5.8179915

110. Nicolaides NC, Holroyd KJ, Ewart SL, et al. Interleukin 9: A candidate gene for asthma.

Proc Natl Acad Sci U S A. 1997;94(24):13175-13180. doi:10.1073/PNAS.94.24.13175/ASSET/4490165B-4F23-407E-8982-65774180F58B/ASSETS/GRAPHIC/PQ2471995004.JPEG

111. Li L, Xia Y, Nguyen A, et al. Effects of Th2 cytokines on chemokine expression in the lung: IL-13 potently induces eotaxin expression by airway epithelial cells. *J Immunol*. 1999;162(5):2477-2487.

112. Gajewski TF, Goldwasser E, Fitch FW. Anti-proliferative effect of IFN-gamma in immune regulation. II. IFN-gamma inhibits the proliferation of murine bone marrow cells stimulated with IL-3, IL-4, or granulocyte-macrophage colony-stimulating factor. *J Immunol*. 1988;141(8):2635-2642.

113. D'andrea A, Aste-Amezaga M, Valiante NM, Ma X, Kubin M, Trinchieri G. Interleukin 10 (IL-10) inhibits human lymphocyte interferon gamma-production by suppressing natural killer cell stimulatory factor/IL-12 synthesis in accessory cells. *J Exp Med*. 1993;178(3):1041-1048. doi:10.1084/JEM.178.3.1041

114. Ito S, Ansari P, Sakatsume M, et al. Interleukin-10 Inhibits Expression of Both Interferon α– and Interferon γ– Induced Genes by Suppressing Tyrosine Phosphorylation of STAT1. *Blood*. 1999;93(5):1456-1463. doi:10.1182/BLOOD.V93.5.1456

115. Baan RA, Stewart BW, Straif K. *Tumour Site Concordance and Mechanisms of Carcinogenesis*. Vol 165.; 2019.

116. Clifford GM, Polesel J, Rickenbach M, et al. Cancer Risk in the Swiss HIV Cohort Study: Associations With Immunodeficiency, Smoking, and Highly Active Antiretroviral Therapy. *JNCI J Natl Cancer Inst*. 2005;97(6):425-432. doi:10.1093/JNCI/DJI072

117. Grulich AE, van Leeuwen MT, Falster MO, Vajdic CM. Incidence of cancers in people

with HIV/AIDS compared with immunosuppressed transplant recipients: a meta-analysis. *Lancet (London, England)*. 2007;370(9581):59-67. doi:10.1016/S0140-6736(07)61050-2

118. Schulz TF. Cancer and viral infections in immunocompromised individuals. *Int J Cancer*. 2009;125(8):1755-1763. doi:10.1002/IJC.24741

119. Wieland U, Kreuter A, Pfister H. Human Papillomavirus and Immunosuppression. *Curr Probl Dermatology*. 2014;45:154-165. doi:10.1159/000357907

120. Salminen A. Clinical perspectives on the age-related increase of immunosuppressive activity. *J Mol Med (Berl)*. 2022;100(5):697-712. doi:10.1007/S00109-022-02193-4

121. Salminen A. Activation of immunosuppressive network in the aging process. *Ageing Res Rev*. 2020;57:100998. doi:10.1016/J.ARR.2019.100998

122. Squire JD, Sher M. Asplenia and Hyposplenism: An Underrecognized Immune Deficiency. *Immunol Allergy Clin North Am*. 2020;40(3):471-483. doi:10.1016/J.IAC.2020.03.006

123. Hartono C, Muthukumar T, Suthanthiran M. Immunosuppressive drug therapy. *Cold Spring Harb Perspect Med*. 2013;3(9). doi:10.1101/CSHPERSPECT.A015487

124. Wiseman AC. Immunosuppressive Medications. *Clin J Am Soc Nephrol*. 2016;11(2):332-343. doi:10.2215/CJN.08570814

125. Mueller TF. Mechanisms of action of thymoglobulin. *Transplantation*. 2007;84(11 S SUPPL.). doi:10.1097/01.TP.0000295420.49063.B1

126. Hardinger KL, Rhee S, Buchanan P, et al. A prospective, randomized, double-blinded comparison of thymoglobulin versus Atgam for induction immunosuppressive therapy: 10-year results. *Transplantation*. 2008;86(7):947-952. doi:10.1097/TP.0B013E318187BC67

127. Webster AC, Playford EG, Higgins G, Chapman JR, Craig JC. Interleukin 2 receptor antagonists for renal transplant recipients: a meta-analysis of randomized trials. *Transplantation*. 2004;77(2):166-176. doi:10.1097/01.TP.0000109643.32659.C4

128. Webster AC, Ruster LP, Mcgee RG, et al. Interleukin 2 receptor antagonists for kidney transplant recipients. *Cochrane database Syst Rev*. 2010;2010(1). doi:10.1002/14651858.CD003897.PUB3

129. Tiede I, Fritz G, Strand S, et al. CD28-dependent Rac1 activation is the molecular target of azathioprine in primary human CD4+ T lymphocytes. *J Clin Invest*. 2003;111(8):1133-1145. doi:10.1172/JCI16432

130. Rhen T, Cidlowski JA. Antiinflammatory Action of Glucocorticoids — New Mechanisms for Old Drugs. *https://doi.org/101056/NEJMra050541*. 2005;353(16):1711-1723. doi:10.1056/NEJMRA050541

131. A W, RC W, RS T, JR C, JC C. Tacrolimus versus cyclosporin as primary immunosuppression for kidney transplant recipients. *Cochrane database Syst Rev*. 2005;(4). doi:10.1002/14651858.CD003961.PUB2

132. Kehrl JH, Wakefield LM, Roberts AB, et al. Production of transforming growth factor beta by human T lymphocytes and its potential role in the regulation of T cell growth. *J Exp Med*. 1986;163(5):1037-1050. doi:10.1084/JEM.163.5.1037

133. Wakeland EK. Immunotherapy as a means to induce transplantation tolerance. *Curr Opin Immunol*. 2002;14(5):660-665. doi:10.1016/S0952-7915(02)00376-X

134. van Sandwijk MS, Bemelman FJ, ten Berge IJM. Immunosuppressive drugs after solid organ transplantation. Netherlands Journal of Medicine. Published 2013. Accessed December 3, 2022. https://pubmed.ncbi.nlm.nih.gov/23956308/

135. A Randomized Clinical Trial of OKT3 Monoclonal Antibody for Acute Rejection of Cadaveric Renal Transplants. *N Engl J Med*. 1985;313(6):337-342. doi:10.1056/nejm198508083130601

136. Noble S, Markham A. Cyclosporin. A review of the pharmacokinetic properties, clinical efficacy and tolerability of a microemulsion-based formulation (Neoral). *Drugs*. 1995;50(5):924-941. doi:10.2165/00003495-199550050-00009

137. Peters DH, Fitton A, Plosker GL, Faulds D. Tacrolimus: A Review of its Pharmacology, and Therapeutic Potential in Hepatic and Renal Transplantation. Drugs. doi:10.2165/00003495-199346040-00009

138. Maxwell L, Singh JA. Abatacept for rheumatoid arthritis. *Cochrane database Syst Rev*. 2009;2009(4). doi:10.1002/14651858.CD007277.PUB2

139. Larsen CP, Pearson TC, Adams AB, et al. Rational Development of LEA29Y (belatacept), a High-Affinity Variant of CTLA4-Ig with Potent Immunosuppressive Properties. *Am J Transplant*. 2005;5(3):443-453. doi:10.1111/J.1600-6143.2005.00749.X

140. Okimura K, Maeta K, Kobayashi N, et al. Characterization of ASKP1240, a Fully Human Antibody Targeting Human CD40 With Potent Immunosuppressive Effects. *Am J Transplant*. 2014;14(6):1290-1299. doi:10.1111/AJT.12678

141. Thomson AW, Bonham CA, Zeevi A. Mode of action of tacrolimus (FK506): molecular and cellular mechanisms. *Ther Drug Monit*. 1995;17(6):584-591. doi:10.1097/00007691-199512000-00007

142. Bennett J, Cassidy H, Slattery C, Ryan MP, McMorrow T. Tacrolimus Modulates TGF-β Signaling to Induce Epithelial-Mesenchymal Transition in Human Renal Proximal Tubule Epithelial Cells. *J Clin Med 2016, Vol 5, Page 50*. 2016;5(5):50.

doi:10.3390/JCM5050050

143. Current and Future Immunosuppressive Therapies Following Transplantation. *Curr Futur Immunosuppr Ther Follow Transplant*. Published online 2001. doi:10.1007/978-94-010-1005-4

144. Fung JJ, Starzl TE. FK506 in solid organ transplantation. *Ther Drug Monit*. 1995;17(6):592-595. doi:10.1097/00007691-199512000-00008

145. Almawi WY, Assi JW, Chudzik DM, Jaoude MMA, Rieder MJ. Inhibition of Cytokine Production and Cytokine-Stimulated T-Cell Activation by FK506 (Tacrolimus)1. *http://dx.doi.org/103727/000000001783986387*. 2017;10(7):615-623. doi:10.3727/000000001783986387

146. Sigal NH, Dumont FJ. Cyclosporin A, FK-506, and Rapamycin: Pharmacologic Probes of Lymphocyte Signal Transduction. *https://doi.org/101146/annurev.iy10040192002511*. 2003;10:519-560. doi:10.1146/ANNUREV.IY.10.040192.002511

147. Almawi WY, Melemedjian OK. Clinical and mechanistic differences between FK506 (tacrolimus) and cyclosporin A. *Nephrol Dial Transplant*. 2000;15(12):1916-1918. doi:10.1093/NDT/15.12.1916

148. Dumont FJ. FK506, an immunosuppressant targeting calcineurin function. *Curr Med Chem*. 2000;7(7):731-748. doi:10.2174/0929867003374723

149. Bultynck G, De Smet P, Weidema AF, et al. Effects of the immunosuppressant FK506 on intracellular Ca2+ release and Ca2+ accumulation mechanisms. Published online June 2000. Accessed December 3, 2022. https://pubmed.ncbi.nlm.nih.gov/10856121/

150. MacMillan D. FK506 binding proteins: Cellular regulators of intracellular Ca2+ signalling. *Eur J Pharmacol*. 2013;700(1-3):181-193. doi:10.1016/J.EJPHAR.2012.12.029

151. Hassanpour SH, Dehghani M. Review of cancer from perspective of molecular. *J Cancer Res Pract*. 2017;4(4):127-129. doi:10.1016/J.JCRPR.2017.07.001

152. Swann JB, Smyth MJ. Immune surveillance of tumors. *J Clin Invest*. 2007;117(5):1137-1146. doi:10.1172/JCI31405

153. Zou W. Immunosuppressive networks in the tumour environment and their therapeutic relevance. *Nat Rev Cancer 2005 54*. 2005;5(4):263-274. doi:10.1038/nrc1586

154. Yang L, Carbone DP. Tumor-host immune interactions and dendritic cell dysfunction. *Adv Cancer Res*. 2004;92:13-27. doi:10.1016/S0065-230X(04)92002-7

155. Kusmartsev S, Gabrilovich DI. Immature myeloid cells and cancer-associated immune suppression. 2002;51(6):293-298. doi:10.1007/S00262-002-0280-8

156. Kim R, Emi M, Tanabe K. Cancer immunosuppression and autoimmune disease: beyond immunosuppressive networks for tumour immunity. *Immunology*. 2006;119(2):254-264. doi:10.1111/J.1365-2567.2006.02430.X

157. Kusmartsev S, Nefedova Y, Yoder D, Gabrilovich DI. Antigen-specific inhibition of CD8+ T cell response by immature myeloid cells in cancer is mediated by reactive oxygen species. *J Immunol*. 2004;172(2):989-999. doi:10.4049/JIMMUNOL.172.2.989

158. Kuzu OF, Nguyen FD, Noory MA, Sharma A. Current State of Animal (Mouse) Modeling in Melanoma Research. *https://doi.org/104137/CGMS21214*. 2015;8s1(s1):CGM.S21214. doi:10.4137/CGM.S21214

159. Overwijk WW, Restifo NP. B16 as a Mouse Model for Human Melanoma. *Curr Protoc Immunol*. 39(1). Accessed December 2, 2022. https://onlinelibrary.wiley.com/doi/full/10.1002/0471142735.im2001s39

160. Potez M, Trappetti V, Bouchet A, et al. Characterization of a B16-F10 melanoma model

locally implanted into the ear pinnae of C57BL/6 mice. *PLoS One*. 2018;13(11):e0206693. doi:10.1371/JOURNAL.PONE.0206693

161. Sun LX, Li WD, Lin Z Bin, et al. Cytokine production suppression by culture supernatant of B16F10 cells and amelioration by Ganoderma lucidum polysaccharides in activated lymphocytes. *Cell Tissue Res*. 2015;360(2):379-389. Accessed December 2, 2022. https://link.springer.com/article/10.1007/s00441-014-2083-6

162. Sun LX, Lin Z Bin, Duan XS, et al. Ganoderma lucidum polysaccharides antagonize the suppression on lymphocytes induced by culture supernatants of B16F10 melanoma cells. *J Pharm Pharmacol*. 2011;63(5):725-735. Accessed December 2, 2022. https://academic.oup.com/jpp/article/63/5/725/6135570

163. Chen YQ, Li PC, Pan N, et al. Tumor-released autophagosomes induces CD4+ T cell-mediated immunosuppression via a TLR2-IL-6 cascade. *J Immunother cancer*. 2019;7(1). doi:10.1186/S40425-019-0646-5

164. Zhou M, Wen Z, Cheng F, et al. Tumor-released autophagosomes induce IL-10-producing B cells with suppressive activity on T lymphocytes via TLR2-MyD88-NF-κB signal pathway. *Oncoimmunology*. 2016;5(7). doi:10.1080/2162402X.2016.1180485/SUPPL_FILE/KONI_A_1180485_SM9171.ZIP

165. Wen ZF, Liu H, Gao R, et al. Tumor cell-released autophagosomes (TRAPs) promote immunosuppression through induction of M2-like macrophages with increased expression of PD-L1. *J Immunother Cancer*. 2018;6(1):1-16. Accessed December 2, 2022. https://jitc.biomedcentral.com/articles/10.1186/s40425-018-0452-5

166. Poulaki V, Iliaki E, Mitsiades N, et al. Inhibition of Hsp90 attenuates inflammation in endotoxin-induced uveitis. *FASEB J*. 2007;21(9):2113-2123. Accessed December 4, 2022. https://onlinelibrary.wiley.com/doi/full/10.1096/fj.06-7637com

167. Dello Russo C, Polak PE, Mercado PR, et al. The heat-shock protein 90 inhibitor 17-allylamino-17-demethoxygeldanamycin suppresses glial inflammatory responses and ameliorates experimental autoimmune encephalomyelitis. *J Neurochem*. 2006;99(5):1351-1362. doi:10.1111/j.1471-4159.2006.04221.x

168. Oparil S, Acelajado MC, Bakris GL, et al. Hypertension. *Nat Rev Dis Prim*. 2018;4. doi:10.1038/nrdp.2018.14

169. Kjeldsen SE. Hypertension and cardiovascular risk: General aspects. *Pharmacol Res*. 2018;129:95-99. doi:https://doi.org/10.1016/j.phrs.2017.11.003

170. Chobanian A V, Bakris GL, Black HR, et al. Seventh report of the Joint National Committee on Prevention, Detection, Evaluation, and Treatment of High Blood Pressure. *Hypertens (Dallas, Tex 1979)*. 2003;42(6):1206-1252. doi:10.1161/01.HYP.0000107251.49515.c2

171. de Gasparo M, Catt KJ, Inagami T, Wright JW, Unger T. International union of pharmacology. XXIII. The angiotensin II receptors. *Pharmacol Rev*. 2000;52(3):415-472.

172. Horiuchi M, Akishita M, Dzau VJ. Recent progress in angiotensin II type 2 receptor research in the cardiovascular system. *Hypertension*. 1999;33(2):613-621. doi:10.1161/01.HYP.33.2.613

173. Abraham HMA, White CM, White WB. The comparative efficacy and safety of the angiotensin receptor blockers in the management of hypertension and other cardiovascular diseases. *Drug Saf*. 2015;38(1):33-54. doi:10.1007/s40264-014-0239-7

174. Barreras A, Gurk-Turner C. Angiotensin II receptor blockers. *Proc (Bayl Univ Med Cent)*. 2003;16(1):123-126. doi:10.1080/08998280.2003.11927893

175. Healey JS, Baranchuk A, Crystal E, et al. Prevention of atrial fibrillation with angiotensin-

converting enzyme inhibitors and angiotensin receptor blockers: a meta-analysis. *J Am Coll Cardiol*. 2005;45(11):1832-1839. doi:10.1016/j.jacc.2004.11.070

176. Kalikar M, Nivangune KS, Dakhale GN, et al. Efficacy and Tolerability of Olmesartan, Telmisartan, and Losartan in Patients of Stage I Hypertension: A Randomized, Open-label Study. *J Pharmacol Pharmacother*. 2017;8(3):106-111. doi:10.4103/jpp.JPP_39_17

177. Gore PN, Badar VA, Hardas MM, Bansode VJ. Comparative effect of telmisartan vs lisinopril on blood pressure in patients of metabolic syndrome. *Endocr Metab Immune Disord Drug Targets*. 2015;15(1):64-70. doi:10.2174/1871530314666141128154152

178. Arif AF, Kadam GG, Joshi C. Treatment of hypertension: postmarketing surveillance study results of telmisartan monotherapy, fixed dose combination of telmisartan + hydrochlorothiazide/amlodipine. *J Indian Med Assoc*. 2009;107(10):730-733.

179. Harrison DG, Guzik TJ, Lob HE, et al. Inflammation , Immunity , and Hypertension. Published online 2011:132-140. doi:10.1161/HYPERTENSIONAHA.110.163576

180. Huang S sha, Zhang Q bing, Yuan Q yan. Inhibitory effects of telmisartan on culture and proliferation of and Kv1 . 3 potassium channel expression in peripheral blood CD4 + T lymphocytes from Xinjiang Kazakh patients with hypertension. Published online 2016. doi:10.1177/1470320316674876

181. Guzik TJ, Hoch NE, Brown KA, et al. Role of the T cell in the genesis of angiotensin II – induced hypertension and vascular dysfunction. 2007;204(10). doi:10.1084/jem.20070657

182. De Miguel C, Rudemiller NP, Abais JM, Mattson DL. Inflammation and hypertension: new understandings and potential therapeutic targets. *Curr Hypertens Rep*. 2015;17(1):507. doi:10.1007/s11906-014-0507-z

183. Crowley SD, Song YS, Lin EE, Griffiths R, Kim HS, Ruiz P. Lymphocyte responses

exacerbate angiotensin II-dependent hypertension. *Am J Physiol Regul Integr Comp Physiol*. 2010;298(4):R1089-97. doi:10.1152/ajpregu.00373.2009

184. Huang SS, He SL, Zhang YM. The effects of telmisartan on the nuclear factor of activated T lymphocytes signalling pathway in hypertensive patients. *JRAAS - J Renin-Angiotensin-Aldosterone Syst*. 2016;17(2):0-7. doi:10.1177/1470320316655005

185. Nakano A, Hattori Y, Aoki C, Jojima T, Kasai K. Telmisartan inhibits cytokine-induced nuclear factor-κB activation independently of the peroxisome proliferator-activated receptor-γ. *Hypertens Res*. 2009;32(9):765-769. doi:10.1038/hr.2009.95

186. Arab HH, Al-Shorbagy MY, Abdallah DM, Nassar NN. Telmisartan attenuates colon inflammation, oxidative perturbations and apoptosis in a rat model of experimental inflammatory bowel disease. *PLoS One*. 2014;9(5). doi:10.1371/journal.pone.0097193

187. De S, Mamidi P, Ghosh S, et al. Telmisartan Restricts Chikungunya Virus Infection In Vitro and In Vivo through the AT1/PPAR-γ/MAPKs Pathways. *Antimicrob Agents Chemother*. 2022;66(1). doi:10.1128/AAC.01489-21

188. Okunuki Y, Usui Y, Nagai N, et al. Suppression of experimental autoimmune uveitis by angiotensin II type 1 receptor blocker telmisartan. *Invest Ophthalmol Vis Sci*. 2009;50(5):2255-2261. doi:10.1167/iovs.08-2649

189. Nilius B, Owsianik G. The transient receptor potential family of ion channels. *Genome Biol*. 2011;12(3):1-11. doi:10.1186/GB-2011-12-3-218/TABLES/2

190. Montell C. The history of TRP channels, a commentary and reflection. *Pflugers Arch Eur J Physiol*. 2011;461(5):499-506. doi:10.1007/S00424-010-0920-3/TABLES/1

191. Venkatachalam K, Montell C. TRP channels. *Annu Rev Biochem*. 2007;76:387-417. doi:10.1146/ANNUREV.BIOCHEM.75.103004.142819

192. Patapoutian A. TRP Channels and Thermosensation. *Chem Senses*. 2005;30(suppl_1):i193-i194. doi:10.1093/CHEMSE/BJH180

193. Chung MK, Jung SJ, Oh SB. Role of TRP channels in pain sensation. *Adv Exp Med Biol*. 2011;704:615-636. doi:10.1007/978-94-007-0265-3_33/FIGURES/2

194. Minke B. The History of the Drosophila TRP Channel: The Birth of a New Channel Superfamily. *http://dx.doi.org/103109/016770632010514369*. 2010;24(4):216-233. doi:10.3109/01677063.2010.514369

195. Cosens DJ, Manning A. Abnormal Electroretinogram from a Drosophila Mutant. *Nat 1969 2245216*. 1969;224(5216):285-287. doi:10.1038/224285a0

196. Minke B, Wu CF, Pak WL. Induction of photoreceptor voltage noise in the dark in Drosophila mutant. *Nat 1975 2585530*. 1975;258(5530):84-87. doi:10.1038/258084a0

197. Montell C, Rubin GM. Molecular characterization of the Drosophila trp locus: a putative integral membrane protein required for phototransduction. *Neuron*. 1989;2(4):1313-1323. doi:10.1016/0896-6273(89)90069-X

198. Montell C, Birnbaumer L, Flockerzi V, et al. A unified nomenclature for the superfamily of TRP cation channels. *Mol Cell*. 2002;9(2):229-231. doi:10.1016/S1097-2765(02)00448-3

199. Sano Y, Inamura K, Miyake A, et al. Immunocyte Ca2+ influx system mediated by LTRPC2. *Science (80-)*. 2001;293(5533):1327-1330. doi:10.1126/SCIENCE.1062473/SUPPL_FILE/1062473S2_THUMB.GIF

200. Montell C. The TRP superfamily of cation channels. *Sci STKE*. 2005;2005(272). doi:10.1126/STKE.2722005RE3

201. Venkatachalam K, Zheng F, Gill DL. Regulation of canonical transient receptor potential

(TRPC) channel function by diacylglycerol and protein kinase C. *J Biol Chem*. 2003;278(31):29031-29040. doi:10.1074/JBC.M302751200

202. Vazquez G, Bird GSJ, Mori Y, Putney JW. Native TRPC7 channel activation by an inositol trisphosphate receptor-dependent mechanism. *J Biol Chem*. 2006;281(35):25250-25258. doi:10.1074/JBC.M604994200

203. Caterina MJ, Schumacher MA, Tominaga M, Rosen TA, Levine JD, Julius D. The capsaicin receptor: a heat-activated ion channel in the pain pathway. *Nat 1997 3896653*. 1997;389(6653):816-824. doi:10.1038/39807

204. Zygmunt PM, Petersson J, Andersson DA, et al. Vanilloid receptors on sensory nerves mediate the vasodilator action of anandamide. *Nature*. 1999;400(6743):452-457. doi:10.1038/22761

205. McNamara FN, Randall A, Gunthorpe MJ. Effects of piperine, the pungent component of black pepper, at the human vanilloid receptor (TRPV1). *Br J Pharmacol*. 2005;144(6):781-790. doi:10.1038/SJ.BJP.0706040

206. Xu H, Blair NT, Clapham DE. Camphor Activates and Strongly Desensitizes the Transient Receptor Potential Vanilloid Subtype 1 Channel in a Vanilloid-Independent Mechanism. *J Neurosci*. 2005;25(39):8924-8937. doi:10.1523/JNEUROSCI.2574-05.2005

207. Liu D, Liman ER. Intracellular Ca2+ and the phospholipid PIP2 regulate the taste transduction ion channel TRPM5. *Proc Natl Acad Sci U S A*. 2003;100(25):15160-15165. doi:10.1073/PNAS.2334159100/SUPPL_FILE/4159FIG7.JPG

208. Perraud AL, Fleig A, Dunn CA, et al. ADP-ribose gating of the calcium-permeable LTRPC2 channel revealed by Nudix motif homology. *Nature*. 2001;411(6837):595-599. doi:10.1038/35079100

209. McKemy DD, Neuhausser WM, Julius D. Identification of a cold receptor reveals a general role for TRP channels in thermosensation. *Nat 2002 4166876*. 2002;416(6876):52-58. doi:10.1038/nature719

210. Peier AM, Moqrich A, Hergarden AC, et al. A TRP channel that senses cold stimuli and menthol. *Cell*. 2002;108(5):705-715. doi:10.1016/S0092-8674(02)00652-9

211. Bautista DM, Jordt SE, Nikai T, et al. TRPA1 mediates the inflammatory actions of environmental irritants and proalgesic agents. *Cell*. 2006;124(6):1269-1282. doi:10.1016/J.CELL.2006.02.023

212. Walker RG, Willingham AT, Zuker CS. A Drosophila mechanosensory transduction channel. *Science*. 2000;287(5461):2229-2234. doi:10.1126/SCIENCE.287.5461.2229

213. Li Y, Wright JM, Qian F, Germino GG, Guggino WB. Polycystin 2 interacts with type I inositol 1,4,5-trisphosphate receptor to modulate intracellular Ca2+ signaling. *J Biol Chem*. 2005;280(50):41298-41306. doi:10.1074/JBC.M510082200

214. Soyombo AA, Tjon-Kon-Sang S, Rbaibi Y, et al. TRP-ML1 regulates lysosomal pH and acidic lysosomal lipid hydrolytic activity. *J Biol Chem*. 2006;281(11):7294-7301. doi:10.1074/JBC.M508211200

215. Kiselyov K, Chen J, Rbaibi Y, et al. TRP-ML1 is a lysosomal monovalent cation channel that undergoes proteolytic cleavage. *J Biol Chem*. 2005;280(52):43218-43223. doi:10.1074/JBC.M508210200

216. Raychowdhury MK, González-Perrett S, Montalbetti N, et al. Molecular pathophysiology of mucolipidosis type IV: pH dysregulation of the mucolipin-1 cation channel. *Hum Mol Genet*. 2004;13(6):617-627. doi:10.1093/HMG/DDH067

217. Handlechner AG, Weiger TM, Hermann A. ACETALDEHYDE AND ION CHANNELS.

Published online 2015.

218. Startek JB, Voets T, Talavera K. To flourish or perish: evolutionary TRiPs into the sensory biology of plant-herbivore interactions. *Pflügers Arch - Eur J Physiol 2018 4712*. 2018;471(2):213-236. doi:10.1007/S00424-018-2205-1

219. Song MY, Yuan JXJ. Introduction to TRP channels: Structure, function, and regulation. *Adv Exp Med Biol*. 2010;661:99-108. doi:10.1007/978-1-60761-500-2_6/FIGURES/1

220. Li M, Yu Y, Yang J. Structural biology of TRP channels. *Adv Exp Med Biol*. 2011;704:1-23. doi:10.1007/978-94-007-0265-3_1

221. Hellmich UA, Gaudet R. Structural biology of TRP channels. *Handb Exp Pharmacol*. 2014;223:963-990. doi:10.1007/978-3-319-05161-1_10

222. Gaudet R. TRP channels entering the structural era. 2008;586(15):3565-3575. Accessed December 3, 2022. https://pubmed.ncbi.nlm.nih.gov/18535090/

223. Owsianik G, Talavera K, Voets T, Nilius B. PERMEATION AND SELECTIVITY OF TRP CHANNELS. *https://doi.org/101146/annurev.physiol68040204101406*. 2006;68:685-717. doi:10.1146/ANNUREV.PHYSIOL.68.040204.101406

224. Pan Z, Capó-Aponte JE, Reinach PS, Pan Z, Capó-Aponte JE, Reinach PS. Transient Receptor Potential (TRP) Channels in the Eye. *Adv Ophthalmol*. Published online March 7, 2012. doi:10.5772/34598

225. Lima M, Destro F, Cantone N, Maffi M, Ruggeri G, Dòmini R. Long-term follow-up after esophageal replacement in children: 45-Year single-center experience. *J Pediatr Surg*. 2015;50(9):1457-1461. doi:10.1016/J.JPEDSURG.2015.03.065

226. Billeter AT, Hellmann JL, Bhatnagar A, Polk HC. Transient receptor potential ion channels: powerful regulators of cell function. *Ann Surg*. 2014;259(2):229-235.

doi:10.1097/SLA.0B013E3182A6359C

227. Tõth BI, Oláh A, Szöllósi AG, Bírõ T. TRP channels in the skin. *Br J Pharmacol*. 2014;171(10):2568-2581. doi:10.1111/BPH.12569

228. Inada H, Iida T, Tominaga M. Different expression patterns of TRP genes in murine B and T lymphocytes. *Biochem Biophys Res Commun*. 2006;350(3):762-767. doi:10.1016/J.BBRC.2006.09.111

229. Entin-Meer M, Levy R, Goryainov P, et al. The Transient Receptor Potential Vanilloid 2 Cation Channel Is Abundant in Macrophages Accumulating at the Peri-Infarct Zone and May Enhance Their Migration Capacity towards Injured Cardiomyocytes following Myocardial Infarction. *PLoS One*. 2014;9(8):e105055. doi:10.1371/JOURNAL.PONE.0105055

230. Schilling T, Miralles F, Eder C. TRPM7 regulates proliferation and polarisation of macrophages. *J Cell Sci*. 2014;127(Pt 21):4561-4566. doi:10.1242/JCS.151068

231. Fonfria E, Murdock PR, Cusdin FS, Benham CD, Kelsell RE, McNulty S. Tissue Distribution Profiles of the Human TRPM Cation Channel Family. *http://dx.doi.org/101080/10799890600637506*. 2008;26(3):159-178. doi:10.1080/10799890600637506

232. Khalil M, Alliger K, Weidinger C, et al. Functional role of transient receptor potential channels in immune cells and epithelia. *Front Immunol*. 2018;9(FEB):174. doi:10.3389/FIMMU.2018.00174/BIBTEX

233. Tano JY, Solanki S, Lee RH, Smedlund K, Birnbaumer L, Vazquez G. Bone marrow deficiency of TRPC3 channel reduces early lesion burden and necrotic core of advanced plaques in a mouse model of atherosclerosis. *Cardiovasc Res*. 2014;101(1):138-144.

doi:10.1093/CVR/CVT231

234. Tano JY, Smedlund K, Lee R, Abramowitz J, Birnbaumer L, Vazquez G. Impairment of survival signaling and efferocytosis in TRPC3-deficient macrophages. *Biochem Biophys Res Commun*. 2011;410(3):643-647. doi:10.1016/J.BBRC.2011.06.045

235. Fernandes ES, Fernandes MA, Keeble JE. The functions of TRPA1 and TRPV1: moving away from sensory nerves. *Br J Pharmacol*. 2012;166(2):510-521. doi:10.1111/J.1476-5381.2012.01851.X

236. Guptill V, Cui X, Khaibullina A, et al. Disruption of the transient receptor potential vanilloid 1 can affect survival, bacterial clearance, and cytokine gene expression during murine sepsis. *Anesthesiology*. 2011;114(5):1190-1199. doi:10.1097/ALN.0B013E318212515B

237. Santoni G, Farfariello V, Liberati S, et al. The role of transient receptor potential vanilloid type-2 ion channels in innate and adaptive immune responses. *Front Immunol*. 2013;4(FRB):34. doi:10.3389/FIMMU.2013.00034/BIBTEX

238. Yamamoto S, Shimizu S, Kiyonaka S, et al. TRPM2-mediated Ca2+ influx induces chemokine production in monocytes that aggravates inflammatory neutrophil infiltration. *Nat Med 2008 147*. 2008;14(7):738-747. doi:10.1038/nm1758

239. Chen S jen, Bao L, Keefer K, et al. Transient receptor potential ion channel TRPM2 promotes AML proliferation and survival through modulation of mitochondrial function, ROS, and autophagy. *Cell Death Dis 2020 114*. 2020;11(4):1-17. doi:10.1038/s41419-020-2454-8

240. Romano B, Borrelli F, Fasolino I, et al. The cannabinoid TRPA1 agonist cannabichromene inhibits nitric oxide production in macrophages and ameliorates murine colitis. *Br J*

Pharmacol. 2013;169(1):213-229. doi:10.1111/BPH.12120

241. Oh-hora M, Rao A. Calcium signaling in lymphocytes. *Curr Opin Immunol*. 2008;20(3):250-258. doi:10.1016/J.COI.2008.04.004

242. Feske S, Skolnik EY, Prakriya M. Ion channels and transporters in lymphocyte function and immunity. *Nat Rev Immunol 2012 127*. 2012;12(7):532-547. doi:10.1038/nri3233

243. Vig M, Kinet JPP. Calcium signaling in immune cells. 10(1):21-27. doi:10.1038/ni.f.220

244. Parenti A, De Logu F, Geppetti P, Benemei S. What is the evidence for the role of TRP channels in inflammatory and immune cells? *Br J Pharmacol*. 2016;173(6):953-969. doi:10.1111/BPH.13392

245. Medic N, Desai A, Olivera A, et al. Knockout of the Trpc1 gene reveals that TRPC1 can promote recovery from anaphylaxis by negatively regulating mast cell TNF-α production. *Cell Calcium*. 2013;53(5-6):315-326. doi:10.1016/J.CECA.2013.02.001

246. Wenning AS, Neblung K, Strauß B, et al. TRP expression pattern and the functional importance of TRPC3 in primary human T-cells. *Biochim Biophys Acta*. 2011;1813(3):412-423. doi:10.1016/J.BBAMCR.2010.12.022

247. Guse AH, Da Silva CP, Berg I, et al. Regulation of calcium signalling in T lymphocytes by the second messenger cyclic ADP-ribose. *Nature*. 1999;398(6722):70-73. doi:10.1038/18024

248. Magnone M, Bauer I, Poggi A, et al. NAD+ levels control Ca2+ store replenishment and mitogen-induced increase of cytosolic Ca2+ by Cyclic ADP-ribose-dependent TRPM2 channel gating in human T lymphocytes. *J Biol Chem*. 2012;287(25):21067-21081. doi:10.1074/JBC.M111.324269

249. Bertin S, Aoki-Nonaka Y, De Jong PR, et al. The ion channel TRPV1 regulates the

activation and proinflammatory properties of CD4+ T cells. *Nat Immunol 2014 1511*. 2014;15(11):1055-1063. doi:10.1038/ni.3009

250. Majhi RK, Sahoo SS, Yadav M, Pratheek BM, Chattopadhyay S, Goswami C. Functional expression of TRPV channels in T cells and their implications in immune regulation. 2015;282(14):2661-2681. Accessed December 2, 2022. https://onlinelibrary.wiley.com/doi/full/10.1111/febs.13306

251. Zhang X, Chen W, Gao Q, et al. Rapamycin directly activates lysosomal mucolipin TRP channels independent of mTOR. *PLOS Biol*. 2019;17(5):e3000252. doi:10.1371/JOURNAL.PBIO.3000252

252. Fernandes ES, Liang L, Smillie SJ, et al. TRPV1 Deletion Enhances Local Inflammation and Accelerates the Onset of Systemic Inflammatory Response Syndrome. *J Immunol*. 2012;188(11):5741-5751. doi:10.4049/JIMMUNOL.1102147

253. Bok E, Chung YC, Kim KS, Baik HH, Shin WH, Jin BK. Modulation of M1/M2 polarization by capsaicin contributes to the survival of dopaminergic neurons in the lipopolysaccharide-lesioned substantia nigra in vivo. *Exp Mol Med 2018 507*. 2018;50(7):1-14. doi:10.1038/s12276-018-0111-4

254. Clark N, Keeble J, Fernandes ES, et al. The transient receptor potential vanilloid 1 (TRPV1) receptor protects against the onset of sepsis after endotoxin. *FASEB J*. 2007;21(13):3747-3755. doi:10.1096/FJ.06-7460COM

255. Motte J, Ambrosius B, Grüter T, et al. Capsaicin-enriched diet ameliorates autoimmune neuritis in rats. *J Neuroinflammation*. 2018;15(1):1-13. doi:10.1186/S12974-018-1165-X/FIGURES/5

256. Shutov LP, Warwick CA, Shi X, et al. The Complement System Component C5a

Produces Thermal Hyperalgesia via Macrophage-to-Nociceptor Signaling That Requires NGF and TRPV1. *J Neurosci*. 2016;36(18):5055-5070. doi:10.1523/JNEUROSCI.3249-15.2016

257. Warwick CA, Shutov LP, Shepherd AJ, Mohapatra DP, Usachev YM. Mechanisms underlying mechanical sensitization induced by complement C5a: the roles of macrophages, TRPV1, and calcitonin gene-related peptide receptors. *Pain*. 2019;160(3):702-711. doi:10.1097/J.PAIN.0000000000001449

258. Amantini C, Farfariello V, Cardinali C, et al. The TRPV1 ion channel regulates thymocyte differentiation by modulating autophagy and proteasome activity. *Oncotarget*. 2017;8(53):90766-90780. doi:10.18632/ONCOTARGET.21798

259. Bertin S, Aoki-Nonaka Y, Lee J, et al. The TRPA1 ion channel is expressed in CD4+ T cells and restrains T-cell-mediated colitis through inhibition of TRPV1. *Gut*. 2017;66(9):1584-1596. doi:10.1136/GUTJNL-2015-310710

260. Hsieh WS, Kung CC, Huang SL, Lin SC, Sun WH. TDAG8, TRPV1, and ASIC3 involved in establishing hyperalgesic priming in experimental rheumatoid arthritis. *Sci Reports 2017 71*. 2017;7(1):1-14. doi:10.1038/s41598-017-09200-6

261. Pohóczky K, Kun J, Szalontai B, et al. Estrogen-dependent up-regulation of TRPA1 and TRPV1 receptor proteins in the rat endometrium. *J Mol Endocrinol*. 2016;56(2):135-149. doi:10.1530/JME-15-0184

262. Tian C, Huang R, Tang F, et al. Transient Receptor Potential Ankyrin 1 Contributes to Lysophosphatidylcholine-Induced Intracellular Calcium Regulation and THP-1-Derived Macrophage Activation. *J Membr Biol*. 2020;253(1):43-55. doi:10.1007/S00232-019-00104-2/FIGURES/6

263. Wang Q, Chen K, Zhang F, et al. TRPA1 regulates macrophages phenotype plasticity and atherosclerosis progression. *Atherosclerosis*. 2020;301:44-53. doi:10.1016/J.ATHEROSCLEROSIS.2020.04.004

264. Usui-kusumoto K, Iwanishi H, Ichikawa K, et al. Suppression of neovascularization in corneal stroma in a TRPA1-null mouse. *Exp Eye Res*. 2019;181(February 2018):90-97.

265. Ma S, Zhang Y, He K, Wang P, Wang DH. Knockout of TRPA1 exacerbates angiotensin II-induced kidney injury. *Am J Physiol Renal Physiol*. 2019;317(3):F623-F631. doi:10.1152/AJPRENAL.00069.2019

266. Ma S, Wang DH. Knockout of Trpa1 Exacerbates Renal Ischemia–Reperfusion Injury With Classical Activation of Macrophages. *Am J Hypertens*. 2021;34(1):110-116. doi:10.1093/AJH/HPAA162

267. Zeng D, Chen C, Zhou W, et al. TRPA1 deficiency alleviates inflammation of atopic dermatitis by reducing macrophage infiltration. *Life Sci*. 2021;266:118906. doi:10.1016/J.LFS.2020.118906

268. Gouin O, L'Herondelle K, Lebonvallet N, et al. TRPV1 and TRPA1 in cutaneous neurogenic and chronic inflammation: pro-inflammatory response induced by their activation and their sensitization. 2017;8(9):644-661. Accessed December 3, 2022. https://link.springer.com/article/10.1007/s13238-017-0395-5

269. Sahoo SSS, Majhi RKK, Tiwari A, et al. Transient receptor potential ankyrin1 channel is endogenously expressed in T cells and is involved in immune functions. 2019;39(9):BSR20191437. Accessed December 3, 2022. /bioscirep/article/39/9/BSR20191437/220415/Transient-receptor-potential-ankyrin1-channel-is

270.   Csekő K, Beckers B, Keszthelyi D, Helyes Z. Role of TRPV1 and TRPA1 Ion Channels in Inflammatory Bowel Diseases: Potential Therapeutic Targets? *Pharm 2019, Vol 12, Page 48*. 2019;12(2):48. doi:10.3390/PH12020048

271.   Kun J, Szitter I, Kemény Á, et al. Upregulation of the Transient Receptor Potential Ankyrin 1 Ion Channel in the Inflamed Human and Mouse Colon and Its Protective Roles. *PLoS One*. 2014;9(9):e108164. doi:10.1371/JOURNAL.PONE.0108164

272.   Trevisan G, Benemei S, Materazzi S, et al. TRPA1 mediates trigeminal neuropathic pain in mice downstream of monocytes/macrophages and oxidative stress. 2016;139:1361-1377. Accessed December 3, 2022. https://pubmed.ncbi.nlm.nih.gov/26984186/

273.   Zhao JF, Shyue SK, Kou YR, Lu TM, Lee TS. Transient Receptor Potential Ankyrin 1 Channel Involved in Atherosclerosis and Macrophage-Foam Cell Formation. 2016;12(7):812-823. doi:10.7150/IJBS.15229

274.   Cameron AM, Steiner JP, Sabatini DM, Kaplin AI, Walensky LD, Snyder SH. Immunophilin FK506 binding protein associated with inositol 1,4,5-trisphosphate receptor modulates calcium flux. *Proc Natl Acad Sci*. 1995;92(5):1784-1788. doi:10.1073/PNAS.92.5.1784

275.   Cameron AM, Steiner JP, Roskams AJ, Ali SM, Ronnettt G V., Snyder SH. Calcineurin associated with the inositol 1,4,5-trisphosphate receptor-FKBP12 complex modulates Ca2+ flux. *Cell*. 1995;83(3):463-472. doi:10.1016/0092-8674(95)90124-8

276.   MacMillan D, McCarron JG. Regulation by FK506 and rapamycin of Ca2+ release from the sarcoplasmic reticulum in vascular smooth muscle: the role of FK506 binding proteins and mTOR. *Br J Pharmacol*. 2009;158(4). Accessed December 3, 2022. https://onlinelibrary.wiley.com/doi/full/10.1111/j.1476-5381.2009.00369.x

277. Van Acker K, Bultynck G, Rossi D, et al. The 12 kDa FK506-binding protein, FKBP12, modulates the Ca(2+)-flux properties of the type-3 ryanodine receptor. *J Cell Sci*. 2004;117(Pt 7):1129-1137. doi:10.1242/JCS.00948

278. Arcas JM, González A, Gers-Barlag K, et al. The Immunosuppressant Macrolide Tacrolimus Activates Cold-Sensing TRPM8 Channels. *J Neurosci*. 2019;39(6):949-969. doi:10.1523/JNEUROSCI.1726-18.2018

279. Taipale M, Jarosz DF, Lindquist S. HSP90 at the hub of protein homeostasis: emerging mechanistic insights. *Nat Rev Mol Cell Biol 2010 117*. 2010;11(7):515-528. doi:10.1038/nrm2918

280. Robert J. Evolution of heat shock protein and immunity. *Dev Comp Immunol*. 2003;27(6-7):449-464. doi:10.1016/S0145-305X(02)00160-X

281. Sreedhar AS, Nardai G, Csermely P. Enhancement of complement-induced cell lysis: A novel mechanism for the anticancer effects of Hsp90 inhibitors. *Immunol Lett*. 2004;92(1-2):157-161. doi:10.1016/j.imlet.2003.11.025

282. Geller R, Taguwa S, Frydman J. Broad action of Hsp90 as a host chaperone required for viral replication. *Biochim Biophys Acta - Mol Cell Res*. 2012;1823(3):698-706. doi:10.1016/J.BBAMCR.2011.11.007

283. Siebelt M, Jahr H, Groen HC, et al. Hsp90 inhibition protects against biomechanically induced osteoarthritis in rats. *Arthritis Rheum*. 2013;65(8):2102-2112. doi:10.1002/ART.38000/ABSTRACT

284. Tukaj S, Węgrzyn G. Anti-Hsp90 therapy in autoimmune and inflammatory diseases: a review of preclinical studies. *Cell Stress Chaperones*. 2016;21(2):213-218. doi:10.1007/S12192-016-0670-Z/FIGURES/2

285. Srisutthisamphan K, Jirakanwisal K, Ramphan S, Tongluan N, Kuadkitkan A, Smith DR. Hsp90 interacts with multiple dengue virus 2 proteins. 2018;8(1). doi:10.1038/s41598-018-22639-5

286. Trepel J, Mollapour M, Giaccone G, Neckers L. Targeting the dynamic HSP90 complex in cancer. 2010;10(8):537-549. doi:10.1038/nrc2887

287. Bhat R, Tummalapalli SR, Rotella DP. Progress in the discovery and development of heat shock protein 90 (Hsp90) inhibitors. *J Med Chem*. 2014;57(21):8718-8728. doi:10.1021/JM500823A/ASSET/IMAGES/LARGE/JM-2014-00823A_0013.JPEG

288. Jhaveri K, Ochiana SO, Dunphy MPS, et al. Heat shock protein 90 inhibitors in the treatment of cancer: current status and future directions. *http://dx.doi.org/101517/135437842014902442*. 2014;23(5):611-628. doi:10.1517/13543784.2014.902442

289. Kim T, Keum G, Pae AN. Discovery and development of heat shock protein 90 inhibitors as anticancer agents: a review of patented potent geldanamycin derivatives. *http://dx.doi.org/101517/135437762013780597*. 2013;23(8):919-943. doi:10.1517/13543776.2013.780597

290. Srivastava P. Roles of heat-shock proteins in innate and adaptive immunity. 2002;2(3):185-194. doi:10.1038/nri749

291. Graner MW. HSP90 and Immune Modulation in Cancer. *Adv Cancer Res*. 2016;129:191-224. doi:10.1016/BS.ACR.2015.10.001

292. Bae J, Munshi A, Li C, et al. Heat shock protein 90 is critical for regulation of phenotype and functional activity of human T lymphocytes and NK cells. *J Immunol*. 2013;190(3):1360-1371. doi:10.4049/JIMMUNOL.1200593

293. Sugita T, Tanaka S, Murakami T, Miyoshi H, Ohnuki T. Immunosuppressive effects of the heat shock protein 90-binding antibiotic geldanamycin. *IUBMB Life*. 1999;47(4):587-595. doi:10.1080/15216549900201633

294. Bijlmakers MJE, Marsh M. Hsp90 is essential for the synthesis and subsequent membrane association, but not the maintenance, of the Src-kinase p56(lck). *Mol Biol Cell*. 2000;11(5):1585-1595.

    doi:10.1091/MBC.11.5.1585/ASSET/IMAGES/LARGE/MK0501207009.JPEG

295. Wax S, Piecyk M, Maritim B, Anderson P. Geldanamycin inhibits the production of inflammatory cytokines in activated macrophages by reducing the stability and translation of cytokine transcripts. *Arthritis Rheum*. 2003;48(2):541-550. doi:10.1002/ART.10780

296. Giannini A, Bijlmakers MJ. Regulation of the Src Family Kinase Lck by Hsp90 and Ubiquitination. *Mol Cell Biol*. 2004;24(13):5667-5676. Accessed December 4, 2022. https://journals.asm.org/doi/10.1128/MCB.24.13.5667-5676.2004

297. De Nardo D, Masendycz P, Ho S, et al. A Central Role for the Hsp90·Cdc37 Molecular Chaperone Module in Interleukin-1 Receptor-associated-kinase-dependent Signaling by Toll-like Receptors. *J Biol Chem*. 2005;280(11):9813-9822. doi:10.1074/JBC.M409745200

298. Rice JW, Veal JM, Fadden RP, et al. Small molecule inhibitors of Hsp90 potently affect inflammatory disease pathways and exhibit activity in models of rheumatoid arthritis. *Arthritis Rheum*. 2008;58(12):3765-3775. doi:10.1002/ART.24047

299. Dello Russo C, Polak PE, Mercado PR, et al. The heat-shock protein 90 inhibitor 17-allylamino-17-demethoxygeldanamycin suppresses glial inflammatory responses and ameliorates experimental autoimmune encephalomyelitis. *J Neurochem*. 2006;99(5):1351-1362. doi:10.1111/J.1471-4159.2006.04221.X

300. Sahoo SS, Pratheek BM, Meena VS, et al. VIPER regulates naive T cell activation and effector responses: Implication in TLR4 associated acute stage T cell responses. *Sci Rep*. 2018;8(1):7118. doi:10.1038/s41598-018-25549-8

301. Gao R, Ma J, Wen Z, et al. Tumor cell-released autophagosomes (TRAP) enhance apoptosis and immunosuppressive functions of neutrophils. *Oncoimmunology*. 2018;7(6). doi:10.1080/2162402X.2018.1438108/SUPPL_FILE/KONI_A_1438108_SM0127.ZIP

302. Nayak TK, Mamidi P, Kumar A, et al. Regulation of Viral Replication, Apoptosis and Pro-Inflammatory Responses by 17-AAG during Chikungunya Virus Infection in Macrophages. *Viruses 2017, Vol 9, Page 3*. 2017;9(1):3. doi:10.3390/V9010003

303. Nayak TK, Mamidi P, Sahoo SS, et al. P38 and JNK Mitogen-Activated Protein Kinases Interact with Chikungunya Virus Non-structural Protein-2 and Regulate TNF Induction during Viral Infection in Macrophages. *Front Immunol*. 2019;10(APR):786. doi:10.3389/FIMMU.2019.00786/BIBTEX

304. Tripathi P, Tripathi P, Kashyap L, Singh V. The role of nitric oxide in inflammatory reactions. *FEMS Immunol Med Microbiol*. 2007;51(3):443-452. doi:10.1111/J.1574-695X.2007.00329.X

305. Bertin S, Aoki-Nonaka Y, De Jong PR, et al. The ion channel TRPV1 regulates the activation and proinflammatory properties of CD4+ T cells. *Nat Immunol*. 2014;15(11):1055-1063. doi:10.1038/ni.3009

306. Bertin S, Raz E. Transient Receptor Potential (TRP) channels in T cells. *Semin Immunopathol*. 2016;38(3):309. doi:10.1007/S00281-015-0535-Z

307. Bielefeldt K, Sharma R V., Whiteis C, Yedidag E, Abboud FM. Tacrolimus (FK506) modulates calcium release and contractility of intestinal smooth muscle. *Cell Calcium*.

1997;22(6):507-514. doi:10.1016/S0143-4160(97)90078-6

308. Kanoh S, Kondo M, Tamaoki J, et al. Effect of FK506 on ATP-induced intracellular calcium oscillations in cow tracheal epithelium. *Am J Physiol*. 1999;276(6). doi:10.1152/AJPLUNG.1999.276.6.L891

309. Cameron AM, Steiner JP, Sabatini DM, Kaplin AI, Walensky LD, Snyder SH. Immunophilin FK506 binding protein associated with inositol 1,4,5-trisphosphate receptor modulates calcium flux. *Proc Natl Acad Sci U S A*. 1995;92(5):1784-1788. doi:10.1073/PNAS.92.5.1784

310. Sanjai Kumar P, Nayak TK, Mahish C, et al. Inhibition of transient receptor potential vanilloid 1 (TRPV1) channel regulates chikungunya virus infection in macrophages. 166(1):139-155. doi:10.1007/S00705-020-04852-8

311. Logu F De, Nassini R, Materazzi S, et al. Schwann cell TRPA1 mediates neuroinflammation that sustains macrophage-dependent neuropathic pain in mice. *Nat Commun 2017 81*. 2017;8(1):1-16. doi:10.1038/s41467-017-01739-2

312. Facchinetti F, Amadei F, Geppetti P, et al. α,β-Unsaturated Aldehydes in Cigarette Smoke Release Inflammatory Mediators from Human Macrophages. *https://doi.org/101165/rcmb2007-0130OC*. 2012;37(5):617-623. doi:10.1165/RCMB.2007-0130OC

313. Ko HK, Lin AH, Perng DW, Lee TS, Kou YR. Lung Epithelial TRPA1 Mediates Lipopolysaccharide-Induced Lung Inflammation in Bronchial Epithelial Cells and Mice. *Front Physiol*. 2020;11:1521. doi:10.3389/FPHYS.2020.596314/BIBTEX

314. Yin S, Wang P, Xing R, et al. Transient Receptor Potential Ankyrin 1 (TRPA1) Mediates Lipopolysaccharide (LPS)-Induced Inflammatory Responses in Primary Human

Osteoarthritic Fibroblast-Like Synoviocytes. *Inflammation*. 2018;41(2):700-709. Accessed December 4, 2022. https://link.springer.com/article/10.1007/s10753-017-0724-0

315. Meseguer V, Alpizar YA, Luis E, et al. TRPA1 channels mediate acute neurogenic inflammation and pain produced by bacterial endotoxins. 2014;5(1). doi:10.1038/ncomms4125

316. Cojocaru F, Șelescu T, Domocoș D, et al. Functional expression of the transient receptor potential ankyrin type 1 channel in pancreatic adenocarcinoma cells. 2021;11(1). doi:10.1038/s41598-021-81250-3

317. Atoyan R, Shander D, Botchkareva N V. Non-Neuronal Expression of Transient Receptor Potential Type A1 (TRPA1) in Human Skin. *J Invest Dermatol*. 2009;129(9):2312-2315.

318. Yusuf N, Nasti TH, Huang CM, et al. Heat Shock Proteins HSP27 and HSP70 Are Present in the Skin and Are Important Mediators of Allergic Contact Hypersensitivity. *J Immunol*. 2009;182(1):675-683. Accessed December 4, 2022. https://journals.aai.org/jimmunol/article/182/1/675/78830/Heat-Shock-Proteins-HSP27-and-HSP70-Are-Present-in

319. Kamal A, Boehm MF, Burrows FJ. Therapeutic and diagnostic implications of Hsp90 activation. *Trends Mol Med*. 2004;10(6):283-290.

320. Prodromou C, Pearl L. Structure and Functional Relationships of Hsp90. *Curr Cancer Drug Targets*. 2005;3(5):301-323. doi:10.2174/1568009033481877

321. Nagata K, Duggan A, Kumar G, García-Añoveros J. Nociceptor and Hair Cell Transducer Properties of TRPA1, a Channel for Pain and Hearing. *J Neurosci*. 2005;25(16):4052-4061. doi:10.1523/JNEUROSCI.0013-05.2005

322. De Logu F, De Prá SDT, de David Antoniazzi CT, et al. Macrophages and Schwann cell

TRPA1 mediate chronic allodynia in a mouse model of complex regional pain syndrome type I. *Brain Behav Immun*. 2020;88:535-546. doi:10.1016/J.BBI.2020.04.037

323. Engel MA, Leffler A, Niedermirtl F, et al. TRPA1 and Substance P Mediate Colitis in Mice. *Gastroenterology*. 2011;141(4):1346-1358. doi:10.1053/J.GASTRO.2011.07.002

324. Beck R, Dejeans N, Glorieux C, et al. Hsp90 Is Cleaved by Reactive Oxygen Species at a Highly Conserved N-Terminal Amino Acid Motif. *PLoS One*. 2012;7(7):e40795. doi:10.1371/JOURNAL.PONE.0040795

325. Scroggins BT, Neckers L. Just say NO: nitric oxide regulation of Hsp90. *EMBO Rep*. 2009;10(10):1093-1094. Accessed December 4, 2022. https://onlinelibrary.wiley.com/doi/full/10.1038/embor.2009.212

326. Giustarini D, Rossi R, Milzani A, Dalle-Donne I. Nitrite and Nitrate Measurement by Griess Reagent in Human Plasma: Evaluation of Interferences and Standardization. *Methods Enzymol*. 2008;440:361-380. doi:10.1016/S0076-6879(07)00823-3

327. Ambade A, Catalano D, Lim A, Mandrekar P. Inhibition of heat shock protein (molecular weight 90 kDa) attenuates proinflammatory cytokines and prevents lipopolysaccharide-induced liver injury in mice. *Hepatology*. 2012;55(5):1585-1595. doi:10.1002/HEP.24802

328. Lei W, Mullen N, McCarthy S, et al. Heat-shock protein 90 (Hsp90) promotes opioid-induced anti-nociception by an ERK mitogen-activated protein kinase (MAPK) mechanism in mouse brain. *J Biol Chem*. 2017;292(25):10414-10428.

329. Kim W, Tokuda H, Kawabata T, et al. Enhancement by HSP90 inhibitor of PGD2-stimulated HSP27 induction in osteoblasts: Suppression of SAPK/JNK and p38 MAP kinase. *Prostaglandins Other Lipid Mediat*. 2019;143:106327.

330. Fujita K, Otsuka T, Kawabata T, et al. Inhibitors of heat shock protein 90 augment

endothelin-1-induced heat shock protein 27 through the SAPK/JNK signaling pathway in osteoblasts. *Mol Med Rep*. 2018;17(6):8542-8547. doi:10.3892/MMR.2018.8878/HTML

331. MOSER C, LANG SA, STOELTZING O. Heat-shock Protein 90 (Hsp90) as a Molecular Target for Therapy of Gastrointestinal Cancer. *Anticancer Res*. 2009;29(6):2031-2042.

332. Picard D. Heat-shock protein 90, a chaperone for folding and regulation. *Cell Mol life Sci C*. 2002;59(10):1640-1648. doi:10.1007/pl00012491

333. Souza Monteiro de Araújo D, De Logu F, Adembri C, et al. TRPA1 mediates damage of the retina induced by ischemia and reperfusion in mice. 2020;11(8). doi:10.1038/s41419-020-02863-6

334. Yin S, Zhang L, Ding L, et al. Transient receptor potential ankyrin 1 (trpa1) mediates il-1β-induced apoptosis in rat chondrocytes via calcium overload and mitochondrial dysfunction. 2018;15(1). Accessed December 4, 2022. https://journal-inflammation.biomedcentral.com/articles/10.1186/s12950-018-0204-9

335. Hoffmann A, Kann O, Ohlemeyer C, Hanisch UK, Kettenmann H. Elevation of Basal Intracellular Calcium as a Central Element in the Activation of Brain Macrophages (Microglia): Suppression of Receptor-Evoked Calcium Signaling and Control of Release Function. *J Neurosci*. 2003;23(11):4410-4419. doi:10.1523/JNEUROSCI.23-11-04410.2003

336. Trebak M, Kinet JP. Calcium signalling in T cells. *Nat Rev Immunol 2018 193*. 2019;19(3):154-169. doi:10.1038/s41577-018-0110-7

337. Friedmann KS, Bozem M, Hoth M. Calcium signal dynamics in T lymphocytes: Comparing in vivo and in vitro measurements. *Semin Cell Dev Biol*. 2019;94:84-93. doi:10.1016/J.SEMCDB.2019.01.004

338. Bertin S, Aoki-Nonaka Y, De Jong PR, et al. The ion channel TRPV1 regulates the activation and proinflammatory properties of CD4+ T cells. *Nat Immunol 2014 1511*. 2014;15(11):1055-1063. doi:10.1038/ni.3009

339. Pang B, Shin DH, Park KS, et al. Differential pathways for calcium influx activated by concanavalin A and CD3 stimulation in Jurkat T cells. *Pflugers Arch Eur J Physiol*. 2012;463(2):309-318. Accessed December 5, 2022. https://link.springer.com/article/10.1007/s00424-011-1039-x

340. Shin DW, Pan Z, Bandyopadhyay A, Bhat MB, Kim DH, Ma J. Ca2+-Dependent Interaction between FKBP12 and Calcineurin Regulates Activity of the Ca2+ Release Channel in Skeletal Muscle. *Biophys J*. 2002;83(5):2539-2549. doi:10.1016/S0006-3495(02)75265-X

341. Chen YQ, Li PC, Pan N, et al. Tumor-released autophagosomes induces CD4+ T cell-mediated immunosuppression via a TLR2–IL-6 cascade. *J Immunother Cancer*. 2019;7(1):178. doi:10.1186/S40425-019-0646-5

342. Racioppi L, Nelson ER, Huang W, et al. CaMKK2 in myeloid cells is a key regulator of the immune-suppressive microenvironment in breast cancer. 2019;10(1). doi:10.1038/s41467-019-10424-5

343. Pla AF, Gkika D. Emerging role of TRP channels in cell migration: From tumor vascularization to metastasis. *Front Physiol*. 2013;4 NOV:311. doi:10.3389/FPHYS.2013.00311/BIBTEX

344. Chang YY, Lu CW, Jean WH, Shieh JS, Lin TY. Phorbol myristate acetate induces differentiation of THP-1 cells in a nitric oxide-dependent manner. *Nitric Oxide*. 2021;109-110:33-41. doi:10.1016/J.NIOX.2021.02.002

345. Kochukov MY, Mcnearney TA, Fu Y, Westlund KN, Westlund KN, Trp T. Thermosensitive TRP ion channels mediate cytosolic calcium response in human synoviocytes. *Am J Physiol - Cell Physiol*. 2006;(3). Accessed December 5, 2022. https://journals.physiology.org/doi/10.1152/ajpcell.00553.2005

346. Stucky CL, Dubin AE, Jeske NA, Malin SA, McKemy DD, Story GM. Roles of transient receptor potential channels in pain. *Brain Res Rev*. 2009;60(1):2-23. doi:10.1016/j.brainresrev.2008.12.018

347. Mickle AD, Shepherd AJ, Mohapatra DP. Nociceptive TRP Channels: Sensory Detectors and Transducers in Multiple Pain Pathologies. *Pharmaceuticals (Basel)*. 2016;9(4). doi:10.3390/ph9040072

348. Omari SA, Adams MJ, Geraghty DP. TRPV1 Channels in Immune Cells and Hematological Malignancies. *Adv Pharmacol*. 2017;79:173-198. doi:10.1016/bs.apha.2017.01.002

349. Naert R, López-Requena A, Talavera K. TRPA1 Expression and Pathophysiology in Immune Cells. *Int J Mol Sci*. 2021;22(21). doi:10.3390/ijms222111460

350. Meneghini M, Bestard O, Grinyo JM. Immunosuppressive drugs modes of action. *Best Pract Res Clin Gastroenterol*. 2021;54-55:101757. doi:https://doi.org/10.1016/j.bpg.2021.101757

351. Parlakpinar H, Gunata M. Transplantation and immunosuppression: a review of novel transplant-related immunosuppressant drugs. *Immunopharmacol Immunotoxicol*. 2021;43(6):651-665. doi:10.1080/08923973.2021.1966033

352. Kumar PS, Mukherjee T, Khamaru S, et al. Correction to: Elevation of TRPV1 expression on T-cells during experimental immunosuppression. *J Biosci*. 2022;47.

353. Acharya TK, Tiwari A, Majhi RK, Goswami C. TRPM8 channel augments T-cell activation and proliferation. *Cell Biol Int*. 2021;45(1):198-210. doi:10.1002/cbin.11483

354. Bertin S, Aoki-Nonaka Y, Lee J, et al. The TRPA1 ion channel is expressed in CD4+ t cells and restrains T-cell-mediated colitis through inhibition of TRPV1. *Gut*. 2017;66(9):1584-1596. doi:10.1136/gutjnl-2015-310710

355. Radhakrishnan A, Mukherjee T, Mahish C, Kumar PS, Goswami C, Chattopadhyay S. TRPA1 activation and Hsp90 inhibition synergistically downregulate macrophage activation and inflammatory responses in vitro. *BMC Immunol*. 2023;24(1):16. doi:10.1186/s12865-023-00549-0

356. Shin DW, Pan Z, Bandyopadhyay A, Bhat MB, Kim DH, Ma J. Ca(2+)-dependent interaction between FKBP12 and calcineurin regulates activity of the Ca(2+) release channel in skeletal muscle. *Biophys J*. 2002;83(5):2539-2549. doi:10.1016/S0006-3495(02)75265-X

357. Landini L, Souza Monteiro de Araujo D, Titiz M, Geppetti P, Nassini R, De Logu F. TRPA1 Role in Inflammatory Disorders: What Is Known So Far? *Int J Mol Sci*. 2022;23(9). doi:10.3390/ijms23094529

358. Trevisani M, Siemens J, Materazzi S, et al. 4-Hydroxynonenal, an endogenous aldehyde, causes pain and neurogenic inflammation through activation of the irritant receptor TRPA1. *Proc Natl Acad Sci U S A*. 2007;104(33):13519-13524. doi:10.1073/pnas.0705923104

359. Andersson DA, Gentry C, Moss S, Bevan S. Transient receptor potential A1 is a sensory receptor for multiple products of oxidative stress. *J Neurosci Off J Soc Neurosci*. 2008;28(10):2485-2494. doi:10.1523/JNEUROSCI.5369-07.2008

360. Benítez-Angeles M, Morales-Lázaro SL, Juárez-González E, Rosenbaum T. TRPV1: Structure, Endogenous Agonists, and Mechanisms. *Int J Mol Sci*. 2020;21(10). doi:10.3390/ijms21103421

361. Morales-Lázaro SL, Simon SA, Rosenbaum T. The role of endogenous molecules in modulating pain through transient receptor potential vanilloid 1 (TRPV1). *J Physiol*. 2013;591(13):3109-3121. doi:10.1113/jphysiol.2013.251751

Elevation of TRPV1 expression on T-cells during experimental immunosuppression

P Sanjai Kumar[†], Tathagata Mukherjee[†], Somlata Khamaru,
Anukrishna Radhakrishnan, Dalai Jupiter Nanda Kishore,
Saurabh Chawla, Subhransu Sekhar Sahoo and Subhasis Chattopadhyay*

*School of Biological Sciences, National Institute of Science Education and Research,
Bhubaneswar 752050, India*

*Corresponding author (Email, subho@niser.ac.in)

[†]*P Sanjai Kumar and Tathagata Mukherjee equal contribution.*

The transient receptor potential vanilloid 1 (TRPV1) channel is a thermo-sensitive, polymodal cation channel. An increase in intracellular calcium (Ca^{2+}) is essential for T-cell responses. Similarly, various immuno-suppressive agents are also reported to induce Ca^{2+} influx. However, the possible involvement of TRPV1 during immunosuppression has not been studied yet. Here, we investigated the possible functional role of TRPV1 in FK506 or B16F10-culture supernatant (B16F10-CS)-driven experimental immunosuppression in T-cells. Intriguingly, it was found that TRPV1 surface expression was further significantly elevated during immunosuppression compared with concanavalin A (ConA) or TCR-activated T-cells. Moreover, in B16F10 tumor-bearing mice, TRPV1 expression was upregulated on splenic T-cells as compared with T-cells derived from control mice. We also observed an immediate increase in intracellular Ca^{2+} levels in FK506 (marked increase) and B16F10-CS treatment (modest increase) or in combination with T-cell activation as compared with resting and activated T-cells. Likewise, in B16F10 tumor-bearing mice, the basal intracellular calcium level was upregulated in T-cells as compared with controls. The elevated Ca^{2+} level(s) were found to be significantly downregulated by 5′-iodoresiniferatoxin (5′-IRTX) (a TRPV1-specific inhibitor), suggesting an important role of TRPV1 during immune activation and immunosuppression. The current study may have implications for immunosuppressive diseases along with inflammatory disorders associated with the coordinating role of TRPV1 and Ca^{2+} influx.

Keywords.   B16F10-CS; FK506; immunosuppression; T-cell; TRPV1

1. Introduction

Ion channels are well-characterized to decipher the functional role of various physiological processes. Moreover, they have been documented to regulate immune responses associated with T-cell activation and effector functions. There are around five major types of ion channels which are found to be operative in T-cells. These ion channels (e.g., Kv1.3, KCa3.1, Orai1+stromal interacting molecule 1 (STIM1) [Ca^{2+}-release activating Ca^{2+} (CRAC) channel]), TRP (transient receptor potential cation channel), and Cl_{swell}) are reported to harbor complex cascades of cellular signaling towards various T-cell-driven immune responses (Cahalan and Chandy 2009). Ca^{2+} channels are indispensable for T-cell activation as they promote the Ca^{2+} influx required for various cellular responses such as cytokine production, T-cell division, and differentiation towards effector responses (Dolmetsch *et al.* 1997; Vig and Kinet 2009; Hogan *et al.* 2010). Transient receptor potential (TRP) channels belong to a superfamily of ion channels that are thermo-sensitive, polymodal-gated,

and permeable to cations such as Ca^{2+} (Nilius 2007). Free Ca^{2+} ions serve as a second messenger of cells, including different immune cells such as T- and B-lymphocytes and macrophages, regulating various physiological processes like differentiation, gene transcription, and effector functions (Oh-hora and Rao 2008; Vig and Kinet 2009). Abnormality in Ca^{2+} signaling or unavailability in immune cells may lead to various immunological disorders like severe combined immunodeficiency (SCID) or may hamper the proper activation of naive T-cell and effector functions (Feske 2007; Majhi et al. 2015). Transient receptor potential vanilloid 1 channels (TRPV1) are reported to regulate Ca^{2+} influx and modulate various T-cell processes, including differentiation, proliferation, and activation (Bertin et al. 2014; Majhi et al. 2015; Amantini et al. 2017).

The association and the involvement of several TRPs and Ca^{2+} in cell-mediated immunity (CMI) are widely reported (Bertin et al. 2014; Majhi et al. 2015; Sahoo et al. 2019; Pathak et al. 2021; Kumar et al. 2021). Experimental analysis of CMI associated with T-cell responses, especially through in vitro and in vivo models, are also well reported. Concanavalin A (ConA) and T-cell receptor (TCR)-driven in vitro T-cell activation and subsequent Ca^{2+} release are described earlier (Komada et al. 1996; Pang et al. 2012; Majhi et al. 2015). Moreover, several immunosuppressive drugs and cancerous cell-driven regulation of T-cell responses are reported as well (Almawi et al. 2001; Zhou et al. 2016).

The functional role of TRPV1 in cell-mediated immunity (CMI) and its involvement in increase in intracellular Ca^{2+} have been reported (Bertin et al. 2014; Majhi et al. 2015; Pathak et al. 2021; Kumar et al. 2021). Moreover, a number of immunosuppressive agents such as rapamycin, tacrolimus (FK506), and cyclosporin have also been reported to induce intracellular increase of Ca^{2+} (Cameron et al. 1995; Bultynck et al. 2000; Van Acker et al. 2004; MacMillan and McCarron 2009). However, information about any alteration of TRP channels towards Ca^{2+} flux associated with immunosuppression remains scanty. It might be possible that TRPV1 may be differentially associated with the intracellular increase in Ca^{2+} levels and cellular responses during immunosuppression, similar to immune activation. Therefore, in the present study, the possible role of TRPV1 during experimental immunosuppression was explored. Moreover, FK506 (an immunosuppressive drug) (Almawi et al. 2001) or B16F10-culture supernatant-driven (B16F10-CS, used as immunosuppressive cell culture media from B16F10 murine melanoma cell line) (Zhou et al. 2016; Gao et al. 2018; Wen et al. 2018)

regulation of T-cell activation, inflammatory cytokine responses, and subsequent Ca^{2+} influx were investigated. The current study may have importance in TRPV1-associated immunosuppression in T-cells, which may have implications for various immunosuppressive diseases as well.

2.   Materials and methods

2.1   Mice

Both male and female C57BL/6 mice, 6 to 8 weeks old, from the National Institute of Science Education and Research (NISER), Bhubaneswar, were used for experimentation. All protocols were approved by the Institutional Animal Ethics Committee (IAEC), NISER, following CPCSEA guidelines.

2.2   Antibodies, reagents, and drugs

FK506 (Cat. no. F4679-5MG), Concanavalin A (ConA) (Cat. no. C0412-5MG), and 5′-IRTX (Cat. no. I9281-1MG) were purchased from Sigma Aldrich (St. Louis, USA); anti-mouse CD25 (Cat. no. 553866), OptEIA kits for IL-2 (Cat. no.555148), IFN-γ (Cat. no.555138), and TNF (Cat. no. 558534) for sandwich ELISA were from BD Biosciences, SJ, USA; anti-mouse CD69 (Cat. no. 35-0691-U100) and anti-mouse CD90.2 (Cat. no. 20-0903-U100) from Tonbo Biosciences, San Diego, CA, USA; anti-mouse TRPV1 (Cat. no. ACC-029) with TRPV1-specific blocking peptide (NSLPMESTPHKSRGS) from Alomone Laboratories (Jerusalem, Israel); anti-mouse CD3 (Cat. no. 40-0032-U500) and anti-mouse CD28 (Cat. no. 40-0281-U500) [functional assay grade] were procured from Tonbo Biosciences, San Diego, USA. Secondary anti-rabbit Alexa Fluor 488 and T-cell isolation kit (Dynabeads™ Untouched™ Mouse T-cells Kit, Cat. no. 11413D) were procured from Invitrogen, Carlsbad, CA, USA. RPMI-1640 cell culture medium and FBS were purchased from PAN Biotech, Germany; DMEM cell culture medium, 10X RBC lysis buffer, 10X PBS, L-glutamine, penicillin, and streptomycin were from Himedia Laboratories, Mumbai, India.

2.3   T-cell isolation, purification, and cell culture

As reported previously, splenocytes from mice were isolated (Sahoo et al. 2018). In brief, spleens of

C57BL/6 mice were disrupted through a 70 μm cell strainer. RBCs were lysed using RBC lysis buffer, washed with 1X PBS, centrifuged, and resuspended in complete RPMI-1640. T-cells were then purified using an Untouched T-cell Isolation Kit according to the manufacturer's protocol (Sahoo *et al.* 2018). Briefly, splenocytes were resuspended in an isolation buffer and incubated with biotinylated antibodies. Cells were then washed with excess isolation buffer, centrifuged, and incubated for 15 min with streptavidin-conjugated magnetic beads, and then placed in a magnet for 2 min. The purity of T-cells was ≥95%, measured using flow cytometry (BD FACSCalibur[TM] flow cytometer, BD Biosciences).

T-cell activation assays were performed using either ConA (5 μg/mL) or anti-CD3 (plate-bound, 2 μg/mL) and anti-CD28 (soluble, 2 μg/mL) as described previously (Majhi *et al.* 2015) in the presence or absence of either FK506 or B16F10-CS for 48 h.

2.4 *B16F10-CS collection and subcutaneous injection*

B16F10 (ATCC® CRL-6475[TM]) cells were cultured in DMEM and maintained as per ATCC protocol. At 60–70% of B16F10 confluency, the culture medium was replaced with a fresh medium, and after 24 h, the cell-free supernatant was collected and stored at −80°C until further use (Zhou *et al.* 2016; Gao *et al.* 2018).

B16F10 cells in the logarithmic growth phase (≤50% confluency) were harvested and suspended in an ice-cold HBSS buffer. After counting, 2×10^5 cells/mouse were injected subcutaneously (sc) in the right flank of wild-type C57BL/6 mice. 5 mice/group as a control group (without B16F10 cell injection) and B16F10 tumor-bearing group (injected with B16F10 cells) were used per experiment. From the 14th day, after the formation of a palpable tumor, tumor growth progression was periodically measured with a digital caliper (Fisher Scientific), and tumor volumes were calculated using [(tumor length × tumor width^2)/2]. On the 21st day, the mice were sacrificed, and the spleens were harvested for further processing (Overwijk and Restifo 2001).

2.5 *Cell viability assay*

Purified mouse T-cells were incubated with different doses of B16F10-CS (5–40% of final volume), 5′-IRTX (2.5–20 μM), and FK506 (1.25–20 μg/mL) for

48 h. Next, the cells were harvested and washed with 1X PBS. Finally, trypan blue was added, and viable cells were manually counted (Sahoo *et al.* 2018). For positive control, T-cells were either heat-killed (65°C for 5 min in a water bath) or UV-treated (30 min) before the cell viability assay.

2.6 *Flow cytometry*

Flow cytometric staining (FACS) of T-cells was performed according to the method reported previously (Majhi *et al.* 2015; Nayak *et al.* 2017; Sahoo *et al.* 2018, 2019). In brief, cells were harvested, washed with 1X PBS, resuspended in FACS buffer, and incubated with the fluorochrome-conjugated antibodies for 30 min on ice in the dark, and then washed twice with FACS buffer. For the extracellular expression of TRPV1 on T-cells after labeling with the anti-mouse TRPV1 Ab and washing, secondary fluorochrome-conjugated Ab was added and incubated for 30 min, followed by washing with FACS buffer. Cells were then fixed and acquired using the BD FACSCalibur[TM] flow cytometer or BD LSRFortessa[TM] (BD Biosciences). Flow cytometry gating was carried out to exclude the low FSC and SSC signals to remove the cellular debris, and 10,000 cells were acquired and further analyzed via Flowjo V10.7.1.

2.7 *Enzyme-linked immunosorbent assay*

Sandwich ELISA was performed to quantitate the cytokine levels in cell culture supernatants. ELISA for IL-2, IFN-γ, and TNF were performed using BD OptEIA ELISA kits according to the manufacturer's protocol (Nayak *et al.* 2017; Sahoo *et al.* 2019; Kumar *et al.* 2021). The cytokine concentration in supernatants was estimated by comparing the corresponding standard curve using different concentrations of the recombinant cytokines in pg/mL.

2.8 *Ca^{2+} influx*

To estimate the intracellular Ca^{2+} contributed by the TRPV1 channel during both immune-activation and immunosuppression of T-cells, we performed a minor modification to the standard Fluo-4 AM staining protocol. First, the T-cells were loaded with Ca^{2+}-sensitive dye (Fluo-4 AM, 2 μM) along with FK506, B16F10-CS, ConA, or TCR for 60 min at 37°C, as per the

experimental conditions (instead of adding the above reagents during acquisition). Additionally, another similar setup of T-cells was pre-treated with 5′-IRTX for 15 min before the addition of FK506, B16F10-CS, ConA, or TCR for 60 min at 37°C, as per the experimental conditions. Next, T-cells were washed twice with 1X PBS and placed inside an incubator for another 30 min for de-esterification. The cell suspension was added to the RIA vials and was acquired via flow cytometer. The rationale behind the idea was to test whether the treatment with these reagents (FK506, B16F10-CS, ConA, or TCR) led to an increase in intracellular Ca^{2+} over time as compared with 5′-IRTX-pre-treated T-cells (Majhi *et al.* 2015; Kumar *et al.* 2021). These values were plotted as a percentage of fluorescence signal relative to the starting signal as % F/F_0.

2.9 *Statistical analysis*

Statistical analysis was performed using the GraphPad Prism 9.0 software (GraphPad Software Inc., San Diego, CA, USA). Data are represented as mean±SEM. The comparison between the groups was performed by ANOVA or Student's *t*-test with the Sidak *post hoc* test. The data presented are representative of at least three independent experiments. Statistical significance is represented by asterisks (*) for *p*-value(s) and is marked correspondingly in the figures (*$p<0.05$, **$p<0.01$, ***$p<0.001$, ****$p<0.0001$).

3. Results

### 3.1 *Upregulation of TRPV1 during immune-activation and immunosuppression*

We performed flow cytometry to determine the surface expression level of TRPV1 channels in splenic purified T-cells. It was observed that the frequency (percentage) of TRPV1-positive cells was 17.86±1.34 as compared with isotype controls (0.02±0.01) (supplementary figure 1A). Further, the specificity of the TRPV1 antibody in T-cells was tested by using control blocking peptide antigen. For that, T-cells were stained with anti-TRPV1 antibody in the presence or absence of the blocking peptide. It was observed that the percentage of positive cells for TRPV1 was markedly reduced in a dose-dependent manner. These results indicate that TRPV1 is expressed on T-cells, and the anti-TRPV1 antibody is specific to TRPV1 expressed on T-cells (supplementary figure 1A).

Figure 1. Upregulation of TRPV1 on mouse T-cells during ▶ both immune activation and immunosuppression. T-cells were treated with either T-cell-activating agents or immunosuppressive agents for 48 h. (**A**) Dose kinetics study showing T-cell viability with (i) B16F10-CS, (ii) FK506, or (iii) 5′-IRTX, as assessed by trypan blue exclusion assay. The inset depicts the percentage of viable cells in heat-killed or UV-treated T-cells. Flow cytometry (FC) dot-plot depicting T-cell activation markers (**B**) CD69 and (**C**) CD25 along with the corresponding bar diagram. (**D**) Histogram representing T-cell proliferation as determined by CFSE staining along with its corresponding bar diagram. (**E**) FC dot-plot showing TRPV1 expression on T-cells along with the corresponding bar diagram. Representative data of three independent experiments are shown. One-way ANOVA was performed for significance calculation between the groups. $p<0.05$ was considered as statistically significant difference between the groups (ns, non-significant; *$p<0.05$; **$p<0.01$; ***$p<0.001$).

The cellular cytotoxicity of 5′-IRTX, FK506, and B16F10-CS in purified mouse T-cells was studied using the trypan blue exclusion method. It was observed that around ∼93% of the cells were viable for 5′-IRTX at 5 μM and FK506 at 5 μg/mL concentration, and ∼95% cells were viable at 20% B16F10-CS with respect to the total media volume (figure 1A). In all the experiments, either heat-killed or UV-treated T-cells were used as a positive control. Accordingly, we chose 5 μM 5′-IRTX, 5 μg/mL FK506, and 20% of B16F10-CS for further experiments.

Next, to determine the status of T-cell activation during immunosuppressive treatment with either FK506 or B16F10-CS, T-cell activation markers, including CD69 and CD25, were analyzed using flow cytometry (Majhi *et al.* 2015). It was observed that in T-cells pre-treated with either FK506 or B16F10-CS stimulated with ConA or TCR, both CD69 and CD25 decreased as compared with those in ConA- or TCR-activated T-cells (figure 1B, C). Additionally, a time kinetics study was performed to elucidate the expression levels of CD69 and CD25 with respect to activation in the presence or absence of FK506 and B16F10-CS treatment (supplementary figure 2). These results indicate that T-cell activation decreases in immunosuppressed T-cells stimulated with ConA or TCR.

T-cell activation is accompanied by T-cell proliferation and effector cytokine responses, as mentioned elsewhere (Majhi *et al.* 2015; Sahoo *et al.* 2018). To ascertain whether immunosuppressed T-cell's stimulation leads to reduced proliferation and cytokine response, we performed CFSE staining and ELISA, respectively. It was observed that in T-cells pre-treated
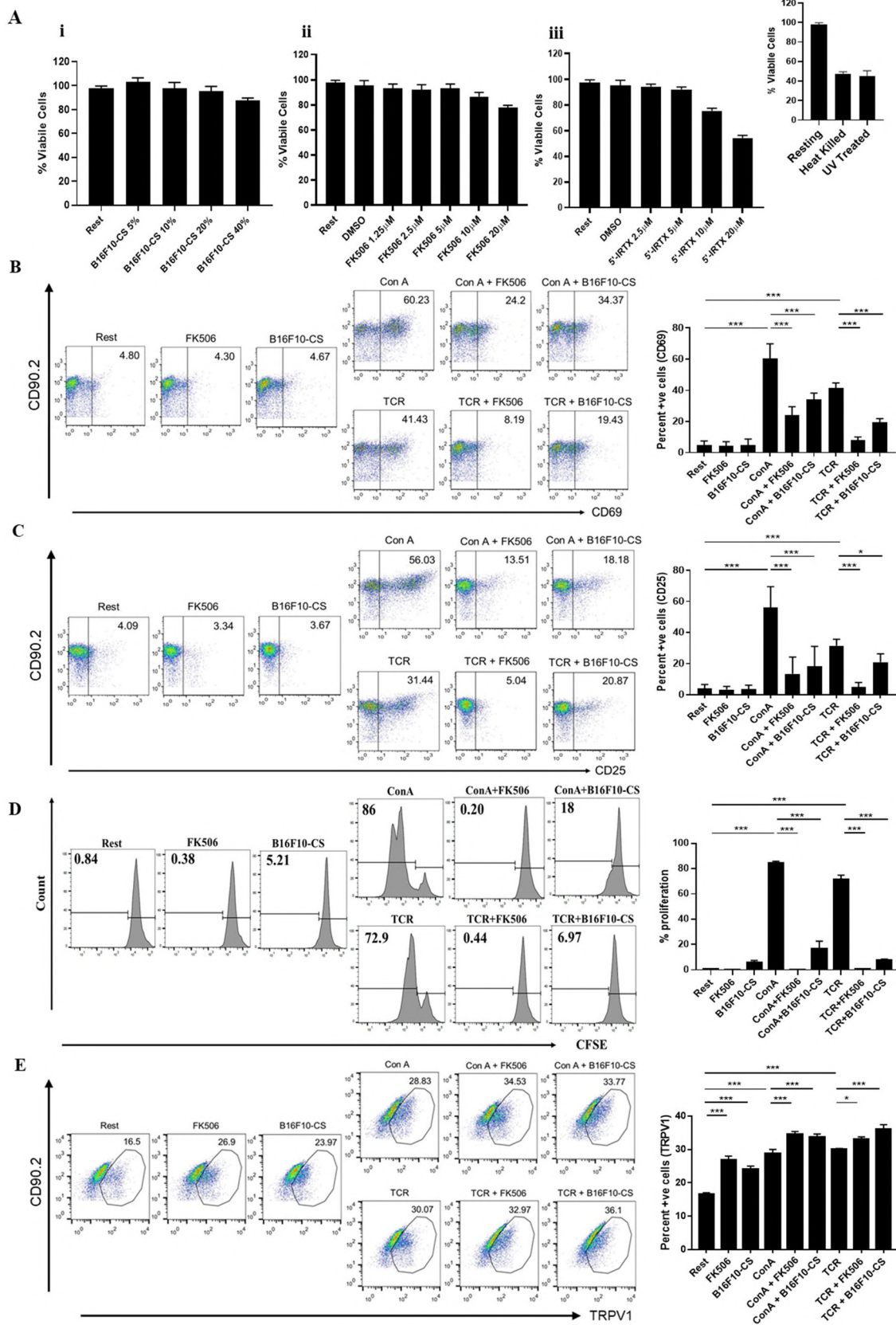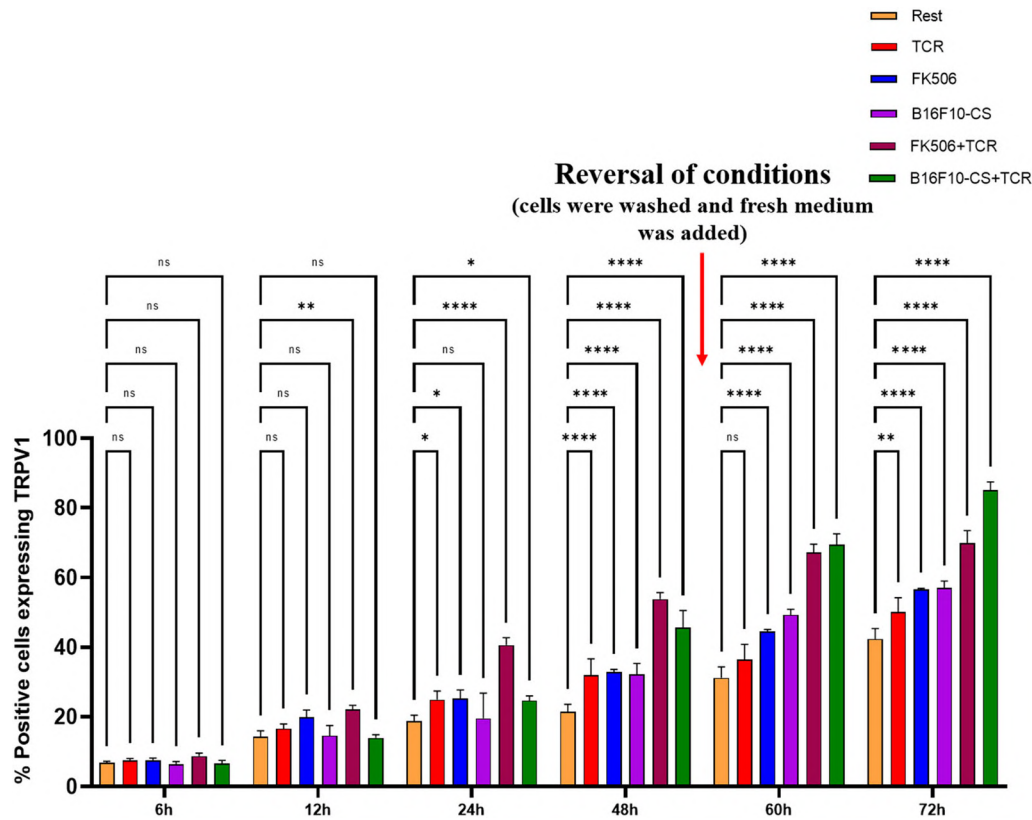
Figure 2. Time kinetics of TRPV1 expression on T-cells and during reversal of conditions. T-cells were treated according to the experimental plan mentioned. The expression profile of TRPV1 on T-cells at time points ranging from 6 h to 48 h is shown. The 48 h T-cells were washed and re-seeded with fresh medium. Those re-seeded T-cells were later harvested at 60 h–72 h and stained for TRPV1. Representative data are from three independent experiments. Two-way ANOVA was performed for significance calculation between the groups (ns, non-significant; *$p<0.05$; **$p<0.01$; ***$p<0.001$, ****$p<0.0001$).

with either FK506 or B16F10-CS stimulated with ConA or TCR, both T-cell proliferation (figure 1D) and pro-inflammatory cytokines, such as IFN-γ, IL-2, and TNF, decreased as compared with the corresponding ConA or TCR controls (supplementary figure 3). Altogether, these results indicate that both proliferation and cytokine response are markedly reduced in immunosuppressed T-cells.

Subsequently, the expression of TRPV1 was assessed in immunosuppressed T-cells. Intriguingly, TRPV1 expression levels significantly increased in T-cells treated with FK506 or B16F10-CS (26.9 ± 1.11 or 23.97 ± 1.04) as compared with resting T-cells (16.5 ± 0.52). Moreover, the TRPV1 expression further increased in FK506- or B16F10-CS-treated T-cells with ConA or TCR stimulation. In FK506- or B16F10-CS-treated T-cells stimulated with ConA or TCR, the TRPV1 expression was 34.53 ± 0.86 or 33.77 ± 0.85, respectively, as compared with control ConA-activated T-cells (28.83 ± 1.19). Similarly, in TCR-activated FK506 or B16F10-CS treated T-cells, the TRPV1

expression was 33.97 ± 0.77 or 36.1 ± 1.31, respectively, as compared with control TCR-activated T-cells (30.07 ± 0.20) (figure 1E). Interestingly, the current findings indicate that the TRPV1 expression also increases significantly in FK506 or B16F10-CS-treated T-cells as compared with the resting T-cells, which were further elevated in FK506- or B16F10-CS-treated T-cells stimulated with either ConA or TCR as compared with ConA or TCR stimulation alone.

3.2 *Time kinetics study of TRPV1 expression on T-cells and during reversal of immunosuppressive conditions*

To determine the effect of FK506 and B16F10-CS on TRPV1, its expression with time and during the reversal of immunosuppressive conditions, we performed a kinetic study via FC. It was observed that in FK506-treated T-cells, the TRPV1 expression significantly increased at an early time point of 24 h,
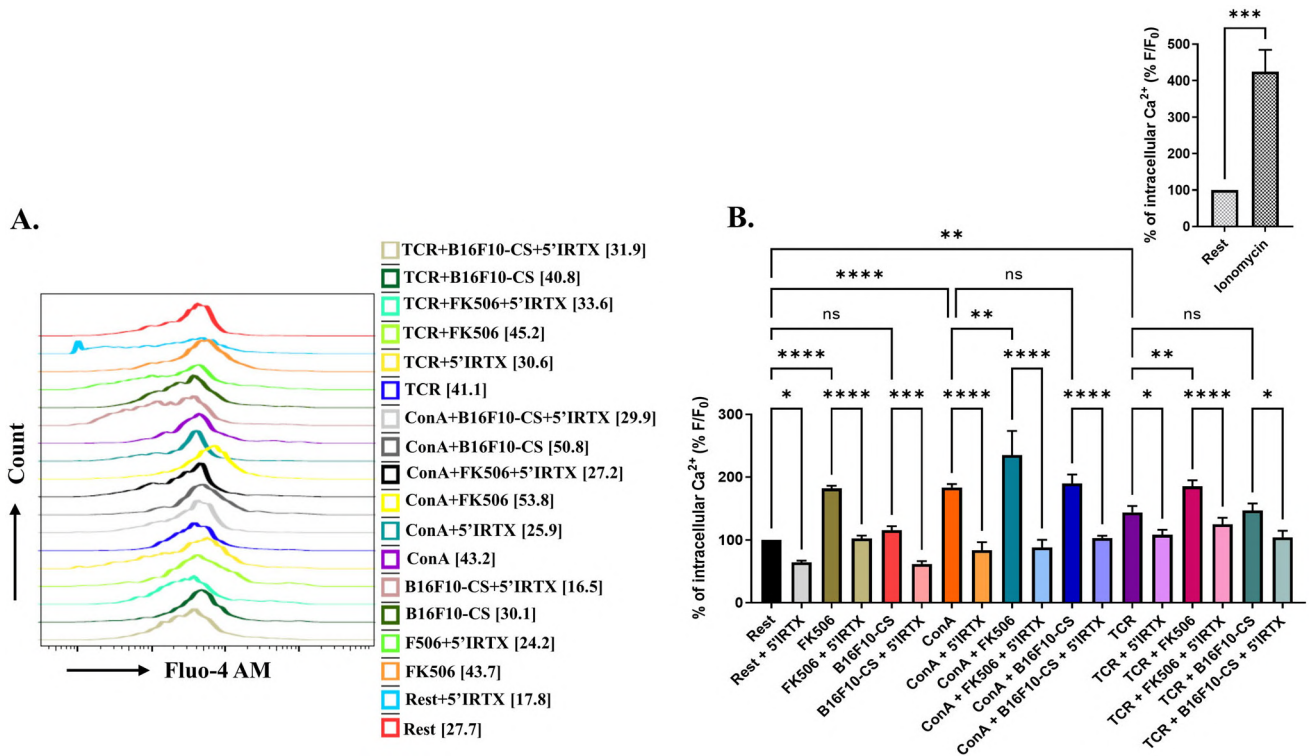
Figure 3. Modulation of intracellular Ca^{2+} in T-cells via TRPV1 channel. T-cells were incubated with calcium-sensitive dye, Fluo-4 AM, along with different experimental conditions for 1 h as mentioned in the materials and methods section and acquired via flow cytometry (FC). The various experimental conditions were pre-treated with 5′-IRTX, followed by treatment as per the experimental setup. (**A**) Histogram analysis of Fluo-4 intensity representing intracellular Ca^{2+} in T-cells. (**B**) Fluo-4 intensity representing intracellular Ca^{2+} has been expressed as a percentage normalized to resting control. The inset depicts the increase in intracellular Ca^{2+} levels in ionomycin-treated T-cells. Representative data are from three independent experiments. One-way ANOVA was performed for significance calculation between the groups (ns, non-significant; *$p<0.05$; **$p<0.01$; ***$p<0.001$, ****$p<0.0001$).

compared with resting T-cells. Further, in B16F10-CS-treated T-cells, the TRPV1 expression significantly increased at 48 h as compared with resting T-cells. The 48 h harvested T-cells were washed to remove FK506 or B16F10-CS and were re-seeded with fresh media. These T-cells were harvested at 60 h and 72 h. Intriguingly, it was observed that the TRPV1 expression levels also further heightened at 60 h and 72 h, as compared with T-cells at 48 h (figure 2). These results indicate that the FK506 or B16F10-CS induced TRPV1 upregulation is irreversible even after the removal of these immunosuppressive conditions.

3.3 *Modulation of intracellular Ca^{2+} via TRPV1 channel*

5′-IRTX is a potent and specific functional inhibitor of the TRPV1 channel and can block TRPV1-directed Ca^{2+} influx (Majhi *et al.* 2015; Kumar *et al.* 2021). Here, the intracellular Ca^{2+} levels were assessed by using the Ca^{2+}-sensitive dye Fluo-4 AM (Majhi *et al.* 2015; Sahoo *et al.* 2019). We have observed that in ConA- or TCR-stimulated T-cells, the calcium levels significantly increased compared with resting T-cells. Additionally, upon immunosuppressive treatment with FK506, the calcium levels further increased significantly compared with ConA or TCR controls. However, in B16F10-CS immunosuppressive conditions, a modest albeit non-significant increase in calcium levels was found (B16F10-CS: ∼115±6.1%, ConA+B16F10-CS: 190±14.3%, TCR+B16F10-CS: 147±11%) as compared with resting (100%), ConA (183±5.52%), or TCR (144±10.5%) controls. Furthermore, in the presence of the TRPV1-specific inhibitor, 5′-IRTX, the calcium levels significantly decreased compared with their corresponding controls (figure 3). These results indicate that other calcium channels fail to replenish the reduced Ca^{2+} levels due to TRPV1 blocking in T-cells. This highlights the fact that TRPV1 is indispensable in increasing intracellular Ca^{2+} levels in T-cells in both T-cell activation and immunosuppressive conditions.
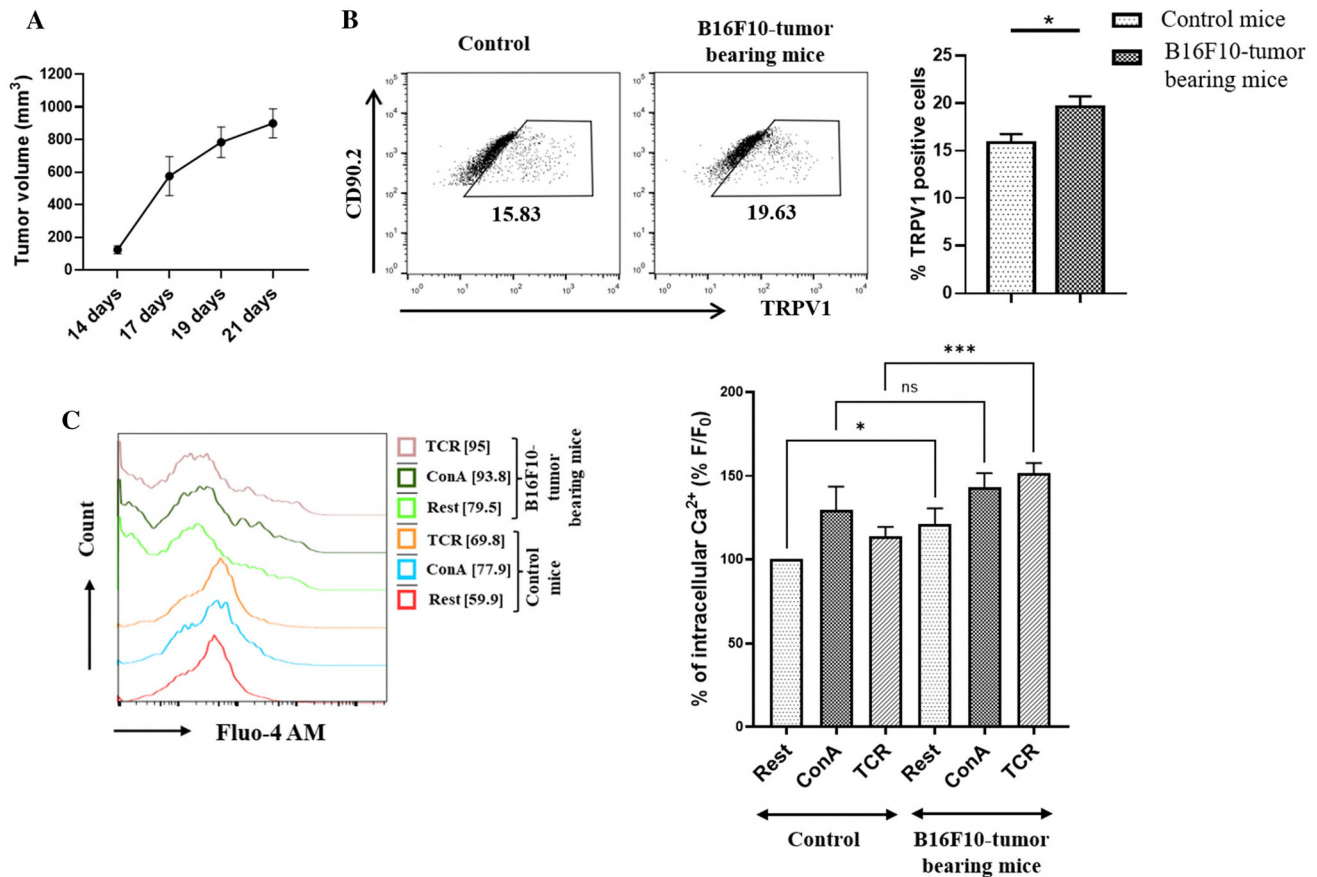
Figure 4. Modulation of TRPV1 expression and intracellular Ca^{2+} levels in splenic T-cells from control and B16F10 tumor-bearing mice. Splenic T-cells were isolated from control and tumor-bearing mice and analyzed via FC. (**A**) B16F10 tumor growth progression in C57BL/6 mice. (**B**) FC dot-plot depicting TRPV1 expression on T-cells along with its corresponding bar diagram. (**C**) Histogram plot of intracellular Ca^{2+} levels in untreated, ConA, or TCR-activated B16F10 tumor-bearing mice as compared with control mice. Fluo-4 intensity representing intracellular Ca^{2+} has been expressed as a percentage normalized to resting T-cells of control mice. Representative data of three independent experiments are shown. The *t*-test (**B**) and one-way ANOVA (**C**) were performed for significance calculation between the groups (ns, non-significant; *$p<0.05$; ***$p<0.001$).

3.4 *Modulation of TRPV1 expression and intracellular Ca^{2+} levels in B16F10 tumor-bearing mice*

B16F10, an immunosuppressive mouse melanoma cell line, was injected subcutaneously as described in the materials and methods section. In order to ascertain the modulation of TRPV1 expression and consequent changes in intracellular Ca^{2+} levels in splenic T-cells, we performed flow cytometry and calcium influx studies. Additionally, we also measured the tumor growth progression as described in the materials and methods section (figure 4A). It was observed that TRPV1 levels significantly increased in T-cells isolated from B16F10 tumor-bearing mice compared with control mice (figure 4B). Next, we assessed whether the increase in TRPV1 expression was associated with a concurrent increase in intracellular Ca^{2+} levels. We found that the basal intracellular Ca^{2+} levels also increased in T-cells isolated from B16F10 tumor-bearing mice as compared with control mice (figure 4C). Altogether, these results indicate that TRPV1 expression increases in T-cells isolated from B16F10 tumor-bearing mice, and consequently, the intracellular Ca^{2+} levels were also increased as compared with control mice.

4. Discussion

TRPV1, a member of the vanilloid group of the TRP family, is reported to have functional expression in a range of immune cells including T-cells, macrophages, dendritic cells, and NK cells (Majhi *et al.* 2015; Kumar *et al.* 2021). A number of T-cell activating agents,
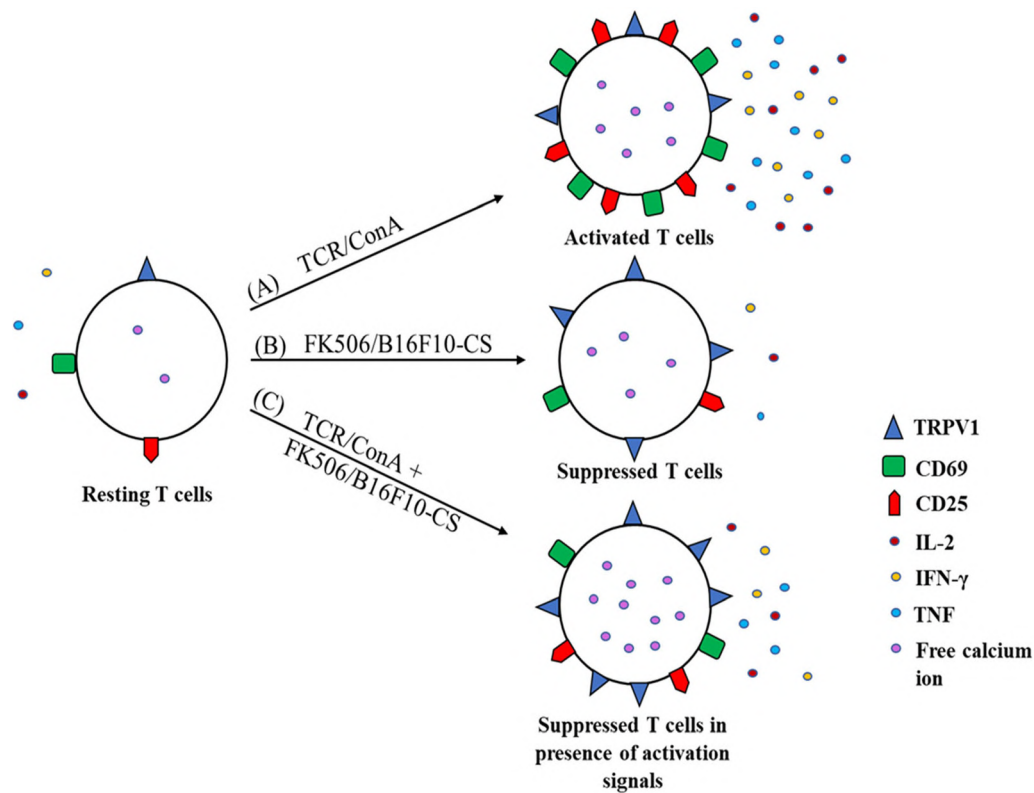
Figure 5. Proposed working model depicting functional expression of TRPV1 and intracellular calcium levels in activated and immunosuppressed T-cells. Resting T-cells maintain low levels of cytosolic Ca^{2+} and basal levels of TRPV1 expression. (**A**) During T-cell activation with either ConA or TCR, both the cytosolic Ca^{2+} level and TRPV1 expression were upregulated significantly along with the induction of robust effector cytokine responses. (**B**) Upon treatment with immunosuppressive FK506 or B16F10-CS, TRPV1 expression increased significantly, and the cytosolic calcium increased either markedly (FK506) or modestly (B16F10-CS). (**C**) During experimental immunosuppression (treated with either FK506 or B16F10-CS) of T-cells in combination with ConA- or TCR-driven stimulations, the cytokine responses markedly decreased. Further, in FK506- or B16F10-CS-treated T-cells stimulated with either ConA or TCR, cytosolic Ca^{2+} either increased markedly or modestly, respectively. Moreover, TRPV1 expression increased significantly in FK506- or B16F10-CS-treated T-cells stimulated with either ConA or TCR, suggesting a possible induction of TRPV1 channel on T-cells during both immune activation and immunosuppression.

including ConA or TCR, as well as immunosuppressive agents, such as rapamycin, tacrolimus (FK506), and cyclosporine, have also been reported to induce intracellular increase of Ca^{2+} (Bultynck *et al.* 2000; Van Acker *et al.* 2004; MacMillan and McCarron 2009). The role of TRPV1 in ConA- or TCR-mediated increase in calcium influx has been recently studied (Bertin *et al.* 2014; Majhi *et al.* 2015). However, the role of TRPV1 in calcium influx induced by immunosuppressive agents is not well studied. The current study provides the first experimental evidence that TRPV1 may also contribute toward FK506- or B16F10-CS-driven increase in intracellular calcium associated with the immunosuppression of T-cells. This study further highlights the modulation of T-cell

activation, proliferation, pro-inflammatory cytokine responses, and modulation of intracellular Ca^{2+} levels.

TRPV1 has been reported to be upregulated during T-cell activation and its associated immune responses (Bertin *et al.* 2014; Majhi *et al.* 2015). Similarly, in treatments with either FK506 or B16F10-CS, the TRPV1 levels were significantly increased compared with resting T-cells. Furthermore, the TRPV1 level was also significantly upregulated in pre-treated FK506 or B16F10-CS T-cells stimulated with either ConA or TCR compared with the corresponding ConA or TCR controls. Intriguingly, it was also observed that TRPV1 expression in T-cells is irreversible as the removal of immunosuppressive conditions also triggered upregulation of TRPV1 expression. Moreover, B16F10

tumor-bearing mice also displayed a significant increase in splenic T-cell TRPV1 expression as compared with control mice. This, in general, may suggest that in an immunosuppressive environment, TRPV1 expression could be upregulated in T-cells.

Modulation of intracellular Ca^{2+} levels is marked by various cellular responses, including activation, migration, and differentiation (Oh-hora and Rao 2008; Pang *et al.* 2012). Hence, modulation of the TRPV1 channel via a functional blocker, 5′-IRTX, has been used to validate the contribution of the TRPV1 channel towards the FK506- or B16F10-CS-driven increase in intracellular Ca^{2+} levels in T-cells (Majhi *et al.* 2015; Kumar *et al.* 2021). In FK506-treated T-cells, stimulated with either ConA or TCR, the accumulated intracellular Ca^{2+} levels markedly increased, and pre-treatment with 5′-IRTX led to a marked decrease in accumulated intracellular Ca^{2+} levels. FK506-driven increases in Ca^{2+} and TRPV1 levels were found in the current study. Furthermore, inhibition of TRPV1 was found to decrease the Ca^{2+} levels during immune activation and suppression of T-cells. FK506 is a potent and fast-acting immunosuppressant, which is known to increase Ca^{2+} levels (Bultynck *et al.* 2000). Moreover, the FK506-binding protein (FKBP12) was found to target calcineurin to the inositol 1,4,5-trisphosphate receptor (IP3R1). The associated calcineurin was found to modulate the phosphorylation of the IP3R1, which might critically induce the Ca^{2+} flux (Cameron *et al.* 1995; Shin *et al.* 2002). However, an involvement of calcineurin-directed release of Ca^{2+} by FK506 associated with immunosuppression towards modulating TRPV1, if any, is warranted for future study. On the other hand, B16F10-CS exerts immunosuppression to induce the generation of IL-10^{+} Bregs, PDL1^{hi} macrophages, and suppress effector T-cell function exerting immunoinhibitory activities (Sun *et al.* 2011, 2015; Zhou *et al.* 2016; Wen *et al.* 2018; Chen *et al.* 2019). In B16F10-CS-treated T-cells, a modest increase in accumulated intracellular Ca^{2+} levels was observed as compared with resting T-cells, and yet, the decrease was prominent with 5′-IRTX. Moreover, B16F10 tumor-bearing mice also showed an increase in intracellular calcium levels in T-cells. This, in general, may suggest that the TRPV1 channel might be acting as a major contributor to elevated intracellular Ca^{2+} levels in T-cells during both immune activation and immunosuppression. Mechanistically, Ca^{2+} has been reported to activate CaMKK2, which further induces an immunosuppressive microenvironment. Moreover, deletion of the *CaMKK2* gene or inhibition of CaMKK2 has been reported to attenuate tumor growth *in vivo* (Racioppi *et al.* 2019). Further studies are warranted on the detailed

mechanisms underlying the possible association between elevated calcium and the immunosuppressive microenvironment.

In brief, the present study provides the first evidence that TRPV1 channel expression is induced in T-cells during both immune activation and immunosuppression. Interestingly, it was found that during immunosuppression, the TRPV1 surface expression and intracellular Ca^{2+} levels in T-cells were further elevated. Moreover, the heightened elevation of intracellular Ca^{2+} during experimental immunosuppression was found to be regulated by the TRPV1 channel. The current understanding of TRPV1 in T-cell activation or suppression is schematically summarized as a proposed working model in figure 5. These findings might also have broad implications for understanding the indispensable role of the TRPV1 channel in various immunosuppressive diseases as well as many inflammatory disorders.

Author contributions

Conceptualization: PSK, TM, SC; methodology: PSK, TM, SK, DJNK, SSS, AR; formal analysis and investigation: PSK, TM, AR, SC; writing—original draft preparation: PSK, TM, SC; funding acquisition and supervision: SC.

Declarations

Conflict of interest The authors declare that they have no conflict of interest.

References

Almawi WY, Assi JW, Chudzik DM, *et al*. 2001 Inhibition of cytokine production and cytokine-stimulated T-cell activation by FK506 (Tacrolimus)1. *Cell Transplant.* **10** 615–623

Amantini C, Farfariello V, Cardinali C, *et al*. 2017 The TRPV1 ion channel regulates thymocyte differentiation by modulating autophagy and proteasome activity. *Onco-target* **8** 90766–99780

Bertin S, Aoki-Nonaka Y, De Jong PR, *et al*. 2014 The ion channel TRPV1 regulates the activation and proinflammatory properties of CD^{4+} T-cells. *Nat. Immunol.* **15** 1055–1063

Bultynck G, De Smet P, Weidema AF, *et al*. 2000 Effects of the immunosuppressant FK506 on intracellular Ca^{2+} release and Ca^{2+} accumulation mechanisms. *J. Physiol.* **525** 681–693

Cahalan MD and Chandy KG 2009 The functional network of ion channels in T lymphocytes. *Immunol. Rev.* **231** 59–87

Cameron AM, Steiner JP, Roskams AJ, *et al*. 1995 Calcineurin associated with the inositol 1,4,5-trisphosphate receptor-FKBP12 complex modulates Ca^{2+} flux. *Cell* **83** 463–472

Chen Y-Q, Li P-C, Pan N, *et al*. 2019 Tumor-released autophagosomes induces CD^{4+} T-cell-mediated immuno-suppression via a TLR2–IL-6 cascade. *J. Immunother. Cancer* **7** 178

Dolmetsch RE, Lewis RS, Goodnow CC, *et al*. 1997 Differential activation of transcription factors induced by Ca^{2+} response amplitude and duration. *Nature* **386** 855–858

Feske S 2007 Calcium signalling in lymphocyte activation and disease. *Nat. Rev. Immunol.* **7** 690–702

Gao R, Ma J, Wen Z, *et al*. 2018 Tumor cell-released autophagosomes (TRAP) enhance apoptosis and immuno-suppressive functions of neutrophils. *Oncoimmunology* **7** 1–11

Hogan PG, Lewis RS and Rao A 2010 Molecular basis of calcium signaling in lymphocytes: STIM and ORAI. *Annu. Rev. Immunol.* **28** 491–533

Komada H, Nakabayashi H, Hara M, *et al*. 1996 Early calcium signaling and calcium requirements for the IL-2 receptor expression and IL-2 production in stimulated lymphocytes. *Cell. Immunol.* **173** 215–220

Kumar PS, Nayak TK, Mahish C, *et al*. 2021 Inhibition of transient receptor potential vanilloid 1 (TRPV1) channel regulates chikungunya virus infection in macrophages. *Arch. Virol.* **166** 139–155

MacMillan D and McCarron J 2009 Regulation by FK506 and rapamycin of Ca^{2+} release from the sarcoplasmic reticulum in vascular smooth muscle: the role of FK506 binding proteins and mTOR. *Br. J. Pharmacol.* **158** 1112–1120

Majhi RK, Sahoo SS, Yadav M, *et al*. 2015 Functional expression of TRPV channels in T-cells and their implications in immune regulation. *FEBS J.* **282** 2661–2681

Nayak TK, Mamidi P, Kumar A, *et al*. 2017 Regulation of viral replication, apoptosis and pro-inflammatory responses by 17-aag during chikungunya virus infection in macro-phages. *Viruses* **9** https://doi.org/10.3390/v9010003

Nilius B 2007 TRP channels in disease. *Biochim. Biophys. Acta Mol. Basis Dis.* **1772** 805–812

Oh-hora M and Rao A 2008 Calcium signaling in lympho-cytes. *Curr. Opin. Immunol.* **20** 250–258

Overwijk WW and Restifo NP 2001 B16 as a mouse model for human melanoma. *Curr. Protoc. Immunol.* **39** https://doi.org/10.1002/0471142735.im2001s39

Pang B, Shin DH, Park KS, *et al*. 2012 Differential pathways for calcium influx activated by concanavalin A and CD3 stimulation in Jurkat T-cells. *Pflugers Arch. Eur. J. Physiol.* **463** 309–318

Pathak S, Gokhroo A, Kumar Dubey A, *et al*. 2021 7-Hydroxy frullanolide, a sesquiterpene lactone, increases intracellular calcium amounts, lowers CD^{4+} T-cell and macrophage responses, and ameliorates DSS-induced colitis. *Int. Immunopharmacol.* **97** 107655

Racioppi L, Nelson ER, Huang W, *et al*. 2019 CaMKK2 in myeloid cells is a key regulator of the immune-suppressive microenvironment in breast cancer. *Nat. Commun.* **10** 2450

Sahoo SS, Majhi RK, Tiwari A, *et al*. 2019 Transient receptor potential ankyrin1 channel is endogenously expressed in T-cells and is involved in immune functions. *Biosci. Rep.* **39** BSR20191437

Sahoo SS, Pratheek BM, Meena VS, *et al*. 2018 VIPER regulates naive T-cell activation and effector responses: Implication in TLR4 associated acute stage T-cell responses. *Sci. Rep.* **8** 7118

Shin DW, Pan Z, Bandyopadhyay A, *et al*. 2002 Ca(2+)-dependent interaction between FKBP12 and calcineurin regulates activity of the Ca(2+) release channel in skeletal muscle. *Biophys. J.* **83** 2539–2549

Sun LX, Bin Lin Z, Duan XS, *et al*. 2011 *Ganoderma lucidum* polysaccharides antagonize the suppression on lymphocytes induced by culture supernatants of B16F10 melanoma cells. *J. Pharm. Pharmacol.* **63** 725–735

Sun LX, Li WD, Bin Lin Z, *et al*. 2015 Cytokine production suppression by culture supernatant of B16F10 cells and amelioration by *Ganoderma lucidum* polysaccharides in activated lymphocytes. *Cell Tissue Res.* **360** 379–389

Van Acker K, Bultynck G, Rossi D, *et al*. 2004 The 12 kDa FK506-binding protein, FKBP12, modulates the Ca^{2+}-

flux properties of the type-3 ryanodine receptor. *J. Cell Sci.* **117** 1129–1137

Vig M and Kinet J-P 2009 Calcium signaling in immune cells. *Nat. Immunol.* **10** 21–27

Wen ZF, Liu H, Gao R, *et al.* 2018 Tumor cell-released autophagosomes (TRAPs) promote immunosuppression through induction of M2-like macrophages with increased expression of PD-L1. *J. Immunother. Cancer* **6** 151

Zhou M, Wen Z, Cheng F, *et al.* 2016 Tumor-released autophagosomes induce IL-10-producing B cells with suppressive activity on T lymphocytes via TLR2-MyD88-NF-κ B signal pathway. *Oncoimmunology* **5** e1180485

Corresponding editor: Dipankar Nandi

Correction

Correction to: Elevation of TRPV1 expression on T-cells during experimental immunosuppression

P Sanjai Kumar[†], Tathagata Mukherjee[†], Somlata Khamaru,
Anukrishna Radhakrishnan, Dalai Jupiter Nanda Kishore,
Saurabh Chawla, Subhransu Sekhar Sahoo and Subhasis Chattopadhyay*

*School of Biological Sciences, National Institute of Science Education and Research, an Off-campus
Centre (OCC) of Homi Bhabha National Institute, Bhubaneswar 752050, India*

*Corresponding author (Email, subho@niser.ac.in)

[†]*P Sanjai Kumar and Tathagata Mukherjee equal contribution.*

Published online 12 July 2022

Correction to: *J. Biosci.* (2022) 47:42
https://doi.org/10.1007/s12038-022-00279-2

In the *Journal of Biosciences* article titled "Elevation of TRPV1 expression on T-cells during experimental immunosuppression" by P Sanjai Kumar *et al.* (*https://doi.org/10.1007/s12038-022-00279-2*; Vol. 47, Art. ID 42), published in July 2022, the affiliation of the authors has been incompletely mentioned as:

> *School of Biological Sciences, National Institute of Science Education and Research, Bhubaneswar 752050, India*

The correct affiliation should read as:

> *School of Biological Sciences, National Institute of Science Education and Research, an Off-campus Centre (OCC) of Homi Bhabha National Institute, Bhubaneswar 752050, India*

The original article can be found online at *https://doi.org/10.1007/s12038-022-00279-2*.

RESEARCH

TRPA1 activation and Hsp90 inhibition synergistically downregulate macrophage activation and inflammatory responses in vitro

Anukrishna Radhakrishnan[1†], Tathagata Mukherjee[1†], Chandan Mahish[1†], P Sanjai Kumar[2], Chandan Goswami[1] and Subhasis Chattopadhyay[1*]

Abstract

Background Transient receptor potential ankyrin 1 (TRPA1) channels are known to be actively involved in various pathophysiological conditions, including neuronal inflammation, neuropathic pain, and various immunological responses. Heat shock protein 90 (Hsp90), a cytoplasmic molecular chaperone, is well-reported for various cellular and physiological processes. Hsp90 inhibition by various molecules has garnered importance for its therapeutic significance in the downregulation of inflammation and are proposed as anti-cancer drugs. However, the possible role of TRPA1 in the Hsp90-associated modulation of immune responses remains scanty.

Results Here, we have investigated the role of TRPA1 in regulating the anti-inflammatory effect of Hsp90 inhibition via 17-(allylamino)-17-demethoxygeldanamycin (17-AAG) in lipopolysaccharide (LPS) or phorbol 12-myristate 13-acetate (PMA) stimulation in RAW 264.7, a mouse macrophage cell lines and PMA differentiated THP-1, a human monocytic cell line similar to macrophages. Activation of TRPA1 with Allyl isothiocyanate (AITC) is observed to execute an anti-inflammatory role via augmenting Hsp90 inhibition-mediated anti-inflammatory responses towards LPS or PMA stimulation in macrophages, whereas inhibition of TRPA1 by 1,2,3,6-Tetrahydro-1,3-dimethyl-N-[4-(1-methylethyl)phenyl]-2,6-dioxo-7 H-purine-7-acetamide,2-(1,3-Dimethyl-2,6-dioxo-1,2,3,6-tetrahydro-7 H-purin-7-yl)-N-(4-isopropylphenyl)acetamide (HC-030031) downregulates these developments. LPS or PMA-induced macrophage activation was found to be regulated by TRPA1. The same was confirmed by studying the levels of activation markers (major histocompatibility complex II (MHCII), cluster of differentiation (CD) 80 (CD80), and CD86, pro-inflammatory cytokines (tumor necrosis factor (TNF) and interleukin 6 (IL-6)), NO (nitric oxide) production, differential expression of mitogen-activated protein kinase (MAPK) signaling pathways (p-p38 MAPK, phospho-extracellular signal-regulated kinase 1/2 (p-ERK 1/2), and phosphor-stress-activated protein kinase/c-Jun N-terminal kinase (p-SAPK/JNK)), and

---

[†]Anukrishna Radhakrishnan, Tathagata Mukherjee and Chandan Mahish contributed equally to this work.

*Correspondence:
Subhasis Chattopadhyay
subho@niser.ac.in

Full list of author information is available at the end of the article

induction of apoptosis. Additionally, TRPA1 has been found to be an important contributor to intracellular calcium levels toward Hsp90 inhibition in LPS or PMA-stimulated macrophages.

Conclusion This study indicates a significant role of TRPA1 in Hsp90 inhibition-mediated anti-inflammatory developments in LPS or PMA-stimulated macrophages. Activation of TRPA1 and inhibition of Hsp90 has synergistic roles towards regulating inflammatory responses associated with macrophages. The role of TRPA1 in Hsp90 inhibition-mediated modulation of macrophage responses may provide insights towards designing future novel therapeutic approaches to regulate various inflammatory responses.

Keywords Macrophages, Pro-inflammatory responses, TRPA1, 17-AAG, Apoptosis, Ca^{2+}

Background

The transient receptor potential (TRP) superfamily integrates 30 closely related non-selective cationic channels, distributed into seven subfamilies and two groups based on their sequence similarity and cellular functions [1, 2]. Subfamilies of TRP channels are named TRPC (Canonical), TRPV (Vanilloid), TRPM (Melastatin), TRPA (Ankyrin), TRPML (Mucolipin), TRPP (Polycystin), and TRPN (NOMPC). TRP channels are found in both excitable and non-excitable vertebrate cells and some non-vertebrate cells, contributing to essential cellular functions [1, 3–6]. TRP channels are pivotal in various cellular processes, including cell division, migration, differentiation, stress responses, and apoptosis [7–9].

TRPA1, the only member of the mammalian TRPA family, is characterized by 14 ankyrin repeats in its N-terminus domain [10]. TRPA1 is required for various immune cells such as T lymphocytes and monocyte/macrophages in regulating their activation, migration, and secretion of different immune molecules [11–15]. In a recent study, it has been reported an important role of TRPA1 in regulating T cell activation and associated responses [16]. TRPA1 is essential in multiple inflammatory and anti-inflammatory functions in different model systems, including tissue injury, inflammatory models, and pain modalities. Recently, it has been reported that in inflammatory models such as acute kidney injury, atopic dermatitis model, and experimental colitis model, the TRPA1 expression levels were significantly elevated at the site of injury or inflammation [17–19]. Further, inflammatory reactions such as pro-inflammatory cytokine release and mast cell infiltration were impaired considerably upon genetic or pharmacological ablation of TRPA1 [20]. TRPA1 modulates pain induction and aggravates injury-induced inflammation. The protective role of TRPA1 is evident in various inflammatory immune responses, including corneal wound healing and mechanical or cold allodynia in chronic post-ischemia pain [21–23]. Similarly, TRPA1 is associated with lipopolysaccharide (LPS) induced inflammatory responses, including lung inflammation, neurogenic inflammation, and Osteoarthritic Fibroblast-Like Synoviocytes [24–26]. Activation of TRPA1 alleviates the LPS-induced nitric

oxide (NO) production in peritoneal macrophages [27]. Like other TRP superfamily members, TRPA1 is associated with various cellular proteins essential for cell survival, including Hsp90, Hsp27, and Hsp70 [28–31].

Hsp90, a cytoplasmic molecular chaperone, is associated with the stabilization and maturation of cellular client proteins and helps in cell fate decisions, including cell cycle, signal transduction, growth regulation, and cell death [32, 33]. Hsp90 is essential for various pathophysiological conditions like cancer, viral infections, and autoimmune disorders [34–39]. Additionally, Hsp90 has been reported to effectively modulate different immune responses by regulating various client proteins involved in innate and adaptive immune responses [40]. Hsp90 inhibition by various pharmacological inhibitors has proven effective in (alleviating) a wide range of inflammatory responses, including macrophage-mediated pro-inflammatory responses, interleukin-1 receptor-associated kinase, Raf-1, mitogen-activated protein kinase kinase, and Src family kinase p56lck activation [41–46]. 17-AAG, a derivative of geldanamycin, is one of the selective inhibitors of Hsp90 and has been reported to actively block various innate immune responses in vitro and in vivo models. 17-AAG administration has been shown to suppress TLR4-mediated pro-inflammatory cytokine production via blockade of the signaling cascade during LPS-induced autoimmune uveitis in rats [47]. Furthermore, 17-AAG inhibits TLR4 stimulation in vitro and alleviates disease incidence and severity in myelin oligodendrocyte glycoprotein-peptide-induced experimental autoimmune encephalomyelitis [48]. These reports suggest the immense therapeutic potential of Hsp90 inhibitors in autoimmune and pro-inflammatory diseases. Although Hsp90 and TRPA1 have been well studied for their immune modulatory effect, the possible association of these proteins and the functional regulation of their effects has not been addressed yet. Accordingly, here we have investigated the association of Hsp90 inhibition-mediated anti-inflammatory effects and the possible contextual involvement of TRPA1-mediated immune regulation, if any. In this study, we have explored the role of TRPA1 in regulating pro-inflammatory responses in Hsp90-inhibited macrophages when

subjected to LPS or PMA stimulation. Additionally, we have also studied the regulation of MAPK signalings, apoptosis, intracellular calcium status, and associated immune responses via 17-AAG and TRPA1 agonist Allyl isothiocyanate (AITC) in macrophages in LPS or phorbol 12-myristate 13-acetate (PMA) stimulation.

Results

TRPA1 is upregulated in Hsp90-inhibited and LPS-stimulated macrophages

TRPA1 is associated with a wide range of cellular and pathophysiological conditions [18, 21, 49, 50]. It has a protective role in macrophage-mediated inflammation in several inflammatory diseases [17, 23, 51–55]. The Hsp90 inhibitor used in the study is 17-AAG, which is accredited as a potential anti-inflammatory agent during LPS stimulation in macrophages via blockade of TLR4 signaling pathways [47, 48]. The working concentration of 17-AAG in RAW 264.7 cells was taken as 0.5 µM as more than 90% of the cells were viable at that concentration (Supplementary Fig. 2A) [56]. To investigate a possible association between TRPA1 and Hsp90-inhibition mediated impairment of inflammation in macrophages, RAW 264.7 cells or THP-1 macrophages were treated with either LPS/PMA or 17-AAG or together. The working concentration of LPS, PMA, and 17-AAG used were 500 ng/mL, 100 ng/mL, and 0.5 µM, respectively. These cells were then harvested, stained, and analyzed to check TRPA1 expression levels via flow cytometry (FC). The TRPA1 antibodies used are specific for mouse TRPA1 proteins, and the specificity was tested using blocking peptides (data not shown). The percentage of cells positive for TRPA1 was observed to be increased significantly in LPS-stimulated RAW 264.7 cells (83.4±1.73%) as compared to resting RAW (mock) 264.7 cells (55.4±3.73%) (Fig. 1A). Further, in macrophages treated with both 17-AAG and LPS, the TRPA1 levels were augmented (94.6±1.67%). Similarly, it was found that the percentage of cells positive for TRPA1 decreased significantly in PMA-stimulated RAW 264.7 cells (48.5±1.74%) as compared to resting RAW 264.7 cells (59.5±2.19%). Furthermore, in macrophages treated with both 17-AAG and PMA, the TRPA1 levels were higher (72.2±1.90%) (Fig. 1A). The samples from each condition were assessed for TRPA1 protein quantification via Western blot. The highest band intensity for TRPA1 was obtained in LPS/PMA stimulated, and 17-AAG treated conditions (Fig. 1B and C). The THP-1 macrophages also followed a similar trend with reaching maximum TRPA1 levels in Hsp90-inhibited and LPS-stimulated macrophages (82.8±2.53%), trailed by LPS-stimulated macrophages (69.7±2.72%) and resting macrophages (56.6±2.61%). These results suggest that the TRPA1 levels are modulated during LPS or PMA stimulation in a dose- and

time-dependent manner. Furthermore, increased TRPA1 expression was observed after the administration of both 17-AAG and LPS as compared to the mock (untreated) macrophages in a dose-independent and reversible manner (Supplementary Fig. 1). The results indicate a possible modulation of TRPA1 expression in Hsp90-inhibited macrophages during LPS or PMA stimulation.

TRPA1 regulates the activation of Hsp90-inhibited macrophages

To investigate whether the differential expression of TRPA1 in the above conditions has any functional implication, TRPA1 specific agonist (AITC) and TRPA1 antagonist (HC-030031) were used [57, 58]. The cytotoxicity levels of the TRPA1-specific modulators were assessed by trypan blue exclusion assay and 7-AAD staining via FC. RAW 264.7 cells were treated with different concentrations of TRPA1 modulators HC-030031 (TRPA1 inhibitor) (40 µM, 20 µM, 10 µM, 5 µM) and AITC (TRPA1 activator) (40 µM, 20 µM, 10 µM, 5 µM) in the presence of 17-AAG for 24 h. DMSO was used as solvent control. More than 95% of the cells were viable at 10 µM and 5 µM of HC-030031 in the presence of 0.5 µM of 17-AAG, and similar results were observed at 20 µM, 10 µM, and 5 µM of AITC in the presence of 0.5 µM of 17-AAG (Supplementary Fig. 2). Henceforth, 10 µM of AITC and 10 µM of HC-030031 were used for further experiments. It was also observed that these pharmacological modulators alone or in combination with 17-AAG have no significant effect on TRPA1 levels in the absence of any inflammatory stimulus (Supplementary Fig. 3).

To determine whether TRPA1 has any role in regulating the activation of Hsp90-inhibited macrophages, cell surface expression of MHCII and CD80/86 were studied via FC; RAW 264.7 were stimulated with LPS or PMA in the presence of TRPA1 modulators and 17-AAG. The cells were harvested at 12 h post-stimulation, immunolabelled with MHCII, CD80, and CD86 antibodies, followed by their acquisition and analysis via FC (Fig. 2A-F). The expression levels of MHCII, CD80, and CD86 were represented in fold change compared to the isotype control. It was observed that inhibition of Hsp90 significantly decreases the expression of MHCII (6.99±0.51), CD80 (17.4±0.72), and CD86 (24.4±0.94) as compared to the LPS stimulated cells (MHCII: 10.40±1.23, CD80: 21.2±1.14 and CD86: 28.1±1.2). Furthermore, the pharmacological inhibition of TRPA1 with HC-030031 significantly downregulated the effect of Hsp90 inhibition (MHCII: 9.85±0.87, CD80: 20.5±0.68, and CD86: 30.3±1.65) as compared to LPS+17-AAG. Conversely, TRPA1 activation with AITC significantly enhanced the Hsp90-mediated downregulation of MHCII (4.63±0.51), CD80 (15.2±0.58), and CD86 (20.7±1.09) as compared to LPS+17-AAG (Fig. 2A and B, and Fig. 2C). Similarly,
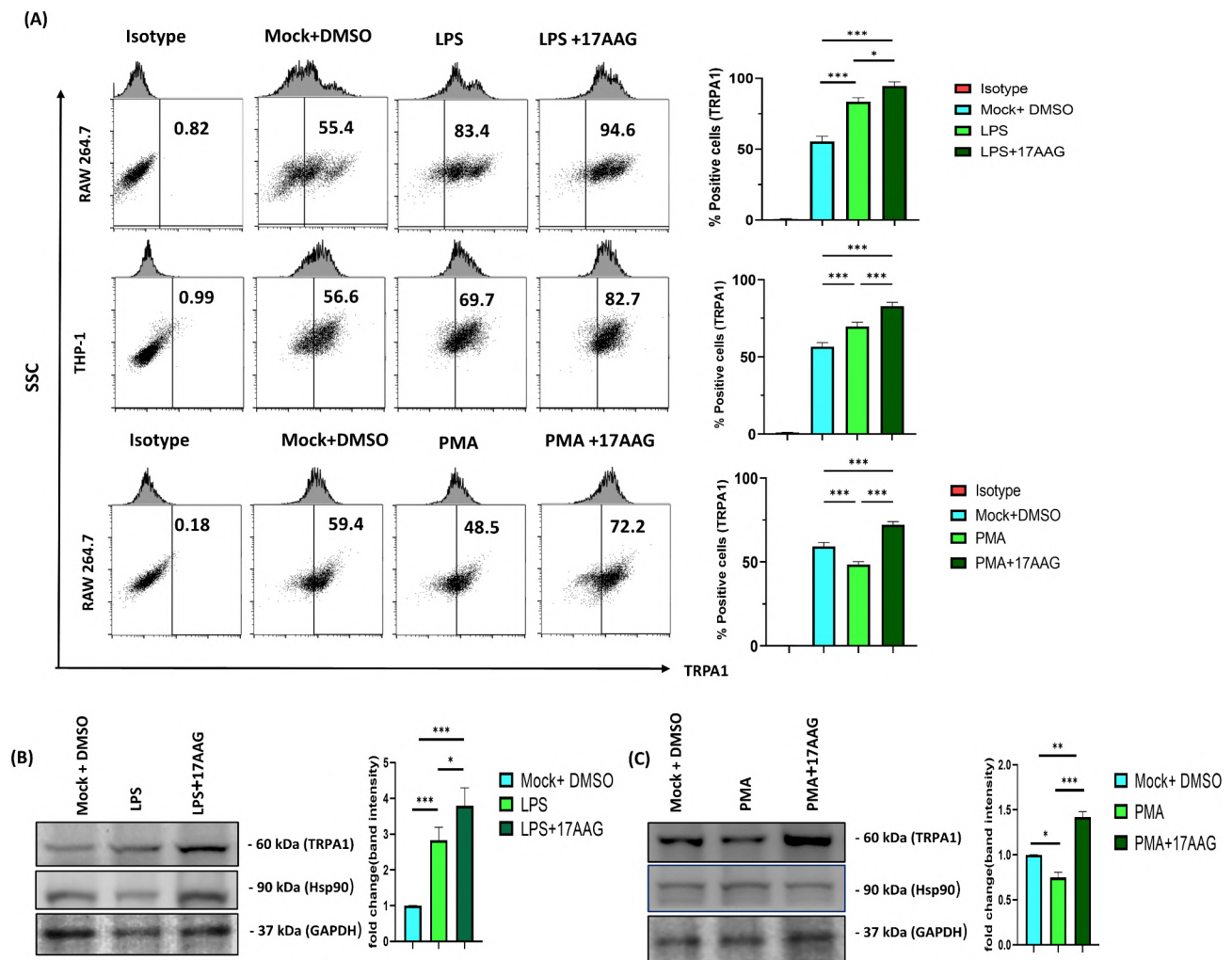
Fig. 1 TRPA1 is upregulated in Hsp90-inhibited and LPS- or PMA-stimulated monocytes/macrophages.
Cells were treated with either LPS 500 ng/ml (both RAW 264.7 and THP-1 macrophages) or PMA 100 ng/ml (only in RAW 264.7) alone or together with 17-AAG. (**A**) FC dot-plot and bar graphs depicting the percentage of positive cells for TRPA1 in mock, LPS/PMA, and 17-AAG + LPS/PMA. Western blot analysis and corresponding bar graphs of TRPA1 expression in RAW 264.7 cells stimulated with LPS (500 ng/ml) (**B**), PMA (100 ng/ml) (**C**), and 17-AAG + LPS/PMA. The blot figures were cropped to omit other conditions. The data represent the mean ± SD of three independent experiments. One-way ANOVA has been performed to find statistical significance among groups. Differences between groups with a p-value < 0.05 were considered statistically significant (*, p < 0.05; **, p < 0.01; ***, p < 0.001)

it was observed that Hsp90 inhibition has significantly downregulated the expression of MHCII (7.90 ± 0.17), CD80 (11.1 ± 0.32), and CD86 (3.46 ± 0.16) as compared to the control PMA-stimulated cells (MHCII: 9.13 ± 0.195, CD80: 12.8 ± 0.59 and CD86: 3.95 ± 0.14). Further, pharmacological inhibition of TRPA1 with HC-030031 significantly reduced the effect of Hsp90 inhibition (MHCII: 9.65 ± 0.73, CD80: 14.1 ± 0.55, and CD86: 3.98 ± 0.13) as compared to PMA + 17-AAG. Conversely, TRPA1 activation with AITC has significantly enhanced the Hsp90-mediated downregulation of MHCII (6.50 ± 0.424), CD80 (9.87 ± 0.06), and CD86 (3.01 ± 0.05) as compared to PMA + 17-AAG (Fig. 2D and E, and Fig. 2F). These results indicate an important role of TRPA1 in the suppression of activation markers of macrophages i.e., MHCII, CD80,

and CD86 in Hsp90-inhibited conditions in the presence of LPS or PMA stimulation.

TRPA1 impairs the nitric oxide (NO) production in Hsp90-inhibited macrophages

Hsp90 is an active modulator of reactive nitrogen species (RNS) and reactive oxygen species (ROS) [59, 60]. To investigate the regulatory effect of TRPA1 in regulating the NO production by 17-AAG-mediated Hsp90 inhibited condition, RAW 264.7 and THP-1 macrophages were stimulated with LPS or PMA in the presence of TRPA1 modulators and 17-AAG. Griess assay was performed from the cell supernatants to assess the nitrite, a breakdown product of NO [61]. Upon LPS stimulation, it was observed that the nitrite production was upregulated at
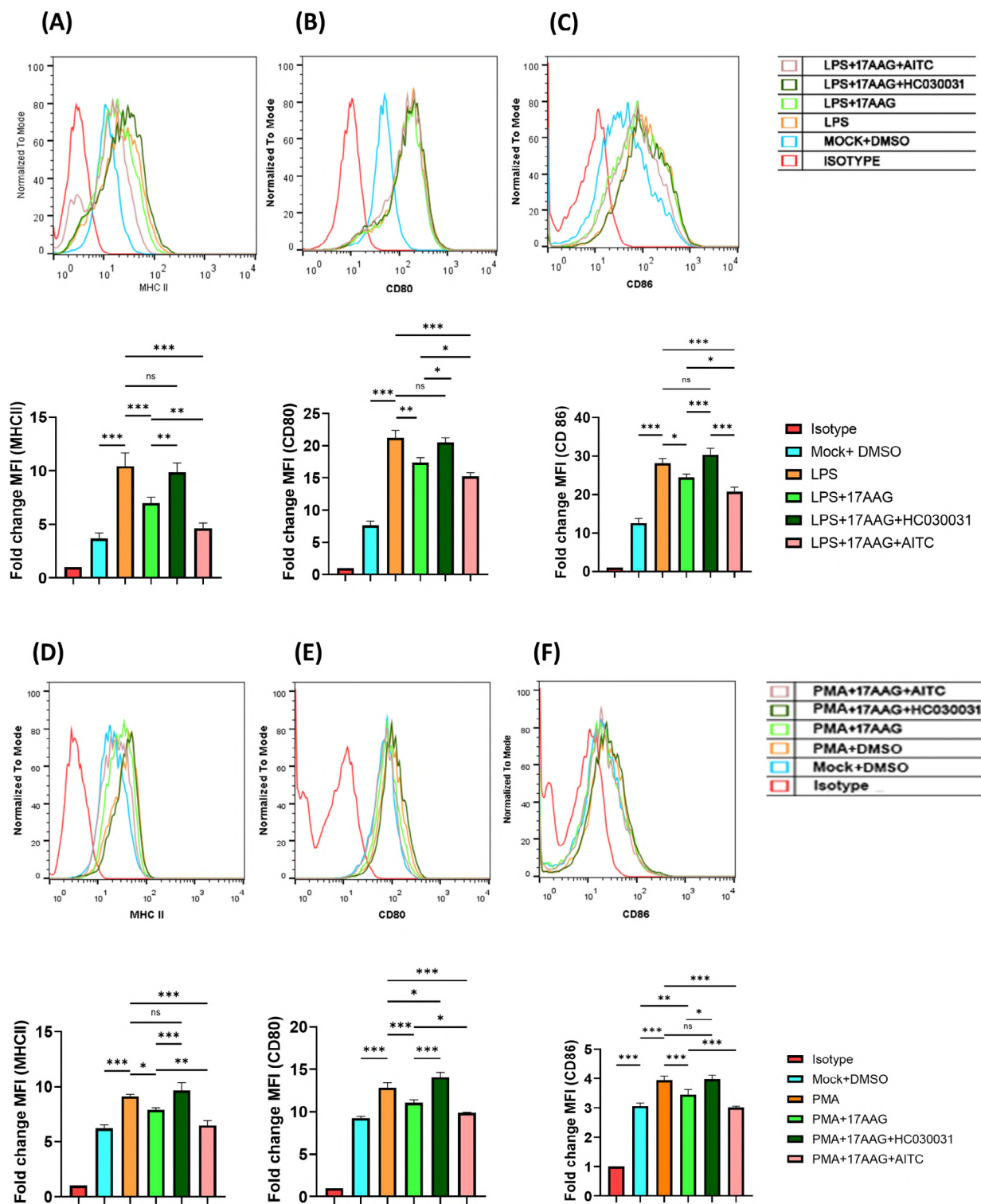
Radhakrishnan *et al. BMC Immunology*   (2023) 24:16

Page 5 of 17

Fig. 2 TRPA1 regulates the activation of macrophages in Hsp90-inhibited condition.
RAW 264.7 cells were treated with different conditions of LPS/PMA, 17-AAG, HC-030031, or AITC and harvested at 12 h. FC histogram depicting fold change in MFI of MHCII (**A**, **D**), CD80 (**B**, **E**), and CD86 (**C**, **F**) of macrophages treated with LPS (500ng/ml, A-C) or PMA (100 ng/ml, D-F) along with their respective bar graphs. The data represent the mean ± SD of at least three independent experiments. One-way ANOVA has been performed to find statistical significance among groups. Differences between groups with a p-value less than 0.05 were considered statistically significant (ns, non-significant; *, p < 0.05; **, p < 0.01; ***, p < 0.001)

24 h (78.7±8.39 μM) as compared to the untreated cells (9.59±0.831 μM). Further, upon Hsp90 inhibition with 17-AAG, the nitrite production was significantly downregulated (53.6±2.42 μM). Surprisingly, in the presence of either HC-030031 (21.58±1.42) or AITC (5.38±0.667 μM), the NO levels decreased significantly (Fig. 3A). This trend was observed at 12 h, while no significant changes in NO production were observed at 6 h post-stimulation. A similar scenario was observed with THP-1 macrophages stimulated with LPS. Activation of TRPA1 along with 17-AAG (10.3±0.6 μM) significantly impaired the NO production compared to the LPS 17.2±0.891 μM) and LPS+17-AAG (14.6±0.97 μM) at 24 h conditions (Fig. 3B). Additionally, a significant uprise in nitrite production was observed in macrophages treated with PMA at 12 and 24 h. Furthermore, TRPA1 activation diminished the nitrite production in 17-AAG treated and

PMA stimulated macrophages successfully compared to the PMA and PMA+17-AAG controls at 12 and 24 h. Surprisingly, no significant changes were observed with HC-030031+17-AAG conditions compared to 17-AAG control in PMA-stimulated macrophages (Fig. 3C). These results indicate that TRPA1 activation augments the downregulation of NO production via Hsp90 inhibition in LPS/PMA-stimulated macrophages.

TRPA1 enhances the Hsp90 inhibition-mediated downregulation of pro-inflammatory cytokine production in LPS or PMA-stimulated macrophages

Hsp90 has been reported to be essential for pro-inflammatory cytokine production from macrophages [62]. To investigate the regulatory effect of TRPA1 in regulating the pro-inflammatory cytokine production by 17-AAG-mediated Hsp90 inhibited condition, RAW
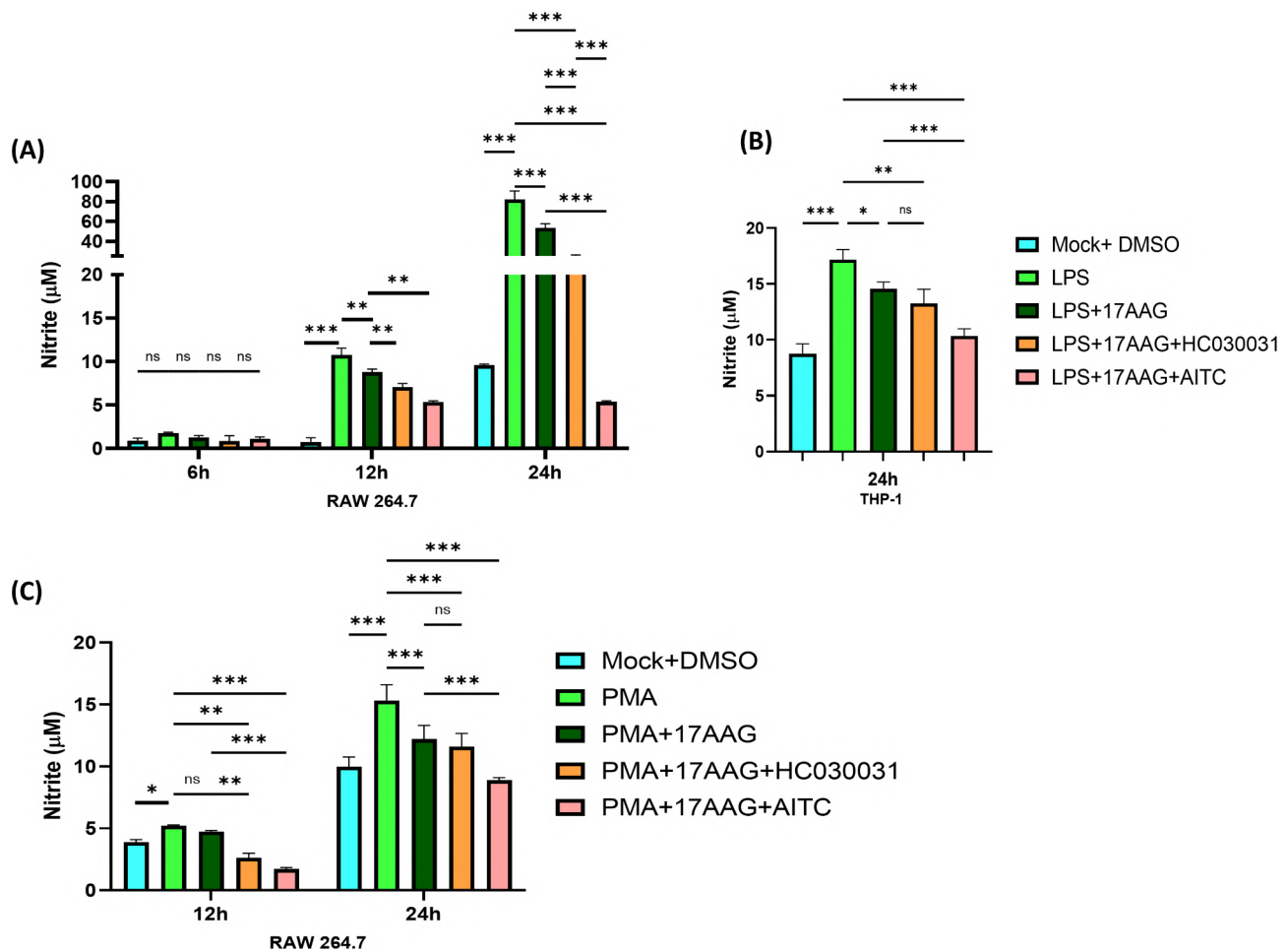

Fig. 3 TRPA1 regulates the nitric oxide (NO) production in Hsp90-inhibited monocytes/macrophages.
RAW 264.7 and THP-1 cells were treated with different conditions of LPS/PMA, 17-AAG, HC-030031, or AITC, and the supernatant was collected at 6 h,12 h, and 24 h. Bar graph depicting nitric oxide production from RAW 264.7 cells treated with LPS (500 ng/ml) (**A**) or PMA (100 ng/ml) (**C**) or THP-1 macrophages treated with LPS (500 ng/ml) (**B**). The data represent the mean ± SD of at least three independent experiments. One-way/two-way ANOVA was performed to find statistical significance among groups. Differences between groups with a p-value less than 0.05 were considered statistically significant (ns, non-significant; *, $p < 0.05$; **, $p < 0.01$; ***, $p < 0.001$)

264.7 cells were subjected to LPS or PMA stimulation under differential conditions of TRPA1 modulation and 17-AAG treatment. The culture supernatant was assessed for TNF and IL-6 cytokine release profiles. In 17-AAG-mediated Hsp90 inhibited and LPS- or PMA-stimulated macrophages, the TNF and IL-6 levels were reduced significantly at 6 and 24 h post-LPS-stimulation compared to only LPS or only PMA controls. Further, the inhibition of TRPA1 by HC-030031 has increased and restored the pro-inflammatory cytokine production in Hsp90-inhibited and LPS-stimulated macrophages, nullifying the effect of 17-AAG as the TNF and IL-6 production of LPS+17-AAG+HC-030031 or PMA+17-AAG+HC-030031 samples were comparable

to only LPS control. Conversely, activation of TRPA1 in the LPS+17-AAG+AITC or PMA+17-AAG+AITC conditions alleviated the pro-inflammatory cytokine production compared to Hsp90-inhibited and LPS- or PMA-stimulated macrophages (Fig. 4). The TNF and IL-6 production were significantly downregulated compared to LPS or PMA, LPS+17-AAG, and PMA+17-AAG samples. Furthermore, AITC administration in LPS-stimulated macrophages could impair TNF and IL-6 production; however, HC-030031 could not significantly change LPS-stimulated macrophages (Supplementary Fig. 4). Similar results were observed with LPS-stimulated THP-1 macrophages at 24 h (Fig. 4B). These results indicate an important role of TRPA1 in
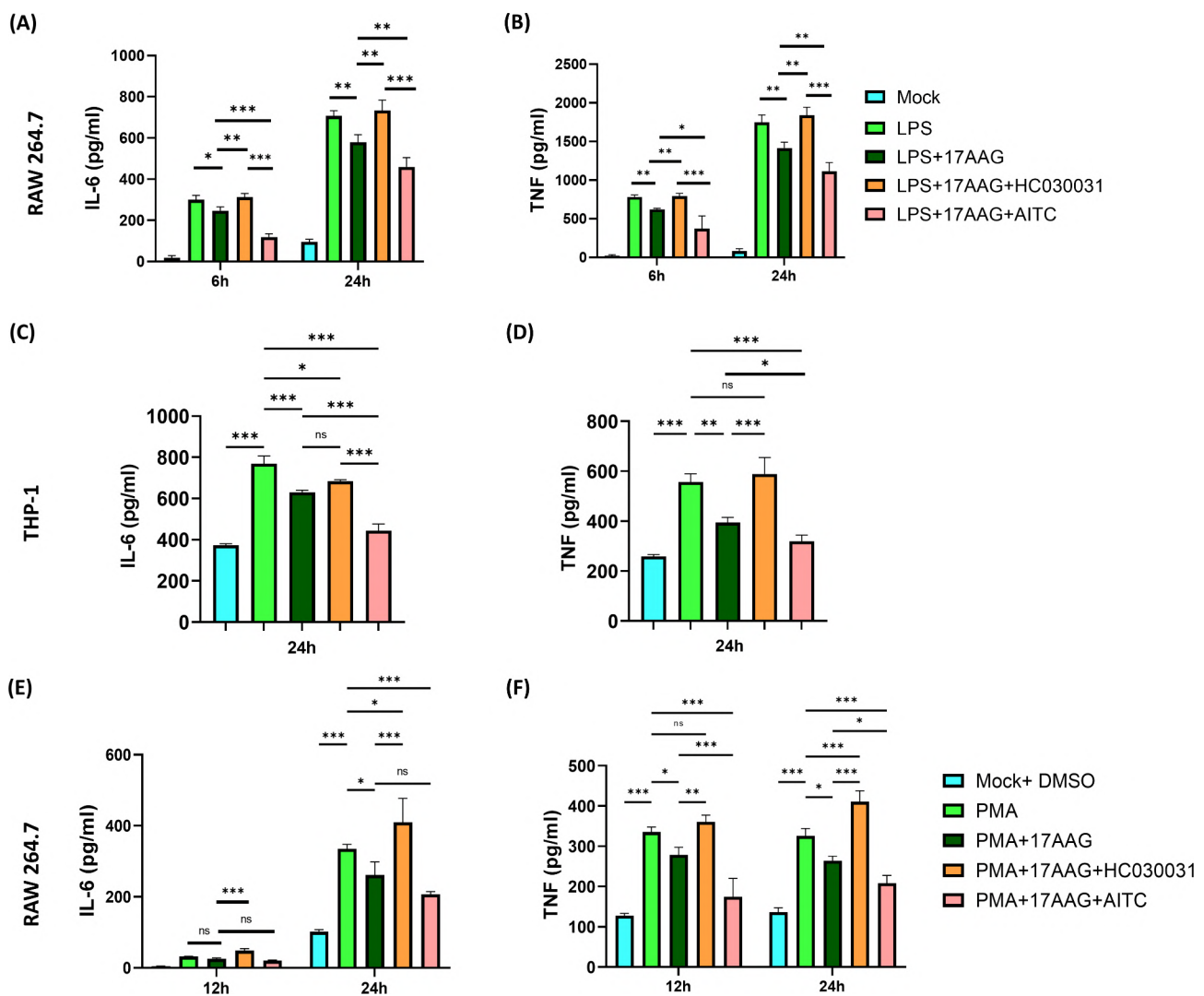

Fig. 4 TRPA1 regulates the pro-inflammatory cytokine production in Hsp90-inhibited monocytes/macrophages.
RAW 264.7 or THP-1 cells were subjected to different conditions of LPS/PMA, 17-AAG, HC-030031, or AITC, and the supernatant was collected at 6 and 24 h and assessed for cytokine profile. Bar graph representing IL-6 (**A**, **C**, **E**) and TNF (**B**, **D**, **F**) levels in RAW 264.7 cells stimulated with either LPS (500 ng/ml) (**A**) / PMA (100 ng/ml) (**C**) and THP-1 macrophages stimulated with LPS (500ng/ml) (**B**). The data represent the mean ± SD of three independent experiments. One-way/two-way ANOVA was performed to find statistical significance among groups. Differences between groups with a p-value less than 0.05 were considered statistically significant (ns, non-significant; *, p < 0.05; **, p < 0.01; ***, p < 0.001)

the anti-inflammatory development effect induced by 17-AAG-mediated Hsp90 inhibition.

TRPA1 modulates the Hsp90 inhibition-mediated downregulation of MAPK activation during LPS stimulation in macrophages

Hsp90 has been well-attributed as a regulator of various signaling complexes of inflammation and associated responses [63]. Hsp90 and inhibitors of Hsp90 have been reported to be associated with the activation of ERK-MAPK signaling pathways and SAPK/JNK pathways in various immune models [64, 65]. To investigate the role of TRPA1 in Hsp90-mediated regulation in MAPK pathways, RAW 264.7 cells were subjected to LPS (500 ng/mL) stimulation under differential conditions of TRPA1 modulators and 17-AAG for 15 min. Samples were collected and assessed to quantify signaling proteins, p38-MAPK, ERK 1/2, SAPK/JNK, and their respective phosphorylated proteins via western blot. Interestingly, it was observed that Hsp90 inhibition via 17-AAG has significantly downregulated the LPS-induced p-p38-MAPK, p-ERK 1/2, and p-SAPK/JNK expression. Further, this development via 17-AAG was reversed with TRPA1 inhibition via HC-030031 treatment. The TRPA1 activation via AITC successfully diminished the expression of the proteins and signaling
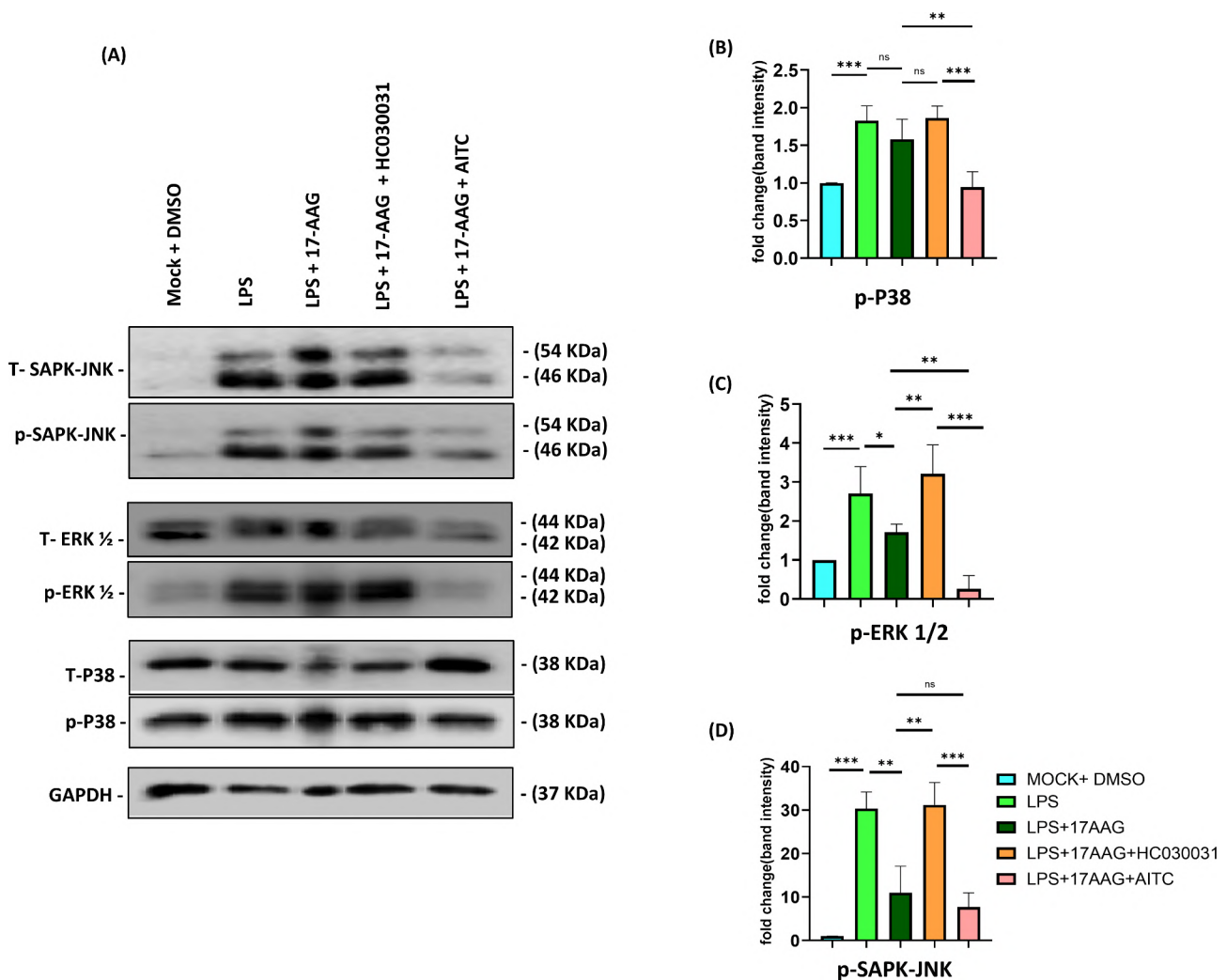

Fig. 5 TRPA1 regulates the Hsp90 inhibition-mediated downregulation of MAPK signaling protein phosphorylation in LPS-stimulated monocytes/macrophages.
RAW 264.7 cells were subjected to different conditions of LPS (500 ng/ml), 17-AAG, HC-030031, and AITC harvested at 15 min and assessed for intracellular signaling proteins p38-MAPK, ERK 1/2, SAPK-JNK and their respective phosphorylated proteins via western blot. (**A**) Western blot images from the samples represent p38-MAPK, ERK 1/2, SAPK-JNK, and their respective phosphorylated proteins. Bar graph representing the fold change in band intensity of phospho-proteins p-p38-MAPK (**B**), p-ERK 1/2 (**C**), and p-SAPK-JNK (**D**) normalized to the corresponding GAPDH controls. The data represent the mean ± SD of three independent experiments. Differences between groups with a p-value less than 0.05 were considered statistically significant (ns, non-significant; *, $p < 0.05$; **, $p < 0.01$; ***, $p < 0.001$)

further compared to the respective 17-AAG+LPS and LPS conditions (Fig. 5). These results indicate that the TRPA1 is required for Hsp90 inhibition-mediated regulation of major MAPK signaling cascades.

TRPA1 modulates Hsp90 inhibition-mediated apoptosis and inflammatory cytokine responses in activated macrophages

Hsp90 has been found to be involved in cell survival during various inflammatory and cancer models [38, 66]. Additionally, our group has reported that Hsp90 inhibition by 17-AAG downregulates the CHIKV-induced apoptosis in host macrophages [56]. To investigate the regulatory role of TRPA1 in Hsp90 inhibition-mediated developments in LPS-induced apoptosis of macrophages, if any, RAW 264.7 cells were incubated with differential conditions of TRPA1 modulators, 17-AAG, and LPS or PMA and assessed for cell death. We have performed cell-death analysis (Annexin V and 7-AAD staining) via FC. The cells were harvested at 5 and 24 h post-stimulation and assessed for apoptosis via Annexin V and

7-AAD staining followed by FC analysis (Fig. 6). We have found that cell death was increased significantly in LPS-stimulated macrophages at 5 h ($12.2\pm1.02\%$) and further augmented at 24 h ($50.8\pm2.30\%$) post-stimulation as compared to untreated cells at 5 h ($2.85\pm0.71\%$) and 24 h ($11.1\pm2.87\%$). As expected, it was significantly diminished with 17-AAG administration at 5 h ($9.65\pm0.55\%$) and 24 h ($40.1\pm1.05\%$) compared to LPS-treated cells. Interestingly, the TRPA1 inhibition via HC-030031 and 17-AAG has significantly upregulated at both 5 and 24 h ($17.6\pm1.40\%$ and $51.1\pm3.14\%$), the apoptosis compared to LPS+17-AAG condition. Conversely, TRPA1 activation via AITC has dramatically diminished the apoptosis at 5 and 24 h ($7.17\pm0.36\%$) and ($25.1\pm3.36\%$). Activation of TRPA1 via AITC exhibited an anti-apoptotic effect in LPS-stimulated macrophages as it diminished cell death compared to LPS-stimulated cells. However, HC-030031 has not modulated the cell death in LPS-stimulated macrophages (Supplementary Fig. 4). Similar results were observed in PMA-induced apoptosis of macrophages. RAW 264.7 cells treated with PMA ($49.1\pm1.46\%$) were
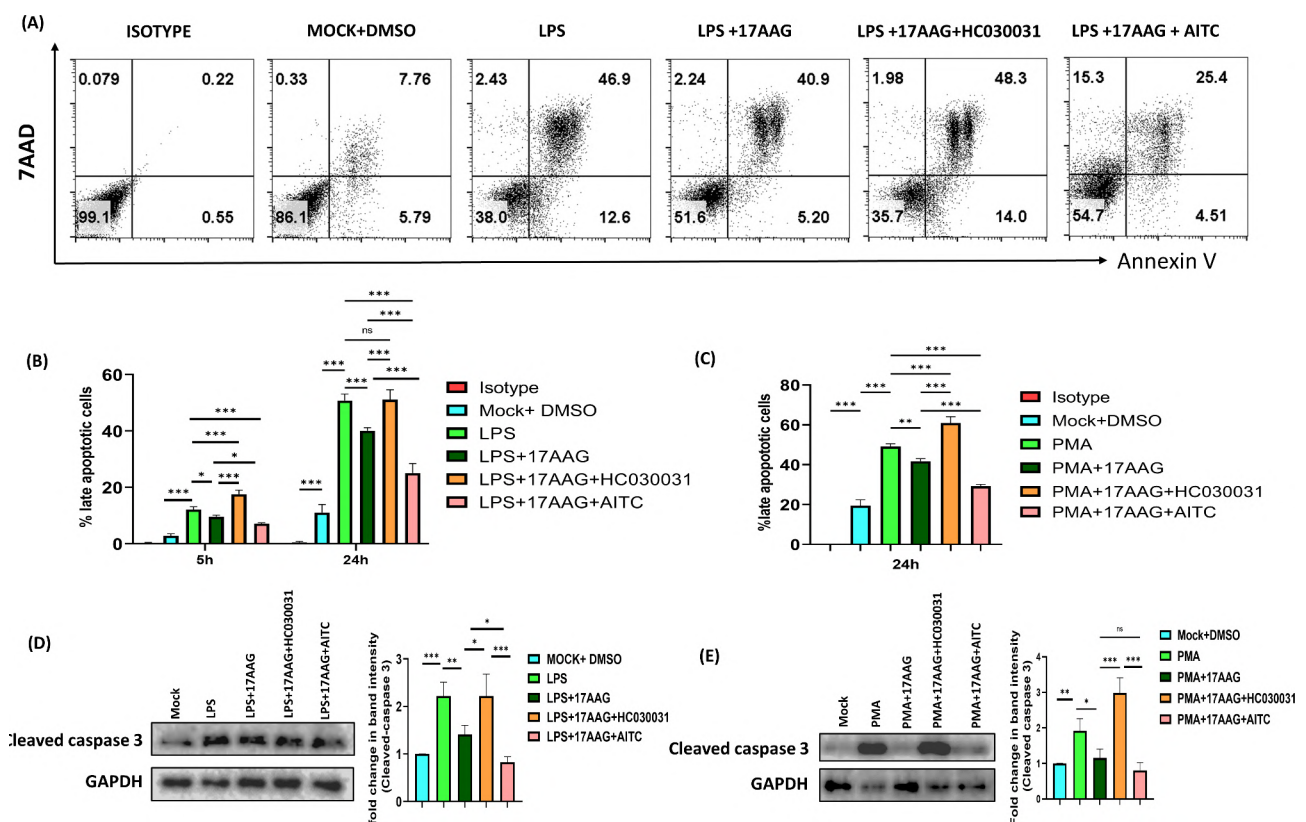

Fig. 6 TRPA1 regulates apoptosis in Hsp90-inhibited and LPS/PMA-stimulated macrophages. RAW 264.7 cells were treated with different conditions of LPS (500 ng/ml)/PMA (100 ng/ml), 17-AAG, HC-030031, and AITC. Cells were harvested at 5 and 24 h. Heat-killed cells were used as a positive control. (**A**) FC dot plots representing the percentage of positive cells for Annexin V and 7-AAD at 24 h. Double-positive cells were considered either dead or late apoptotic. Representative bar graphs of sample stimulated with LPS (500 ng/ml) (**B**)/PMA (100 ng/ml) (**C**). (**D**, **E**) Western blot image and bar graph representing fold change in band intensity for cleaved caspase 3 (**D**, **E**) for the respective samples. The data represent the mean ± SD of three independent experiments. Differences between groups with a p-value less than 0.05 were considered statistically significant (ns, non-significant; *, p < 0.05; **, p < 0.01; ***, p < 0.001)

susceptible to apoptosis at 24 h compared to untreated cells (19.4±2.90%). The highest percentage of apoptotic cells at 24 h was observed in samples treated with PMA+LPS+HC-030031 (60.9±3.16%) and the lowest in cells treated with PMA+17-AAG+AITC (29.2±0.872%) compared to PMA+17-AAG (41.7±1.35%) and PMA controls (49.1±1.46%). These samples were also assessed for caspase 3 protein levels via western blot (Fig. 6C). Band intensity levels were the lowest for cleaved caspase 3 in LPS/PMA+17-AAG+HC-030031 samples compared to LPS/PMA, LPS/PMA+17-AAG, and LPS/PMA+17-AAG+HC-030031. Inhibition of TRPA1 with HC-030031 augmented the cleaved caspase 3 levels to the respective LPS/PMA samples, nullifying the effect of 17-AAG, indicating the important role of TRPA1 towards regulating the Hsp90-associated apoptosis of macrophages.

TRPA1 is an important contributor to intracellular Ca²⁺-influx in Hsp90-inhibited and LPS-stimulated macrophages

Ca^{2+} currents via TRPA1 have been reported to modulate various immune responses and cell fate decisions [11, 12, 14, 17, 53, 67–69]. Studies have reported that intracellular Ca^{2+} increases after LPS stimulation [70]. To investigate the regulatory role of TRPA1 in intracellular Ca^{2+}-influx in Hsp90-inhibited and LPS-stimulated macrophages, Ca^{2+}-influx studies via FC were performed. RAW 264.7 cells were stained with Fluo-4 AM, and Ca^{2+}-influx was analyzed via FC continuously for 200s. The mean value for every 20s interval was obtained, and two-way ANOVA was carried out for statistical analysis. The intracellular Ca^{2+} levels were compared before and after the addition of TRPA1 modulators, 17-AAG, and LPS in different conditions. Colorless RPMI media was used as a vehicle. Interestingly, we observed that the Ca^{2+} levels were augmented upon LPS stimulation in macrophages compared to mock or vehicle-treated cells, whereas 17-AAG administration could not evoke any changes in Ca^{2+}-influx of its own (data not shown). Additionally, 17-AAG treatment along with LPS has significantly diminished the intracellular Ca^{2+} levels compared to the LPS-stimulation control. Similarly, HC-030031 administration reduced the elevated calcium levels during LPS stimulation, whereas the TRPA1 activation via AITC has upregulated it. HC-030031 treatment along with 17-AAG and LPS resulted in reduced Ca^{2+} levels compared to LPS only, LPS+17-AAG, LPS+HC-030031. Additionally, the activation of TRPA1 via AITC along with 17-AAG and LPS resulted in elevated Ca^{2+}-levels compared to LPS, or 17-AAG, LPS+17-AAG, and LPS+AITC treated cells (Fig. 7). These results indicate that TRPA1 might be an important contributor to Ca^{2+}-influx in Hsp90-inhibited and LPS-stimulated macrophages.

Together, these results suggest the anti-inflammatory nature of TRPA1 in LPS-stimulated macrophages and its synergistic role in Hsp90 inhibition-mediated pro-inflammatory responses in macrophages. A proposed comprehensive working model of the same is depicted in Fig. 8.

Discussion

The role of TRPA1, a non-selective cation channel, and Hsp90, a chaperone molecule in various immune responses has been well studied over recent years. TRPA1 plays an essential role in many immune cells, including T cells, macrophages, and monocytes [11–15]. The potential of TRPA1 in regulating various inflammatory pathways and its association with various intracellular proteins has provided insights toward TRPA1 targeted therapeutic development in various autoimmune disorders and infectious diseases [12, 19, 20, 25, 26, 71, 72]. Similarly, Hsp90 has been well attributed as a critical component in regulating various immune responses. Inhibition of HSp90 via various biological and synthetic compounds is effective in downregulating various inflammatory responses, including monocyte/macrophage-associated pro-inflammatory responses [34–39]. Even though these two molecules are effective modulators of inflammatory responses, their possible associations or the functional regulation between them in inflammatory responses are not yet been assessed. Our study highlights the role of TRPA1 channels in regulating the anti-inflammatory effect of Hsp90 inhibition. We also emphasized a novel approach to downregulate macrophage-mediated pro-inflammatory responses. We have chosen mouse RAW 264.7, and human THP-1 macrophages stimulated with LPS or PMA as model systems for studying the pro-inflammatory responses. Hsp90 inhibition mediated downregulation of macrophage activation was obtained through 17-AAG.

This study suggests an important role of a TRP channel in regulating the Hsp90 inhibitor's effect on inflammatory responses. Additionally, we have demonstrated the association of TRPA1 with Hsp90 in inflammatory responses in vitro. Our results suggest that TRPA1 has an anti-inflammatory role in 17-AAG-mediated development in macrophages during inflammation, supporting various other studies. TRPA1 is associated with and upregulated in various inflammatory conditions [14, 15, 73, 74, 17, 23, 51–55, 69]. Here, we have demonstrated that TRPA1 is upregulated during LPS/PMA stimulation and further augmented with 17-AAG administration in macrophages. Additionally, the frequency of TRPA1 positive cells and expression was significantly increased upon LPS stimulation, while it was diminished upon PMA stimulation. This might be a reflection of the different activation mechanisms these molecules induce. Although
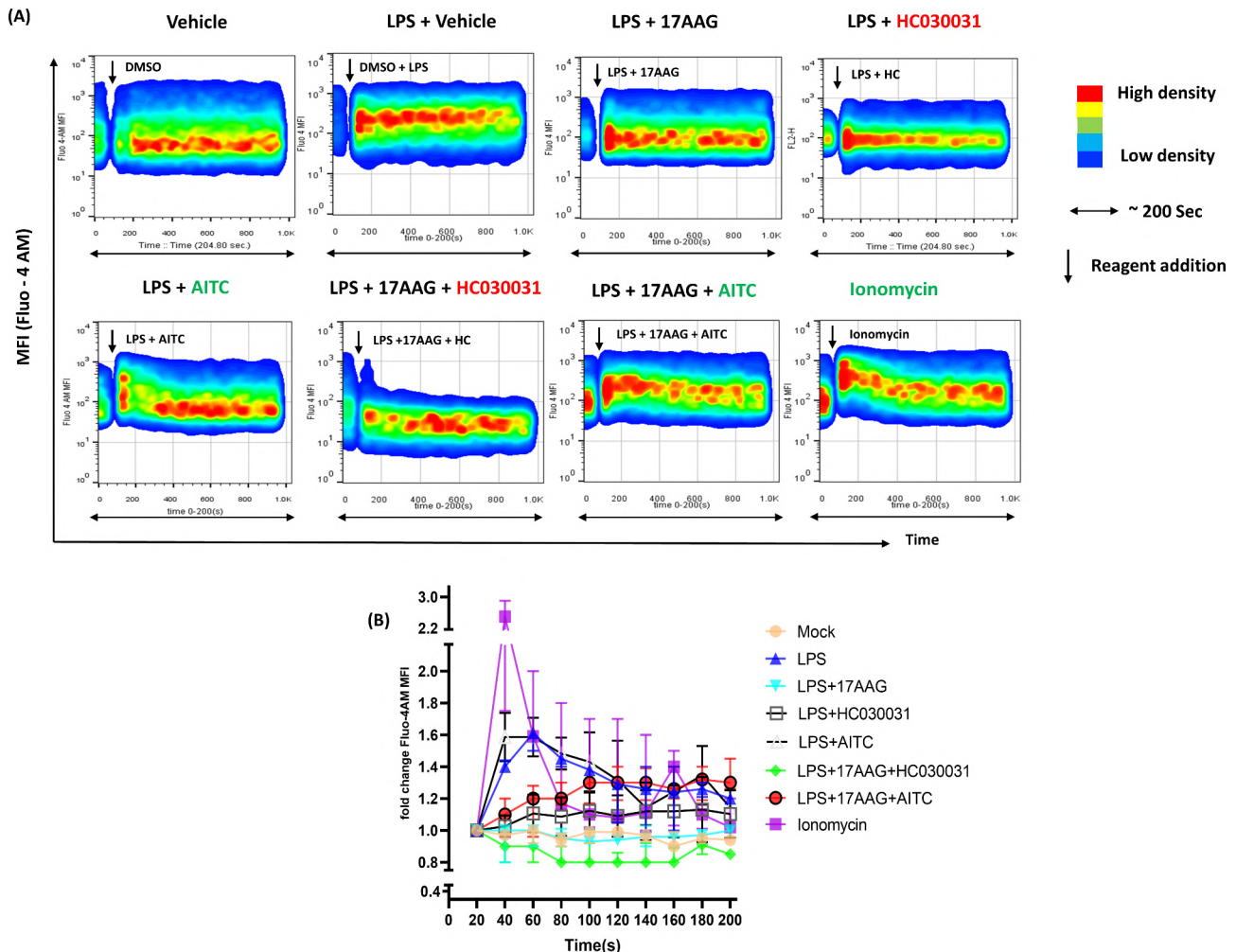
Fig. 7 TRPA1 regulates intracellular calcium influx in LPS-stimulated and Hsp90-inhibited macrophages. RAW 264.7 cells were treated with Fluo-4 AM and assessed via FC for intracellular calcium levels upon combinatorial treatment with either ionomycin, vehicle (DMSO), vehicle + LPS, LPS + 17-AAG, LPS + 17-AAG + HC-030031, and LPS + 17-AAG + AITC. (**A**) Time-lapse kinetics of intracellular calcium influx. The X-axis of the flow cytometric plots represent approximately 200 s and '↓' represents the addition of reagents/modulators to stimulate cells. (**B**) Representative line graph depicting fold changes in mean Fluo-4 intensity. The data represent the mean ± SD of three independent experiments.

these expression patterns are previously reported, the actual mechanisms behind these observations are yet to be reported. Furthermore, we highlight that the effect of Hsp90 inhibition in TRPA1 positive cell frequency is augmented in a time-dependent and reversible manner. This elevation of TRPA1 in macrophages indicates a possible association of TRPA1 in 17-AAG-induced Hsp90 inhibition-mediated anti-inflammatory developments in LPS or PMA-stimulated macrophages.

Here in this report, we have examined the effect of TRPA1 in 17-AAG-mediated downregulation of various inflammatory responses in macrophages. This study addresses the essential role of a TRP channel in regulating the Hsp90 inhibitor's effect on inflammatory responses. Additionally, we have demonstrated the association of TRPA1 with Hsp90 in inflammatory responses in vitro. Our results suggest that TRPA1 has

an anti-inflammatory role in 17-AAG-mediated development in macrophages during inflammation, supporting various other studies. 17-AAG is widely reported to regulate various autoimmune disorders and inhibit the TLR4-mediated inflammatory signaling cascade in macrophages [47, 48]. Our findings support these studies as 17-AAG administration in macrophages stimulated with LPS/PMA has significantly downregulated the LPS-induced pro-inflammatory responses in macrophages such as cell surface expression of MHCII, CD80, CD86, production of NO and inflammatory cytokines (TNF and IL-6). Our work highlights the regulatory role of TRPA1 in this case. The results suggest that the pharmacological modulation of TRPA1 has a significant impact on the 17-AAG-mediated anti-inflammatory developments in LPS/PMA-stimulated macrophages. HC-030031-mediated inhibition of TRPA1 has significantly impaired
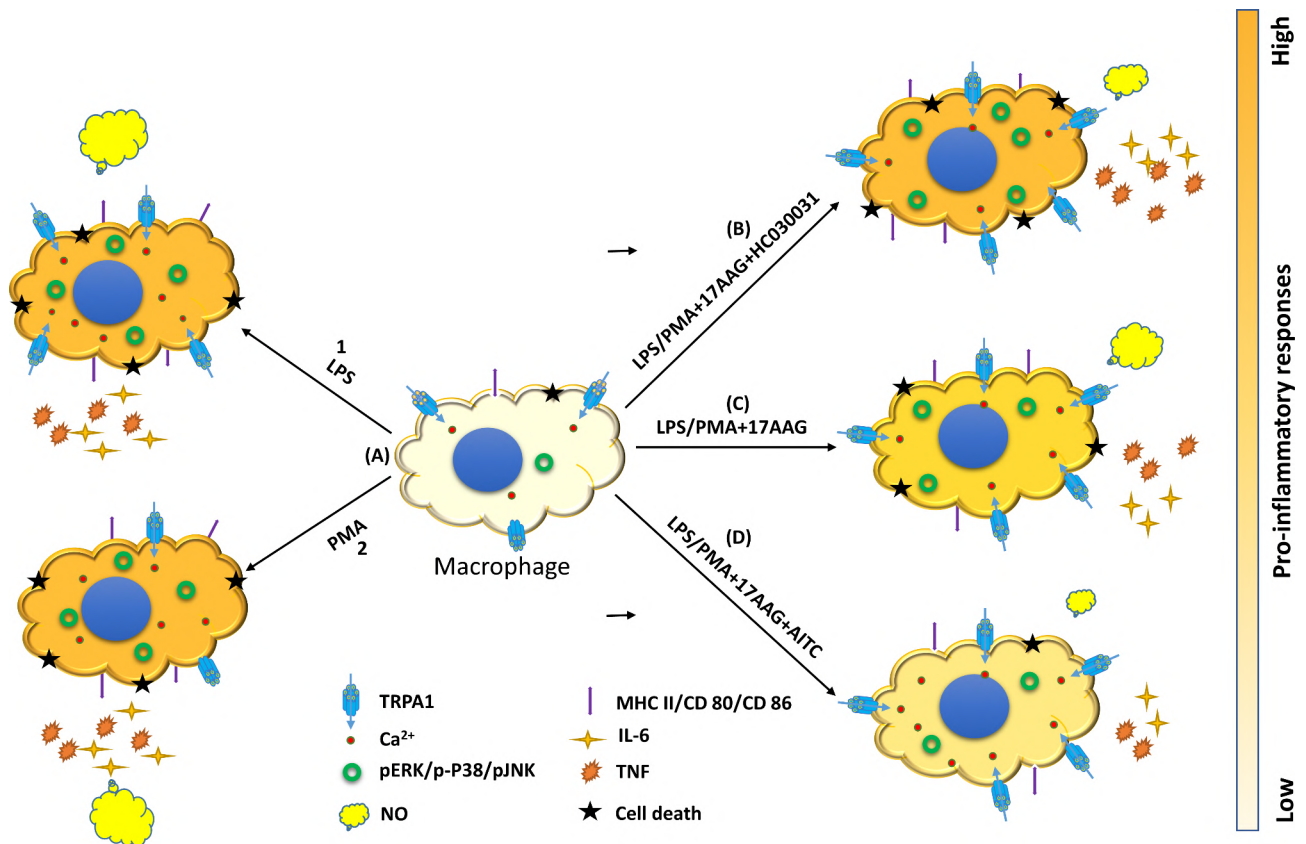
Fig. 8 A proposed comprehensive working model.

A detailed working model depicting the role of TRPA1 in 17-AAG mediated regulation of inflammation in LPS or PMA stimulated macrophages. TRPA1 is modulated upon LPS/PMA stimulation (**A**). pro-inflammatory responses including IL-6, TNF, MHCII, CD80/86, NO, intracellular calcium, and intracellular signaling proteins p38-MAPK, p-ERK 1/2, p-SAPK-JNK are significantly upregulated with LPS (**A.1**) or PMA stimulation (**A.2**). Upon administration of 17-AAG along with LPS or PMA, the pro-inflammatory responses are downregulated (**C**). Inhibition of TRPA1 via HC-030031 with 17-AAG and LPS or PMA administration reverses the pro-inflammatory responses, intracellular signaling proteins p38-MAPK, p-ERK 1/2, p-SAPK-JNK back to the LPS or PMA stimulated levels with a further diminished intracellular calcium level (**B**). Activation of TRPA1 via AITC and 17-AAG in LPS or PMA stimulated macrophages by impairing the proinflammatory responses, intracellular calcium, and intracellular signaling proteins p-p38-MAPK, p-ERK 1/2, p-SAPK-JNK to a greater extent exhibiting an anti-inflammatory property (**D**). The pro-inflammatory responses are represented according to the color code.

the suppression of pro-inflammatory responses in LPS/PMA-stimulated macrophages. HC-030031 administration, along with 17-AAG and LPS, has abolished or diminished the 17-AAG-mediated downregulation of inflammatory responses as the MHCII, CD80, CD86 surface expression, inflammatory cytokines such as TNF and IL-6 production were comparable or higher than that of LPS/PMA stimulated macrophages, clearly depicting that TRPA1 is important for 17-AAG-mediated anti-inflammatory responses. Further, the TRPA1 activation via AITC has significantly augmented the 17-AAG-mediated downregulation of inflammation as MHCII, CD80, and CD86 surface expression, secretion of inflammatory cytokines such as TNF and IL-6, and NO production are the lowest. Hsp90 inhibition in macrophages follows a suppression of various macrophage-activation signaling processes. Macrophage activation via LPS or PMA induces apoptosis due to various secreted molecules such as NO and inflammatory cytokines.

Our observations suggest that macrophages are prone to apoptosis at 12–24 h post-stimulation. Additionally, Hsp90 is well known to be involved in various cell fate decisions, including cell differentiation and apoptosis [35, 36, 39]. Our results suggest that TRPA1 has a significant regulatory role in the 17-AAG-mediated down-regulation of apoptosis. Functional activation of TRPA1 could significantly increase cell death compared to the 17-AAG and LPS administration in macrophages. Similarly, the 17-AAG-mediated downregulation apoptosis was reversed by HC-030031-mediated TRPA1 inhibition.

Our experiments on various signaling protein expressions upon Hsp90 inhibition with TRPA1 modulators suggested that TRPA1 has a critical role in Hsp90 inhibition-mediated down-regulation of macrophage activation signaling. The MAPK signaling proteins p-p38-MAPK, p-ERK 1/2, and p-SAPK/JNK expressions were significantly downregulated with 17-AAG treatment in LPS-stimulated macrophages as expected. Interestingly,

TRPA1 inhibition via HC-030031 has reversed the down-regulated expression of signaling proteins p-p38-MAPK, p-ERK 1/2, p-SAPK/JNK by 17-AAG, indicating that TRPA1 is required for the 17-AAG-mediated down-regulation of MAPK signaling pathways. Furthermore, the expression of the signaling proteins p-p38-MAPK, p-ERK 1/2, and p-SAPK/JNK were successfully diminished with TRPA1 activation and Hsp90 inhibition via 17-AAG. Modulation of the signaling cascade can be the active mechanism behind the effect of TRPA1 in regulating Hsp90 inhibition-mediated anti-inflammatory effects. These results suggest that TRPA1 and its activation may augment the efficiency of 17-AAG in ant-inflammatory responses, leading to a novel combinatorial approach to regulating inflammatory responses.

Even though TRP channels are considered non-selective cation channels, the calcium influx through these channels has an important role in TRP channel functions. A high Ca^{2+} influx is preceded by LPS stimulation in macrophages. Our results demonstrated that 17-AAG (Hsp90 antagonist) or HC-030031 (TRPA1 antagonist) administration significantly diminishes LPS-mediated elevation of intracellular calcium in macrophages. The TRPA1 activation has augmented these Ca^{2+} levels, while the TRPA1 antagonist has further reduced it, indicating that the calcium influx occurring via LPS and 17-AAG administration is dependent on TRPA1. These changes in Ca^{2+} levels could reflect the activity of additional TRPA1 channels recruited by 17-AAG administration in LPS-stimulated macrophages. This Ca^{2+} status may not correspond to calcium levels for the regulatory role of TRPA1 in the 17-AAG (Hsp90 antagonist)-mediated effect. Still, it may trigger various downstream signaling cascades that lead to the observed anti-inflammatory developments by 17-AAG.

The present study may have implications for the synergistic role of TRPA1 activation and Hsp90 inhibition toward developing future regulatory measures against various inflammatory responses. The future perspective of the study may include the sub-cellular mechanism associated with domains of TRPA1 and 17-AAG interactions and the replication of these results in different inflammatory models.

Conclusion
In conclusion, our study indicates an important role of TRPA1 in Hsp90 inhibition-mediated anti-inflammatory developments in LPS or PMA-stimulated macrophages. TRPA1 activation and Hsp90 inhibition synergistically may regulate the inflammatory responses in macrophages and this combinatorial approach may have implications towards designing future therapeutic strategies in various diseases and inflammatory disorders.

Materials and methods
Cell culture
Mouse macrophage cell line, RAW 264.7 (source – ATCC (ATCC® TIB-71™)) was cultured in complete Roswell Park Memorial Institute-1640 medium (RPMI-1640) (PAN Biotech, Aidenbach, Germany) with penicillin (100 U/mL), Streptomycin (0.1 mg/mL), and 2.0 mM L-Glutamine (Himedia Laboratories Pvt. Ltd., Mumbai, MH, India), 10% heat-inactivated fetal bovine serum (FBS) (PAN Biotech, Aidenbach, Germany) at 37°C in a sterile incubator with 5% CO_2 and appropriate humidity. Enzyme-free cell dissociation reagent (ZymeFree™; Himedia Laboratories Pvt. Ltd, Mumbai, MH, India) was used to maintain the cells [56].

Undifferentiated human leukemia monocytic cell line, THP-1 (source – ATCC (ATCC® TIB-202™)) was maintained in complete RPMI-1640 (PAN Biotech, Aidenbach, Germany) supplemented with Penicillin (100 U/mL), Streptomycin (0.1 mg/mL), and 2.0 mM L-Glutamine (Himedia Laboratories Pvt. Ltd., Mumbai, MH, India), 10% heat-inactivated FBS (PAN Biotech, Aidenbach, Germany) at 37°C in a sterile incubator with 5% CO_2 and appropriate humidity. THP-1 cells were further treated with 100 ng/ml PMA for 24 h to differentiate monocytes into macrophage-like cells [75].

Antibodies, reagents, and pharmacological modulators
Rabbit polyclonal antibody against extracellular TRPA1 with specific blocking peptide [TRPA1, INSTGIINETS-DHSE] was obtained from Alomone Laboratories (Jerusalem, Israel). Mouse antibodies against Hsp90, CD80, CD86, I-Ad/I-Ed (MHCII) were purchased from BD Biosciences (SJ, USA). The anti-mouse Alexa Fluor 647 (AF-647), anti-rabbit Alexa Fluor 488 (AF-488), and Fluo-4 AM were procured from Invitrogen (Carlsbad, CA, USA). Mouse IgG1 isotype control and rabbit IgG1 isotype control were bought from Abgenex India Pvt. Ltd. (Bhubaneswar, India). Saponin and Bovine serum albumin (BSA) fraction-V were procured from Merck Millipore (Billerica, MA, USA). 17-AAG and the pharmacological modulators of TRPA1 channel-antagonist HC-030031, agonist Allyl isothiocyanate (AITC) were purchased from Alomone Laboratories (Jerusalem, Israel). HC-030031 and AITC are proven to be functional modulators of TRPA1, and their administration may not alter the TRPA1 expression levels.

Cell viability assay
To assess the cytotoxicity of pharmacological modulators, RAW 264.7 and PMA differentiated THP-1 macrophages were administrated with differential doses of TRPA1 modulators HC-030031 and AITC along with 17-AAG (0.5 µg/ml) and incubated for 24 h. Cells were immediately assessed by trypan blue exclusion assay.

Additionally, samples were stained with Annexin V and 7-AAD and evaluated for cell viability. The percentage of viable cells was calculated in comparison to the control cells.

LPS/PMA stimulation in macrophages

RAW 264.7 cells were harvested and seeded in a six-well plate. After the cells had reached monolayer confluency of ~80%, they were washed with 1X PBS and subjected to LPS (500 ng/ml) or PMA (100 ng/ml) [76] dissolved in fresh complete RPMI-1640. The supernatant and the cells were then harvested. They were stored or processed at various time points. 17-AAG was used to promote the Hsp90-inhibited condition in the cells. For assessing the effect of TRPA1 in the Hsp90-inhibited cells in presence of LPS-induced inflammatory responses, RAW 264.7 cells were subjected to 17-AAG (0.5 µM) and TRPA1 pharmacological modulators incubation followed by LPS or PMA administration for 6 to 24 h. DMSO was used as solvent control. The further proceedings were executed by following the protocols mentioned above.

Similarly, undifferentiated THP-1 cells were harvested and seeded in a six-well plate with the administration of 100 ng/ml PMA for 24 h. After the cells reached a monolayer confluency of ~80%, they were washed with 1X PBS and kept in PMA-free media for another 24 h before LPS treatment (500 ng/ml) [77]. PMA-differentiated THP-1 macrophages were stimulated with LPS only for later experiments and no further PMA stimulation was carried out. Post-treatment, the supernatant, and the cells were harvested, then stored or processed at various time points. Further experiments were conducted as mentioned above.

Indirect immunofluorescence and Flow cytometry (FC)

RAW 264.7 and THP-1 macrophages were subjected to different stimuli and pharmacological modulators of TRPA1 and Hsp90. For TRPA1 extracellular staining, cells were harvested, resuspended in staining buffer (1X PBS, 1% BSA, 0.01% NaN$_3$), and then incubated with primary anti-mouse TRPA1 antibody for 30 min on ice. After direct staining, any excess unbound antibody was washed out with an additional staining buffer. Subsequently, a secondary fluorochrome-conjugated (AF-488) antibody was administered and incubated for 30 min followed by washing with staining buffer. The rabbit IgG was used as isotype control [56]. Samples (10,000 cells/sample) were then acquired via BD FACS Calibur/BD LSRFortessa (BD Biosciences) and analyzed using FlowJo v10.8.1.

Cell death/apoptosis analysis was conducted using PE Annexin V Apoptosis Detection Kit I (BD Biosciences). Freshly harvested cells were washed with 1X PBS followed by incubation with Annexin V in Annexin V binding buffer for 15 min. The assay was conducted by following the manufacturer's protocol [78]. Samples were immediately acquired via FC and analyzed using FlowJo v10.8.1.

Enzyme-linked Immunosorbent Assay (ELISA)

ELISA was performed to quantify and analyze the cytokine levels in RAW 264.7 and THP-1 cell culture supernatants under different experimental conditions of LPS/PMA, 17-AAG, HC-0300031, and AITC. Sandwich ELISA was executed using the BD OptEIA™ sandwich ELISA kit (BD Biosciences) following the instructions of the manufacturer's protocol [56]. The cytokine concentration in each sample was estimated in pg/ml from the standard curve.

Western blotting

To analyze the expression of various proteins of interest, a western blot was performed after stimulating the cells with LPS (500 ng/ml) and pharmacological modulators. In brief, respective cells (RAW 264.7 and THP-1) were treated with LPS (500 ng/ml) for 15 min, washed with 1X PBS, and immediately harvested. Cell lysis, protein estimation, and western blotting were done according to the protocol mentioned earlier [56]. Briefly, cells were harvested and washed with 1X PBS and whole cell lysates (WCL) were prepared using Radio Immuno Precipitation Assay (RIPA) buffer. The lysates were centrifuged at 13,000 rpm for 30 min at 4 °C. The protein concentrations were then quantified using the Bradford reagent (Sigma-Aldrich). The same amount of proteins was loaded in 10% SDS-gel. After running, the gels were blotted on a PVDF membrane (Millipore, MA, USA) and then blocked by 3% BSA in TBST. The blots were cut before antibody staining, then incubated overnight with primary antibodies, Hsp90 (1:1000), TRPA1 (1:1000), GAPDH (1:5000), Cleaved Caspase 3 (1:1000), p38 (1:2000), SAPK/JNK (1:2000), ERK (1:2000). The blots were then washed with TBST, 3 times, 5 min each. Then, HRP-conjugated secondary antibodies were added and blots were incubated for 2 h at RT. Blots were then washed with TBST, 3 times, 5 min each, and chemiluminescent detection reagent (Immobilon Western Chemiluminescent HRP substrate, Millipore) was added and images were captured by ChemiDoc (Bio-Rad). The ImageLab analysis software was used for band intensity quantification of western blot images with normalization to the corresponding loading controls.

Calcium (Ca²⁺) influx analysis

To evaluate the Ca^{2+} influx after the administration of various stimuli and pharmacological modulators, the cells were incubated with 5 µM Fluo-4 AM for 45–60 min in HBSS buffer and subjected to de-esterification for

15 min in 1X PBS. Cells were then incubated in an HBSS medium and Ca^{2+} influx was analyzed in FC by measuring the time-dependent fluorescence intensity upon adding the respective modulators, as mentioned earlier [79]. The data were analyzed using FlowJo for kinetic studies and obtaining mean fluorescence every 10 s.

Nitrite estimation

The supernatant of macrophages was treated with the differential conditions of LPS/PMA,17-AAG, HC-0300031, and AITC for 6, 12, and 24 h in colorless RPMI-1640. About 100 µl of supernatants were used to measure NO levels with 100 µl of 1% sulfanilamide and 100 µl of 0.1% N-1-naphthylenediamine dihydrochloride [80]. Samples were incubated for 10 min and the absorbance values were read at 540 nm using a microplate reader (Epoch 2 microplate reader, BioTek, USA). Nitrite concentrations were calculated from a standard graph prepared using different concentrations of sodium nitrite dissolved in colorless RPMI-1640.

Statistical analysis

Statistical analyses were performed using GraphPad Prism 9.0 software (GraphPad Software Inc., San Diego, CA, USA). The comparison between the groups was performed by one-way ANOVA or two-way ANOVA with the Bonferroni posthoc test unless otherwise mentioned. The data is represented as the mean±SD of three independent experiments (n=3). $p < 0.05$ was reflected as a statistically significant relation between the respective groups (ns, non-significant; * $p < 0.05$; ** $p < 0.01$; *** $p < 0.001$).

List of Abbreviations

TRPA1	Transient receptor potential ankyrin channel 1
Hsp90	Heat shock protein 90
17-AAG	17-(allylamino)-17-demethoxygeldanamycin
LPS	Lipopolysaccharide
PMA	Phorbol 12-myristate 13-acetate
AITC	Allyl isothiocyanate
HC-030031	1,2,3,6-Tetrahydro-1,3-dimethyl-N-[4-(1-methylethyl) phenyl]-2,6-dioxo-7 H-purine-7- acetamide,2-(1,3-Dimethyl-2,6-dioxo-1,2,3,6-tetrahydro-7 H-purin-7-yl)-N-(4-isopropylphenyl) acetamide
MHCII	Major histocompatibility complex II
CD80	Cluster of differentiation 80
CD86	Cluster of differentiation 86
TNF	Tumor necrosis factor
IL-6	Interleukin 6
NO	Nitric oxide
MAPK	Mitogen-activated protein kinase
ERK	Extracellular signal-regulated kinase
SAPK	Stress-Activated Protein Kinase
JNK	C-Jun N-terminal kinase
Lck	Lymphocyte-specific protein tyrosine kinase
FBS	Fetal bovine serum
FC	Flow cytometry
DMSO	Dimethyl sulfoxide

Declarations

Ethics approval and consent to participate

All the experimental protocols were performed as per the Institutional Ethical Guidelines.

Consent for publication

Not applicable.

Competing interests

The authors have no relevant competing interests to disclose.

Author details

[1]National Institute of Science Education and Research, an Off-campus Centre (OCC) of Homi Bhabha National Institute, Bhubaneswar, Odisha 752050, India
[2]Institute of Life Sciences, Nalco Nagar Rd, NALCO Square, NALCO Nagar, Chandrasekharpur, Bhubaneswar, Odisha 751023, India

References

1. Flockerzi V, Bruford EA, Caterina MJ et al. For the superfamily of TRP cation channels the TRP superfamily includes a diversity of non-voltage-. 2002;9:229–31.
2. Ramsey I, Delling M, Clapham D. An introduction to TRP channels. Annu Rev Physiol. 2006;68:619–47. https://doi.org/10.1146/annurev.physiol.68.040204.100431

Radhakrishnan *et al. BMC Immunology*   (2023) 24:16

Page 16 of 17

3. Gaudet R. TRP channels entering the structural era. J Physiol. 2008;586(15):3565–75. https://doi.org/10.1113/jphysiol.2008.155812

4. Gees M, Colsoul B, Nilius B. The role of transient receptor potential cation channels in Ca2 + signaling. Cold Spring Harb Perspect Biol. 2010;2(10):a003962. https://doi.org/10.1101/cshperspect.a003962

5. Vay L, Gu C, Mcnaughton PA. The thermo-TRP ion channel family: properties and therapeutic implications. Published online. 2012. https://doi.org/10.1111/j.1476-5381.2011.01601.x

6. Clapham DE. TRP channels as cellular sensor. Nature. 2003;426(December):517–24.

7. Smani T, Shapovalov G, Skryma R, Prevarskaya N, Rosado JA. Biochimica et Biophysica Acta Functional and physiopathological implications of TRP channels. BBA - Mol Cell Res. 2015;1853(8):1772–82. https://doi.org/10.1016/j.bbamcr.2015.04.016

8. Pla AF, Gkika D. Emerging role of TRP channels in cell migration: from tumor vascularization to metastasis. 2013;4(November):1–13. https://doi.org/10.3389/fphys.2013.00311

9. Sukumaran P, Schaar A, Sun Y, Singh BB. Functional role of TRP channels in modulating ER stress and autophagy. Cell Calcium Published online 2016:1–10. https://doi.org/10.1016/j.ceca.2016.02.012

10. Montell C, Birnbaumer L, Flockerzi V, et al. A unified nomenclature for the superfamily of TRP cation channels. Mol Cell. 2002;9(2):229–31. https://doi.org/10.1016/s1097-2765(02)00448-3

11. Payrits M, Helyes Z, Szentagothai J, Sciences AE. Oestrogen-dependent up-regulation of TRPA1 and TRPV1 receptor proteins in the rat endometrium. 2015;(December):1–49.

12. Tian C, Huang R, Tang F, et al. Transient receptor potential ankyrin 1 contributes to Lysophosphatidylcholine – Induced Intracellular Calcium Regulation and THP – 1 – derived macrophage activation. J Membr Biol. 2019;0123456789. https://doi.org/10.1007/s00232-019-00104-2

13. Amraiz D, Zaidi N, us sahar S, Fatima M. Antiviral evaluation of an Hsp90 inhibitor, gedunin, against dengue virus. 2017;16(May):997–1004.

14. Logu F, De, Nassini R, Materazzi S et al. Schwann cell TRPA1 mediates neuroinflammation that sustains macrophage-dependent neuropathic pain in mice. Nat Commun Published online 1887:1–16. https://doi.org/10.1038/s41467-017-01739-2

15. Facchinetti F, Amadei F, Geppetti P et al. A, b -Unsaturated aldehydes in cigarette smoke release Inflammatory Mediators from Human Macrophages. https://doi.org/10.1165/rcmb.2007-0130OC

16. Sahoo SS, Majhi RK, Tiwari A, et al. Transient receptor potential ankyrin1 channel is endogenously expressed in T cells and is involved in immune functions. Biosci Rep. 2019;39(9):BSR20191437. https://doi.org/10.1042/BSR20191437

17. Ma S, Zhang Y, He K, Wang P, Wang DH. Knockout of TRPA1 exacerbates angiotensin II-induced kidney injury.

18. Zeng D, Chen C, Zhou W, et al. TRPA1 deficiency alleviates inflammation of atopic dermatitis by reducing macrophage infiltration. Life Sci. 2021;266:118906. https://doi.org/10.1016/j.lfs.2020.118906

19. Kun J, Szitter I, Kemény A, et al. Upregulation of the transient receptor potential ankyrin 1 ion channel in the inflamed human and mouse colon and its protective roles. PLoS ONE. 2014;9(9):e108164. https://doi.org/10.1371/journal.pone.0108164

20. Ma S, Wang DH. Knockout of Trpa1 exacerbates renal ischemia-reperfusion injury with classical activation of macrophages. *Am J Hypertens*. Published online October 2020. https://doi.org/10.1093/ajh/hpaa162

21. Usui-kusumoto K, Iwanishi H, Ichikawa K, et al. Suppression of neovascularization in corneal stroma in a TRPA1-null mouse. Exp Eye Res. 2019;181(February 2018):90–7. https://doi.org/10.1016/j.exer.2019.01.002

22. Shepherd AJ, Copits BA, Mickle AD, et al. Angiotensin II triggers peripheral macrophage-to-sensory Neuron Redox Crosstalk to Elicit Pain. J Neurosci. 2018;38(32):7032–57. https://doi.org/10.1523/JNEUROSCI.3542-17.2018

23. Logu F, De, Prá SDtoé, De DCT, De et al. Macrophages and Schwann cell TRPA1 mediate chronic allodynia in a mouse model of complex regional pain syndrome type I. *Brain Behav Immun*. Published online 2020. https://doi.org/10.1016/j.bbi.2020.04.037

24. Meseguer V, Alpizar YA, Luis E, et al. TRPA1 channels mediate acute neurogenic inflammation and pain produced by bacterial endotoxins. Nat Commun. 2014;5:3125. https://doi.org/10.1038/ncomms4125

25. Yin S, Wang P, Xing R, et al. Transient receptor potential ankyrin 1 (TRPA1) mediates lipopolysaccharide (LPS)-Induced inflammatory responses in Primary Human Osteoarthritic Fibroblast-Like Synoviocytes. Inflammation. 2018;41(2):700–9. https://doi.org/10.1007/s10753-017-0724-0

26. Ko HK, Lin AH, Perng DW, Lee TS, Kou YR. Lung epithelial TRPA1 mediates Lipopolysaccharide-Induced Lung inflammation in bronchial epithelial cells and mice. Front Physiol. 2020;11. https://doi.org/10.3389/fphys.2020.596314

27. Romano B, Borrelli F, Fasolino I, et al. The cannabinoid TRPA1 agonist cannabichromene inhibits nitric oxide production in macrophages and ameliorates murine colitis. Br J Pharmacol. 2013;169(1):213–29. https://doi.org/10.1111/bph.12120

28. Yusuf N, Nasti TH, Huang CM, et al. Heat shock proteins HSP27 and HSP70 are Present in the skin and are important mediators of allergic contact hypersensitivity. J Immunol. 2009;182(1):675–83. https://doi.org/10.4049/jimmunol.182.1.675

29. Atoyan R, Shander D, Botchkareva NV. Non-neuronal expression of transient receptor potential type A1 (TRPA1) in human skin. J Invest Dermatol. 2009;129(9):2312–5. https://doi.org/10.1038/jid.2009.58

30. Cojocaru F, Şelescu T, Domocoş D, et al. Functional expression of the transient receptor potential ankyrin type 1 channel in pancreatic adenocarcinoma cells. Sci Rep. 2021;11(1):2018. https://doi.org/10.1038/s41598-021-81250-3

31. Gouin O, L'Herondelle K, Lebonvallet N, et al. TRPV1 and TRPA1 in cutaneous neurogenic and chronic inflammation: pro-inflammatory response induced by their activation and their sensitization. Protein Cell. 2017;8(9):644–61. https://doi.org/10.1007/s13238-017-0395-5

32. Prodromou C, Pearl LH. Structure and functional relationships of Hsp90. Curr Cancer Drug Targets. 2003;3(5):301–23. https://doi.org/10.2174/1568009033481877

33. Kamal A, Boehm MF, Burrows FJ. Therapeutic and diagnostic implications of Hsp90 activation. Trends Mol Med. 2004;10(6):283–90. https://doi.org/10.1016/j.molmed.2004.04.006

34. Srisutthisamphan K, Jirakanwisal K, Ramphan S, Tongluan N, Kuadkitkan A, Smith DR. Hsp90 interacts with multiple dengue virus 2 proteins. Sci Rep. 2018;8(1):4308. https://doi.org/10.1038/s41598-018-22639-5

35. Geller R, Taguwa S, Frydman J. Broad action of Hsp90 as a host chaperone required for viral replication. Biochim Biophys Acta. 2012;1823(3):698–706. https://doi.org/10.1016/j.bbamcr.2011.11.007

36. Siebelt M, Jahr H, Groen HC, et al. Hsp90 inhibition protects against Biomechanically Induced Osteoarthritis in rats. Arthritis \& Rheum. 2013;65(8):2102–12. https://doi.org/10.1002/art.38000

37. Tukaj S, Węgrzyn G. Anti-Hsp90 therapy in autoimmune and inflammatory diseases: a review of preclinical studies. Cell Stress Chaperones. 2016;21(2):213–8. https://doi.org/10.1007/s12192-016-0670-z

38. Moser C, Lang SA, Stoeltzing O. Heat-shock protein 90 (Hsp90) as a Molecular Target for Therapy of Gastrointestinal Cancer. Anticancer Res. 2009;29(6):2031–42. https://ar.iiarjournals.org/content/29/6/2031

39. Trepel J, Mollapour M, Giaccone G, Neckers L. Targeting the dynamic HSP90 complex in cancer. Nat Rev Cancer. 2010;10(8):537–49. https://doi.org/10.1038/nrc2887

40. Srivastava P. Roles of heat-shock proteins in innate and adaptive immunity. Nat Rev Immunol. 2002;2(3):185–94. https://doi.org/10.1038/nri749

41. Rice JW, Veal JM, Fadden RP, et al. Small molecule inhibitors of Hsp90 potently affect inflammatory disease pathways and exhibit activity in models of rheumatoid arthritis. Arthritis Rheum. 2008;58(12):3765–75. https://doi.org/10.1002/art.24047

42. Wax S, Piecyk M, Maritim B, Anderson P. Geldanamycin inhibits the production of inflammatory cytokines in activated macrophages by reducing the stability and translation of cytokine transcripts. Arthritis Rheum. 2003;48(2):541–50. https://doi.org/10.1002/art.10780

43. Sugita T, Tanaka S, Murakami T, Miyoshi H, Ohnuki T. Immunosuppressive effects of the heat shock protein 90-binding antibiotic geldanamycin. Biochem Mol Biol Int. 1999;47(4):587–95. https://doi.org/10.1080/15216549900201633

44. Giannini A, Bijlmakers MJ. Regulation of the src family kinase lck by Hsp90 and ubiquitination. Mol Cell Biol. 2004;24(13):5667–76. https://doi.org/10.1128/MCB.24.13.5667-5676.2004

45. Bijlmakers MJJE, Marsh M. Hsp90 is essential for the synthesis and subsequent membrane Association, but not the maintenance, of the src-kinase p56 lck. Mol Biol Cell. 2000;11(5):1585–95. https://doi.org/10.1091/mbc.11.5.1585

46. *J Biol Chem*. 2005;280(11):9813–9822. doi:10.1074/jbc.M409745200.

47. Poulaki V, Iliaki E, Mitsiades N, et al. Inhibition of Hsp90 attenuates inflammation in endotoxin-induced uveitis. FASEB J. 2007;21(9):2113–23. https://doi.org/10.1096/fj.06-7637com

48. Dello Russo C, Polak PE, Mercado PR, et al. The heat-shock protein 90 inhibitor 17-allylamino-17-demethoxygeldanamycin suppresses glial inflammatory responses and ameliorates experimental autoimmune

encephalomyelitis. J Neurochem. 2006;99(5):1351–62. https://doi.org/10.1111/j.1471-4159.2006.04221.x

49. Bautista DM, Pellegrino M, Tsunozaki M. TRPA1: a gatekeeper for inflammation. Annu Rev Physiol. 2013;75:181–200. https://doi.org/10.1146/annurev-physiol-030212-183811

50. Nagata K, Duggan A, Kumar G, Garcı J. Nociceptor and Hair Cell Transducer Properties of TRPA1, a Channel for Pain and hearing. 2005;25(16):4052–61. https://doi.org/10.1523/JNEUROSCI.0013-05.2005

51. Bertin S, Aoki-nonaka Y, Lee J et al. The TRPA1 ion channel is expressed in CD4 + T cells and restrains T-cell-mediated colitis through inhibition of TRPV1. Published online 2016:1–13. https://doi.org/10.1136/gutjnl-2015-310710

52. Engel MA, Leffler A, Niedermirtl F et al. TRPA1 and substance P mediate colitis in mice. Published online 2011:1346–58. https://doi.org/10.1053/j.gastro.2011.07.002

53. Trevisan G, Benemei S, Materazzi S, et al. TRPA1 mediates trigeminal neuropathic pain in mice downstream of monocytes/macrophages and oxidative stress. Brain. 2016;139(5):1361–77. https://doi.org/10.1093/brain/aww038

54. Parenti A, Logu F, De, Geppetti P, Benemei S. What is the evidence for the role of TRP channels in in fl ammatory and immune. 2016;16:953–69. https://doi.org/10.1111/bph.13392

55. Khalil M, Alliger K, Weidinger C, et al. Functional role of transient receptor potential channels in Immune cells and Epithelia. Front Immunol. 2018;9:174. https://doi.org/10.3389/fimmu.2018.00174

56. Nayak TK, Mamidi P, Kumar A, et al. Regulation of viral replication, apoptosis and pro-inflammatory responses by 17-aag during chikungunya virus infection in macrophages. Viruses. 2017;9(1). https://doi.org/10.3390/v9010003

57. Eid SR, Crown ED, Moore EL, et al. HC-030031, a TRPA1 selective antagonist, attenuates inflammatory- and neuropathy-induced mechanical hypersensitivity. Mol Pain. 2008;4. https://doi.org/10.1186/1744-8069-4-48

58. Hansted AK, Bhatt DK, Olesen J, Jensen LJ, Jansen-Olesen I. Effect of TRPA1 activator allyl isothiocyanate (AITC) on rat dural and pial arteries. Pharmacol Rep. 2019;71(4):565–72. https://doi.org/10.1016/j.pharep.2019.02.015

59. Scroggins BT, Neckers L. Just say NO: nitric oxide regulation of Hsp90. EMBO Rep. 2009;10(10):1093–4. https://doi.org/10.1038/embor.2009.212

60. Beck R, Dejeans N, Glorieux C, et al. Hsp90 is cleaved by reactive oxygen species at a highly conserved N-terminal amino acid motif. PLoS ONE. 2012;7(7):e40795–5. https://doi.org/10.1371/journal.pone.0040795

61. Giustarini D, Rossi R, Milzani A, Dalle-Donne I. Nitrite and nitrate measurement by Griess reagent in human plasma: evaluation of interferences and standardization. Methods Enzymol. 2008;440:361–80. https://doi.org/10.1016/S0076-6879(07)00823-3

62. Ambade A, Catalano D, Lim A, Mandrekar P. Inhibition of heat shock protein (molecular weight 90 kDa) attenuates proinflammatory cytokines and prevents lipopolysaccharide-induced liver injury in mice. Hepatology. 2012;55(5):1585–95. https://doi.org/10.1002/hep.24802

63. Lei W, Mullen N, McCarthy S, et al. Heat-shock protein 90 (Hsp90) promotes opioid-induced anti-nociception by an ERK mitogen-activated protein kinase (MAPK) mechanism in mouse brain. J Biol Chem. 2017;292(25):10414–28. https://doi.org/10.1074/jbc.M116.769489

64. Fujita K, Otsuka T, Kawabata T, et al. Inhibitors of heat shock protein 90 augment endothelin–1–induced heat shock protein 27 through the SAPK/JNK signaling pathway in osteoblasts. Mol Med Rep Published online April. 2018;12. https://doi.org/10.3892/mmr.2018.8878

65. Kim W, Tokuda H, Kawabata T, et al. Enhancement by HSP90 inhibitor of PGD2-stimulated HSP27 induction in osteoblasts: suppression of SAPK/JNK and p38 MAP kinase. Prostaglandins Other Lipid Mediat. 2019;143:106327. https://doi.org/10.1016/j.prostaglandins.2019.03.002

66. Subramanian C, Grogan PT, Wang T, et al. Novel C-terminal heat shock protein 90 inhibitors target breast cancer stem cells and block migration, self-renewal, and epithelial–mesenchymal transition. Mol Oncol. 2020;14(9):2058–68. https://doi.org/10.1002/1878-0261.12686

67. Yin S, Zhang L, Ding L, et al. Transient receptor potential ankyrin 1 (trpa1) mediates il-1β-induced apoptosis in rat chondrocytes via calcium overload and mitochondrial dysfunction. J Inflamm. 2018;15(1):27. https://doi.org/10.1186/s12950-018-0204-9

68. de Souza Monteiro D, De Logu F, Adembri C, et al. TRPA1 mediates damage of the retina induced by ischemia and reperfusion in mice. Cell Death Dis. 2020;11(8):633. https://doi.org/10.1038/s41419-020-02863-6

69. Kun J, Szitter I, Kemény A, et al. Upregulation of the transient receptor potential ankyrin 1 ion channel in the inflamed human and mouse colon and its protective roles. PLoS ONE. 2014;9(9):e108164. https://doi.org/10.1371/journal.pone.0108164

70. Hoffmann A, Kann O, Ohlemeyer C, Hanisch UK, Kettenmann H. Elevation of basal intracellular calcium as a central element in the activation of brain macrophages (microglia): suppression of receptor-evoked calcium signaling and control of release function. J Neurosci. 2003;23(11):4410–9. https://doi.org/10.1523/JNEUROSCI.23-11-04410.2003

71. Zhao J, Shyue S, kun, Kou YR, Lu T, min, Lee T. Transient receptor potential ankyrin 1 Channel involved in atherosclerosis and. Macrophage-Foam Cell Formation. 2016;12. https://doi.org/10.7150/ijbs.15229

72. Billeter AT, Galbraith N, Walker S, et al. TRPA1 mediates the effects of hypothermia on the monocyte inflammatory response. Surgery. 2015;158(3):646–54. https://doi.org/10.1016/j.surg.2015.03.065

73. Kochukov MY, Mcnearney TA, Fu Y, Westlund KN, Westlund KN, Trp T. Thermosensitive TRP ion channels mediate cytosolic calcium response in human synoviocytes. 2006;1043:424–33. https://doi.org/10.1152/ajpcell.00553.2005

74. Romano B, Borrelli F, Fasolino I, et al. The cannabinoid TRPA1 agonist cannabichromene inhibits nitric oxide production in macrophages and ameliorates. Published online. 2013. https://doi.org/10.1111/bph.12120

75. Chang YY, Lu CW, Jean WH, Shieh JS, Lin TY. Phorbol myristate acetate induces differentiation of THP-1 cells in a nitric oxide-dependent manner. Nitric Oxide - Biol Chem. 2021;July 2020109–10. https://doi.org/10.1016/j.niox.2021.02.002

76. Jones E, Adcock IM, Ahmed BY, Punchard NA. Modulation of LPS stimulated NF-kappaB mediated nitric oxide production by PKCε and JAK2 in RAW macrophages. J Inflamm. 2007;4:1–9. https://doi.org/10.1186/1476-9255-4-23

77. Bai G, Matsuba T, Niki T, Hattori T. Stimulation of THP-1 macrophages with LPS increased the production of osteopontin-encapsulating Exosome. Int J Mol Sci. 2020;21(22). https://doi.org/10.3390/ijms21228490

78. Properties C, Properties T. Technical data sheet technical data sheet. Cell. 2005;123(May):98–9.

79. Papaioannou NE, Voutsas IF, Samara P, Tsitsilonis OE. A flow cytometric approach for studying alterations in the cytoplasmic concentration of calcium ions in immune cells following stimulation with thymic peptides. Cell Immunol. 2016;302:32–40. https://doi.org/10.1016/j.cellimm.2016.01.004

80. Tripathi P, Tripathi P, Kashyap L, Singh V. The role of nitric oxide in inflammatory reactions. FEMS Immunol Med Microbiol. 2007;51(3):443–52. https://doi.org/10.1111/j.1574-695X.2007.00329.x

Publisher's Note

Upregulation, Functional Association, and Correlated Expressions of TRPV1 and TRPA1 During Telmisartan-Driven Immunosuppression of T Cells

Tathagata Mukherjee, Kshyama Subhadarsini Tung, Parthasarathi Jena, Chandan Goswami & Subhasis Chattopadhyay

View supplementary material 🗗

Published online: 07 Apr 2024.

Submit your article to this journal 🗗

View related articles 🗗

View Crossmark data 🗗

Check for updates

Upregulation, Functional Association, and Correlated Expressions of TRPV1 and TRPA1 During Telmisartan-Driven Immunosuppression of T Cells

Tathagata Mukherjee, Kshyama Subhadarsini Tung, Parthasarathi Jena, Chandan Goswami, and Subhasis Chattopadhyay

School of Biological Sciences, National Institute of Science Education and Research (NISER), Jatni, India

ABSTRACT

TRPV1 and TRPA1, are known to be functionally expressed in T cells, where these two channels differentially regulate effector immune responses. Telmisartan (TM), an anti-hypertension drug, has been recently repurposed to suppress various inflammatory responses. However, the possible involvement of TRP channels during TM-driven suppression of T cells responses has not been explored yet. In this study, we investigated the potential role of TRPV1 and TRPA1 during TM-driven immunosuppression of T cells *in vitro*. We observed a significant elevation of both TRPV1 and TRPA1 during TM-induced immunosuppression of T cells.We found that TRPA1 activation-driven suppression of T cell activation and effector cytokine responses during TM treatment is partially, yet significantly overridden by TRPV1 activation. Moreover, the expressions of TRPV1 and TRPA1 were highly correlated in various conditions of T cell. Mechanistically, it might be suggested that TRPV1 and TRPA1 are differentially involved in regulating T cell activation despite the co-elevation of both these TRP channels' expressions in the presence of TM. T cell activation was delineated by CD69 and CD25 expressions along with the effector cytokine levels (IFN-γ and TNF) in TM-driven suppression of T cell. These findings could have broad implications for designing possible future immunotherapeutic strategies, especially in the repurposing of TM for T cell-TRP-directed immune disorders.

Introduction

TRP channels are thermosensitive, cation-permeable ion channels with polymodal activation properties that regulate various physiological processes, including immune functions (Omari et al., 2017; Samanta et al., 2018; Zhang et al., 2023). These channels are expressed on various immune cells, such as macrophages, B cells, and T cells, playing a crucial role in cell differentiation, gene transcription, and effector responses (Acharya et al., 2021; Majhi et al., 2015; Oh-Hora & Rao, 2008; Sahoo et al., 2019; Vig & Kinet, 2009). Among these TRP channels, TRPV1 and TRPA1 are shown to be functionally associated with T cell-mediated immune responses. Pharmacological inhibition or genetic knockout of TRPV1 in T cells has

been reported to reduce intracellular Ca^{2+} levels, T cell activation, and effector immune functions. On the other hand, genetic deletion of TRPA1 in T cells has been shown to elevate TCR-induced Ca^{2+}influx, T cell activation, and result in higher proinflammatory responses (Bertin et al., 2014, 2017; Majhi et al., 2015; Sahoo et al., 2019).

TM is an ARB that is currently used to treat patients having hypertension (Arif et al., 2009; Gore et al., 2015; Kalikar et al., 2017). Reports indicate that TM reduces T cell responses by inhibiting the NFAT signaling and diminishing TNF-α-induced NF-κB activation (Huang et al., 2016; Nakano et al., 2009). Furthermore, the repurposing of TM has been documented to regulate various inflammatory immune diseases by its anti-inflammatory or immunosuppressive effects (Arab et al., 2014; De et al., 2022; Okunuki et al., 2009).

TRPA1 and TRPV1 are non-selective cation channels that can conduct Ca^{2+}-influx and recruit a series of downstream signaling events. Both TRPV1 and TRPA1 are known to be endogenously expressed in T cells (Majhi et al., 2015; Sahoo et al., 2019). Notably, various endogenous and exogenous factors can act on both TRPV1 as well as TRPA1, suggesting that, in several cases, these two channels are modulated simultaneously and/or mediate similar functions. Upregulation of TRPV1 and TRPA1 expressions during T cell activation has been reported previously (Majhi et al., 2015; Sahoo et al., 2019). However, studies regarding the involvement of the TRP channels in T cells during an immunosuppressive or anti-inflammatory stateare limited. Moreover, any potential involvement of TRP channels during TM-driven downregulation of T cell responses has yet to be investigated.

Against this backdrop, we hypothesized that there might be differential functional involvement of TRPV1 and TRPA1 in TM-induced immunosuppression of T cells. Accordingly, our aim in this study was to explorethe possible functional roles of TRPV1 and TRPA1 during TM-driven experimental immunosuppression of T cells. We examined TCR-induced T cell activation (e.g., CD69 and CD25 expression) and T cell proliferation in the presence or absence of TM. Additionally, we investigated the expressions of TRPV1 and TRPA1 on resting and activated T cells in the presence or absence of TM. Furthermore, we explored the regulation of T cell activation and effector cytokine production (e.g., IFN-γ and TNF) through TRPV1 and/or TRPA1 activation or inhibition in the presence or absence of TM. The current study might hold potential implications for immunotherapeutic strategies, particularly in the repurposing of TM in T cell-TRP-associated altered immune responses, with relevance to various health disorders and pathophysiological conditions.

Materials and methods

Animals

Male and female C57BL/6 mice aged 6–8 weeks were sourced from the NCARE animal house facility of NISER. The experimental procedures were conducted following protocols approved (Protocol no. AH-274) by the IAEC in accordance with the CPCSEA guidelines. The mice were housed in IVCs, maintaining 12-hour day-night cycles, at a temperature of approximately $22 \pm 2°C$ with 40–60% humidity. Prior to harvesting spleens, mice were euthanized in CO_2 chambers. In each experiment, spleens from multiple animals (ranging from 2 to 4) were collected in a 50 mL centrifuge tube containing 5 mL complete RPMI-

1640 cell culture medium (RPMI-1640 + heat-inactivated FBS 10% + Penicillin (100 U/mL) + Streptomycin (0.1 mg/mL) + L-glutamine (2.0 mM) + 2-ME (55 μM)). The number of spleens was determined by the experiment plans. The 50 mL tube containing the spleens was then placed on ice until further processing. Splenocytes were isolated from these spleens within 15 to 30 min after harvesting and subjected to downstream processes.

Reagents

The following reagents were obtained from Alomone Laboratories (Jerusalem, Israel): Anti-mouse TRPV1 antibody, anti-mouse TRPA1 antibody, RTX, and 1,2,3,6-Tetrahydro-1,3-dimethyl-N-[4-(1-methylethyl)phenyl]-2,6-dioxo-7 H-purine-7-acetamide,2-(1,3-Dimet hyl-2,6-dioxo-1,2,3,6-tetrahydro-7 H-purin-7-yl)-N-(4-isopropylphenyl)acetamide(HC-0300 31) (HC). 4-(3-Chloro-2-pyridinyl)-N-[4-(1,1-dimethylethyl)phenyl]-1-piperazinecarboxamide (BCTC) was procured from Tocris Bioscience (Bristol, UK). DMSO, ConA, AITC, and 2-ME were procured from Sigma Aldrich (St. Louis, MO, USA). Anti-mouse CD25, anti-mouse CD90.2, functional grade anti-mouse CD3, and functional grade anti-mouse CD28 antibodies were procured from Tonbo Biosciences (San Jose, CA, USA). Anti-mouse CD69 antibody was procured from eBiosciences (San Diego, CA, USA). BDOptEIA™(trademark; immunoassay ELISA reagents of BD Biosciences) mouse sandwich ELISA sets for IFN-γ and TNF were procured from BD Biosciences (San Jose, CA, USA). Secondary anti-rabbit AF488 antibody, CellTrace™ (trademark; fluorescence stains of Invitrogen) CFSE, and Dynabeads™ Untouched™ Mouse T Cells Kit were procured from Invitrogen (Carlsbad, CA, USA). RPMI-1640 medium and FBS were procured from Gibco (Billings, MT, USA). TM was obtained from Glenmark Life Sciences Ltd., Ankleshwar, Gujrat, India. 10X RBC lysis buffer, 10X PBS, BSA, L-glutamine, and penicillin-streptomycin were from HiMedia Laboratories (Mumbai, Maharashtra, India).

T cell purification and culture

T cells were purified from mouse splenocytes, following a previously reported method (Kumar et al., 2022; Sahoo et al., 2018). In brief, mouse spleens were disrupted with a syringe plunger in 5 mL RPMI-1640 medium on a Petri plate and passed through a 70 μM strainer. The resulting cells were collected in a 50 mL centrifuged tube. Next, the RBCs were lysed using RBC-lysis buffer. Afterward, cells were washed with 1X PBS and resuspended in complete RPMI-1640 medium. Splenocytes were counted using a hemocytometer, and T cells were purified using a T cell isolation kit (Dynabeads™ Untouched™ Mouse T Cells Kit, Invitrogen) following the manufacturer's protocol. In brief, the splenocytes were resuspended in isolation buffer (1XPBS+ FBS 2%) after hemocytometer-based counting, and incubated with biotinylated antibodies for 20 min in a 15 mL centrifuge tube. After washing with isolation buffer, the cells were incubated for an additional 15 min with streptavidin-conjugated magnetic beads. The 15 mL centrifuge tube containing cells was then placed in a magnetic stand (DynaMag™-15 Magnet) for 2 min, allowing T cells to be collected from the bead-free solution. The purified T cells were washed with 1X PBS, resuspended in complete RPMI-1640 medium, and subjected to downstream experiments. The purity of the isolated T cells was determined by flow cytometry (BD LSRFortessa™, BD Biosciences) and found to

be ≥ 95% pure. T cells were subsequently seeded in 48-well plates according to the experimental plans.

Cell viability assay

Purified murine T cells were incubated with varying concentrations of TM (10–1000 μM), RTX (TRPV1 activator; 25–400 nM), AITC (TRPA1 activator; 5–40 μM), BCTC (TRPV1 inhibitor; 1.34–53.63 μM), and HC-030031 (TRPA1 inhibitor; 10–400 μM) for 48 hours. Subsequently, T cells were then harvested and washed with 1X PBS. The viability of T cells was determined through trypan blue exclusion assays (Kumar et al., 2022). As a positive control (heat-killed cells), cells were heated at 55°C for 10 min prior to the addition of trypan blue.

Experimental setups and T cell activation

To investigate different cell surface expressions (CD69 and CD25) on T cells in the presence or absence of TM, purified murine T cells were pre-incubated with either DMSO or TM (35 μM) for 1 hour. Cells were then activated with TCR (1 μg/mL of plate-bound anti-CD3 and 1 μg/mL of soluble anti-CD28 antibodies) stimulation in the presence or absence of TM and incubated for 48 hours. Next, cells were harvested, surface stained, and analyzed by flow cytometry (Figure 1a–f).

To study the T cell proliferation in the presence or absence of TM, purified murine T cells were first loaded with CFSE (3.75 μM). Next, CFSE-loaded cells were incubated with either DMSO or TM for 1 hour. Cells were subsequently activated with TCR stimulation in the presence or absence of TM and further incubated for 72 hours. Cells were then harvested and analyzed by flow cytometry (Figure 1g–h).

To examine different cell surface expressions (TRPV1 and TRPA1) on T cells in the presence or absence of TM, purified murine T cells were pre-incubated with either DMSO or TM for 1 hour. Cells were subsequently activated with either TCR or ConA (5 μg/mL) stimulation in the presence or absence of TM and incubated for 48 hours. Next, cells were harvested, surface stained, and analyzed by flow cytometry (Figure 2).

To explore the status of T cell activation (cell surface expressions of CD69 and CD25 on T cells) and cytokine production (IFN-γ and TNF) by T cells in the presence of different modulators of TRPV1 [RTX (100 nM) and BCTC (1.34 μM)] and TRPA1 [AITC (12.5 μM) and HC (100 μM)] in the presence or absence of TM, purified murine T cells were pre-incubated either with DMSO or with TM and/or with different functional modulators of TRPV1 and TRPA1. Next, T cells were activated with TCR stimulation and incubated for 48 hours along with the modulators in the presence or absence of TM. Cell culture supernatants were then collected to quantify cytokine levels using sandwich ELISA (Figure 4), and cells were harvested, surface stained, and subjected to flow cytometry (Figure 3). Additionally, a schematic depiction has been presented in Fig S2.

For correlation analysis (Figure 5), different experimental conditions are as follows: for Figure 5a,b: DMSO, TM, DMSO+TCR, DMSO+ConA, TM+TCR, and TM+ConA; for Figure 5c,d: DMSO, DMSO+TCR, RTX+TCR, AITC+TCR, RTX+AITC+TCR, TM+TCR, RTX+TM+TCR, AITC+TM+TCR,RTX+AITC+TM+TCR, BCTC+TCR, HC+TCR, BCTC+HC+TCR, BCTC+TM+TCR, HC+TM+TCR, BCTC+HC+TM+TCR).
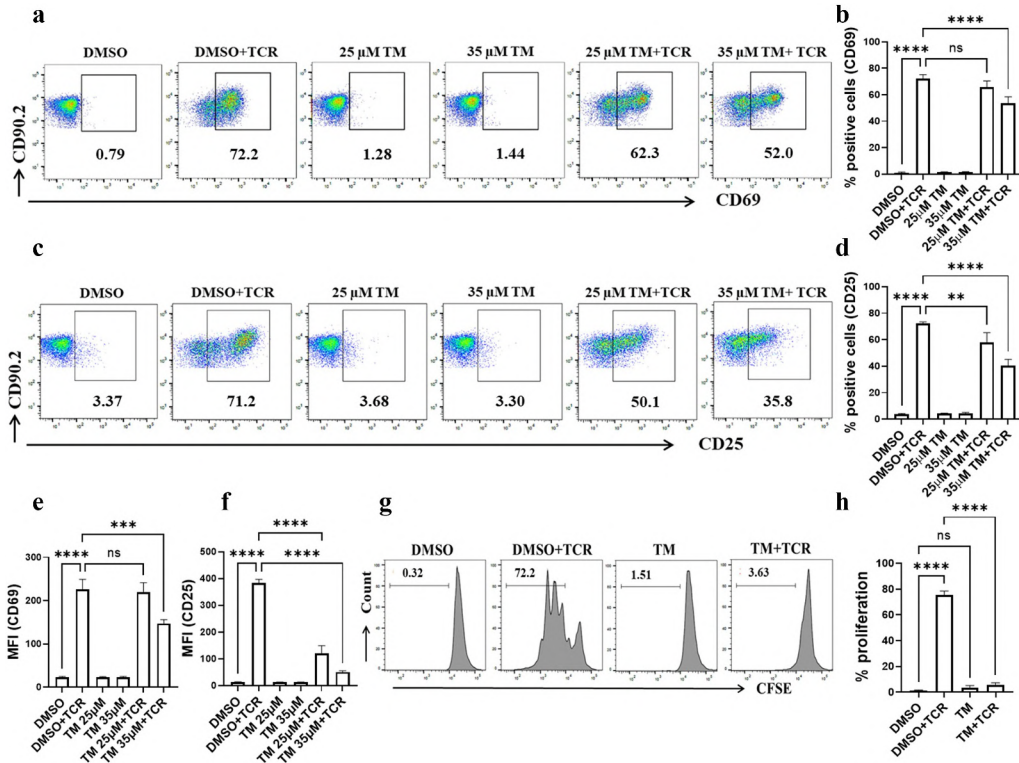
Figure 1. Telmisartan (TM) suppresses TCR-induced T cell activation and proliferation. Flow cytometric dot-plots of T cells showing frequencies of (a) CD69 and (c) CD25 positive T cells in different conditions. Bar diagrams (representing the mean ± SD of three independent experiments) showing (b) frequency of CD69 positive T cells, (d) frequency of CD25 positive T cells, (e) MFI of CD69 and (f) MFI of CD25. TM at 35 μM concentration downregulates both CD69 and CD25 levels significantly, and this concentration was used in further experiments. Flow cytometric histograms in (g) showing T cell proliferation [proliferation assay of T cells stained with CFSE] in the presence or absence of TM with or without activation along with the corresponding bar diagram in (h). Statistical analysis: one-way ANOVA; $p \leq 0.05$ was considered statistically significant. ns = non-significant; ** = $p \leq 0.01$; *** = $p \leq 0.001$; **** = $p \leq 0.0001$. The X and Y axes of the flow cytometric dot plots in (a) and (c) denote the log scale from 10^0 to 10^5. For the flow cytometric histograms in (g), the X-axis represents the log scale from 10^2 to 10^5 and the Y-axis denotes the count from 0 to 100.

Flow cytometry

Cell staining and flow cytometric analysis were conducted following established protocols (Kumar et al., 2022; Majhi et al., 2015; Sahoo et al., 2019). In brief overview, cells were harvested, washed with 1X PBS, and resuspended in staining buffer (1X PBS+ BSA 1%). Cells were incubated with either fluorophore-conjugated antibodies (for CD90.2, CD69, and CD25 detection) or unconjugated antibodies (in case of TRPV1 and TRPA1 detection). The incubation period was 30 min on ice, with protection from light for fluorochrome-conjugated antibodies. Following incubation, the cells were washed with 1X PBS and resuspended in staining buffer containing 1% PFA. For samples with fluorophore-unconjugated antibodies, after primary antibody incubation, cells were washed with 1X PBS, an anti-rabbit AF488-conjugated secondary antibody was added, and incubated on ice for 30 min, with protection from light. Subsequently, cells were washed with 1X PBS and resuspended in staining buffer containing PFA (1%).
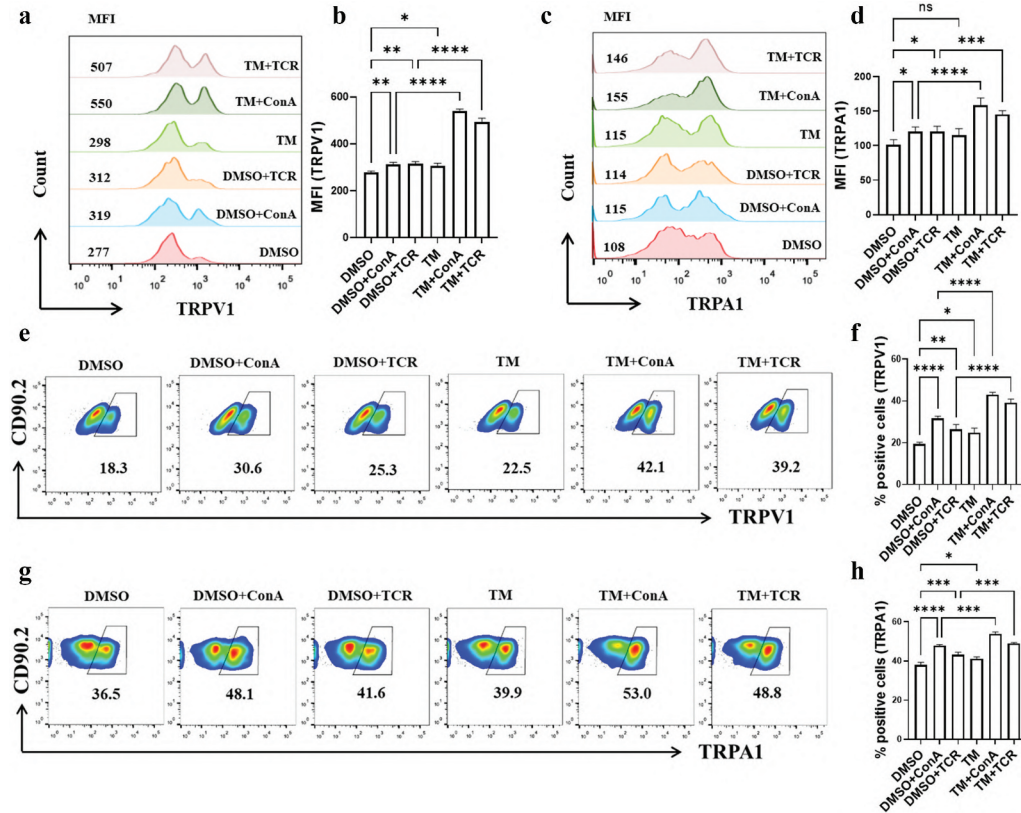
Figure 2. Elevation of cell surface TRPV1 and TRPA1 on T cells during TM-mediated immunosuppression. Flow cytometric histograms of T cells show the MFIs of (a) TRPV1 and (c)TRPA1. Bar diagrams (representing the mean ± SD of 3 independent experiments) in (b) and (d) represent the MFIs of TRPV1 and TRPA1, respectively. Percentages of TRPV1 positive and TRPA1 positive T cells are shown in (e) and (g), respectively, along with the corresponding bar diagrams in (f) and (h). Statistical analysis: one-way ANOVA; $p \leq 0.05$ was considered statistically significant. ns = non-significant; * = $p \leq 0.05$; ** = $p \leq 0.01$; *** = $p \leq 0.001$; **** = $p \leq 0.0001$. The X and Y axes of the flow cytometric plots in (e) and (g) denote the log scale from 10^0 to 10^5.

In the case of cell proliferation assays, T cells were first stained with CFSE, washed with 1X PBS, and seeded in 48 well plates according to the experimental plans. Cells were harvested 72 hours after TCR stimulation. All flow cytometry samples were acquired using BD LSRFortessa[TM] flow cytometer. In each case 10,000 cells/sample were recorded, and further analyses were done using FlowJo software (BD Biosciences). FlowJo analysis was performed by gating the total cell population, excluding the low FSC-A and SSC-A signals, and then excluding the doublets. The CD90.2 positive population (T cells) against SSC-A were then selected and further cellular expressions were analyzed within the CD90.2 positive T cell population.

Elisa

Sandwich ELISAs were performed to quantify IFN-γ and TNF levels in cell culture supernatants using BD OptEIA[TM] mouse ELISA sets following the manufacturer's protocol (Kumar et al., 2022; Majhi et al., 2015; Sahoo et al., 2019). Cytokine concentrations (pg/mL) in culture
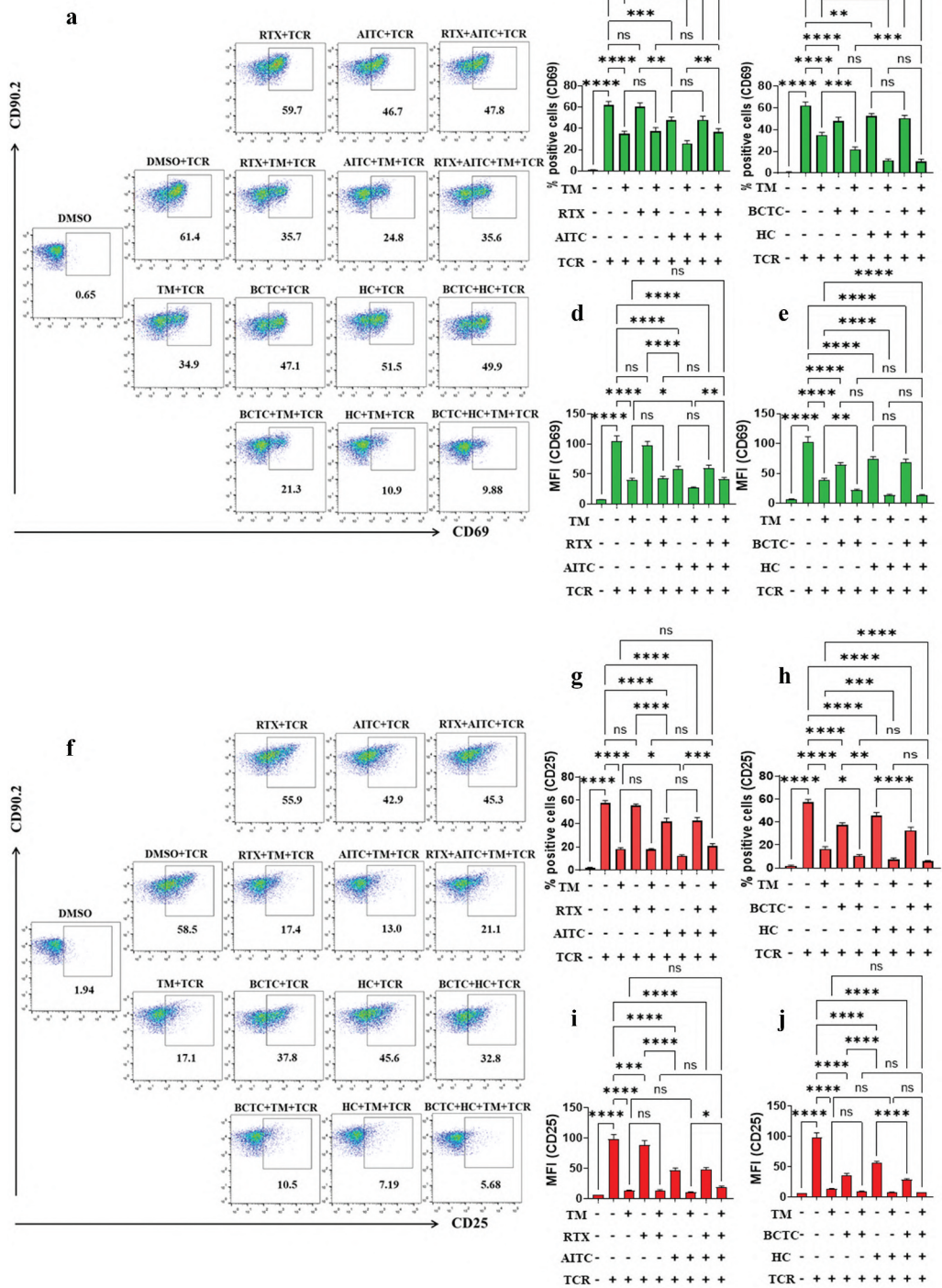
supernatants were determined from the corresponding standard curves derived from recombinant mouse IFN-γ and TNF.

Statistical analysis

Statistical analyses were performed using GraphPad Prism 9.0 software. Data were represented as mean ± SD of 3 independent experiments(3 biological replicates). One-way ANOVA was performed for comparison between groups [Figure 1 (cell surface expressions of CD69 and CD25 on T cells in the presence or absence of TM; T cell proliferation assay in the presence or absence of TM), Figure 2 (cell surface expressions of TRPV1 and TRPA1 on T cells in the presence or absence of TM), Figure 3 (cell surface expressions of CD69 and CD25 on T cells in TRP-modulated conditions in the presence or absence of TM), Figure 4 (IFN-γ and TNF production by T cells in TRP-modulated (activated or inhibited) conditions in the presence or absence of TM)]. Linear fit and correlation between points were used for the correlation analysis (Figure 5). $p \leq 0.05$ was considered statistically significant.

Results

Telmisartan (TM) suppresses TCR-induced T cell activation and proliferation

To determine the impact of TM on CD69 and CD25 levels, T cells were pre-incubated with either DMSO or 25 and 35 μM of TM, and experiments were conducted as described in the materials and methods (Figure 1a–f). No cytotoxicity was observed in the presence of 25 and 35 μM of TM; therefore, these concentrations were selected for further experiments (Fig S1A). Flow cytometric dot-plots in Figure 1a and c represent frequencies of CD69[+ve] and CD25[+ve] T cells along with the corresponding bar diagrams in Figure 1b and c, respectively. Figure 1e and f represent the MFI values of CD69 and CD25 expressions on T cells, respectively. Flow cytometric histograms in Figure 1g represent T cell proliferation along with the corresponding bar diagram in Figure 1h. Notably, 35 μM of TM significantly downregulated T cell activation (even in the presence of TCR, i.e., in TM+TCR condition) as the frequencies of both CD69[+ve] (53.7 ± 3.90; $p \leq 0.0001$) and CD25[+ve] (40.3 ± 3.94; $p \leq 0.0001$) T cells were reduced compared to only TCR (CD69: 72.26 ± 2.36; CD25:72.33 ± 0.93) (Figure 1a–d). This downregulation was consistent with the MFI values of CD69 (147.33 ± 7.40; $p \leq 0.001$) and CD25 (50.6 ± 3.88; $p \leq 0.0001$) in TM+TCR condition compared to TCR alone (CD69: 226.33 ± 18.87; CD25: 383.33 ± 11.02) (Figure 1e–f). Next, a T cell proliferation assay was carried out in the presence or absence

Figure 3. TRPV1 activation during TM-mediated immunoregulation overrides TRPA1-driven suppression of T cell activation. Flow cytometric dot-plots of T cells showing frequencies of (a) CD69 and (f) CD25 positive T cells in different experimental conditions. Bar diagrams (representing the mean ± SD of 3 independent experiments) showing frequency (b) and MFI (d) of CD69 positive T cells in TRPV1- and/or TRPA1-activated conditions. Bar diagrams showing frequency (g) and MFI (i) of CD25 positive T cells in TRPV1- and/or TRPA1-activated conditions. Bar diagrams showing frequency (c) and MFI (e) of CD69 positive T cells in TRPV1- and/or TRPA1-inhibited conditions. Bar diagrams showing frequency (h) and MFI (j) of CD25 positive T cells in TRPV1 and/or TRPA1-inhibited conditions. In each case, one-way ANOVA was performed. $p \leq 0.05$ was considered statistically significant. ns = non-significant; * = $p \leq 0.05$; ** = $p \leq 0.01$; *** = $p \leq 0.001$; **** = $p \leq 0.0001$. The X and Y axes of the flow cytometric dot plots in (a) and (f) denote the log scale from 10^0 to 10^5 (Oh-Hora & Rao, 2008).
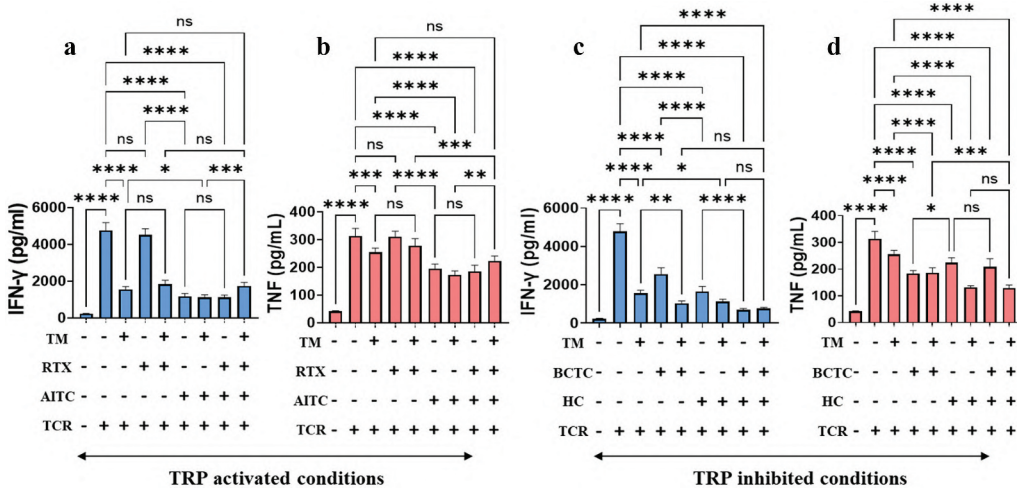
Figure 4. TRPV1 activation during TM-mediated immunoregulation overrides TRPA1-driven suppression of effector cytokine production by T cells. Bar diagrams (representing the mean ± SD of 3 independent experiments) showing production of IFN-γ (a) and TNF (b) in TRPV1- and/or TRPA1-activated conditions. Bar diagrams showing productions of IFN-γ (c) and TNF (d) in TRPV1- and/or TRPA1-inhibited conditions. Statistical analysis: one-way ANOVA; $p \leq 0.05$ was considered statistically significant. ns = non-significant; * = $p \leq 0.05$; ** = $p \leq 0.01$; *** = $p \leq 0.001$; **** = $p \leq 0.0001$.

of TM, revealing a significant downregulation of T cell proliferation in the TM+TCR condition (5.55 ± 0.99; $p \leq 0.0001$) compared to only TCR (75.4 ± 1.74) (Figure 1g and h).

Elevation of cell surface TRPV1 and TRPA1 on T cells during TM-mediated immunosuppression

To assess the cell surface expressions of TRPV1 and TRPA1 in TM-induced immunosuppressed T cells, purified murine T cells were pre-incubated with either DMSO or TM, and experiments were conducted as described in the materials and methods. Flow cytometric histograms in Figure 2a,c represent MFIs of TRPV1 and TRPA1 expressions on T cells along with their corresponding bar diagrams in Figures 2b and c, respectively. Flow cytometric density-plots in Figures 2e and g represent the frequencies of TRPV1[+ve] and TRPA1[+ve] T cells along with the corresponding bar diagrams in Figure 2f,h, respectively. Interestingly, the frequencies of both TRPV1[+ve] and TRPA1[+ve] T cells were significantly elevated in TM+TCR (TRPV1: 39.2 ± 1.34, $p \leq 0.0001$; TRPA1: 48.9 ± 0.37, $p \leq 0.001$) and TM+ConA (TRPV1: 43.13 ± 0.85, $p \leq 0.0001$; TRPA1: 53.73 ± 0.89, $p \leq 0.001$) conditions compared to only TCR (TRPV1: 26.46 ± 1.79; TRPA1: 43.1 ± 1.08) or only ConA (TRPV1: 31.73 ± 0.83; TRPA1: 47.86 ± 0.40), respectively (Figures 2e–h). Similar trends were observed for the MFIs of TRPV1 and TRPA1 in TM+TCR (TRPV1: 494.33 ± 11.58, $p \leq 0.0001$; TRPA1: 145.33 ± 4.92, $p \leq 0.001$) and TM+ConA (TRPV1: 538 ± 8.52, $p \leq 0.0001$; TRPA1: 158.33 ± 10.07, $p \leq 0.0001$) conditions as compared to only TCR (TRPV1: 316.33 ± 6.84; TRPA1: 120.5 ± 6.5) or only ConA (TRPV1: 312.66 ± 6.94; TRPA1: 120.33 ± 6.18) controls, respectively (Figures 2a–d).
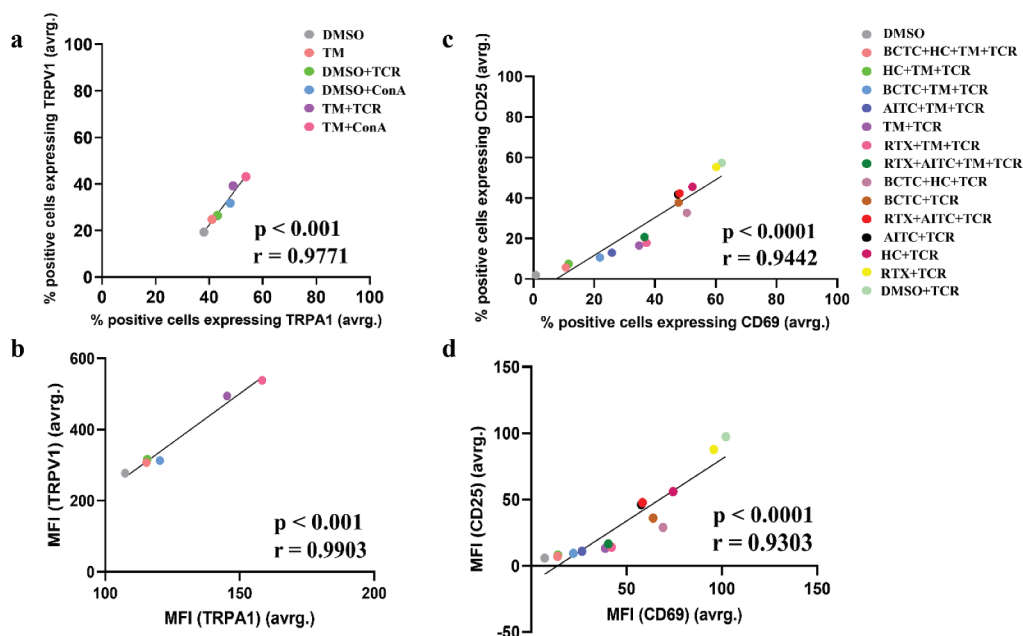
Figure 5. Expression of TRPV1 correlates well with TRPA1 in T cells in different immunological conditions. (a) Correlation between frequencies of TRPV1^{+ve} with TRPA1^{+ve} T cells in different conditions is shown. (b) Correlation between MFIs of TRPV1 with TRPA1 in different conditions is shown. (c) Correlation between frequencies of CD69 with CD25 positive T cells in different conditions is shown. (d) Correlation between MFIs of CD69 and CD25 in different conditions is shown. Linear fit and correlation between points were used for the correlation analysis. In each case, the r and p values are indicated.

TRPV1 activation during TM-mediated immunoregulation overrides TRPA1-driven suppression of T cell activation and effector cytokine responses

To determine the functional role of TRPV1 and TRPA1 in TM-induced immunosuppressed T cells, TRPV1 and TRPA1 were modulated with different functional modulators (no cytotoxicity was observed in each of the modulator's concentrations used for this study, **Figure S1b–S1e**). Experiments were conducted as described in the materials and methods (Figures 3 and 4). Flow cytometric dot-plots in Figure 3a and f represent the frequencies of CD69^{+ve} and CD25^{+ve} T cells, respectively.Bar diagrams in Figure 3b and g represent the frequencies of CD69^{+ve} and CD25^{+ve} T cells in TRP-activated conditions whereas Figure 3c and h represent the frequencies of CD69^{+ve} and CD25^{+ve} T cells in TRP-inhibited conditions, respectively. Bar diagrams in Figure 3d and i represent the MFIs of CD69 and CD25 expressions on T cells in TRP-activated conditions whereas Figure 3e and j represent the MFIs of CD69 and CD25 expressions on T cells in TRP-inhibited conditions, respectively. It was observed that frequencies of both CD69^{+ve} and CD25^{+ve} T cells were significantly reduced in AITC+TCR (CD69: 47.6 ± 2.49, $p \leq 0.001$; CD25: 41.8 ± 2.29, $p \leq 0.0001$) and AITC+TM+TCR (CD69: 25.86 ± 2.25, $p \leq 0.05$; CD25: 12.26 ± 0.65, $p \leq 0.05$) conditions compared to TCR (CD69: 62 ± 2.72; CD25: 57.4 ± 1.92) and TM+TCR (CD69: 34.83 ± 2.12; CD25: 18.16 ± 0.85), respectively (Figure 3a,b,f,g). RTX+TCR condition (CD69: 60.2 ± 3.08; CD25: 55.26 ± 1.26) showed no suppression of T cell activation, but maintained similar trends (in TCR and RTX+TCR) of TCR-driven activation (TCR: CD69: 62 ± 2.72;

CD25: 57.4 ± 1.92) compared to resting T cells (only DMSO) (CD69: 0.82 ± 0.39; CD25: 1.99 ± 0.43) or AITC+TCR treated T cells (CD69: 47.6 ± 2.49; CD25: 41.8 ± 2.29) (for AITC+TCR, the p-value: for CD69: $p \leq 0.01$; for CD25: $p \leq 0.0001$ respectively, as compared to RTX+TCR (CD69: 60.2 ± 3.08; CD25: 55.26 ± 1.26)).

Moreover, the activation of both TRPV1 (by RTX) and TRPA1 (by AITC) in T cells treated with TM and TCR, i.e., in RTX+AITC+TM+TCR (CD69: 36.6 ± 2.62, $p \leq 0.01$; CD25: 20.73 ± 1.61, $p \leq 0.001$) condition partially yet significantly upregulated the frequencies of both CD69^{+ve} and CD25^{+ve}T cells as compared to AITC+TM+TCR (CD69: 25.86 ± 2.25; CD25: 12.26 ± 0.65) (Figure 3a,b,f,g). However, in the absence of TM, the AITC-driven T cell suppression in the presence of TCR (i.e., in AITC+TCR) as compared to TCR alone or RTX+TCR was not reversed by the RTX+AITC+TCR condition. The partial restoration of T cell activation was only observed in T cells treated with TM and TCR, where TRPV1 activation was found to override TRPA1 activation-driven T cell suppression (i.e., RTX+AITC+TM+TCR was found to restore T cell activation as compared to AITC+TM+TCR). However, no such reversal of T cell activation was observed in TCR-treated T cells (in the absence of TM), where TRPV1 activation was not found to override the TRPA1 activation-driven suppression (i.e., RTX+AITC+TCR did not restore T cell activation as compared to AITC+TCR) of T cells.

Corresponding MFIs of CD69 and CD25 are depicted in Figure 3d and i. Similar to the frequencies of CD69 and CD25, the MFI values of CD69 and CD25 in RTX+AITC+TM+TCR (CD69: 41.28 ± 3.01, $p \leq 0.01$; CD25: 18.56 ± 1.97, $p \leq 0.05$) condition moderately yet significantly upregulated the MFIs of both CD69 and CD25 expressions in T cells as compared to AITC+TM+TCR (CD69: 27.10 ± 1.53; CD25: 10.90 ± 0.41) (Figure 3d and i). However, no reversal effects in the MFIs of CD69 and CD25 expressions were observed in the RTX+AITC +TCR (CD69: 59.73 ± 4.92, non-significant; CD25: 48.10 ± 3.082, non-significant) condition in the absence of TM as compared to AITC+TCR (CD69: 58.90 ± 4.16; CD25: 46.76 ± 3.99).

The T cell activation in different conditions, as mentioned above, was further supportedby cytokine levels (IFN-γ and TNF) (Figure 4a and b). Bar diagrams in Figure 4a and b represent the amount of IFN-γ and TNF released by T cells in TRP-activated conditions whereas Figure 4c and d represent the amount of IFN-γ and TNF released by T cells in TRP-inhibited conditions, respectively. RTX+AITC+TM+TCR (IFN-γ: 1749 ± 195.3, $p \leq 0.001$; TNF: 223.7 ± 17.46, $p \leq 0.01$) condition partly yet significantly upregulated both IFN-γ and TNF productions by T cells as compared to AITC+TM+TCR (IFN-γ: 1119 ± 153; TNF: 172.8 ± 15.03) (Figure 4a and b). However, no reversal effects in IFN-γ and TNF production were observed in the RTX+AITC +TCR (IFN-γ: 1124 ± 129.8, p = ns; TNF: 186.2 ± 22.27, non-significant) condition in the absence of TM as compared to AITC+TCR (IFN-γ: 1180 ± 150.4; TNF: 195.4 ± 17.28). In addition, no such reversal of T cell suppression was observed in the BCTC+HC+TM+TCR condition compared to BCTC+TM+TCR and HC+TM+TCR (Figures 3a,c,e,f,h,j and 4c,d).

Expression of TRPV1 correlates well with TRPA1 in T cells in different immunological conditions

Correlation analyses were performed to assess the association between surface expressions of TRPV1 and TRPA1, as well as CD69 and CD25 in various experimental conditions (as shown in Figure 5a). Frequencies of TRPA1^{+ve} and TRPV1^{+ve} T cells in six different immunological conditions remain highly correlated (r = 0.9771; $p \leq 0.001$) (Figure 5a). Comparable results were observed for MFIs of TRPA1 and TRPV1 (r = 0.9903; $p \leq 0.001$) (Figure 5b).

To explore the relationship between TRPV1 and TRPA1 in the context of T cell function, a standard pair of immune activation markers, i.e., a correlation between CD69 and CD25, was analyzed in sixteen different experimental conditions (as shown in Figure 5c). A high correlation between frequencies of CD69^{+ve} and CD25^{+ve} T cells ($r = 0.9442$; $p \leq 0.0001$) and MFIs of CD69 and CD25 ($r = 0.9303$; $p \leq 0.0001$) in various immunomodulated conditions was observed (Figure 5c and d).

Discussion

Many TRP channels, including TRPV1 and TRPA1 channels, are expressed in neurons and play a crucial role in transmitting a variety of sensory signals, such as inflammation, pain, and chemical and thermal nociception (Mickle et al., 2016; Stucky et al., 2009). TRPV1 and TRPA1 are members of the TRP family and have been reported to be functionally associated with diverse immune cells, including macrophages, dendritic cells, T cells, and NK cells (Majhi et al., 2015; Naert et al., 2021; Omari et al., 2017; Sahoo et al., 2019). The functional role of TRPV1 and TRPA1 in TCR- or ConA-mediated T cell activation has been reported previously (Majhi et al., 2015; Sahoo et al., 2019). TM, an anti-hypertension drug, has been experimentally repurposed towards regulating various inflammatory disorders (De et al., 2022; Harrison et al., 2011; Okunuki et al., 2009). However, the possible involvement and association of TRPV1 and/or TRPA1 channels in TM-driven immunosuppression of T cells, if any, have not been reported until now. This study presents the initial evidence that both TRPV1 and TRPA1 participate in TM-driven suppression of T cell responses. Accordingly, our aim was to explore the possible functional involvement of TRPV1 and TRPA1 during TM-driven experimental immunosuppression of T cells. We observe that the surface expressions of TRPV1 and TRPA1 were elevated in TM-mediated immunosuppression of T cells. Moreover, TRPA1 activation-driven suppression of T cell responses during TM treatment was found to be partially yet significantly overridden by TRPV1 activation. Collectively, the data suggest that during immune activation from the basal level as well as in immunosuppressed conditions, expressions of TRPV1 and TRPA1 are upregulated, and these channels are functionally associated with T cell effector responses.

Immunosuppression promotes anti-inflammatory responses, demonstrating a critical impact in both clinical and experimental cases of altered immunity (Meneghini et al., 2021; Parlakpinar & Gunata, 2021). In this study, we used TM, an anti-hypertension drug reported to induce immunosuppression by regulating inflammatory responses (Arab et al., 2014; De et al., 2022; Nakano et al., 2009; Okunuki et al., 2009). Pre-incubation of T cells with TM effectively reduces T cell responses (CD69 and CD25 expressions, proliferation, and cytokine profile), indicating that TM-induced immunosuppression predominates over TCR-mediated T cell activation. Additionally, under TM-induced immunosuppressed conditions, activation of TRPA1 by AITC further induced immunosuppression. However, such stringent levels of immunosuppression could be partially overcome through the activation of TRPV1. Furthermore, in TM-driven immunosuppressed conditions, activation of TRPV1 by RTX was found to enhance T cell activation and effector cytokine production by overriding TRPA1-driven suppression of T cell responses. In contrast, the inhibition of TRPV1 by BCTC and TRPA1 by HC was found to induce higher immunosuppression. Therefore, it appears that the activation of endogenous TRPV1 may enhance T cell activation, especially under stringent immunosuppressive conditions.

Elevation of TRPV1 and TRPA1 during T cell activation and their functional association with T cell effector responses have been previously reported (Majhi et al., 2015; Sahoo et al., 2019). In

our recent work, we demonstrated an increase in cell surface expression of TRPV1 levels in immunosuppressed T cells (Kumar et al., 2022). Additionally, our previous findings indicated an upregulationof different TRP channels during T cell activation (Acharya et al., 2021; Majhi et al., 2015; Sahoo et al., 2019) aligning well with the results presented in this study.

TRPV1 activation facilitates TCR-driven Ca^{2+}-influx, T cell signaling, and effector responses in $CD4^+$ T cells (Bertin et al., 2014). Additionally, pharmacological inhibition of TRPV1 or genetic knockout mice showed reduced disease scores, colitogenic T cell responses, and intestinal inflammation in the T cell-mediated colitis model (Bertin et al., 2014). Conversely, $IL-10^{-/-}TRPA1^{-/-}$ mice in colitis and inflammatory bowel disease (IBD) models have been reported to develop more severe $CD4^+$ T cell-mediated chronic inflammation as compared to mice with only $IL-10^{-/-10}$. Moreover, TRPA1 knockout mutation has also been associated with sustained TCR-driven Ca^{2+} influx, leading to Th1 (IFN-γ, IL-2 producing type 1 $CD4^+$ helper T cells) polarization and the production of IFN-γ and IL-2 (Bertin et al., 2017). Furthermore, TRPA1 has been shown to play a suppressive role in regulating macrophage activation and proinflammatory responses (Radhakrishnan et al., 2023). In addition, immunosuppression has been reported elsewhere to upregulate intracellular Ca^{2+}concentrations (Bultynck et al., 2000; Kumar et al., 2022; Racioppi et al., 2019; Shin et al., 2002) and both TRPV1 and TRPA1 have been found to play an important functional role in regulating intracellular Ca^{2+}levels associated with immunosuppression (Kumar et al., 2022; Radhakrishnan et al., 2023). However, the underlying mechanisms involving immunosuppression-driven elevation of TRPV1 and TRPA1 and their possible association in regulating T cell functions require further exploration in future studies. It could be speculated that TRPV1 and TRPA1 might differentially contribute to the regulation of immune function, in addition to their upregulated expressions during cell-mediated immunosuppression.

In addition to pharmacological modulations, various endogenous molecules have been shown to have agonistic effects on TRPV1 and TRPA1 (Andersson et al., 2008; Benítez-Angeles et al., 2020; Landini et al., 2022; Morales-Lázaro et al., 2013; Trevisani et al., 2007). These include lysophosphatidic acid, N-acyl-ethanolamines, N-acyl-dopamines, oxytocin ATP, hydrogen sulfide, nitric oxide, arachidonic acid and lipoxygenase products, ammonia, intracellular pH, divalent cations (Ca^{2+}, Mg^{2+}), which have been reported to activate TRPV1 channels (Benítez-Angeles et al., 2020; Morales-Lázaro et al., 2013). In contrast, alkenyl aldehydes (4-hydroxynonenal, 4-oxo-nonenal, and 4-hydroxyhexenal), hydrogen peroxide, 15-deoxy-Δ12,14-prostaglandin J2, reactive oxygen species, and reactive nitrogen species have been shown to activate TRPA1 channels (Andersson et al., 2008; Landini et al., 2022; Trevisani et al., 2007). However, further investigations are warranted to decipher the direct involvement of various endogenous molecules in activating TRPV1 and TRPA1 in T cells.

Our data further indicate the existence of a strong correlation between surface expressions of TRPV1 and TRPA1 in T cells in different immunological conditions, such as resting, activated, and immunosuppressed states. Notably, the correlation between TRPV1 and TRPA1 surface expressions is at least the equal range, if not stronger than the CD69 and CD25, suggesting that TRPV1 and TRPA1 could be considered as contextual immunoregulatory markers. Nevertheless, the high correlation between the surface expressions of TRPV1 and TRPA1 in T cells is striking. This is also relevant as in the diverse cellular systems, both TRPV1 and TRPA1 engage in reciprocal signaling functions.

Based on these findings, we suggest that functional modulation of TRPV1 and TRPA1 could be helpful in regulating the immunosuppression of T cells. A proposed working model of the current study has been summarized in Figure 6. This study might have broad
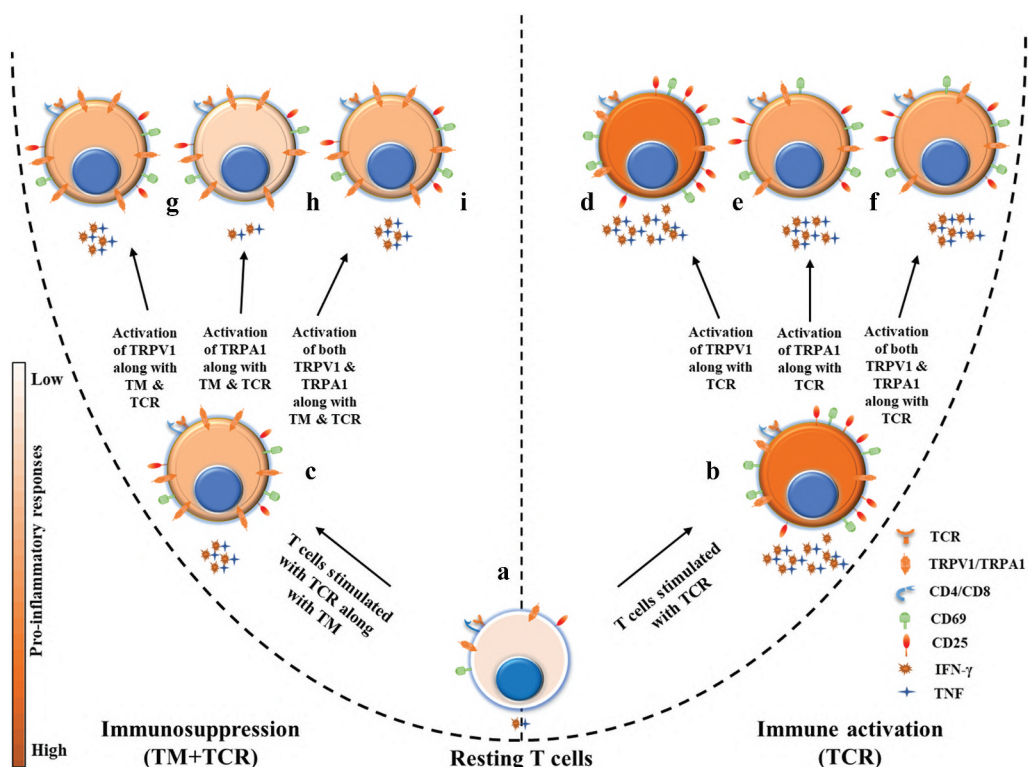
Figure 6. The proposed model depicting the possible involvement of TRPV1 and TRPA1 during TM-induced immunosuppression of T cells. Resting (condition (a), i.e., T cells treated with only DMSO) murine T cells were activated by TCR (i.e., T cells pre-incubated with DMSO and then stimulated with TCR) in the presence (c) or absence (b) of TM. TCR activation upregulates T cell responses relating to T cell activation markers (CD69 and CD25 expressions) and effector cytokine (IFN-γ and TNF) production as compared to resting cells (i.e., T cells treated with only DMSO). TM treatment suppresses T cell responses by downregulating T cell activation markers (i.e., CD69 and CD25 expressions) and effector cytokine (IFN-γand TNF) productions in TM+TCR condition (depicted by condition c) (i.e., pre-incubated with TM and then stimulated with TCR) as compared to only TCR activation (depicted by condition (b). Cell surface expressions of TRPV1 and TRPA1 were upregulated in TM-induced immunosuppressed T cells (c) as compared to T cells activated with only TCR stimulation (b). TRPA1 activation by AITC reduces T cell responses by reducing T cell activation markers (CD69 and CD25 expressions) and effector cytokine (IFN-γand TNF) productions in both AITC+TCR (depicted by condition (e) (i.e., T cells pre-incubated with AITC and then activated with TCR stimulation) and AITC+TM+TCR (h) (i.e., T cells pre-incubated with TM and AITC and then stimulated with TCR) conditions. TRPV1 activation by RTX during TM-mediated immunoregulation overrides TRPA1-driven suppression of T cell responses by upregulating T cell activation markers (CD69 and CD25 expressions) and effector cytokine (IFN-γ and TNF) responses i.e., in RTX+AITC+TM+TCR condition (depicted in (i), T cells pre-incubated with RTX, AITC, and TM and then stimulated with TCR) as compared to TRPA1-activated cells treated with TM and TCR, i.e., in AITC+TM+TCR condition (depicted in (h), T cells pre-incubated with AITC and TM, and then stimulated with TCR). However, in the "absence of TM", activation of TRPV1 by RTX in TCR-activated cells fails to override TRPA1 activation (by AITC)-driven suppression of T cell responses, i.e., in RTX+AITC+TCR condition (depicted in (f), i.e., T cells pre-incubated with RTX and AITC, and then stimulated with TCR) relating to T cell activation markers (CD69 and CD25 expressions) and effector cytokine (IFN-γand TNF) productions as compared to TRPA1-activated cells treated with TCR, i.e., in AITC+TCR condition (depicted in (e), T cells pre-incubated with AITC and then stimulated with TCR), suggesting a possible functional involvement of TRPV1 and TRPA1 in TM-mediated immunosuppression of T cells.

implications for the role of TRPV1 and TRPA1 in immunosuppressive diseases and might be important in designing strategies for possible future immunotherapy, especially the repurposing of TM in regulating TRP-directed cell-mediated immune responses associated with immune disorders. The current study may open future translational implications for other TRP channels in altered cell-mediated immune responses associated with various diseases.

Acknowledgments

Disclosure statement

No potential conflict of interest was reported by the author(s).

Funding

Author contributions

Conceptualization: Tathagata Mukherjee, Chandan Goswami, and Subhasis Chattopadhyay; Methodology: Tathagata Mukherjee, Shyama SubhadarsiniTung, Parthasarathi Jena; Formal analysis and investigation: Tathagata Mukherjee, Chandan Goswami, and SubhasisChattopadhyay; Writing/ original draft preparation: Tathagata Mukherjee, Chandan Goswami, and SubhasisChattopadhyay.

Data availability statement

Data supporting the findings of the study are available from the corresponding author upon reasonable request.

Ethical approval

All protocols used for animal (mice) experiments (Protocol no. AH-274) were approved by the IAEC, NISER. This study does not contain any human participants.

References

Acharya, T. K., Tiwari, A., Majhi, R. K., & Goswami, C. (2021). TRPM8 channel augments T-cell activation and proliferation. *Cell Biology International*, *45*(1), 198–210. https://doi.org/10.1002/cbin.11483

Andersson, D. A., Gentry, C., Moss, S., & Bevan, S. (2008). Transient receptor potential A1 is a sensory receptor for multiple products of oxidative stress. *Journal of Neuroscience*, *28*(10), 2485–2494. https://doi.org/10.1523/JNEUROSCI.5369-07.2008

Arab, H. H., Al-Shorbagy, M. Y., Abdallah, D. M., & Nassar, N. N. (2014). Telmisartan attenuates colon inflammation, oxidative perturbations and apoptosis in a rat model of experimental inflammatory bowel disease. *PLoS One*, *9*(5), e97193. https://doi.org/10.1371/journal.pone.0097193

Arif, A. F., Kadam, G. G., & Joshi, C. (2009). Treatment of hypertension: Postmarketing surveillance study results of telmisartan monotherapy, fixed dose combination of telmisartan + hydrochlorothiazide/amlodipine. *Journal of the Indian Medical Association*, *107*(10), 730–733.

Benítez-Angeles, M., Morales-Lázaro, S. L., Juárez-González, E., & Rosenbaum, T. (2020). TRPV1: Structure, Endogenous Agonists, and Mechanisms. *International Journal of Molecular Sciences*, *21*(10), 3421. https://doi.org/10.3390/ijms21103421

Bertin, S., Aoki-Nonaka, Y., De Jong, P. R., Nohara, L. L., Xu, H., Stanwood, S. R., Srikanth, S., Lee, J., To, K., Abramson, L., Yu, T., Han, T., Touma, R., Li, X., González-Navajas, J. M., Herdman, S., Corr, M., Fu, G., & Jefferies, W. A. (2014). The ion channel TRPV1 regulates the activation and proinflammatory properties of CD4+ T cells. *Nature Immunology*, *15*(11), 1055–1063. https://doi.org/10.1038/ni.3009

Bertin, S., Aoki-Nonaka, Y., Lee, J., de Jong, P. R., Kim, P., Han, T., Yu, T., To, K., Takahashi, N., Boland, B. S., Chang, J. T., Ho, S. B., Herdman, S., Corr, M., Franco, A., Sharma, S., Dong, H., Akopian, A. N., & Raz, E. (2017). The TRPA1 ion channel is expressed in CD4+ t cells and restrains T-cell-mediated colitis through inhibition of TRPV1. *Gut*, *66*(9), 1584–1596. https://doi.org/10.1136/gutjnl-2015-310710

Bultynck, G., De Smet, P., Weidema, A. F., Ver Heyen, M., Maes, K., Callewaert, G., Missiaen, L., Parys, J.B., & De Smedt, H. (2000, June). Effects of the immunosuppressant FK506 on intracellular Ca2+ release and Ca2+ accumulation mechanisms. *The Journal of Physiology*. Advance online publication. https://pubmed.ncbi.nlm.nih.gov/10856121/

De, S., Mamidi, P., Ghosh, S., Keshry, S.S., Mahish, C., Pani, S.S., Laha, E., Ray, A., Datey, A., Chatterjee, S., & Singh, S. (2022). Telmisartan Restricts Chikungunya Virus Infection In Vitro and In Vivo through the AT1/PPAR-γ/MAPKs Pathways. *Antimicrobial Agents and Chemotherapy*, *66*(1). https://doi.org/10.1128/AAC.01489-21

Gore, P. N., Badar, V. A., Hardas, M. M., & Bansode, V. J. (2015). Comparative effect of telmisartan vs lisinopril on blood pressure in patients of metabolic syndrome. *Endocrine, Metabolic & Immune Disorders Drug Targets*, *15*(1), 64–70. https://doi.org/10.2174/1871530314666141128154152

Harrison, D. G., Guzik, T. J., Lob, H. E., Madhur, M. S., Marvar, P. J., Thabet, S. R., Vinh, A., & Weyand, C. M. (2011). Inflammation, immunity, and hypertension. *Hypertension*, *57*(2), 132–140. Published online. https://doi.org/10.1161/HYPERTENSIONAHA.110.163576

Huang, S. S., He, S. L., & Zhang, Y. M. (2016). The effects of telmisartan on the nuclear factor of activated T lymphocytes signalling pathway in hypertensive patients. *J Renin-Angiotensin-Aldosterone Syst*, *17*(2), 0–7. https://doi.org/10.1177/1470320316655005

Kalikar, M., Nivangune, K. S., Dakhale, G. N., Bajait, C. S., Sontakke, S. D., Motghare, V. M., & Budania, R. (2017). Efficacy and tolerability of Olmesartan, Telmisartan, and losartan in patients of stage I hypertension: A randomized, open-label study. *Journal of Pharmacology & Pharmacotherapeutics*, *8*(3), 106–111. https://doi.org/10.4103/jpp.JPP_39_17

Kumar, P. S., Mukherjee, T., Khamaru, S., Radhakrishnan, A., Kishore, D. J. N., Chawla, S., Sahoo, S. S., & Chattopadhyay, S. (2022). Correction to: Elevation of TRPV1 expression on T-cells during experimental immunosuppression. *Journal of Biosciences*, *47*(4), 47. https://doi.org/10.1007/s12038-022-00305-3

Landini, L., Souza Monteiro de Araujo, D., Titiz, M., Geppetti, P., Nassini, R., & De Logu, F. (2022). TRPA1 role in inflammatory disorders: What is known so far? *International Journal of Molecular Sciences*, *23*(9), 4529. https://doi.org/10.3390/ijms23094529

Majhi, R. K., Sahoo, S. S., Yadav, M., Pratheek, B. M., Chattopadhyay, S., & Goswami, C. (2015). Functional expression of TRPV channels in T cells and their implications in immune regulation. *The FEBS Journal*, *282*(14), 2661–2681. https://doi.org/10.1111/febs.13306

Meneghini, M., Bestard, O., & Grinyo, J. M. (2021). Immunosuppressive drugs modes of action. *Best Practice & Research Clinical Gastroenterology*, *54–55*, 101757. https://doi.org/10.1016/j.bpg.2021.101757

Mickle, A. D., Shepherd, A. J., & Mohapatra, D. P. (2016). Nociceptive TRP channels: Sensory detectors and transducers in multiple pain pathologies. *Pharmaceuticals (Basel)*, *9*(4), 72. https://doi.org/10.3390/ph9040072

Morales-Lázaro, S. L., Simon, S. A., & Rosenbaum, T. (2013). The role of endogenous molecules in modulating pain through transient receptor potential vanilloid 1 (TRPV1). *The Journal of Physiology*, *591*(13), 3109–3121. https://doi.org/10.1113/jphysiol.2013.251751

Naert, R., López-Requena, A., & Talavera, K. (2021). TRPA1 expression and pathophysiology in Immune Cells. *International Journal of Molecular Sciences*, *22*(21), 11460. https://doi.org/10.3390/ijms222111460

Nakano, A., Hattori, Y., Aoki, C., Jojima, T., & Kasai, K. (2009). Telmisartan inhibits cytokine-induced nuclear factor-κB activation independently of the peroxisome proliferator-activated receptor-γ. *Hypertension Research*, *32*(9), 765–769. https://doi.org/10.1038/hr.2009.95

Oh-Hora, M., & Rao, A. (2008). Calcium signaling in lymphocytes. *Current Opinion in Immunology*, *20*(3), 250–258. https://doi.org/10.1016/J.COI.2008.04.004

Okunuki, Y., Usui, Y., Nagai, N., Kezuka, T., Ishida, S., Takeuchi, M., & Goto, H. (2009). Suppression of experimental autoimmune uveitis by angiotensin II type 1 receptor blocker telmisartan. *Investigative Opthalmology & Visual Science*, *50*(5), 2255–2261. https://doi.org/10.1167/iovs.08-2649

Omari, S. A., Adams, M. J., & Geraghty, D. P. (2017). TRPV1 Channels in Immune Cells and Hematological Malignancies. *Advances in Pharmacology (San Diego, California)*, *79*, 173–198. https://doi.org/10.1016/bs.apha.2017.01.002

Parlakpinar, H., & Gunata, M. (2021). Transplantation and immunosuppression: a review of novel transplant-related immunosuppressant drugs. *Immunopharmacology and Immunotoxicology*, *43*(6), 651–665. https://doi.org/10.1080/08923973.2021.1966033

Racioppi, L., Nelson, E. R., Huang, W., Mukherjee, D., Lawrence, S. A., Lento, W., Masci, A. M., Jiao, Y., Park, S., York, B., Liu, Y., Baek, A. E., Drewry, D. H., Zuercher, W. J., Bertani, F. R., Businaro, L., Geradts, J., Hall, A., & Chang, C.-Y. (2019). CaMKK2 in myeloid cells is a key regulator of the immune-suppressive microenvironment in breast cancer. *Nature Communications*, *10*(1). https://doi.org/10.1038/s41467-019-10424-5

Radhakrishnan, A., Mukherjee, T., Mahish, C., Kumar, P. S., Goswami, C., & Chattopadhyay, S. (2023). TRPA1 activation and Hsp90 inhibition synergistically downregulate macrophage activation and inflammatory responses in vitro. *BMC Immunology*, *24*(1), 16. https://doi.org/10.1186/s12865-023-00549-0

Sahoo, S. S. S., Majhi, R. K. K., Tiwari, A., Acharya, T., Kumar, P., Saha, S., Kumar, A., Goswami, C., & Chattopadhyay, S. (2019). Transient receptor potential ankyrin1 channel is endogenously expressed in T cells and is involved in immune functions. *Bioscience Reports*, *39*(9), BSR20191437/220415. https://doi.org/10.1042/BSR20191437

Sahoo, S. S., Pratheek, B. M., Meena, V. S., Nayak, T. K., Kumar, P. S., Bandyopadhyay, S., Maiti, P. K., & Chattopadhyay, S. (2018). VIPER regulates naive T cell activation and effector responses: Implication in TLR4 associated acute stage T cell responses. *Scientific Reports*, *8*(1), 7118. https://doi.org/10.1038/s41598-018-25549-8

Samanta, A., Hughes, T. E. T., & Moiseenkova-Bell, V. Y. (2018). Transient Receptor Potential (TRP) Channels. *Sub-Cellular Biochemistry*, *87*, 141–165. https://doi.org/10.1007/978-981-10-7757-9_6

Shin, D. W., Pan, Z., Bandyopadhyay, A., Bhat, M. B., Kim, D. H., & Ma, J. (2002). Ca(2+)-dependent interaction between FKBP12 and calcineurin regulates activity of the Ca(2+) release channel in skeletal muscle. *Biophysical Journal*, *83*(5), 2539–2549. https://doi.org/10.1016/S0006-3495(02)75265-X

Stucky, C. L., Dubin, A. E., Jeske, N. A., Malin, S. A., McKemy, D. D., & Story, G. M. (2009). Roles of transient receptor potential channels in pain. *Brain Research Reviews*, *60*(1), 2–23. https://doi.org/10.1016/j.brainresrev.2008.12.018

Trevisani, M., Siemens, J., Materazzi, S., Bautista, D. M., Nassini, R., Campi, B., Imamachi, N., Andrè, E., Patacchini, R., Cottrell, G. S., Gatti, R., Basbaum, A. I., Bunnett, N. W., Julius, D., & Geppetti, P. (2007). 4-hydroxynonenal, an endogenous aldehyde, causes pain and neurogenic inflammation through activation of the irritant receptor TRPA1. *Proceedings of the National Academy of Sciences*, *104*(33), 13519–13524. https://doi.org/10.1073/pnas.0705923104

Vig, M., & Kinet, J. P. (2009). Calcium signaling in immune cells. *Nature Immunology*, *10*(1), 21–27. https://doi.org/10.1038/ni.f.220

Zhang, M., Ma, Y., Ye, X., Zhang, N., Pan, L., & Wang, B. (2023). TRP (transient receptor potential) ion channel family: Structures, biological functions and therapeutic interventions for diseases. *Signal Transduction and Targeted Therapy*, *8*(1). https://doi.org/10.1038/s41392-023-01464-x